Central Role of Cystathionine γ-Lyase in the Regulation of Cardiac Functions

Re Ea Tay

Doctor of Philosophy

Aston University

January 2024

Central Role of Cystathionine γ-Lyase in the Regulation of Cardiac Functions

Re Ea Tay

Doctor of Philosophy

January 2024

Summary

Cardiovascular diseases have been the leading cause of global mortality and morbidity, estimating to kill 18 million people per year. Cardiomyopathy (CM), a disease that affects the myocardium, is considered one of the main drivers. Affected individuals could face heart failure and sudden cardiac deaths due to impaired contractility of the heart. As the underlying causes for CMs remained unknown, there is no cure for this disease and there is a growing interest in discovering therapeutic interventions.

Hydrogen sulfide (H_2S) is a gasotransmitter that is mainly produced by the cystathionine γ-lyase (CSE) enzyme in the heart. Previous research from our lab emphasised the importance of CSE in cardiovascular adaptations during pregnancy but its physiological effects on age-related changes remains unexplored. The aim of this project was to investigate the effects of global CSE deletion on cardiac function, structure, cellular dynamics and molecular pathways using a transgenic murine model.

The longitudinal study revealed that disruption in the CSE/H_2S pathway caused age-dependent systolic and diastolic dysfunction preceding structural abnormalities using echocardiography. This includes a significant reduction in ejection fraction, increased cardiac volumes, elevated myocardial performance index, and prolonged isovolumetric relaxation time, indicative of compromised contractility and myocardial stiffening. Given the pivotal role of mitochondria in cellular energetics, such functional alterations may result from mitochondrial dysfunction, including reductions in biogenesis and bioenergetics due to loss of CSE. Subsequently, reduced ATP produced is due to electron transport chain inefficiencies. Furthermore, perturbations in mitochondrial dynamics were evident, characterised by reduced fission, fusion and mitophagy in $CSE^{-/-}$ mice. At the molecular level, dysregulated calcium signalling was observed, accompanied by upregulation of genes associated with hypertrophy and inflammation, at the onset of the disease process. In conclusion, proper regulation of the CSE/H_2S pathway is essential in maintaining normal cardiovascular functions even under non-energy demanding, resting conditions.

Keywords: cystathionine γ-lyase; cardiomyopathy; mitochondrial dysfunction; gene expression

Acknowledgements

This thesis is dedicated to my loved ones who stood by me unconditionally throughout this whole journey.

First, I would like to express my heartfelt gratitude towards my supervisor, Dr Keqing Wang, for her support and guidance throughout my studies. Her mentorship and patience have taught me to become a good researcher. I extend my sincere appreciation to Dr Francisco Leyva-Leon for sharing his expertise in cardiology. His extensive experiences and advice provided me new research ideas and insights to my PhD project. I would also like to thank the Fletchers for their donation, which has provided me with the opportunity to successfully complete my research.

Thank you to Dr Lissette Sanchez-Aranguren for her unwavering support and motivation in the lab. Her guidance and mentoring have been pivotal in my mitochondrial studies. Special thanks to Dr Theo Kantidakis, Dr Sophie Broadway-Stringer and Dr Lorena Diaz Sanchez for their invaluable feedback on my thesis. Many thanks to everyone in Aston Medical Research Institute for their help and support during my research career. Thank you to my fellow PhD colleagues and friends for the continuous encouragement over the past three years, you are one of the main reasons where I would look forward to going to the lab every day.

To my family and friends, there are no words to express my gratitude towards each and every one of you for being a part of this journey. To my mum and dad, thank you for raising me into the person I am today and being the driving force behind my accomplishments. I cannot wait to repay all your sacrifices, even though I know that it will never be enough. To my brother and sister, thank you both for being my rock and always being there for me. Without all the laughs and encouragements, I would not have the courage to finish this arduous journey. To all my friends, both old and new, thanks for the constant motivation and belief. You guys made my PhD more bearable and kept me sane, and I am truly grateful for all the memories we have made together. Thank you all from the bottom of my heart for believing in me, even during moments when I doubted myself.

Finally, I would like to thank the mice that have sacrificed their lives for my research and for the advancement of mankind.

Table of Contents

List of Figures

List of Tables

List of Equations

List of Abbreviations

-SH	Persulfide groups
-SHH	Hydropersulfide group
3-MP	3-mercaptopyruvate
3-MST	3-mercaptopyruvate sulfurtransferase
ACE-I	Angiotensin-converting enzymes inhibitor
CoA	Coenzyme A
ACTC1	α-actine
ADP	Adenosine diphosphate
AET	Aortic ejection time
AMPK	AMP-activated protein kinase
Ang-II	Angiotensin II
ANP	Atrial natriuretic peptide
$ApoE^{-/-}$	Apolipoprotein-E deficient
AR	Aortic regurgitation
ARB	Angiotensin reception-II blocker
ARE	Antioxidant response element
AT1	Angiotensin II Type I receptor
ATP	Adenosine triphosphate
AV	Atrioventricular
BHF	British Heart Foundation
BNP	B-type natriuretic peptide
BP	Biological processes
BPM	Beats per minute
BSA	Bovine serum albumin
Ca^{2+}	Calcium
CAT	Cysteine aminotransferase
CBS	Cystathionine β-synthase
CC	Cellular components
CCHS	Copenhagen City Heart Study
CE-MRI	Contrast-enhanced MRI
CM	Cardiomyopathy
cMyBPC	Myosin binding protein C
CO	Cardiac output
CO	Carbon monoxide
CO_2	Carbon dioxide
CoQ	Coenzyme Q
CSE	Cystathionine γ-lyase
$CSE^{-/-}$	CSE knockout
$CSE^{+/+}$	CSE wild-type
Ct	Cycle number
CVDs	Cardiovascular diseases
DAO	D-amino acid oxidase
DCM	Dilated cardiomyopathy

DEG	Differential expression gene
DES	Desmin
DHLA	Dihydrolipoic acid
DMD	Dystrophin
DOX	Doxorubicin
Drp1	Dynamin related protein 1
DT	Deceleration time
EC	Excitation-contraction
ECM	Extracellular matrix
ED	Endothelial dysfunction
EDV	End diastolic volume
EF	Ejection fraction
EHN	European Heart Network
EKV	Electrocardiogram-gated kilohertz visualisation
eNOS	Endothelial nitric oxide synthase
ESV	End systolic volume
ETC	Electron transport chain
ETHE1	Ethylmalonic encephalopathy 1
$FADH_2$	Flavin adenine dinucleotide
FCCP	Carbonyl cyanide-4-phenylhydrazone
FDA	Food and Drug Administration
Fis1	Fission 1 protein
FKPM	Fragments per Kilobase of transcript sequence of per Millions base pairs sequences
GBP1	Guanylate-binding protein 1
GO	Gene Ontology
GPX1	Glutathione peroxidase-1
GSEA	Gene set enrichment analysis
GSH	Glutathione
GTPases	Guanosine triphosphatases
H_2O_2	Hydrogen peroxide
H_2S	Hydrogen sulfide
HCM	Hypertrophic cardiomyopathy
HF	Heart failure
HFmrEF	Heart failure with mid-range ejection fraction
HFpEF	Heart failure with preserved ejection fraction
HFrEF	Heart failure with reduced ejection fraction
HIP/Rpl29	Heparin/heparan sulfate interacting protein
HO-1	Heme oxygenase-1
HR	Heart rate
HUVECs	Human umbilical vein endothelial cells
I/R	Ischaemia and reperfusion
ICAM-1	Intracellular adhesion molecule-1
ICD	Cardioverter defibrillator
IFN-γ	Interferon-gamma
IL-1β	Interleukin-1 beta

IL-10	Interleukin-10
IL-6	Interleukin-6
IMF	Intermyofibrillar mitochondria
IMM	Inner mitochondrial membrane
Itga	Integrin a
Itgb	Integrin b
IVCT	Isovolumetric contraction time
IVRT	Isovolumetric relaxation time
IVS	Interventricular septum
K_{ATP}	ATP-sensitive potassium channel
Keap1	Kelch-like ECH-associated protein 1
KEGG	Kyoto Encyclopaedia of Genes and Genomes
LAMTOR3	Mammalian target of rapamycin activator 3
LBBB	Left bundles branch blocks
LC3	Atg8-light chain 3
LGE-CMR	Late gadolinium enhancement cardiovascular magnetic resonance
LMNA	Lamin A/C
LV	Left ventricle/ Left ventricular
LVH	Left ventricular hypertrophy
LVID	Left ventricular internal diameter
LVMI	Left ventricular mass index
LVOT	Left ventricular outflow tract
LVPW	Left ventricular posterior wall
LVRR	Left ventricular reverse remodelling
MAPK	Ras-mitogen activated protein kinase
MAPKSP1	Mitogen-activated protein kinase scaffold protein 1
MAS	Mitochondria assay solution
MF	Molecular functions
Mff	Mitochondrial fission factor
Mfn1	Mitofusin 1
Mfn2	Mitofusin 2
MI	Myocardial Infarction
Midiv-1	Mitochondrial division inhibitor-1
MIM	Mitochondrial isolation media
miR-21	MicroRNA 21
miR-22	MicroRNA 22
MMPs	Matrix metalloproteinases
MnSOD	Manganese superoxide dismutase
MPI	Myocardial performance index
mPTP	Mitochondria permeability transition pore
mRNA	Messenger-RNA
MSEA	Multi-Ethnic Study of Atherosclerosis
Mt-ND3	Mitochondrially encoded NADH:ubiquinone oxidoreductase core subunit 3
mtDNA	Mitochondrial DNA

MuRF1	Muscle RING finger-1
MyBPC3	Myosin binding protein C
MYH7	β-myosin heavy chain
NADH	Nicotinamide adenine dinucleotide
NaHS	Sodium hydrosulfide
NDMA	N-methyl-D-aspartate
nDNA	Nuclear DNA
Nf-kB	Nuclear factor-kappa B
NGS	Next-generation sequencing
nHCM	Non-obstructive hypertrophic cardiomyopathy
NMDA	N-methyl-D-aspartate
NO	Nitric oxide
Nrf2	Nuclear factor erythroid 2-related factor 2
NYHA	New York Heart Association
OCR	Oxygen consumption rate
oHCM	Obstructive hypertrophic cardiomyopathy
OMM	Outer mitochondrial membrane
OPA1	Optic atrophy protein 1
Osbpl3	Oxysterol-binding protein-like 3
Ox-LDL	Low-density lipoprotein
OXPHOS	Oxidative phosphorylation
PAG	Propargylglycine
PCA	Principal component analysis
PGC1α	Proliferator-activated receptor gamma coactivator 1-alpha
PINK1	PTEN-induced kinase
PLP	Pyroxidal-5'-phosphate
PM	Perinuclear mitochondria
PP2A	Protein phosphatase 2A
PPCM	Peripartum cardiomyopathy
PSLAX	Parasternal long axis B-mode view
qPCR	Real-time PCR
RBC	Red blood cells
RBPs	RNA binding proteins
RCM	Restrictive cardiomyopathy
RCR	Respiratory control ratio
RNA-seq	RNA sequencing
ROS	Reactive oxygen species
Rpl29	Ribosomal protein L29
RPs	Ribosomal proteins
rRNA	Ribosomal RNA
S_2	Second heart sound
$S_2O_3^{2-}$	Thiosulfate
S_4	Fourth heart sound
SCD	Sudden cardiac death
SENP1	Sentrin-specific protease 1
Serca2a	Sarcoplasmic reticulum Ca^{2+} ATPase

siRNA	small interfering RNA
SIRT-1	Sirtuin-1
SIRT3	Sirtuin 3
SO_3^{2-}	Sulfite
SO_4^{2-}	Sulfate
SOD2	Superoxide dismutase 2
SQR	Sulfide quinone oxireductase
SR	Sarcoplasmic reticulum
SSM	Subsarcolemmal mitochondria
SV	Stroke volume
TAC	Transverse aortic constriction
TCA	Tricarboxylic cycle
TEMT	Thiolether S-methylransferase
TFAM	Mitochondrial transcription factor A
TGF-β	Transforming growth factor beta
TIMPs	Tissue inhibitors of metalloproteinases
TMT	Thiol S-methylransferase
Tn1	Troponin I
TNF-α	Tumor necrosis factor alpha
TNNC1	Troponin C
TnT2	Troponin T
TPM1	Tropomyosin
Trx	Thioredoxin
TST	Thiosulfate sulfurtransferase
TTN	Titin
VDAC-1	Voltage-dependent anion-selective channel 1
VEGF	Vascular endothelial growth factor
WHO	World Health Organisation

1 Introduction

1.1 Cardiovascular Diseases

Cardiovascular diseases (CVDs) are a group of conditions that affect the cardiac and vascular functions of our body. These conditions reduce the life expectancy and quality of life of patients, and have been the leading cause of death worldwide for the past decade (Roth *et al.*, 2020). The World Health Organisation (WHO) estimated that CVDs contributed to 18 million deaths globally, making up 32% of total deaths in 2019. 85% of these deaths are caused by strokes and heart attacks, and having a higher prevalence in middle- and low-income countries, accounting for more than 75% of global deaths (WHO, 2021). The European Heart Network (EHN) (2018) also reported that approximately 4 million deaths per year in Europe were due to heart diseases, which is half of the total number of deaths in Europe. This posed significant burdens on the EU economy, and is estimated to cost €210 billion each year due to productivity losses and healthcare costs (Wilkins *et al.*, 2017). According to the British Heart Foundation (BHF) (2020), one person dies of a heart condition every three minutes in the United Kingdom. Coronary heart disease and stroke are the leading causes of death, followed by arrhythmias and cardiomyopathies (CM). These patients suffer from heart failure (HF), where their cardiac output (CO) is unable to meet the metabolic demands of the body as the heart has less ability to pump blood due to systolic or diastolic dysfunction (Savarese and Lund, 2017).

1.1.1 The Cardiac Physiology

The cardiovascular system consists of the heart and the blood vessels, which are the arteries, veins and capillaries that provide blood supply throughout our bodies (Iaizzo, 2015). This was divided into the (i) systemic circulation, responsible for carrying oxygenated blood to all tissues and organs, and (ii) pulmonary circulation, which facilitates the return of deoxygenated blood to the lungs. The concept of the closed-looped cardiovascular system was first discovered by a British physiologist William Harvey in 1628, documented in his book *de Motu Cordis* (Ribatti, 2009). The heart, located in the middle mediastinum, is a

fibromuscular organ composed of 4 chambers, namely the right and left atria and ventricles. The ‘right heart’, characterised by thin walls, operates as a low-pressure system, whereas the ‘left heart’ possesses more myocardial tissue to produce higher pressure (Mahadevan, 2018).

The cardiac cycle consists of diastole, a period of relaxation and systole, a period of contraction. These phases can be further divided into seven distinct stages: atrial systole, isovolumetric contraction, rapid ejection, reduced ejection, isovolumetric relaxation, rapid filling and reduced filling (Figure 1.1). The cardiac cycle begins with atrial systole, initiated by the electrical depolarisation of atria (P wave of ECG). When the atrial contracts, the pressure rises (‘a’ wave), forcing blood into the ventricles through the atrioventricular (AV) valves. At the end of this phase, known as the end-diastolic volume, the ventricles are filled. This is followed by isovolumetric contraction and ventricular depolarisation as shown by the QRS complex. All valves are closed during this stage, and the ventricular volumes remain unchanged as the ventricles contract. The ventricular pressure continues to increase, exceeding the pressure in pulmonary artery and aorta, causing the aortic and pulmonary valves to open and the rapid ejection of blood into the respective ventricles. Ventricular repolarisation, reflected by the T-wave, occurs approximately after 200 ms after systole. As the ventricles continue to contract, the rate of ejection slows due to decreasing ventricular pressure and active tension. Isovolumetric relaxation begins when intraventricular pressure falls, resulting in all valve closure and producing the second heart sound (S_2). During this phase, the volume of blood in the ventricles, known as end-systolic volume (ESV), remains constant as the ventricles relax. When the intraventricular pressure falls below arterial pressure, the AV valves open, initiating rapid passive filling begins as blood flows from the atria into the ventricles. As the ventricles fill and become less compliant, the intraventricular pressure rises. The ventricles are almost 90% filled at this point in normal resting hearts. The rate of filling slows, marking the end of diastole and the start of the next cardiac cycle (Klabunde, 2011).

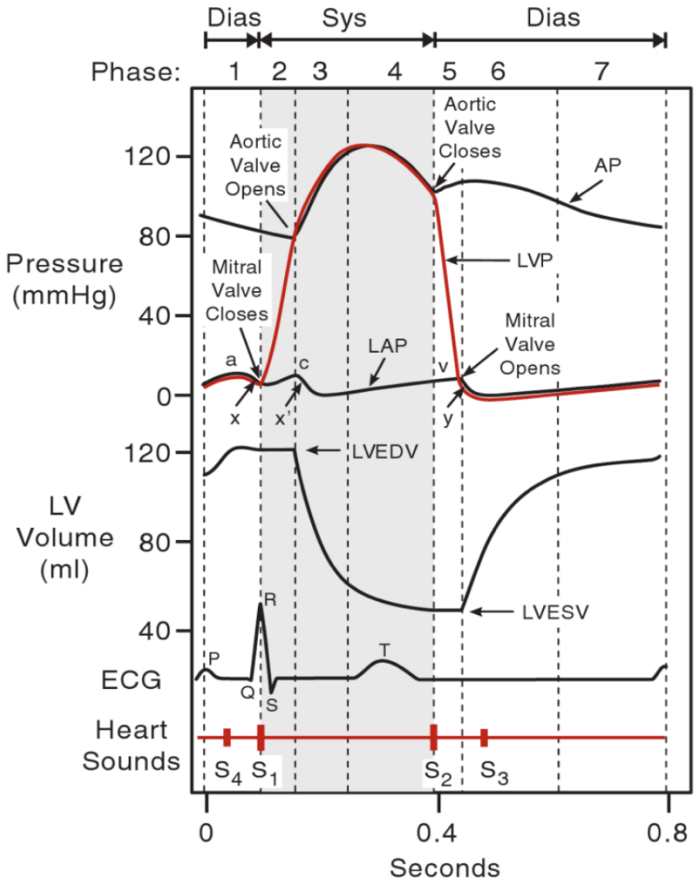

Figure 1.1 Wiggers diagram of the cardiac cycle plotted with left atrial and aortic pressure, and left ventricular pressure (mmHg) and volume, against time.
The 7 phases include (1) atrial systole; (2) isovolumetric contraction; (3) rapid ejection; (4) reduced ejection; (5) isovolumetric relaxation; (6) rapid filling; and (7) reduced filling. Sys, systole; Dias, diastole; AP, aortic pressure; LVP, left ventricular pressure; LAP, left atrial pressure; a, a wave; c, c wave; v, v wave; x, x descent; x', x' descent; y, y descent; LV, left ventricle; ECG, electrocardiogram; LVEDV, left ventricular end-diastolic volume; LVESV, left ventricular end-systolic volume, S_1–S_4, four heart sounds. Adapted from (Klabunde, 2011).

1.1.2 Pathophysiology of HF

Despite advances in medical technology, the morbidity and mortality rate of HF remains high, posing a significant global health problem. For the past two decades, HF is the only heart disease that has an increasing prevalence worldwide (Hazebroek, Dennert and Heymans, 2012). In 2016, the Global Burden of Disease Study found that there was a 54% increase in deaths due to HF compared to the 1990s, from the changes in global demographics with increasing ageing population (Moraga and Collaborators, 2017). Age is a dominant factor in developing circulatory diseases and HF. Even in healthy individuals,

cardiac ageing causes heart function and structure to deteriorate. Hence, it is especially important to understand the underlying pathological pathways and processes that affect the ageing heart, as it will reduce the risk and delay the onset of age-related HF in our growing ageing population (Chiao and Rabinovitch, 2015). Another major cause of HF is CM, a disease that affects heart muscle. Due to alterations in the myocardium, dysregulations in the ventricles arise. This subsequently changes the heart rate, causing hemodynamic overload, ventricular filling defects and abnormalities (Cubero *et al.*, 2004).

HF occurs when the heart is unable to pump enough blood to meet the body's metabolic needs. It is a multifactorial, symptomatic LV dysfunction that often results from coronary artery disease, valvular disease, hypertension and CM. HF can be chronic, *de novo* or subacute, and is further categorised as systolic or diastolic based on EF: HF with reduced EF (HFrEF) (≤ 40%), HF with preserved EF (HFpEF) (≥ 50%) and HF with mid-range EF (41 – 49%) (HFmrEF) (Ponikowski *et al.*, 2016). Notably, HFrEF had a higher incidence in male sex whereas HFpEF affected more females and older patients (Lee *et al.*, 2009). HFrEF has been associated with eccentric hypertrophy with a dilated LV chamber and loss of cardiomyocytes following volume overload, myocarditis or myocardial infarction. This results in reduced contractility and weak pumping of the heart, leading to systolic dysfunction (Simmonds *et al.*, 2020). In contrast, HFpEF is linked to concentric hypertrophy with increased LV wall thickness, and was shown to be a clinical manifestation of microvascular complications and chronic pro-inflammatory state of the heart, resulting in cardiomyocyte stiffening and hypertrophy and the development of diastolic dysfunction (Paulus and Tschöpe, 2013; Tromp *et al.*, 2019).

1.1.3 Cardiac Ageing and its Implications

Age is a significant risk factor for CVDs and mortality. As the heart ages, it undergoes changes that affects its overall performance, increasing the susceptibility to HF.

Cardiomyocytes make up more than 70% of the human heart, with a turnover rate of less than 1% annually until 25 years old, decreasing to 0.45% at 75 years old (Bergmann *et al.*, wa2009). Age-related cardiac deterioration and increasing risk of HF have become a growing global phenomenon due to the expanding elderly population. A population-based cohort study with a 13-year follow-up, involving 24675 participants without a history of HF, emphasised the importance of preventative efforts throughout adult life. Although the incidence of HF in lower in younger people (≤ 55 years), risk factors of HF such as diabetes, smoking, hypertension and past myocardial infarction confer a greater relative risk of HF (75% vs 53%) among young population compared to older individuals (≥ 65 years) (Tromp *et al.*, 2021).

The common pathological changes in an ageing heart include left ventricular hypertrophy (LVH), fibrosis, reduced CO, diastolic dysfunction, increased arterial stiffness and electrical defects (Steenman and Lande, 2017). Ventricular dysfunction in ageing is characterised by fibrosis and hypertrophy from progressive myocyte loss, enlargement of remaining cells, increased collagen content and thicker collagen type I fibres (Olivetti *et al.*, 1991; Debessa, Maifrino and de Souza, 2001). Consequently, ventricular stiffening and impaired diastole develop in ageing hearts. LV fibrosis precedes global LV functional impairment, where a rodent study estimated that systolic and diastolic dysfunction only occurred approximately at 20 months, which is equivalent to 60 years of human age (Sangaralingham *et al.*, 2011). Impaired cardiac contractility and diastolic dysfunction were also commonly caused by decline in calcium handling proteins, specifically the levels of cardiac sarcoplasmic reticulum Ca^{2+} ATPase (SERCA2a) (Dai *et al.*, 2009). These LV remodelling processes result in concentric hypertrophy and HFpEF, which are typical hallmarks of age-associated cardiac deterioration (Zile *et al.*, 2015). However, Cheng *et al.* (2009) used cardiac magnetic resonance imaging on participants without CVDs to show that preserved EF does not reflect a reduction in stroke volume (SV), impaired systolic and diastolic function. Despite the decline of absolute LV mass in ageing, the marked increase in

mass-to-volume ratio of the heart was driven by the significantly reduced EDV (Cheng *et al.*, 2009). In addition, alterations in the electrical conduction of an ageing myocardium, modulated by the cardiac autonomic nervous system, increases risks of elderly to arrythmias (Chadda *et al.*, 2018). This could be attributed to decreased β-adrenergic responsiveness, maximal heart rate and cardiac contractility (Ferrara *et al.*, 2014).

1.2 Idiopathic Cardiomyopathies: Dilated and Hypertrophic

Idiopathic CM is a heterogenous group of myocardium diseases without an identifiable cause. It is defined as abnormalities in the structure and functions of heart muscle, in the absence of coronary heart disease, congenital heart disease, valvular disease and hypertension (Charron *et al.*, 2010). This affects cardiac biomechanics and morphology by altering the shape and function of the heart through ventricular remodelling. The irregularities in conductivity and contractility leads to progressive cardiac dysfunction, which eventually results in sudden cardiac death (SCD) and HF as the onset of this disease is often asymptomatic (Tsipis, 2018). CMs may be primary or secondary. The former can be genetic, acquired, or mixed genetic and non-genetic cases that are mainly confined to the heart. The latter develops as the consequences of different systemic disorders and medical conditions like inflammation, myocardial ischemia, toxins, infections and autoimmune diseases (Sisakian, 2014).

There are several types of cardiomyopathies, such as dilated cardiomyopathy (DCM), hypertrophic cardiomyopathy (HCM), restrictive cardiomyopathy (RCM) and arrhythmogenic right ventricle cardiomyopathy (ARVC), peripartum cardiomyopathy (PPCM) and Takotsubo (stress) cardiomyopathy (Tsipis, 2018). They are most diagnosed by in vivo imaging, either with cardiac MRI or echocardiography. DCM and HCM are principal primary CMs, and a considerable amount of research has been carried out on them (Figure 1.2). DCM is the most prevalent type of CM, but up to 50% of these are idiopathic (Parks *et al.*,

2008). It is an incurable heart disease with 50% rate of fatality in 5 years and up to 80% in 8 years, along with chronic, progressive HF (Mahmaljy, Yelamanchili and Singhal, 2022). This is followed by HCM, the most common inherited CVD, with up to 30% of cases with unknown causes (members *et al.*, 2014). Most of the cases are intractable and result in SCD, even at initial stages (Roberts, Siegel and McManus, 1987). Therefore, early diagnosis of this disease is especially important as it is asymptomatic and progresses silently in relatively young patients, particularly affecting patients between 20 – 60 years old (Hazebroek, Dennert and Heymans, 2012).

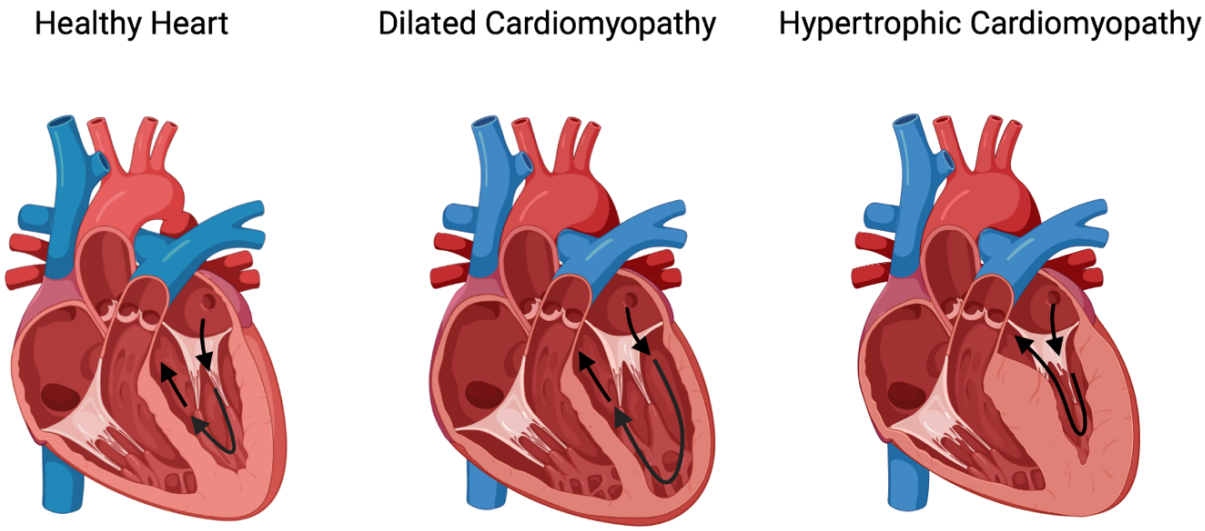

Figure 1.2 Cardiomyopathic versus normal heart.
In DCM, the LV is significantly dilated, and the cardiac walls become thinner, resulting in systolic dysfunction. This reduces the ability of the heart to squeeze and therefore, leading to inefficient pumping and less blood flow around the body. In contrast, HCM is usually associated with diastolic dysfunction as the LV and septal walls becomes significantly thickened, making it difficult for the heart to relax and fill properly with blood. Created in BioRender.com.

The heart possesses the ability to adapt to changes in load, whether it be pressure or volume overload. It responds to these alterations by undergoing dilation or hypertrophy as a compensatory mechanism. However, when the heart fails to adapt to the overload in chronic HF or CMs, it undergoes irreversible LV remodelling. DCM is defined as systolic dysfunction with the progressive enlargement of LV, without any global impairment caused by coronary

heart disease or abnormal loading conditions (Pinto *et al.*, 2016). It accounts for approximately 60% of all cases, making it the most prevalent type of CM and the main cause of non-ischemic HF (Schultheiss *et al.*, 2019). Systolic HF occurs when the LVEF is less than 40% or fractional shortening <25%, due to reduced strength during pumping of the heart. Previous research has suggested that before a patient appears to be symptomatic, their blood pressure is maintained by vasoconstriction of the peripheral vascular system and increased heart rate (Hirota *et al.*, 1984). This is followed by the initial ventricular dilation and thinning of LV walls. Geometrical remodelling acts as a compensatory mechanism for SV and contraction force to support CO. However, as the disease progresses gradually, the larger cavity continues to lower CO and EF while increasing wall stress and ESV. With restrictive and inefficient pumping, the myocardial injury worsens, and the cardiovascular system fails eventually from prolonged exhaustion (Mahmaljy, Yelamanchili and Singhal, 2022).

In contrast to IDCM, HCM has reduced LV chamber size, stiffening and unexplained asymmetrical thickening (wall thickness ≥15 mm) of myocardium. HCM results in diastolic dysfunction due to impaired relaxation and enhanced cardiac contractility. Its complex pathophysiology includes obstruction in left ventricular outflow tract (LVOT), mitral valve problems causing regurgitation, arrhythmias and myocardial ischemia (Gersh *et al.*, 2011). It is classified into obstructive (oHCM) or nonobstructive HCM (nHCM) based on the presence of LVOT. oHCM, caused by the hypertrophied septum which obstructs blood flow from LV to aorta, is the more usual form of the disease, making up two-thirds of the patients (Zaiser *et al.*, 2020). The classic asymmetrical LVH most commonly involve basal interventricular septum (IVS) and the anterior free wall (Ommen *et al.*, 2020). HCM is widely recognised as the most typical cause of SCD and deaths among younger individuals, affecting 1:200 – 1:500 adults, which corresponds to approximately 15 to 20 million people worldwide (Maron *et al.*, 2006). A recent study using cardiac MRI in Multi-Ethnic Study of Atherosclerosis

(MSEA) then found a higher prevalence of 1 in 74 participants with unexplained LVH, suggesting that the actual figures could be higher as HCM could be underdiagnosed (Massera *et al.*, 2019). HCM is often misdiagnosed as the athlete's heart in younger patients and as hypertensive heart disease in older patients (Ommen *et al.*, 2020). At initial stages of HCM, the stiffening and decreased compliance of LV precedes any visible morphological changes, contributing to reduced diastolic and systolic long-axis functions. There will be significant thickening of myocardial walls as HCM progresses, affecting the heart's ability to relax, decreasing LV cavity size and LV filling. However, LVEF was preserved due to reduced LV volumes (Haland *et al.*, 2017). Late phases or end-stage of HCM, also known as dilated HCM, is associated with higher SCDs and can be characterised by dilated LV and systolic dysfunction that resembles an IDCM heart (Goto *et al.*, 2013).

1.2.1 Genetic Causes of DCM and HCM

DCM and HCM are primary myocardial disorders that are affected by genetic mutations in cytoskeletal and sarcomeric protein genes (Hershberger, Hedges and Morales, 2013; Lopes, Rahman and Elliott, 2013). DCM mutations result in impaired force transmission in sarcomere contraction causing reduced contractility; HCM causes defective force generation with poor sarcomere relaxation and enhanced contractility (Garfinkel, Seidman and Seidman, 2018). Although there could be mutations of the same genes, the resultant phenotype and type of CM caused by sarcomere CM were highly variable as it is also dependent on external factors such as lifestyle, environmental exposures, and background genotypes.

The aetiology of DCM is multifactorial and can be classified as a primary or mixed CM. IDCM is an inherited familial DCM that makes up around 20–40% of individuals with the disease (Michels *et al.*, 1992; Grünig *et al.*, 1998; Mahon *et al.*, 2005). Approximately 57 autosomal dominant genetic mutations in structural and sarcomeric proteins are 60% of the

cause of IDCM (Burke *et al.*, 2016; Pérez-Serra *et al.*, 2016). Although it is predominantly autosomal dominant inheritance, there are also less common autosomal recessive, X-linked and mitochondrial inheritance present as well (Towbin and Bowles, 2002). The most common cause is the frameshifting mutation of TTN, a sarcomeric gene that encodes for a large muscle filament titin, which is responsible for the sarcomere's M-, A-, I-bands and Z disk (Haas *et al.*, 2015). TTN mutation is estimated to account for 20% of the familial and 18% of the sporadic cases (Herman *et al.*, 2012). As titin controls the viscoelasticity of the heart, this subsequently changes the contractility of myofibril and affects the pumping mechanisms in the LV. Systolic dysfunction often arises as a complication of DCM due to the reduced stiffness (Vikhorev and Vikhoreva, 2018). The second most frequent mutation is the *LMNA* gene. This non-sarcomeric gene codes for the Lamin A/C protein in the nuclear lamina that is responsible for nuclear stability (Parks *et al.*, 2008). Carriers of this mutation showed conduction abnormalities, arrythmias and reduced force development due to decreased myofibril density that precedes the development of LV dysfunction and dilation (Hoorntje *et al.*, 2017; Hasselberg *et al.*, 2018). Some other mutations that cause defective contractility and force transmission of the myofibrils are stated in Table 1. Bollen *et al.* (2017) showed that mutations in gene encoding cardiac troponin I (Tn1) and cardiac troponin T (TnT2) in IDCM patients has higher calcium sensitivity, reduced length-dependent activation of sarcomeres, increased passive stiffness in cardiomyocytes and haploinsufficiency. Cytoskeletal gene mutation and deletion in dystrophin (DMD) can cause X-linked DCM and DCM in Duchenne and Becker muscular dystrophies from muscle weakness and impairment (Mestroni *et al.*, 2014). Interestingly, MYH3 mutation is associated with late onset of DCM in a population study (Villard *et al.*, 2005).

HCM is inherited as an autosomal dominant trait caused by mutations in sarcomere-associated genes to cause hypercontractility and impaired relaxation. More than 1400 mutations were identified in at least 11 genes encoding the cardiac sarcomere, which is responsible for the contractile function of the heart (Maron, Maron and Semsarian, 2012).

MYH7, which encodes β-myosin heavy chain (β-MHC), and MYBP3, which encodes myosin binding protein C (cMyBPC), are the two predominant genes in the thick filament implicated in HCM, together accounting for 50% of the genetic causes of this condition (Lopes, Rahman and Elliott, 2013). Both mutations lead to poor relaxation and hypercontractility of the myocardium. Missense mutations in the former gene were associated with defective force generation and ATPase activity, altering the interaction of myosin head and neck domains of β-MHC and affecting its binding with actin (Walsh *et al.*, 2009). In contrast, mutations in MYBP3 are predominantly caused by frameshift mutations, premature stop codon mutations or in-frame insertion/deletions that leads to haploinsufficiency, mainly impacting cardiac contraction through cMYBPC content reduction (Weissler-Snir *et al.*, 2017; Helms *et al.*, 2020) . However, there are conflicting views on the severity of HCM depending on the type of thick-filament mutation. Velicki *et al.* (2020) observed that MYH7 mutation showed a more severe phenotype when compared to MYBP3 whereas others reported no significant differences in clinical phenotypes between these mutations (Lopes, Rahman and Elliott, 2013; Weissler-Snir *et al.*, 2017; Viswanathan *et al.*, 2017).

Additionally, thin-filaments mutations were detected in HCM as well. A comprehensive meta-analysis involving 7675 HCM patients across 51 studies by Sedaghat-Hamedani *et al.* (2018) revealed that MYH7 and MYBP3 average mutation frequency were much higher, 20% and 14% respectively, as compared to 2% prevalence in thin filament protein encoding genes TnT2 and TnI, which are regulators of act-myosin interaction. In the same study, it was reported that patients with MYH7 and TnT2 faced earlier onset of HCM than HCM patients with MYBP3, TnI or no mutations (Sedaghat-Hamedani *et al.*, 2018). While thin-filament mutation is less frequent, patients with thin-filament HCM had milder, concentric and atypically distributed LVH at initial examination compared to thick-filament mutations. However, these patients had poorer prognosis during final evaluation, as thin-filament mutation progresses into a more severe phenotype of systolic dysfunction and

restrictive diastolic pattern overtime, with LVEF<50% (Coppini *et al.*, 2014). Generally, patients with sarcomeric mutations were significantly younger at diagnosis, with a much higher risk of SCD and family history of HCM (Lopes *et al.*, 2015). There is a gene-dose effect on the mutations, where compound mutations increased the risks, but not severity, of HCM and its associated SCD (Lopes *et al.*, 2015; Viswanathan *et al.*, 2017).

1.2.2 Non-genetic Pathogenesis of CM

Myocardial damage in CMs can also result from non-genetic, secondary causes and involves a complex interplay of these mechanisms during the pathogenesis of CM. These include inflammation, immunological responses, metabolic abnormalities, toxic triggers, oxidative stress, mechanical stress, and vascular and mitochondrial dysfunction.

Inflammation plays a crucial role in the pathogenesis of CM, potentially acting as an initial trigger or exacerbating existing cardiac damage during disease progression. Inflammatory CM, also known as myocarditis, is caused by autoimmunity and infections and can progresses into DCM (Bironaite *et al.*, 2015). Viral infections, particularly by enteroviruses, initiates inflammation by activating systemic autoimmune system, causing fibrosis and HF via the direct cytotoxic effect, cytoskeleton disruption and myocyte necrosis (Caforio *et al.*, 2017). Endomyocardial biopsy samples from myocarditis patients often showed significant expressions of pro-inflammatory cytokines and infiltrations of inflammatory cells such as $CD3^+$ T lymphocytes, $CD68^+$ macrophages and $CD20^+$ B cells, indicating chronic inflammatory response (Tschöpe *et al.*, 2021). In HCM patients, Kuusisto *et al.* (2012) observed low-grade systemic inflammation characterised by increased infiltration of both pro- and anti-inflammatory cytokines and activation of nuclear factor-kappa B (Nf-kB). They suggested that this inflammatory response was induced by injury to the myocardium and played an important role in modifying the active process of myocardial fibrosis in HCM. This was later supported by Fang *et al.* (2017), who found that the degree of

systemic inflammation correlated with the disease severity of HCM, including the extent of hypertrophy, fibrosis and diastolic dysfunction. Nf-kB was also found to be a predictor of long-term clinical outcomes in HCM patients in a 10-year follow-up study (Pelliccia *et al.*, 2022). Moreover, Shimada *et al.* (2021) preformed a large-scale proteomics profiling in HCM patients compared to controls with hypertensive LVH and revealed the upregulation in the transforming growth factor-β (TGF-β) and Ras-mitogen activated protein kinase (MAPK) pathways, including their upstream and downstream pathways, contributing to the development of a more severe form of HCM.

Furthermore, CM caused by long-term use of alcohol and cocaine can induce toxicity and myocardial damage (Awtry and Philippides, 2010). According to a recent longitudinal cohort study, DCM patients with previous history of moderate excess alcohol consumption showed a globally impaired cardiac phenotype, including increased ventricular mass, greater ventricular dilation and reduced biventricular functions (Tayal *et al.*, 2022). Similarly, these deleterious effects and depressed LV functions were seen in long-term users of cocaine, as this drug was shown to be prothrombotic, consequently impairing calcium signalling and increasing myocardial oxygen demand. In addition, it also stimulates vasoconstrictor endothelin-1 production and inhibits the release of vasodilator nitric oxide (NO) (Schwartz, Rezkalla and Kloner, 2010). Excessive stress in CM triggers different forms of cell death through signalling mechanisms involving apoptosis, autophagy and pyroptosis (Sheng *et al.*, 2023). Cancer chemotherapeutic drugs like doxorubicin (DOX), can induce CM and congestive HF as side-effects (Volkova and Russell, 2011). Despite being designed to interfere with mitosis, DOX adversely affects healthy organs by progressively increasing ROS generation, cardiomyocyte apoptosis and destabilising DNA strands to downregulate mitochondria biogenesis (Zhang *et al.*, 2012c).

Another notable cause of DCM is vascular factors that lead to reduced blood flow, impaired angiogenesis, and hypertension. An example of this is pregnancy related PPCM.

European Society of Cardiology defines PPCM as an idiopathic CM that occurs towards late pregnancy or early post-partum, characterised by LVEF <45% and no other cause of HF (Sliwa *et al.*, 2010). PPCM is a complex, multifactorial disease that involves oxidative stress, hormonal, metabolic and angiogenic factors, therefore making it difficult to determine its aetiology and pathophysiology. Studies have also shown that vascular complications such as preeclampsia and eclampsia are highly associated with PPCM, as they are both triggered by excess ROS, placental antiangiogenic and anti-vascular factors secretion (Patten *et al.*, 2012).

Table 1.1 Etiologies of DCM and HCM

Common Causes	DCM	HCM
Genetic	Titin (*TTN*), Lamin A/C (*LMNA*), β-myosin heavy chain (*MYH7*), myosin binding protein C (*MyBPC3*), troponin T (*TnT2*), troponin I (*Tn1*), Desmin (*DES*), Dystrophin (*DMD*)	β-myosin heavy chain (*MYH7*), myosin binding protein C (*MyBPC3*), troponin T (*TNNT2*), troponin I (*TNN13*), troponin C (*TNNC1*), α-actine (*ACTC1*), α-tropomyosin (*TPM1*), Desmin (*DES*)
Non-genetic	Neuromuscular disorders (Duchenne muscular dystrophy, Becker muscular dystrophy); Inflammatory/Myocarditis (viral, bacterial, fungal, parasitic); Autoimmune diseases (polymyositis, dermatomyositis, sarcoidosis, rheumatoid arthritis); Toxicity/Drugs (Alcohol, cocaine, iron-overload, anabolic steroids, amphetamines, amyloidosis, arsenic); Metabolic/Endocrine (Diabetes mellitus, hypo- or hyperthyroidism, Cushing's disease, acromegaly, pheochromocytoma); Pregnancy (Peripartum cardiomyopathy)	Mitochondrial disorders, hypertension, ageing, obesity

1.2.3 Histopathological Changes During DCM and HCM

Myocardial structures undergo alterations at macro- and microscopic levels, in the form of LV dilation in DCM or hypertrophy in HCM. The myocardium is composed of approximately 24% of extracellular matrix (ECM) and 76% of cardiomyocytes (Mirut, Stephan and Pirici, 2018). Cardiomyocytes are muscle cells that are responsible for cardiac excitation-contraction coupling and the ECM is crucial for the maintenance and homeostasis of cardiac muscles. The ECM compromises myofibrils, blood vessels, myocytes, and collagen fibres. Fibrillar collagen Type I constitutes over 80% of a healthy human heart, while Type III accounts for 10%, both linked to the non-fibrillary basement membrane by fibronectin and collagen type IV (Weber, 1989; Silva *et al.*, 2021). Type I collagen provides mechanical tensile strength, while Type III contributes to heart elasticity (Monte-Nieto *et al.*, 2020).

Changes in the ECM can significantly the influence onset progression of CM (Louzao-Martinez *et al.*, 2016). Myocardial fibrosis is a major hallmark in DCM, resulting from ECM protein accumulation and expansion that causes myocardial remodelling (Chute *et al.*, 2019). Alterations in the interstitial collagen concentration profoundly impact the heart and its mechanisms. For example, increased collagen content in response to pressure overload stiffens the heart, while decreased collagen leads to a more compliant, dilated ventricle with systolic dysfunction (Janicki and Brower, 2002). Clinical pictures and histology of DCM showed dilated cavities in the LVs, myocytolysis and post necrotic scars in the myocardium, without other CVDs (McKenna, Maron and Thiene, 2017). DCM is associated with increased collagen deposition, but the newly produced collagen may be functionally defective and have weaker crosslinks, resulting in heart dilation and wall-thinning (Gunja-Smith *et al.*, 1996). A study highlighted that the total collagen content and collagen type III/I ratio in all patients with idiopathic, hypertensive or diabetic DCM were much higher than the controls, with the increase in type I collagen leading to significantly lowered LVEF (Soufen *et*

al., 2008). Histological images also revealed both fibrosis and loss of collagen scaffold around cardiomyocytes in idiopathic DCM patients (López, González and Díez, 2010). Overexpression of matrix metalloproteinases (MMPs) in patients with mild LV dilation suggests that remodelling occurs in early stages of DCM. This accelerates collagen degradation and metabolism, reduces cardiac tensile strength, leading to poor LV integrity and systolic dysfunction as the heart's pumping ability becomes compromised (Picard *et al.*, 2006; Rubiś *et al.*, 2016). Midwall myocardial fibrosis is another predictor of adverse outcomes in DCM. A study by McCrohon and colleagues (2003) found that 30% of DCM patients with systolic dysfunction and HF exhibited mid-wall myocardial fibrosis when being evaluated using late gadolinium enhancement cardiovascular magnetic resonance (LGE-CMR) imaging. This finding is supported by later studies, where mid-wall fibrosis is found to be an independent predictor for morbidity and mortality in DCM patients after cardiac transplantation (Leyva *et al.*, 2012; Gulati *et al.*, 2012). With mid-wall fibrosis, the circumferential fibres in the myocardium are impaired. This decreases the torsion, global circumferential strain and strain rate during both systole and diastole. Therefore, there is higher risk of heart failure as the heart becomes more rigid and stiffens (Taylor *et al.*, 2015). In addition, nuclear pleomorphism is another characteristic of DCM, where the nuclei of cardiomyocytes were observed to appear larger, dysmorphic and unsymmetrical (Mitruț *et al.*, 2019). The myocytes of DCM patients are associated with cardiomyocyte hypertrophy and elongation throughout the myocardium, with deterioration in intercalated discs, myofibrillar loss and disorganisation of sarcomeres (Ito *et al.*, 2021)

Histopathologically, HCM is characterised by cardiomyocyte hypertrophy in affected regions, replacement or interstitial fibrosis, increased loose connective tissue with fibre disarray and endocardial thickening, all of which would impede myocyte force generation and impair relaxation in cardiac muscles (Cui *et al.*, 2021). Hypertrophied myocyte is determined by its diameter. Healthy cardiomyocytes are usually rod-shaped, measuring around 5 – 12 μm in diameter. When the diameter reaches up to 25 μm diameter, it is

considered as moderate hypertrophy, while a diameter exceeding 30 μm indicates severe hypertrophy (Tejado and Jou, 2018). Furthermore, these cells would display characteristics such as binucleation, irregular nuclear shapes and enlarged nuclei, and are usually surrounded by narrow small arteries with thickened vessel wall (Hughes, 2004). Cui *et al.* (2021) reported moderate or severe myocyte hypertrophy in 97.3% of HCM patients, with the degree of hypertrophy correlating to septal thickness and LV mass index (LVMI). Moreover, both replacement and interstitial fibrosis were seen in HCM patients. A study by Galati *et al.* (2016) on 30 explanted hearts of end-stage HCM patients with severely depressed LVEF and HF detected an average of 37.3% of different fibrosis types, which includes interstitial, combination or replacement, scar-like fibrosis. Replacement fibrosis was the most predominant type – it was present in more than half of the patients, with the midventricular layer exhibiting the most extensive presence of fibrosis (Galati *et al.*, 2016). During HCM progression, the extent of fibrosis could be measured using LGE on contrast-enhanced MRI (CE-MRI) as it indicates extensive scarring (Eijgenraam, Silljé and de Boer, 2020). Rubinshtein *et al.* (2010) evaluated 424 patients with HCM and concluded that gene-positive patients had higher prevalence of LGE, which was significantly associated to SCD and reduced LVEF.

The presence of myocyte disarray is another hallmark of HCM and an independent predictor of SCDs, distinguishing it from other hypertensive disorders (Ariga *et al.*, 2019). It leads to cardiac arrythmias and diastolic dysfunction as electromechanical coupling is disrupted from the disorganisation of intercellular junctions of hypertrophied myocytes (Hughes, 2004). Surprisingly, Cui *et al.* (2021) suggested that myocyte disarray could be a trigger, rather than the consequence of HCM, as higher degree of myocyte disarray was found in younger oHCM patients. This was supported by a recent study using MYBPC3-targeted knockout HCM mouse model that mimic human HCM patients with cMYBPC haploinsufficiency, which showed that myoarchitectural disarray precedes LVH and was already present before birth in fetal hearts (Garcia-Canadilla *et al.*, 2019). Autopsy of

patients with TNNT2 mutations who faced SCDs had severe disarray despite showing mild hypertrophy and fibrosis, and this could be a direct response of structural or functional abnormalities from sarcomeric mutations (Varnava *et al.*, 2001).

1.2.4 Diagnosis and Treatment of CMs

The clinical presentations of both DCM and HCM are similar to those seen in HF. Patients will generally find themselves with typical symptoms of HF, which includes chest pain or tightness, atrial fibrillation, progressive dyspnea on exertion, and paroxysmal nocturnal dyspnea (Wahls, 2012; Zaiser *et al.*, 2020). The diagnostic process for DCM and HCM involves a comprehensive evaluation through a combination of medical assessment, physical examination, and diagnostic tests. After excluding other forms of heart dysfunction, genetic screenings are carried out to identify any underlying genetic mutations associated with the conditions (Rapezzi *et al.*, 2013). The initial clinical evaluation includes screenings of first-degree relatives and a thorough assessment of family history of at least three generations of family pedigree to identify relatives with DCM or HCM (Vogiatzi *et al.*, 2022). Diagnostic tests like chest X-ray examination, transthoracic echocardiography, ECG, CMR imaging and B-type natriuretic peptide (BNP) blood tests are usually carried out to examine the underlying causes (Wexler *et al.*, 2009; Maron *et al.*, 2022). Chest radiography is an accurate method to inspect for abdominal distension and oedema. Echocardiography is a valuable tool for assessing LV remodelling, functions and detecting any abnormalities, including wall thickness and motion (Inamdar and Inamdar, 2016). In cases of DCM, enlarged ventricles, systolic dysfunction, and normal or reduced wall thickness are typically observed. ECGs of individuals with CMs also revealed arrhythmia, conduction irregularities, and lower QRS voltages and amplitudes (Finocchiaro *et al.*, 2020). Rodrigues *et al.* (2018) found that changes in ST segments, AV conduction, and left bundles branch blocks (LBBB) that cause cardiac desynchronisation, may suggest the presence of idiopathic DCM. On the other hand, the diagnosis of HCM involves similar steps, but focuses on assessing the

thickness of the heart muscles. Physical examination may reveal the presence of a heart murmur or fourth heart sound (S_4), indicating oHCM, and up to 96% of HCM patients exhibit ECG abnormalities (Nourani *et al.*, 2023). Two-dimensional echocardiography is the primary method for diagnosing HCM as it allows evaluation systolic and diastolic functions, mitral valve function, the degree of hypertrophy, and presence of LVOT obstruction (Ommen *et al.*, 2020). However, sometimes the results of echocardiography can be inconclusive or overestimate the thickness, requiring the use of CMR imaging to provide further clarification and assess the specific wall segment affected (Corona-Villalobos *et al.*, 2016). HCM is diagnosed when LV wall thickness $\geq$ 15 mm with a non-dilated cavity (Maron, Rowin and Maron, 2017).

Currently, there is no cure available for CMs as the prognosis is often poor and causes are unidentifiable. The treatment options for DCM and HCM aim to manage symptoms, improve heart functions and prevents complications. The specific treatment plan for each patient may vary based on the severity of the condition and individual factors. For DCM, the primary focus is on addressing HF and improving cardiac function whereas for HCM, treatment strategies focus on managing symptoms to reduce the risks of complications such as arrythmias and SCDs. In both conditions, lifestyle modifications play a crucial role to prevent disease progression, which mainly include for example, exercise, healthier diet, abstinence of alcohol and smoking cessation (Hazebroek, Dennert and Heymans, 2012).

In DCM, standard medications for HF like angiotensin-converting enzymes inhibitor (ACE-I), angiotensin reception-II blocker (ARB) (for patients who are intolerant to ACE-I) and beta-blocker (in addition to ACE/ARB treatments) are provided to alleviate the disease by vasodilation and improving the LVEF. ACE-Is have been shown to be the gold standard in reducing deaths in HFrEF (McDonagh *et al.*, 2021). Hoshikawa and colleagues (2011) predicted the long-term prognosis of IDCM patients using ARBs and beta-blockers or the

ACEs therapy and found rather successful left ventricular reverse remodelling (LVRR) and improved left ventricular systolic functions. Furthermore, oral diuretics for example, loop diuretics or thiazide, also help to decrease retention of fluids and oedema (Inamdar and Inamdar, 2016).

The primary therapy for HCM is beta-blockers or calcium channel blockers to reduce heart rate and relax the heart muscles (Ommen *et al.*, 2020). Just last year, the first ever HCM medication, Mavacamten, that targets underlying mechanism to treat patients with symptomatic oHCM and New York Heart Association (NYHA) class II – III symptoms was developed and approved by the Food and Drug Administration (FDA) (Keam, 2022). Mavacamten is a selective allosteric cardiac myosin inhibitor, affecting cardiac contractility by targeting myosin ATPase to reduce the actin-myosin crossbridge formation and enhance myocardial energetics (Rohde *et al.*, 2018). Mavacamten was shown to lower the LVEF and diastolic dysfunction, inducing relaxations by inhibiting hypercontractility in the myocardium of HCM patients (Edelberg *et al.*, 2022)

If all forms of medications have failed, the chances of survival of an individual suffering from DCM and HCM without any surgical interventions is relatively low. Different studies have found that implantations of devices such as the cardioverter defibrillator (ICD) and pacemakers aids CM recovery, reduces hospitalisation, mortality and morbidity rates (Cleland et al., 2006; Tang et al., 2010). A randomised controlled trial by the Danish Study to Assess the Efficacy of ICDs in Patients with Non-ischemic Systolic Heart Failure on Mortality (DANISH) (2016) suggested that although ICDs implantations could lower the risks of patients facing SCD, they are unable to decrease the total mortality rate in the long run (Køber et al., 2016). Septal reduction therapy such as septal myectomy and alcohol septal ablation are well-established in HCM for symptomatic relief to relieve LVOT obstruction (Ommen *et al.*, 2020). Heart transplantation is the last resort of CM management, but even so, there is often lack of donors and a high risk of infection and potential tissue rejection

(Mahmaljy et al., 2020). It is therefore crucial to increase our understanding about the aetiologies of the condition to introduce more effective therapies.

1.3 Changes in Cardiac Mitochondria During Disease States

Mitochondria are double-membraned intracellular organelles that are most abundant in tissues that requires high-energy, particularly the heart and skeletal muscles. They are the main energy producers in eukaryotic cells, and hence are known as the 'powerhouses' of cells (Sabbah, 2020). Mitochondria generate more than 90% of adenosine triphosphate (ATP) that are required for cardiac function, and it compromises around 30 – 40% of cardiomyocyte volume (Cao and Zheng, 2019). Being the most metabolic active organ with limited regenerative capacity, the mammalian heart is extremely susceptible to mitochondrial damage and dysfunctions. Hence, healthy mitochondrial functions for proper regulation of electron transport chain (McFarland *et al.*) and oxidative phosphorylation (OXPHOS) are vital in mammalian bodies. They produce ATP during cardiac excitation-contraction coupling, controls 'programmed' cell death and mediates the differentiation of cardiomyocytes (Dorn, 2015). When there is an imbalance in oxygen demand and supply due to diminished ATP production and increased cardiac remodelling, the mitochondrion was described as an "engine out of fuel" (Neubauer, 2007). This could have undesirable outcomes like the acceleration of cardiac failure, modulation of calcium signalling, excess oxidative stress circulation and dysregulation in redox reactions (Karamanlidis *et al.*, 2013).

1.3.1 Alterations in Mitochondrial Structure

The mitochondrion is made up of the matrix, inner mitochondrial membrane (IMM), intermembrane space and outer mitochondrial membrane (OMM). OMM is porous, allowing molecules to freely diffuse into the intermembrane space from cytoplasm through transport proteins porins. In contrast, the impermeable IMM made up of phospholipid cardiolipin, folds inwards to form the cristae, and contains the ETC complexes and membrane protein

transporters (Glancy *et al.*, 2020). Cardiac mitochondria contain more densely-packed, lamellar cristae with higher ETC content to increase energy conversion capacity during OXPHOS due to its high energy demand, with less matrix volume (Phillips *et al.*, 2012). The tricarboxylic cycle (TCA) situates in the mitochondrial matrix, and it is also a site for DNA transcription, replication, and protein synthesis. Each copy of mitochondrial DNA (mtDNA) is packed into a spherical nucleoid by mitochondrial transcription factor A (TFAM) (Kukat *et al.*, 2015). Higher pH (7.9 – 8.0) of the matrix also creates the proton gradient that is necessary to drive ATP synthesis (Kühlbrandt, 2015). There are 3 subtypes of cardiac mitochondria: perinuclear (PM), subsarcolemmal (SSM) and intermyofibrillar (IMF) (Kalkhoran *et al.*, 2017). Under the electron microscope, IMF and SSM mitochondria of adult cardiomyocytes were around the same size whereas the PM mitochondria was smaller. Additionally, the IMF mitochondria was observed to be elongated compared to the other two subsets (Kalkhoran *et al.*, 2017).

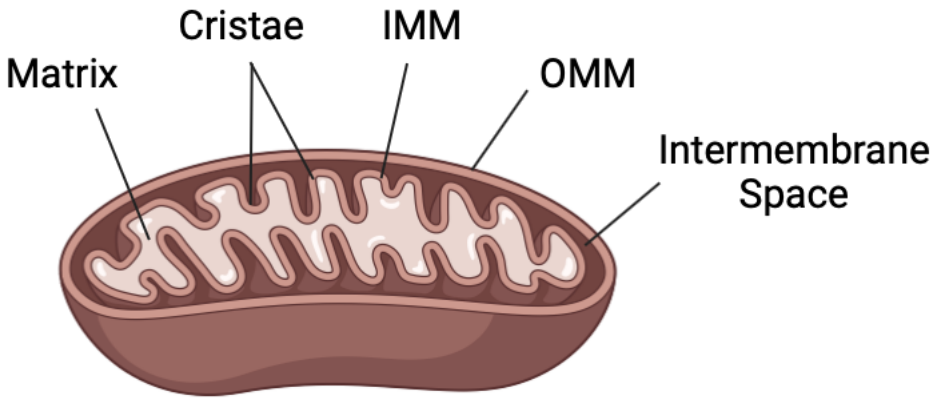

Figure 1.3 Structure of a mitochondrion.
Mitochondria contains two membranes: the inner (IMM) and outer mitochondria membranes (OMM). This is separated by the intermembrane space. The IMM forms multiple folds, known as cristae, that extends into the matrix. Created in BioRender.com.

The structure and organisation of the cardiac mitochondria are highly dependent on cardiomyocytes. Electron microscopy have revealed abnormalities in different heart diseases, including mitochondrial membrane disruptions, hyperplasia, depletion in electron-

dense matrix and organelle fragmentation (Sabbah, 2020). In cardiac hypertrophy, the mitochondria increase in size due to enlarged cardiomyocytes (Rosca and Hoppel, 2010). Wüst *et al.* (2016) found that HF individuals have compromised mitochondrial morphology and integrity, characterised by solitary larger mitochondria with more vacuoles. This is probably because of the downregulation of mitochondria inner membrane protein mitofilin, which functions to ensure cristae organisation (John *et al.*, 2005). Similar effects were observed by Sabbah *et al.* (2018) in patients with ischemic and idiopathic DCM, where there was marked reduction in the mitofilin expression. Moreover, patients with HFrEF showed more pronounced changes in their mitochondria ultrastructure as compared to HFpEF, with enhanced mitochondrial fragmentation and degradation in their vacuoles and cristae (Chaanine *et al.*, 2019).

1.3.2 Mitochondrial Bioenergetics in the Heart

Mitochondria generate ATP through 2 key processes: the TCA cycle and OXPHOS. The TCA cycle, also known as Krebs cycle, is a series of chemical reactions that generates reducing equivalents nicotinamide adenine dinucleotide (NADH) and flavin adenine dinucleotide ($FADH_2$) that are required for the ETC. The TCA cycle involves the stepwise oxidation of acetyl coenzyme A (CoA) from amino acids, fatty acid, and pyruvate to release carbon dioxide (CO_2), reducing NAD^+ to NADH and FAD to $FADH_2$ during the process. Due to its high energy demand, the heart relies primarily on fatty acid β-oxidation for acetyl CoA production, generating 50 – 70% of ATP through this pathway (Lopaschuk *et al.*, 2010). The reducing equivalents feed into the ETC as electron carriers (Martínez-Reyes and Chandel, 2020). The ETC consists of membrane-spanning proteins in the IMM: NADH dehydrogenase (Complex I), succinate dehydrogenase (Complex II), coenzyme Q (CoQ), ubiquinol cytochrome c reductase (Complex III), cytochrome C oxidase (Complex IV) and the ATP synthase. All of these complexes are encoded by both nuclear DNA (nDNA) and mtDNA, except Complex II, which is only encoded by nDNA (Bezawork-Geleta *et al.*, 2017). The

electrons are transferred from NADH and $FADH_2$ to the ETC through Complex I and II respectively. These were then passed on to Complex III via electron carrier CoQ to reduce cytochrome c. Complex IV oxidises cytochrome c and transfer the electrons to oxygen to form water. The proton gradient generated from the transport of protons from matrix into intermembrane space across the IMM is used by ATP synthase in Complex V to form ATP from phosphorylation of ADP (Ahmad, Wolberg and Kahwaji, 2018).

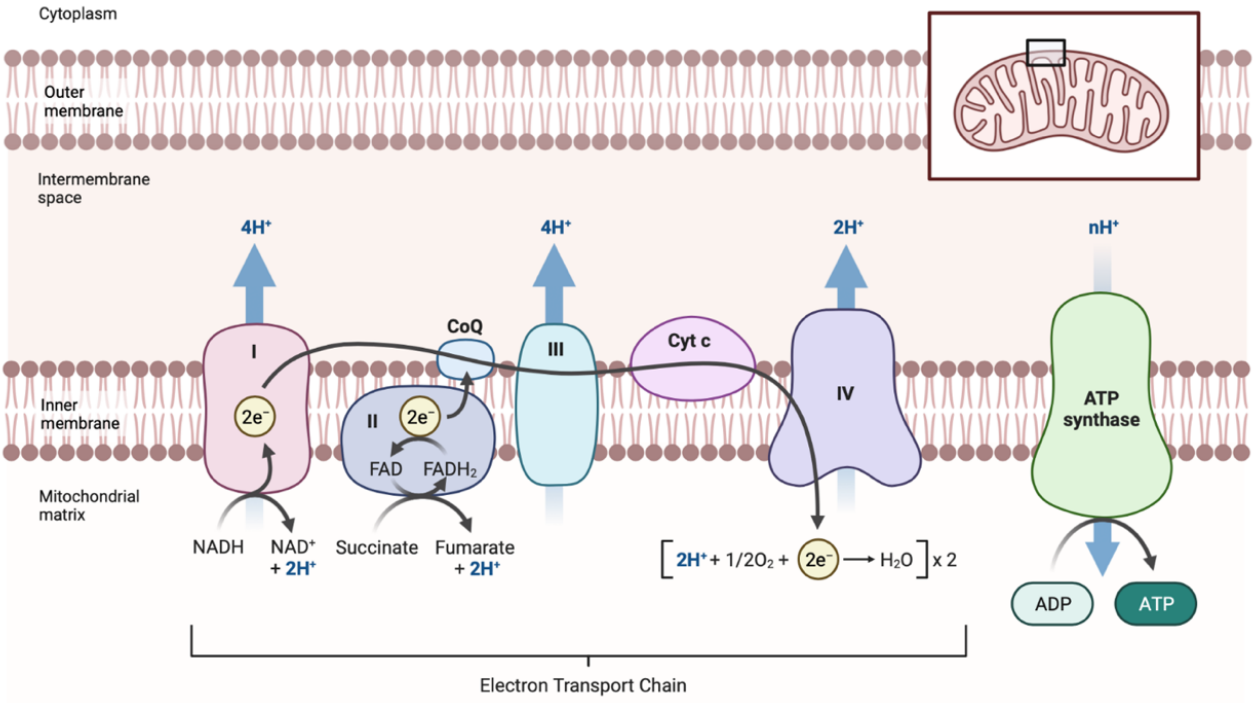

Figure 1.4 Schematic representation of the ETC in IMM.
Electrons enter the ETC through electron carriers NADH and $FADH_2$ in complex I and II respectively and are transferred to complex III via CoQ. Cyct Cyct c then carries the electrons to complex IV. As the electrons pass through complexes I, III and IV, protons (H^+) are pumped from the mitochondrial matrix into the intermembrane space, creating an electrochemical gradient across the IMM. This gradient drives ATP synthesis by ATP synthase. Created in BioRender.com.

Mitochondrial dysfunction, often reflected by defective OXPHOS and mtDNA depletion, is a common characteristic in CMs and HF due imbalance in energy supply and demand (Neubauer, 2007). Under physiological conditions, there is a fine balance between ROS generation and clearance, thereby maintaining ROS at low levels (Zorov, Juhaszova and Sollott, 2014). However, this redox homeostasis is disrupted in diseases and is associated with ETC dysfunction. Excessive production of ROS in complexes I and III damages mtDNA and inhibits the activities of ATP synthase and TCA cycle enzymes,

resulting in reduced energy production and impaired contractility (Sabbah, 2020). Peroxidation of cardiolipin in the IMM further decrease the activities of complexes, halts ATP production, and aggravates cardiomyocyte apoptosis by inducing OMM permeability and cytochrome c release into the cytosol (Dolinsky *et al.*, 2016). Furthermore, this oxidative stress is exacerbated by the loss of antioxidants such as manganese superoxide dismutase (MnSOD), further disrupting mitochondria function during disease state, increasing the prevalence of DCM and premature death (Zhang *et al.*, 2009).

Another factor that affected the mitochondrial bioenergetics and ATP production during CM is pathogenic mtDNA mutation in complex I, the largest component of the ETC (Wirth *et al.*, 2016). Complex I deficiency is commonly seen in HCM cases, often inherited as an autosomal recessive trait and accounting for one-third of OXPHOS defects (Fassone and Rahman, 2012). Under unstressed conditions, Karamanlidis *et al.* (2013) observed no changes in the ATP supply or ROS production with this deficiency in mice. However, in response to chronic cardiac stressed induced by pressure overload using transverse aortic constriction (TAC), complex I deficiency led to worsened cardiac functions, increased myocyte deaths and mitochondria permeability transition pore (mPTP) opening, and the development of CM. A failing heart also shifts towards less efficient glycolysis rather than fatty acid oxidation as an energy source, further reducing myocardial ATP production by up to 40% and affecting cardiac energy metabolism compared to a normal heart (Karwi *et al.*, 2018).

1.3.3 Mitochondrial Dynamics in the Heart

Mitochondria dynamics are essential for energy production and cellular quality control in cardiomyocytes. These dynamics processes involve mitochondrial fission, fusion, mitophagy and biogenesis. Fission refers to mitochondria division and fragmentation to form new organelles, while fusion allows the formation of mitochondrial networks and facilitates

the exchange of mtDNA between mitochondria (Westermann, 2010). The process of mitochondrial biogenesis is mediated by large guanosine triphosphatases (GTPases). Specifically, fission is controlled by cytosolic dynamin related protein 1 (Drp1) and fission 1 protein (Fis1) in the OMM, while fusion is mediated by mitofusins (Mfn1 and Mfn2) in the OMM and optic atrophy protein 1 (OPA1) in the IMM (Martínez *et al.*, 2020). OPA1 is particularly important for maintaining mitochondrial cristae tightness and energetics, as its deficiency can lead to reduced mtDNA levels and dysregulation of OXPHOS (Lee, Smith and Yoon, 2017). Membrane-anchored Mfn1 and Mfn2 are critical for maintaining normal mitochondrial morphology, respiration, and cardiac contractility. Deletion of these proteins can rapidly cause lethal CM and HF due to mitochondrial fragmentation (Chen, Liu and Dorn, 2011). Interestingly, OPA1 requires Mfn1, but not Mfn2, to induce fusion (Cipolat *et al.*, 2004). The opposite action of fission is mediated by outer membrane integrated Fis1, mitochondrial fission factor (Mff) and mitochondrial dynamic proteins, Mi49 and Mi51, which promote the assembly recruitment of Drp1 (Losón *et al.*, 2013). However, a small fraction of Drp1 localises to the constriction regions of mitochondria tubules where division occurs, suggesting that it cycles between the membrane and cytosol (Smirnova *et al.*, 2001). Drp1 would form into a helical multimeric structure to wrap around the scission site and constricts the lipid bilayer upon GTP hydrolysis, leading to fission (Mears *et al.*, 2011). Without proper division, excess fusion can cause mitochondrial swelling, increased oxidative damage and impaired ETC activities (Kageyama *et al.*, 2012).

Following fission, mitophagy serves as a process for quality control. Damaged mitochondria are selectively targeted by autophagosomes and delivered to lysosomes for degradation, to maintain a healthy population of mitochondria (Youle and Narendra, 2011). Mitophagy is mediated by PTEN-induced kinase (PINK1) and E3 ubiquitin ligase Parkin. Under normal conditions, PINK1 would be imported into the mitochondria for degradation. However, in damaged mitochondria, depolarisation triggers PINK1 accumulation and autophosphorylation on the OMM (Narendra *et al.*, 2010). Activated PINK1 then

phosphorylates ubiquitin and Parkin on Ser65 to form ubiquitin chains, recruiting more Parkin from the cytosol. Mfn2 also recruits Parkin to damaged mitochondria and acts a receptor for Parkin in a PINK1-dependent manner, suggesting the mechanistic relationship between fusion and mitophagy (Chen and Dorn, 2013). Activated Parkin further ubiquitylates mitochondrial substrates such as Mfn1, Mfn2 and voltage-dependent anion-selective channel 1 (VDAC-1) in the OMM (Geisler *et al.*, 2010). The ubiquitination of Mfn1 and 2 prevents fusion by promoting proteasomal degradation and disrupting Mfn2-mediated tethering of mitochondria-endoplasmic reticulum contacts (Gegg *et al.*, 2010; McLelland *et al.*, 2018). These ubiquitinated substrates serves as signals for autophagy receptors like p62, which directly recruit autophagic effector protein Atg8-light chain 3 (LC3) to form an autolysosome for mitochondria clearance (Pankiv *et al.*, 2007).

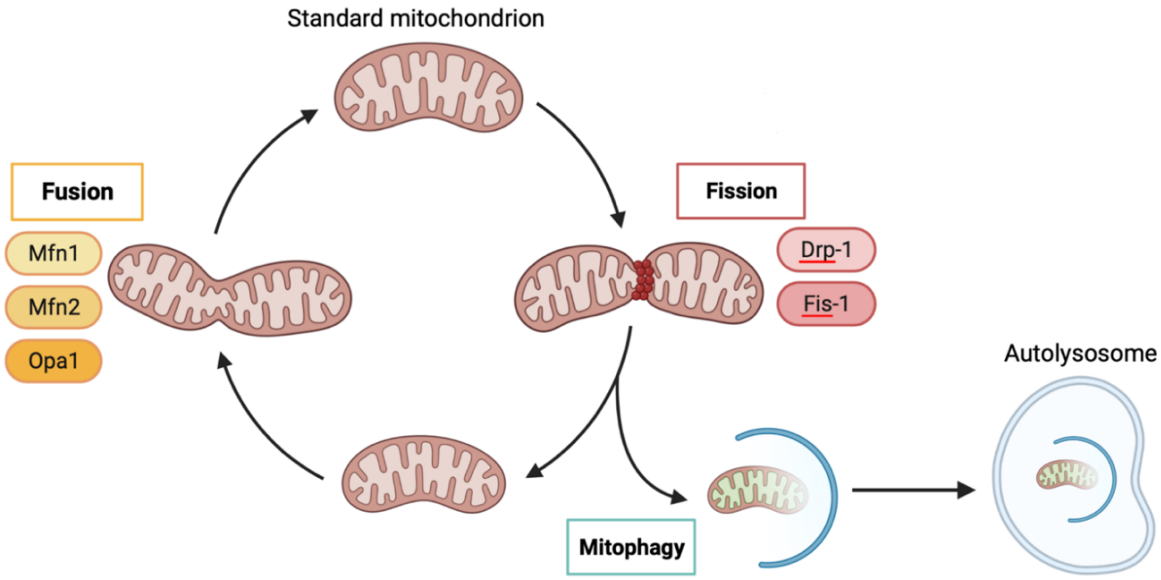

Figure 1.5 Overview of mitochondria homeostasis.
Mitochondrial dynamics involve fission, fusion and mitophagy, which play critical roles in maintaining mitochondrial health. Under damage or stress, mitochondria undergo fission, mediated by Drp1 and Fis1, to remove dysfunctional mitochondria for degradation by mitophagy. LC3-assocaited autophagosomes engulf the damaged mitochondria and fuse with lysosomes to form autolysosomes for the removal. Fusion is regulated by Mfn1, Mfn2 and Opa 1, where they merge the mitochondria, allowing the exchange of contents and mtDNA for mitochondrial biogenesis. Created in Biorender.com.

During HF, LV tissues from both humans and dogs showed significant increases in fission proteins Fis1 and Drp1, accompanied by marked reductions in the fusion proteins Mfn2 and Opa1 (Sabbah *et al.*, 2018). They also reported a downregulation in the regulator of mitochondrial biogenesis, proliferator-activated receptor gamma coactivator 1-alpha (PGC1α), indicating an overall impairment in mitochondrial dynamics. LV tissues from HF guinea pigs showed more than 50% downregulation in mRNA levels of Mfn1 and Mfn2, leading to significant decrease in their protein expressions and disruptions in mitochondrial network structure and tethering between mitochondria (Goh *et al.*, 2016). Furthermore, mitochondrial dysfunction in HCM patients was found to be associated with disorganisation of interfibrillar mitochondria, which appeared clustered or not properly aligned to myofilaments (Nollet *et al.*, 2023). Deletion of Drp1 in mice led to progressive LV dilation and DCM, with larger and more elongated mitochondria, whereas combined ablation of Mfn1/Mfn2 resulted in eccentric hypertrophy, accompanied by smaller mitochondria with abnormal cristae (Song *et al.*, 2015b). Mutations in mtDNA causing reduced biogenesis have been reported in patients with HF, contributing to over 50% of familial HCM (Limongelli *et al.*, 2010). Similarly, dysfunctional biogenesis was observed in DCM hearts due to mtDNA damage, with increased mitochondrial fragmentation and doubled cellular volume density as compared to ischemic CM hearts (Ahuja *et al.*, 2013).

Dysregulation in fission and fusion also affects mitochondrial quality control via mitophagy (Song *et al.*, 2015b). Mitochondria fission precedes mitophagy, as damaged mitochondria were segregated for removal (Twig *et al.*, 2008). In Drp-deficient hearts where fission was suppressed, Song *et al.* (2015b) suggested that there was progressive degradation of the damaged mitochondria until it reached a mitophagic threshold, where the whole organelle would be removed with no healthy daughter produced for the cellular pool. Therefore, mitochondrial depletion occurs due to the accumulation of damaged mitochondria and increased mitophagy. Conversely, ablation of Mfn2 suppressed mitophagy and led to the accumulation of defective mitochondria in cardiomyocytes (Chen and Dorn, 2013). Inhibition

of mitophagy was associated to various forms of CMs, including diabetic, obesity-associated and age-related CM (Liu *et al.*, 2022). Interestingly, deletion of Parkin could inhibit the ubiquitination and degradation of Drp1 and leads to increased fragmentation, highlighting the importance of regulating mitochondria dynamics (Wang *et al.*, 2011).

1.3.4 Age-dependent Mitochondrial Changes

At a molecular level, mitochondria play a central role in controlling the ageing process. Age is associated with increased oxidative stress and the overproduction of reactive oxygen species (ROS), which affects OXPHOS and cellular functions. Harraan (1955) first proposed that ageing in mitochondria is caused by ROS resulting from high rates of mtDNA mutations. As ROS accumulates overtime, oxidative metabolism becomes impaired, leading to significantly less energy production. Simultaneously, impaired mitochondria release excess ROS, causing further cellular and tissue damage, forming a 'vicious cycle' that exacerbates cardiomyocyte apoptosis in ageing tissues (Harman, 1972). Mice with accumulated somatic mtDNA mutations exhibited premature ageing, reduced lifespan, respiratory chain, and age-related cardiac phenotypes such as increased heart-to-body weight ratio, CM, LVH and cardiomyocytes with abnormally enlarged mitochondria dysfunction at 40 weeks (Trifunovic *et al.*, 2004). Mitochondrial respiration, determined by oxygen consumption rate of the ETC complexes, was greatly affected by the accumulation of oxidative damage, especially in Complex IV (Tatarkova *et al.*, 2011). However, a recent study using duplex sequencing, the most accurate next generation sequencing, on naturally aged mouse tissues dismissed the theory where accumulation of ROS drives mtDNA mutagenesis. Instead, it suggested that the impact of mtDNA mutation on ageing was rather tissue-specific, where different tissues experience different levels of ROS damage earlier in life but maintain a steady state throughout the ageing process (Sanchez-Contreras *et al.*, 2023).

1.4 Hydrogen Sulfide Pathway in the Heart

Hydrogen sulfide (H_2S), originally known as a hazardous and toxic gas with a strong smell of 'rotten eggs', is the third gasotransmitter that was found after nitric oxide (NO) and carbon monoxide (CO) in the human body (Wang, 2002). Epidemiological studies conducted in geothermal areas have shown a positive correlation between H_2S exposure and increased incidence of CVDs, while others suggest that H_2S actually protects against CVD, indicating its hormetic effect (Gorini *et al.*, 2020). H_2S exhibits concentration-dependent effects: at low concentrations, it stimulates oxygen consumption and ATP production, while higher concentrations (20 – 40 μM) inhibit mitochondrial cytochrome c-oxidase, suppressing these reactions (Olson and Straub, 2015).

H_2S began to gain the interest of the scientific community after being first discovered by Abe and Kimura (1996) as an important neuromodulator produced in mammalian bodies, where it promotes the long-term potentiation in the hippocampus by amplifying the activities of N-methyl-D-aspartate (NMDA) receptors that are fundamental for memory and learning. H_2S is now recognised as essential for physiological and homeostatic processes in various tissues, exerting beneficial effects such as neuromodulation, anti-inflammatory, anti-apoptosis, and antioxidative actions (Szabó, 2007). Its high permeability contributes to its biological potency, as H_2S can diffuse through membranes approximately 400,000 times faster than water molecules, independent of membrane proteins or transporters (Mathai *et al.*, 2009; Riahi and Rowley, 2014). In the heart, H_2S is present at concentrations of approximately 0.18 μM, while plasma concentrations range from 0.4 to 0.9 μM (Wintner *et al.*, 2010; Sonobe and Haouzi, 2016).

1.4.1 H_2S Production

In mammalian cells and tissues, H_2S can be produced by both enzymatic and non-enzymatic pathways. Endogenously, the non-enzymatic pathway is considered less

important. It consists of generating H_2S through glucose oxidation, reduction of elemental sulfur and glutathionine (GSH), and reduction of thiocysteine or thiosulfate (Searcy and Lee, 1998). However, Yang *et al.* (2019) suggested that the non-enzymatic production of H_2S by catalysing cysteine in the presence of iron and vitamin B_6, can be crucial in blood as it regulates of red blood cell (RBC) integrity. Cystathionine γ-lyase (CSE), cystathionine β-synthase (CBS) and 3-mercaptopyruvate sulfurtransferase (3-MST) are the three key enzymes responsible for H_2S biosynthesis (Kimura, 2014). They can be found in the vascular smooth muscles, myocardium, placenta, kidney and liver. Both CSE and CBS are cytosolic pyroxidal-5′-phosphate (PLP)-dependent enzymes with tissue-specific expression. The former is predominantly present in the kidney, liver and cardiovascular system whereas the latter is found commonly in the brain and nervous system (Kamoun, 2004; Pan *et al.*, 2012). To produce H_2S, they catalyse L-cysteine from homocysteine and cystathionine in the cytosol via the transsulfuration pathway (Figure 1.3).

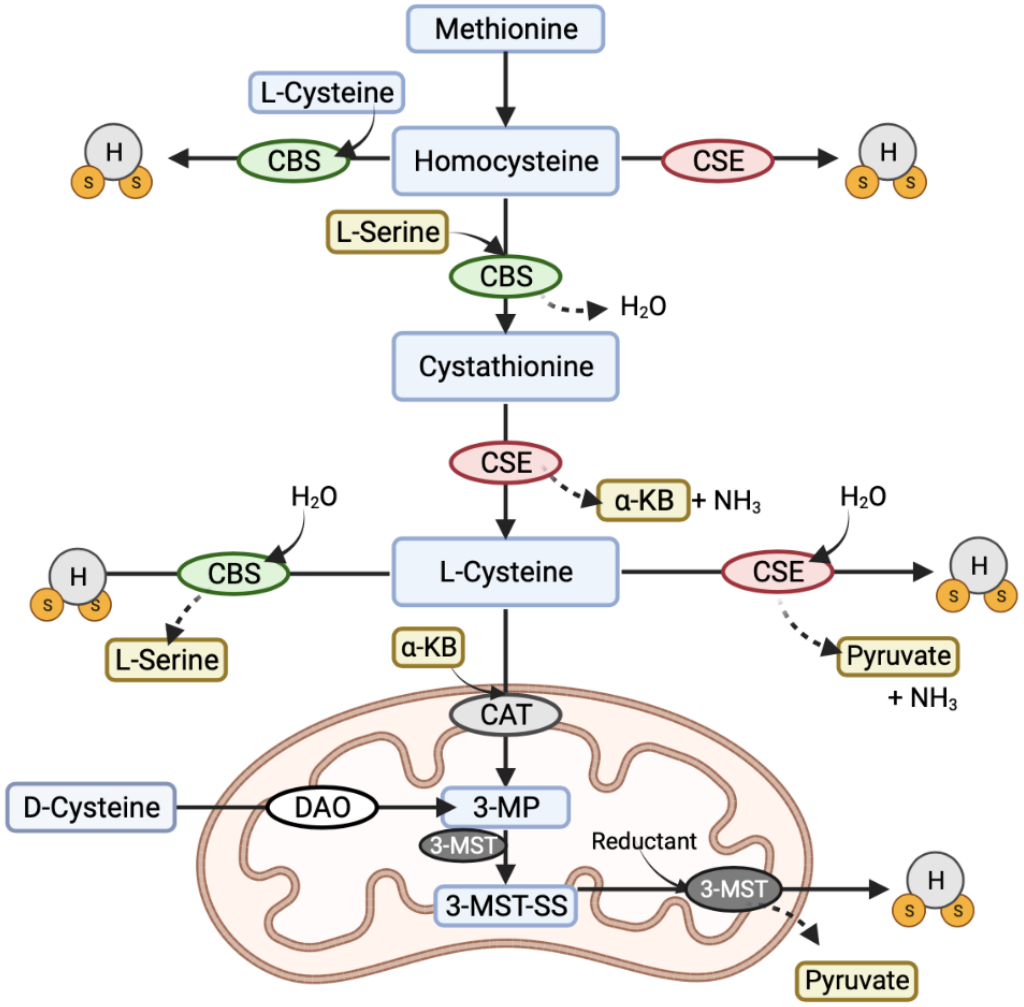

Figure 1.6 Endogenous production of H_2S via the enzymatic transsulfuration pathway. CBS catalyses homocysteine and serine to form cystathionine, a precursor for CSE to produce cysteine. In addition, CBS and CSE can use both homocysteine and cysteine to generate gaseous H_2S. During these processes, serine is produced as a by-product by CBS whereas for the CSE enzyme, α-ketobutyrate, ammonia and pyruvate are released. In the mitochondria, 3-MST and DAO uses L-cysteine and D- cysteine respectively to produce H_2S. Created in BioRender.com.

This pathway begins with the condensation of homocysteine, derived from dietary methionine, and L-serine by CBS into cystathionine. The CSE enzyme then uses this as a substrate to produce cysteine via α,γ-elimination, releasing α-ketobutyrate and ammonia as by-products. Subsequently, both CSE and CBS undergo a β-replacement reaction, where they utilise two molecules of cysteine, in combination with water, to produce H_2S (Chiku *et al.*, 2009). In addition, these enzymes can catalyse homocysteine into H_2S in the presence of cysteine as well (Sbodio, Snyder and Paul, 2019). Under normal physiological

circumstances, H_2S generation using β-replacement of cysteine is preferred by CSE, and it accounts for about 70% of the H_2S created by this enzyme. However, an additional step for production can also occur when there are high levels of homocysteine (i.e., hyperhomocysteinemia) (Chiku *et al.*, 2009). It undergoes γ-replacement of two moles of homocysteine to yield homolanthionine, a novel sulfur metabolite that is first found in the urine of patients with homocystinuria (Perry, Hansen and MacDougall, 1966). This therefore suggests that the production route of H_2S by the CSE enzyme is dependent on the homocysteine concentrations and can be more versatile as compared to CBS. Although CSE is a cytosolic enzyme, it can translocate into the mitochondria in response to increased intracellular calcium levels and under stress conditions like hypoxia to sustain H_2S and ATP production by using mitochondria metabolised cysteine, which is three times the amount of cytosolic cysteine (Fu *et al.*, 2012). The third enzyme, 3-MST, is both a cytosolic and mitochondrial zinc-dependent enzyme. Cysteine aminotransferase (CAT) catalyses cysteine and α-ketobutyrate as its primary substrates to form 3-mercaptopyruvate (3-MP) (Kohl, Mellis and Schwarz, 2019). In the presence of reductants like thioredoxin (Trx) and dihydrolipoic acid (DHLA), 3MST produces H_2S from the persulfide provided by 3-MP, releasing pyruvate as a by-product (Mikami *et al.*, 2011). Recently, a novel D-cysteine-dependent pathway has also been discovered in producing H_2S from 3-MST and D-amino acid oxidase (DAO), specifically in the kidney and cerebellum (Shibuya *et al.*, 2013).

1.4.2 H_2S Breakdown

The catabolism of H_2S is crucial for maintaining steady levels of endogenous H_2S under physiological conditions, complementing its biogenesis. The catabolism and oxidation of H_2S occurs in the mitochondrial matrix and are determined by oxygen levels (Fu *et al.*, 2012). As described by Hildebrandt and Grieshaber (2008), the first step to mitochondrial sulfide oxidation is catalysed by sulfide-quinone oxidoreductase (SQR), which oxidises two H_2S molecules to sulfane sulfur. Simultaneously, cysteine disulfide of the SQR enzyme is

reduced to form persulfide groups (-SH). Two electrons are released in this reaction, where they feed into complex III and IV of the ETC via CoQ to produce ATP. One persulfide group is oxidised by ethylmalonic encephalopathy 1 (ETHE1) to form sulfite (SO_3^{2-}) in the presence of water and oxygen. The other persulfide group is utilised by thiosulfate sulfurtransferase (TST) to convert SO_3^{2-} to thiosulfate ($S_2O_3^{2-}$). SO_3^{2-} can also be further oxidised by sulfite oxidase (SO) in the intermembrance space into sulfate (SO_4^{2-}), which both this and $S_2O_3^{2-}$ will be excreted in urine (Hildebrandt and Grieshaber, 2008). This process is tightly regulated to prevent high levels of H_2S, which can be toxic and inhibit mitochondrial respiration. Inhibiting SQR through siRNA silencing in a murine Hepa1c1c7 hepatoma cell line resulted in impaired breakdown of H_2S, leading to reduced basal bioenergetics and respiration, as well as affecting 3-MST/3-MP pathway in stimulating mitochondrial respiration (Módis *et al.*, 2013). ETHE1 deficiency was also found to disrupt redox homeostasis by downregulating the antioxidant GSH, Krebs cycle intermediates and redox cofactors NAD^+ and NADH in cultivated patients fibroblasts (Sahebekhtiari *et al.*, 2016).

H_2S metabolism also involves methylation and reaction with metalloproteins, occurring in the cytoplasm. Thiol S-methylransferase (TMT) metabolises H_2S to methanethiol, which is then converted to dimethylsulfide. Thiolether S-methylransferase (TEMT) further convert dimethylsulfide to trimethylsulfonium for urinary excretion (Furne *et al.*, 2001). Another catabolic pathway involves scavenging of methemoglobin to form oxidised GSH or sulfhemoglobin. Understanding of the H_2S-hemoglobin interaction is crucial for the removal of toxic H_2S in heart and blood, as mitochondria is not present in the RBCs. Interestingly, Vitvitsky *et al.* (2015) established that the mechanism of homeostasis in the circulatory system is that H_2S produced by 3-MST in RBCs is cleared in the form of thiosulfate and polysulfides by methemoglobin-catalysed oxidation, suggesting the involvement of additional hemeproteins in sulfide homeostasis in other tissues.

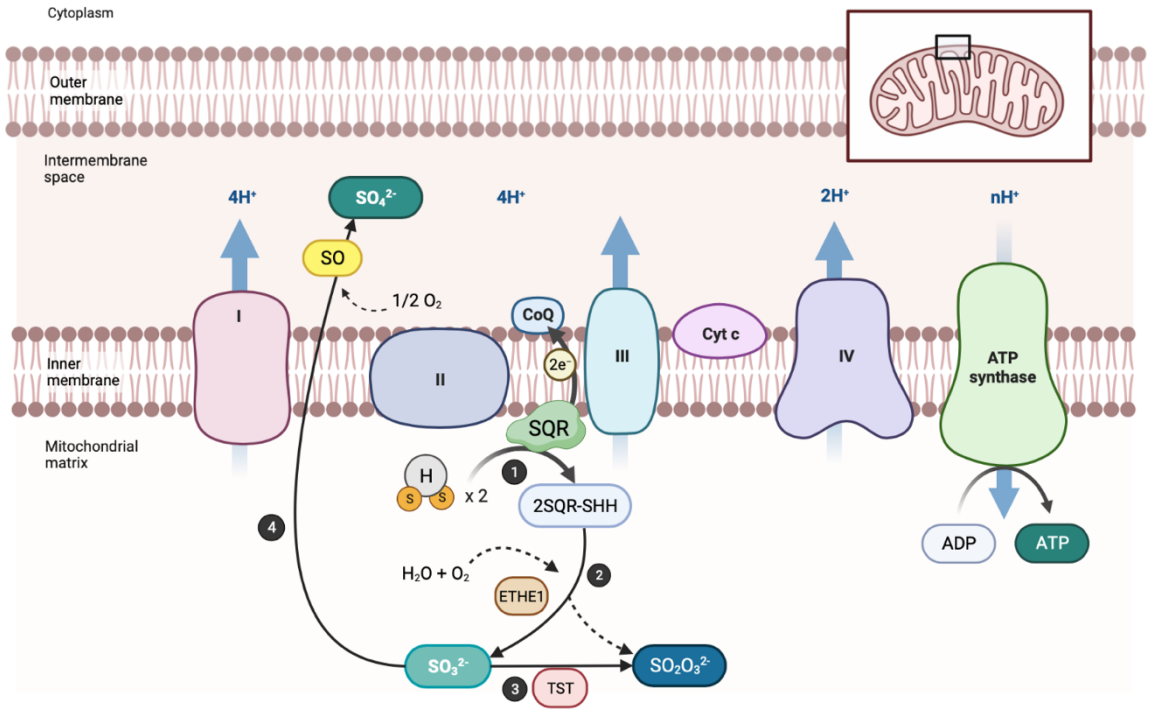

Figure 1.7 Catabolism of H_2S in IMM of the mitochondria.
(1) SQR oxidises 2 molecules of H_2S to sulfane sulfur and persulfide. (2) In the presence of water and oxygen, ETHE1 converts one persulfide group into sulfite (SO_3^{2-}). (3) TST uses the other persulfide group to oxidise SO_3^{2-} to thiosulfate ($S_2O_3^{2-}$), for urinay excretion. (4) SO, in the mitochondrial intermembrane space, converts $S_2O_3^{2-}$ to sulfate in an oxygen-dependent reaction, to be excreted in urine. *Created in BioRender.com.*

1.4.3 CSE/H_2S pathway in CVDs

Cardiac dysfunction and LV remodelling in CM typically involves oxidative stress, inflammation, myocardial fibrosis, cardiomyocyte apoptosis and mitochondria dysfunction as biological responses (Maack *et al.*, 2003). The CSE/H_2S pathway, which is mediated by CSE as the main H_2S-producing enzyme in the cardiovascular system, has shown an increasing importance in maintaining cardiovascular health. Dysregulation of this pathway, through genetic deletion or pharmacological inhibition of CSE, can lead to aggravation of myocardial damage and has been implicated in the pathophysiology of CVDs, such as atherosclerosis and myocardial infarction (MI), which eventually leads to chronic HF (Yang *et al.*, 2008; Zhang *et al.*, 2012a).

H_2S exerts cardioprotective effects through various pathways, including protein post-translational modification, interaction with NO, activation of molecular signalling cascades, and redox-dependent reactions, resulting in diverse physiological processes such as vasodilation, anti-inflammation, anti-apoptosis, angiogenesis, and anti-oxidation (Kolluru *et al.*, 2023). One significant mechanism is sulfhydration, a post translational modification of reactive cysteine residues of protein to either enhance or diminish their activity by converting their -SH group to a hydropersulfide group (-SHH) (Mustafa *et al.*, 2009). For example, H_2S facilitates vasorelaxation through sulfhydration of Kir6.1 subunit of the ATP-sensitive potassium (K_{ATP}) channels (Mustafa *et al.*, 2011). Furthermore, H_2S can also directly regulate NO metabolism or interact with its metabolites to influence vascular functions (Kolluru, Shen and Kevil, 2013). The NO-H_2S crosstalk serves as an important molecular switch in controlling vascular tone as NO also modulates H_2S levels by upregulating both CSE activity and expression in VSMCs (Zhao *et al.*, 2001). The cardioprotective effects of H_2S were more pronounced in smaller resistance vessels, such as mesenteric arteries (Mustafa *et al.*, 2011).

1.4.3.1 CSE/H_2S pathway in Atherosclerosis

Many CVDs, especially atherosclerosis, are associated with an inflammatory response triggered by endothelial dysfunction (ED), infections or lipoprotein accumulation in the sub endothelium (Henein *et al.*, 2022). The recruitment and accumulation of inflammatory cells, along with increased ROS, contributes to atherosclerotic plaque formation at lesion sites, leading to disturbed blood flow and development of vascular disease (Davies *et al.*, 2013). Notably, cellular adhesion molecules such as ICAM-1, responsible for adhesion of inflammatory cells to the endothelium, have been proposed to be a marker of inflammation in this disease (Tzoulaki *et al.*, 2005). Apolipoprotein-E deficient ($ApoE^{-/-}$) mice is a common model for studying human atherosclerosis (Lo Sasso *et al.*, 2016). Using this model in conjunction with carotid artery ligation, Bibli *et al.* (2019) reported that despite the increase in CSE protein, endogenous H_2S production decreased due to

serine phosphorylation and inactivation of CSE. Mice lacking CSE exhibited greater plaque size, a smaller carotid lumen, and elevated levels of circulating L-cystathionine, a biomarker for ED. They further confirmed this in human subjects, suggesting that CSE inhibition was linked to accelerated progression of atherosclerosis and inflammation (Bibli *et al.*, 2019).

The relationship of H_2S and inflammation has been controversial. H_2S exerts anti-inflammatory effects at low physiological concentrations by inhibiting NF-kB activation, but it can become pro-inflammatory at higher concentrations (Whiteman *et al.*, 2010). The anti-inflammatory effect was also found to be dependent on the rate of production, where fast-releasing NaHS causes inflammation whereas slow-releasing GYY4137 has the opposite reaction (Whiteman *et al.*, 2010). Li *et al.* (2005) reported increased CSE mRNA and H_2S after either LPS or NaHS injection, causing inflammation and tissue damage as indicated by the increased myeloperoxidase activity, which was then improved by CSE inhibitor DL-propargylglycine (PAG). The author later demonstrated that slow and sustained release of H_2S via GYY4137, which reflects endogenous production, inhibited the formation of pro-inflammatory mediators and cytokines through the inhibition of NF-kB signalling (Li *et al.*, 2009). GYY4137 was also found to increase the anti-inflammatory cytokine interleukin-10 (IL-10) in isolated macrophages (Whiteman *et al.*, 2010).

In addition to supressing pro-inflammatory mediators, H_2S demonstrated the ability to inhibit leukocyte adhesion and oedema formation. Wang *et al.* (2009) reported upregulation in mRNA and protein levels of ICAM-1 in ApoE$^{-/-}$ mice, which was attenuated by H_2S administration, indicating the anti-atherosclerotic effects. H_2S also suppressed ICAM-1 expression in tumour necrosis factor-α (TNF-α)-induced human umbilical vein endothelial cells (HUVECs) through the NF-kB signalling pathway (Wang *et al.*, 2009). Zanardo *et al.* (2006) observed that H_2S donors modulate acute inflammatory responses by suppressing leukocyte infiltration and adherence on vascular endothelium by activating K_{ATP} channels on both leukocyte and endothelium. Inhibition of H_2S synthesis resulted in significant increase in

endothelial permeability and ICAM-1 expression and a reduction in rolling velocity of leukocytes, resulting in oedema (Zanardo *et al.*, 2006; Guan *et al.*, 2013).

1.4.3.2 Protective Mechanisms in Myocardial Infarction

MI, also known as heart attack, is a common manifestation of coronary artery disease that causes sudden cardiomyocyte deaths due prolonged ischaemia (Thygesen *et al.*, 2007). This condition occurs after flow restriction and thrombosis caused by a ruptured atherosclerotic plaque in the coronary artery. Overtime, MI leads to myocardial fibrosis and LV remodelling, ultimately reducing pumping efficiency and causing chronic HF. Furthermore, myocardial ischaemia disrupts metabolic responses and cause mitochondria dysfunction, excessive ROS production and Ca^{2+} overload (Chen *et al.*, 2020). Although reperfusion alleviates ischaemia, it can exacerbate oxidative stress and inflammatory responses (Dhalla *et al.*, 2000).

Jiang *et al.* (2005) found that plasma H_2S levels, which correlate with disease severity, were significantly reduced in patients with acute MI and coronary heart disease. King *et al.* (2014) reported the exacerbated response to myocardial ischaemia and reperfusion (I/R) injury and increased oxidative stress in CSE KO mice. which were accompanied by reduced activity of endothelial nitric oxide synthase (eNOS) and NO production. In a rat model induced with myocardial ischaemia, H_2S showed beneficial effects as mortality rates, infarct sizes, and cardiac post loads were significantly reduced when treated with sodium hydrosulfide (NaHS), compared to the group treated with PAG, a CSE inhibitor (Zhu *et al.*, 2007). H_2S has been shown to reduce MI size by approximately 70%, mitigated inflammation and preserve LV functions and structure in an *in vivo* mouse model of MI/R injury (Elrod *et al.*, 2007). This was also shown in an ex vivo model of isolated rat hearts, where H_2S dose-dependently decreased their infarct size (Johansen, Ytrehus and Baxter, 2006). Interestingly, the cardioprotective effects of H_2S is biphasic and concentration

dependent, where the therapeutic, infarct-reducing response is only effective at low doses (NaHS 0.1–1 μM or Na_2S ≤50 μg/kg body weight) and has no effect at higher doses (NaHS 10 μM or Na_2S ≥100 μg/kg) (Johansen, Ytrehus and Baxter, 2006; Elrod *et al.*, 2007).

The cardioprotective effects of H_2S in MI/R injury mainly include anti-inflammation, anti-apoptosis, anti-oxidation and preservation of mitochondria functions. Apoptosis is a tightly regulated mode of cell death that maintains cellular homeostasis by eliminating unwanted cells (Movassagh and Foo, 2008). Imbalances in this physiological process led to increased oxidative stress, LV dysfunction and myocardial damage. CSE knockdown in human hepatocellular cancer cell line were less proliferative and showed 60 – 70% decrease in cell viability (Yin *et al.*, 2012). Yang *et al.* (2013) later demonstrated that isolated CSE KO mice embryonic fibroblasts showed accelerated cardiomyocyte senescence and increased oxidative stress due to increased p53 and p21 expression, proteins involved in tumour suppression and cellular growth arrest. H_2S protected against cardiomyocyte apoptosis under oxidative stress via sirtuin-1 (SIRT-1) activation by increasing PGC-1α and eNOS for ROS scavenging and ATP generation in the mitochondria (Wu *et al.*, 2015).

ROS is typically generated within the mitochondria through molecular oxygen reduction, resulting in hydrogen peroxide (H_2O_2) and superoxide. Increased ROS production under stressful conditions such as ageing and CVDs can lead to gradual functional decline in the heart, reduced stress tolerance and premature cellular senescence (Rizvi *et al.*, 2021). H_2S has been demonstrated to be crucial in redox homeostasis and could act as a direct ROS scavenger (Corsello, Komaravelli and Casola, 2018). It reduces oxidative stress and ROS by upregulating antioxidant response element (ARE) gene expression for production of antioxidants such as Trx, GSH or heme oxygenase-1 (HO-1) through the nuclear factor erythroid 2-related factor 2 (Nrf2) signalling pathway (Calvert *et al.*, 2009). In an ischaemic-induced HF mouse model, Trx-1 protein and mRNA levels were upregulated, resulting in attenuation of cardiac remodelling (Nicholson *et al.*, 2013). In addition, by inducing protective

microRNA 21 (miR-21) expression through the formation of an anti-apoptotic cycle that propagates itself to supress inflammasome, H_2S successfully ameliorated ischaemic injury in mice (Toldo *et al.*, 2014).

1.4.3.3 CSE/H_2S pathway in Heart Failure

HF manifests as a consequence of LV remodelling and various cardiac conditions including MI and CM, resulting in reduced CO. Cardiac hypertrophy is a compensatory mechanism that develops following MI, or in response to chronic pressure- or volume-overload and cell deaths (Ponikowski *et al.*, 2016). However, the transition to HF occurs when vascularisation of the heart fails to keep up with the rate of pathological myocyte growth (Izumiya *et al.*, 2006). In rodent models of HF, pressure-overload is induced using TAC, whereas volume-overload is established by aortic regurgitation (AR) (You *et al.*, 2018). Often, ED develops, a recognised hallmark of HF due to compromised angiogenesis. Polhemus *et al.* (2014) found a substantial reduction in circulating H_2S levels in HF patients with end-stage CM. A similar depletion was observed in pressure-overload rodent model following TAC, and CSE-deficient mice showed more severe cardiac dysfunction and LV dilation (Kondo *et al.*, 2013). However, LV remodelling and dysfunction were alleviated after H_2S treatment via the upregulation of angiogenesis (Polhemus *et al.*, 2014). H_2S also preserved cardiac functions in volume overload-induced chronic HF by increasing mRNA and protein levels of HO-1 (Zhang *et al.*, 2013).

Angiogenesis, the formation of new blood vessels from existing vasculature, is essential for wound healing, tissue repair and the growth and development of organs. Proper vessel maintenance relies on a balance between pro-angiogenic factors (e.g. vascular endothelial growth factor (VEGF)) and anti-angiogenic factors (e.g. endostatin) that regulate endothelial cell proliferation, migration, vessel formation and ECM remodelling (Carmeliet, 2003). H_2S plays a significant role in mediating VEGF-induced angiogenesis. Its

administration in a HF mouse model increased VEGF expression, leading to improved vascular density, reduced fibrosis, and attenuated LV dysfunction, dilation and hypertrophy (Polhemus *et al.*, 2013). In addition, H_2S can inhibit the formation of anti-angiogenic factors, preserving LV functions and enhancing cardiac angiogenesis (Qipshidze *et al.*, 2012). Papapetropoulos *et al.* (2009) studied the pro-angiogenic effects of H_2S *in vitro*, *in vivo* and *ex vivo*. As a direct effect, H_2S doubled the proliferation and migration of HUVECs through the K_{ATP}/ MAPK pathway. *In vivo*, topical administrations of H_2S promoted wound healing, whereas H_2S suppression in CSE KO mice delayed wound healing (Papapetropoulos *et al.*, 2009). The authors also demonstrated H_2S regulating VEGF-induced angiogenesis as there was significantly less microvessel formation in CSE KO mice in response to VEGF (Papapetropoulos *et al.*, 2009).

Furthermore, calcium (Ca^{2+}) homeostasis is crucial in maintaining cardiac functions. Impaired contractility is also a common defect that arise during HF, hence reducing CO. One of the most important contributor is the reduction of Ca^{2+} release from the sarcoplasmic reticulum (SR), leading to decreased generation of contractile force (Kubalova *et al.*, 2005). Ca^{2+} signalling in cardiomyocytes is dependent on intracellular Ca^{2+} concentration that is regulated by voltage gated Ca^{2+} channels and H_2S was shown to be an important regulator of intracellular Ca^{2+} levels (Yong *et al.*, 2010). H_2S could exert a negative inotropic effect by reducing Ca^{2+} influx through blocking L-type Ca^{2+} channels in cardiomyocytes in spontaneously hypertensive rats and reduce myocardial contractility to reduce cardiac workload (Zhang *et al.*, 2012b; Sun *et al.*, 2008).

1.5 Therapeutic Applications of H_2S

1.5.1 Protective Mechanisms of CSE/H_2S pathway in Mitochondria

Due to its ability to diffuse freely across cellular and intracellular membranes without prior activation or processing, H_2S can easily affect cells and their organelles, namely the

mitochondria (Szabo *et al.*, 2014). H_2S acts as an energy substrate and is crucial in regulating ATP production in mitochondria, especially under hypoxic conditions (Fu *et al.*, 2012). This was also observed in hibernation when there is supressed oxygen consumption and metabolism, where the total sulfide concentration remained unchanged. Instead, under metabolic depression, H_2S was found generate high levels of GSH antioxidant and was regenerated by recycling its oxidation products, polysulfides and thiosulfate in the mitochondria (Revsbech *et al.*, 2014). It was first established by Goubern *et al.* (2007) that H_2S serves as an alternative energetic substrate and electron donor that contributes to the ETC through CoQ. By the H_2S oxidation pathway, the electrons are transferred from SQR complex to CoQ, and then to oxygen via Complex III, cytochrome c and Complex IV to form water (Goubern *et al.*, 2007). However, H_2S exerts both beneficial and adverse effects on mitochondria: at low concentrations (0.1-1μM), it increased activities of the ETC whereas the cellular bioenergetics was hindered at higher concentrations by inhibiting cytochrome *c* oxidase in Complex IV (3-30μM) (Módis *et al.*, 2013). Under physiological concentrations, H_2S was able to enhance mitochondrial bioenergetics and activities through sulfhydration of ATP synthase (Módis *et al.*, 2016). However, Hildebrandt (2011) presented that the effects of sulfide toxicity was observed at 50 μM NaHS as there was a complete respiratory inhibition and 75% reduction in respiration at 10 μM NaHS.

H_2S is crucial in preserving mitochondrial functions. Following H_2S administration in a myocardial infarction murine model, cardiac mitochondrial respiration improved, with less mitochondria swelling and well-organised matrix density, leading to reduced infarct size (Elrod *et al.*, 2007). Not only does H_2S plays a role in energy expenditure of the mitochondria, it is also an important regulator of mitochondria biogenesis and cardiac mitochondrial content. Using CSE KO mice, Shimizu *et al.* (2018) depicted the direct relationship between H_2S and mitochondrial content, where these mice had depressed mtDNA levels and citrate synthase activity. They also reported diminished levels of H_2S and

mitochondrial content in end-stage HF patients. These were rescued when SG-1002 H_2S releasing drug was administered to induce mitochondrial biogenesis via the AMP-activated protein kinase (AMPK)/PGC-1α signalling pathway (Shimizu *et al.*, 2018).

Meng at al. (2017) has proved that H_2S improved Ang II-induced cardiac hypertrophy by specifically targeting H_2S donors NaHS and GYY4137 on the Sirtuin 3 (SIRT3) molecule in mitochondria. In addition, H_2S can also upregulate antioxidants to inhibit ROS production, decrease oxidative stress and promotes fission (Siasos et al., 2018). SIRT3 can directly be influenced by the PGC-1α pathway, as its expression levels were depressed in PGC-1α KO transgenic mice and elevated ROS were detected. Conversely, the basal ROS level was rescued in mice that overexpress PGC-1α and production of antioxidative enzymes like the superoxide dismutase 2 (SOD2) and gluthathione peroxidase-1 (GPX1) was stimulated (Kong et al., 2010). Zhu et al. (2019) showed cardiac structural and functional deterioration, influx of inflammatory proteins and increased cardiac stress in mice when there was loss of molecule, and subsequently recovered these reactions by overexpressing it. Another method how H_2S controls the PGC-1α levels and subsequently mitochondrial biogenesis is via the phosphorylation of AMPK. This was discovered by Shizumu et al. (2018) to have improved respiration and bioenergetics in the mitochondria, alongside with better cardiac functions in a myocardial ischemia mouse model.

1.5.2 Current H_2S Donors for CVDs

Although H_2S has shown to exert protective effects on multiple organs with its ability to diffuse freely across cellular membranes, more research must be done for clinical translation. Currently, rapid-releasing NaHS and slow-releasing GYY4137 are the most common exogenous H_2S donors used to improve cardiac functions in preclinical studies (Li, Polhemus and Lefer, 2018). When NaHS dissolves in aqueous solution, H_2S will be generated instantaneously and has a short-half life. Therefore, it may not be the ideal

therapeutic for chronic CVDs as the rapid release and decline in circulating H_2S levels do not reflect the constant, steady-state of H_2S production endogenously (Szabo and Papapetropoulos, 2017). Li *et al.* (2008) then developed GYY4137 as one of the first sustained, slow-releasing H_2S donor, where both acute and chronic GYY4137 administration was able to exert anti-hypertensive effects without having signs of toxicity. Ellmers *et al.* (2020) recently demonstrated the preservation of cardiac functions long term and post-infarct remodelling using GYY4137 treatment following myocardial infarction in CSE WT and KO mice.

In addition, a mitochondria-targeted donor, AP39, was introduced in 2014 (Szczesny *et al.*, 2014). 100 nM of AP39 resulted in significant mitochondrial stimulation, as it increased mitochondria respiration, improved mitochondrial DNA integrity and reduced intracellular oxidative stress in vitro (Szczesny *et al.*, 2014). Interestingly, AP39 supplementation in preservation solution protected heart graft functions and maintained tissue viability from prolonged ischemic injury in an in vivo murine heart transplant model, suggesting that AP39 could be useful in human heart transplantations as well (Zhu *et al.*, 2019). Finally, SG1002 is the only synthetic H_2S prodrug that has completed phase I clinical trial in both healthy and chronic HF patients (Polhemus *et al.*, 2015). SG1002 has previously shown to attenuate LV remodelling and preserved cardiac functions in a pressure-overload HF mouse model (Kondo *et al.*, 2013). The results of this clinical trial were promising as they determined the safety of SG1002 in humans through oral administration and managed to elevate circulating H_2S and NO bioavailability. However, a larger phase II clinical trial would be needed to determine the drug's efficacy to improve cardiac functions (Polhemus *et al.*, 2015).

1.6 Research Rationale

Despite the improvements in CVD management, the prevalence and mortality rates in CM remains high as its underlying mechanisms are not fully understood. Considering the

cardioprotective effects of H_2S and its regulatory role in numerous physiological processes, H_2S releasing compounds hold promise as potential therapeutics. Building upon previous research, we hypothesised that the CSE/H_2S pathway is fundamentally necessary to support normal cardiac function under physiological conditions during physiological ageing. Conversely, deletion of the CSE enzyme impairs this protective mechanism, leading to myocardial dysfunction and CM. To test this hypothesis, we used a previously generated CSE knockout ($CSE^{-/-}$) mouse model to determine if the loss of CSE compromises cardiac adaptation and function under physiological conditions over a 16-month period, stimulating the ageing transition in human. As most existing murine studies on CM or HF were performed in male adolescent mice at 2 months, this is a longitudinal study that observe the changes across 16 months, as HF usually occurs in elderly individuals. Changes in the heart as the mice mature and age were taken into consideration in this study.

1.7 Hypothesis

I. CSE/H_2S pathway is essential in maintaining normal cardiac functions under physiological conditions. Loss of CSE enzyme leads to age-dependent LV dysfunction and CM.

II. Loss of CSE leads mitochondrial dysfunction and changes in gene expression profile in cardiomyocytes.

1.8 Aims

I. To explore the role of CSE on myocardial function and structure longitudinally using a transgenic $CSE^{-/-}$ mouse model.

II. To investigate the underlying molecular mechanisms of loss of CSE-induced cardiac dysfunction.

III. To determine the gene expression profile in hearts lacking CSE enzyme.

2 Materials and Methods

2.1 Animal Experimentation

2.1.1 Transgenic Model

2- to 18 months old CSE wild-type ($CSE^{+/+}$) and transgenic CSE knockout ($CSE^{-/-}$) male mice (n=30) were utilized in this study. The $CSE^{-/-}$ mice was kindly provided by Yang *et al.* (2008), where they also published a protocol for generating them. The positive cell clones were microinjected into C57BL/6j mice blastocysts and planted in a surrogate mother. Chimera was chosen for mating and generating F1. The heterozygous genotypes ($CSE^{+/-}$) were then used to produce F2. The resulting experimental mice were generated by C57BL/6j × 129SvEV. The mice were previously genotyped with ear clips in our lab using a three-primer assay as described by Yang *et al.* (2008) to determine successful transgenic generation. Bands were identified at 400 base pairs for $CSE^{+/+}$ mice using qPCR whereas there were no bands present for $CSE^{-/-}$ mice.

Mice were housed in a controlled environment with 12 hours of light/dark cycle. Animal experimentation in this study was approved and regulated by the UK Government Home Office in accordance with the United Kingdom Animals (Scientific Procedures) Act, 1986, with the use of procedures approved by Aston University institutional guidelines and regulations for ethical animal use and care.

2.1.2 Animal Preparation

Mice were anesthetised with isoflurane at a concentration of 3.0% during induction and a concentration of 2.5% for maintenance under 100% oxygen. The chest was shaved using Veet depilatory cream, after being placed in a supine position with limbs taped to electrodes with conductance gel on a platform. Before imaging, a thick layer of prewarmed ultrasound gel was applied to the scan area. The body temperature of each mouse was maintained at approximately 37.0°C using a heating lamp, and its average heart rate above

450 ± 50 beats/min (BPM). Eye gel was applied to keep the eyes lubricated and pedal reflex test was carried out to ensure adequate unconsciousness throughout the procedure.

2.2 Ultrasound Imaging

Cardiac ultrasound was performed using the Vevo 3100 Imaging System (FUJIFILM VisualSonics, Toronto, Canada), with a MS550D (40MHz) transducer, according to the manufacturer's imaging guide and an echocardiography position paper (Zacchigna et al., 2020).

2.2.1 Parasternal Long Axis and Left Mid-Papillary Short Axis of the Heart

After securing the mouse on the heated platform, the stage was slightly tilted to the left and the transducer was placed parallel to the mouse's sternum, the notch pointing toward its head. The probe was turned approximately 35° anti-clockwise, until the LV was in the centre of the view, the aorta aligned with the LV and the apex clearly seen. Following this position, the probe was rotated 90° clockwise (until the papillary muscles were seen) to image the view of the short axis. Both normal B-mode and electrocardiogram-gated kilohertz visualisation (EKV) images were recorded.

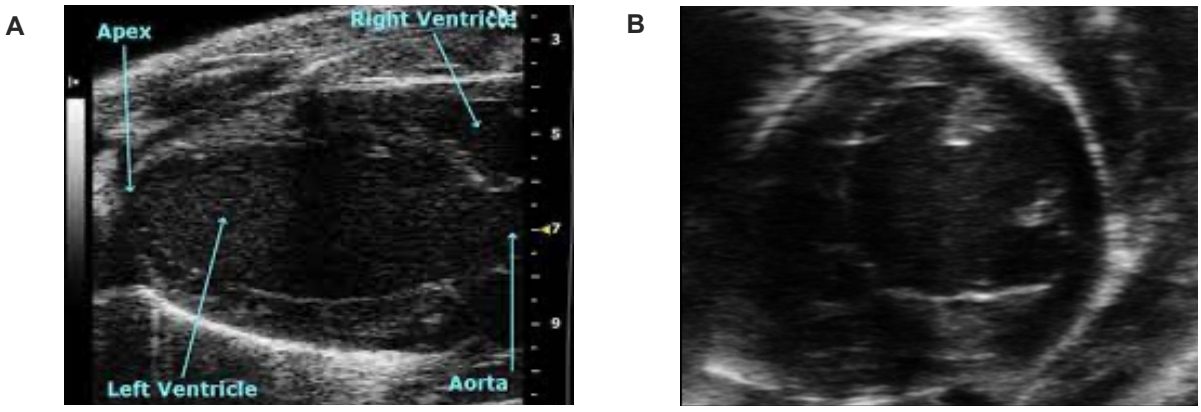

Figure 2.1 Echocardiography analysis.
(A) Parasternal long axis (PSLAX) view of the heart in diastole. **(B)** Short axis view of the heart after rotating the probe 90° clockwise.

2.2.2 M-mode Imaging

The m-mode images were selected and taken following the correct positions of the heart mentioned previously. This provided an indication of changes in the size and wall thickness, as well as the systolic function. The LV mass was also calculated from the m-mode analysis (Table 1).

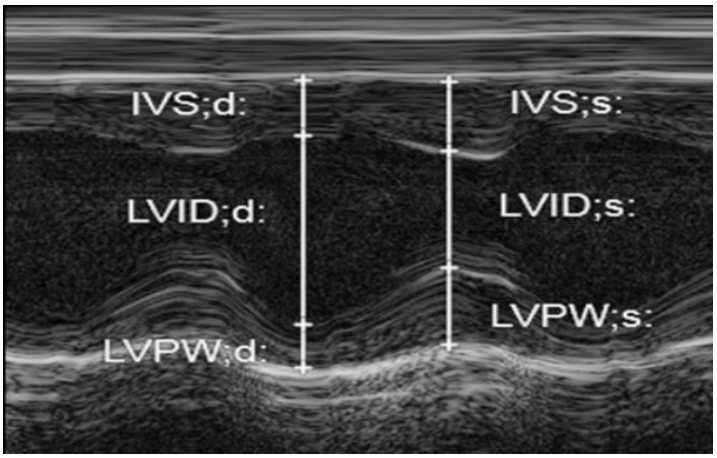

Figure 2.2 M-mode echocardiography analysis.
Cross-sectional view of the left ventricular wall with wall thickness calculations. IVS: Inter ventricular septum, IVID: Left ventricle internal diameter, LVPW: left ventricle posterior wall, d: diastole, s: systole.

2.2.3 Mitral Inflow

Mitral flow was assessed for the diastolic functions. The stage was moved into a Trendelenburg position (with the upper left corner of the platform tilted all the way down). The transducer was positioned to follow the plane of the chest, in the same orientation as it was for the short axis view. Colour Doppler was used to detect the mitral valve blood flow, by placing the measurement gate in the direction of flow (approximately ±10°). This was imaged and the E (early filling velocity) and A (late filling velocity) peaks, isovolumetric contraction time (IVCT), isovolumetric relaxation time (IVRT), aortic ejection time (AET) and deceleration time (DT) were analysed using the Vevolab software.

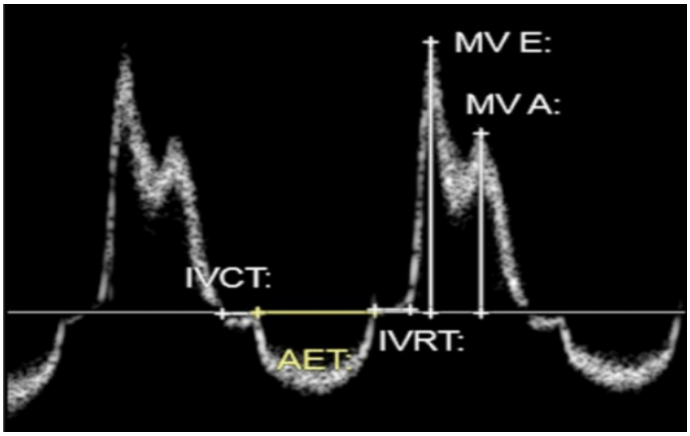

Figure 2.3 Analysis of diastolic functions.
Mitral inflow calculations using colour Doppler waveform. IVCT; isovolumetric contraction time, IVRT; isovolumetric relaxation time, AET; aortic ejection time.

Cardiac Output (CO)	$\boldsymbol{CO\ (ml/min) = \frac{SV\ \times\ HR}{1000}}$
Ejection Fraction (EF)	$\boldsymbol{EF\ (\%) =\ 100\ \times \frac{SV}{EDV}}$
LV Mass/Body Weight (LVMI)	$\boldsymbol{LVMI\ (mg/g) = 0.8\ [1.053(IVS;d + IVID;d + LVPW;d)^3 - (IVID;d)^3}$
Myocardial Performance Index (MPI)	$\boldsymbol{MPI = \frac{(IVCT + IVRT)}{AET}}$

Equation 2.1 Formulas used by Vevolabs® software to calculate the heart parameters.

2.2.4 Tissue collection

Following the cardiac puncture, the mice were euthanised via cervical dislocation and their hearts were harvested and snap frozen for further analysis.

2.3 Mitochondria Respirometry Assay

2.3.1 Cardiac Mitochondria Isolation

To investigate the function of the electron transport chain in murine hearts, the oxygen consumption rate was measured directly using the Seahorse assay. Cardiac

mitochondria of mice were freshly isolated using a method adapted from Sakamuri et al. (2018) and optimised by Sanchez-Aranguren et al. (2020). Freshly harvested mouse hearts were placed in mitochondrial isolation medium (MIM) (5 ml, pH 7.4; 1 mM EGTA, 5 mM HEPES, 210 mM mannitol, 70 mM sucrose) with 0.5% (w/v) bovine serum albumin (BSA) on ice. To ensure that the tissues were clean, they were further rinsed in MIM with BSA to remove any remaining blood. A tweezer and scalpel were used to remove the fat surrounding the tissue. The left ventricle was isolated and chopped into smaller pieces in a Petri dish on ice, transferred to a Precellys tube with beads, and homogenised in VelociRuptor V2 Microtube Homogeniser (Scientific Laboratories Supplies, U.K.) (10 s, speed 7, 2 cycles). The homogenate was transferred to a 15 ml polycarbonate tube and centrifuged at 500 × g, 4 °C for 5 min. The supernatant was carefully removed using a 1 ml syringe and a 26-gauge × 3/8-inch needle and transferred to a new 15 ml falcon tube, which was then continuously drawn and expelled for about 7 to 10 times for further mechanical disruption. This mitochondrial suspension was centrifuged at 600 × g, 4 °C for 5 min to wash. This supernatant was removed and transferred to 1.5 ml Eppendorf tubes and centrifuged at 10,000 × g, 4°C for 10 min. The supernatant was discarded, the final pellet containing mitochondria was resuspended with 200 ml of MIM and kept on ice, which was to be used within 4 h. The purity of the mitochondrial isolation was confirmed by western blot prior to the experiments.

2.3.2 Mitochondrial Protein Quantification

The concentration of mitochondrial proteins was determined using the Bio-Rad DC protein assay (Bio-Rad, Watford, U.K.) according to the manufacturer's instructions. 20 μl of Reagent S and 1 ml of Reagent A were mixed in an Eppendorf tube and added to a non-binding 96-well plate, with 25 μl per well. A series of standards (0 – 2 mg/ml) were made from diluting MIM and added in duplicate (5 μl per well), followed by 5 μl of protein per well. 200 μl of Reagent B was pipetted into each well to cause colour development that

corresponds to the protein concentration. The plate was incubated in the dark for 10 min and read with a Tecan Spark plate reader (Mannedorf, Switzerland), where the absorbance was measured at 690nm. A standard curve was plotted with the values obtained, in which the equation of the best-fit line was used to calculate the unknown protein concentration.

2.3.3 Mitochondrial Respiration Assay (Seahorse XFe24)

The respirometry assay was carried out using a method adapted from Boutagy et al. (2015) and Sanchez-Aranguren et al. (2020), with an XF24 Extracellular Flux Analyser (Seahorse Bioscience, Billerica, MA). 800 ml of Seahorse XF calibrant solution was added to each well of the sensor cartridges (Seahorse Bioscience, Agilent, UK) and hydrated at 37°C overnight.

Mitochondria assay solution (MAS) (10 mM KH_2PO_4, 5 mM $MgCl_2$, 1 mM EGTA, 2 mM HEPES, 210 mM mannitol, 70 mM sucrose, 0.2% (w/v) fatt-acid free BSA; pH 7.4) with either: i) 10 mM pyruvate/2 mM malate or, ii) 10 mM succinate/2 mM rotenone was made. The isolated mitochondria (10 mg/50 ml per well) were seeded in a V7 Seahorse XF24 microplate in the respective substrate solutions to investigate the activities of Complexes I and II. MAS with only substrate were loaded to A1, B4, C3 and D6 blank wells. For mitochondrial attachment, the microplate was centrifuged at 2000 × g, 4°C for 10 min. 450 ml of prewarmed (37°C) MAS-containing substrate were added to each respective well. After incubating at 37°C for 10 min, it was placed in the XF24 Analyser to measure the respiration rate, where the oxygen concentration (pmol O_2) was plotted against time (min).

The first injection would be 1 mM of ADP in the substrate to begin measuring mitochondrial respiration. This was to determine state 3 (ADP-dependent) respiration, where coupled active respiration was at the maximum. It was then followed by the injection of 2 mM oligomycin A, which is an ATP synthase inhibitor, to measure non-ATP dependent respiration

from protein leak (state 4_o respiration). 4 mM carbonyl cyanide-4-phenylhydrazone (FCCP) was injected to represent uncoupled respiration at the maximum level (state 3u respiration) and lastly, 4 mM antimycin A for inhibition of OXPHOS. By taking the state 3/state 4_o respiration ratio, the respiratory control ratio (RCR) could be calculated, which reflects the efficiency of ETC in the mitochondria during ATP synthesis.

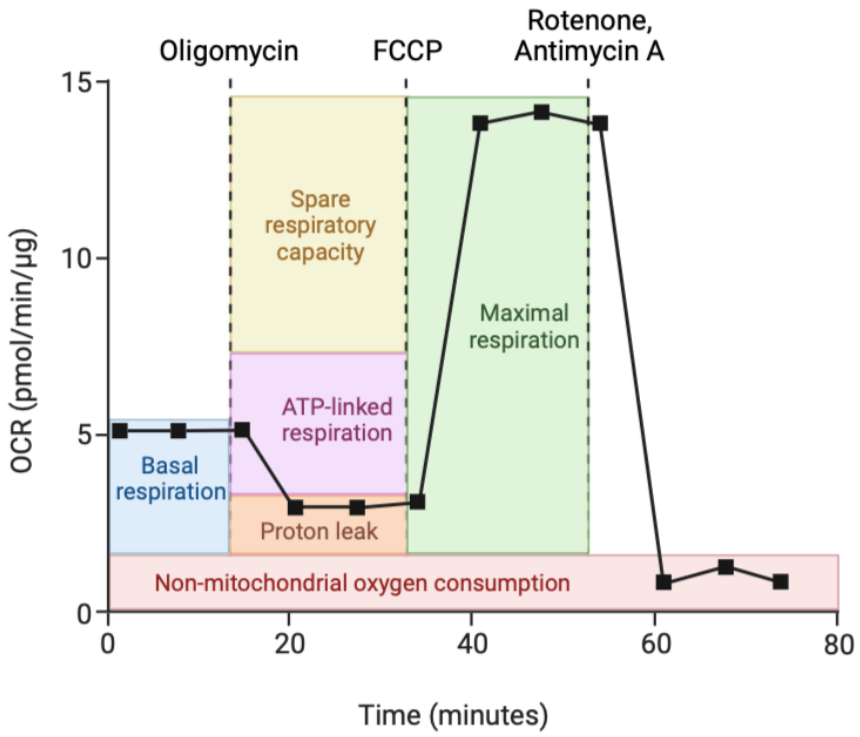

Figure 2.4 Representative graph of seahorse analysis using XF24 analyser.
Parameters such as basal respiration, ATP-dependent respiration and non-mitochondrial oxygen consumption were measured after injections with different complexes modulators compounds such as oligomycin, FCCP and rotenone/antimycin A. Adapted from Mito Stress Kit Datasheet.

2.4 Protein Analysis

2.4.1 Protein Isolation

Frozen heart tissues were lysed in 150 µl of RIPA buffer with 1% (v/v) protease and phosphatase inhibitor cocktail (Sigma) to prevent protein degradation and preserve its quality. This was transferred into a tube containing silica beads and centrifuged at 10000 × g, 4 °C for 10 min. The supernatant was collected and stored at -80 °C for future protein assay and western blots.

2.4.2 Protein Quantification

The protein concentration was measured with the Bio-Rad DC protein assay (Bio-Rad, Watford, U.K.) according to the manufacturer's instructions (as noted in Section 2.3.2.).

2.4.3 Western Blotting

25 μg of protein lysates was mixed with 900 μL of Laemmli protein sample buffer and 100 μl of 2-mercaptoethanol (1:10) and heated at 95 °C for 5 min. Samples were separated using gel electrophoresis (100V for 2h) on 10% SDS-PAGE gel. The gels were then transferred to nitrocellulose membrane using a semi-dry transfer system for 30 min at 25 V. The membrane was washed in TBS (Sigma) for 5 min and incubated with 5% (w/v) non-fat milk in TBS-T (0.5% (v/v) Tween 20) for 1 h to ensure all non-specific binding of antibodies is blocked. The membrane was washed again in TBS-T and incubated overnight at 4 °C with relevant primary antibodies at recommended concentrations. Membranes were washed three times in TBS-T and incubated with 1:20000 of either IR Dye 800CW Donkey anti-rabbit or Goat anti-mouse IgG secondary antibody accordingly (Li-cor, Lincoln, USA) for 1 h at room temperature. The membrane was imaged using Li-cor Odyssey, Image Studio 5.2 program.

2.5 Gene expression

2.5.1 RNA Isolation

The miRNeasy Mini Kit (Qiagen) was used to isolate total RNA from the cardiac samples. Snap frozen tissues (<30 mg) were mechanically homogenised using VelociRuptor V2 Microtube Homogeniser in Precellys tubes containing ceramic beads, in 700 μl of QIAzol Lysis Reagent. The homogenate was incubated at room temperature for 5 min. For the RNA to separate, each sample was added with 140 μl of chloroform and vigorously shaken for 15

s. The homogenate was then incubated for 2 min at room temperature and centrifuged at 12,000 × g for 15 min at 4 °C.

The upper aqueous (clear) phase (approx. 350 μl) was transferred into a new Eppendorf tube and 1.5 volumes (usually 525 μl) of 100% (v/v) ethanol was added. The solution was mixed by gentle pipetting and was added to the column provided. These columns were centrifuged at 8000 × g for 15 s at room temperature and the flow-through was discarded. 350 μl of RWT stringent wash buffer was pipetted into the RNeasy Mini column, centrifuged at the same setting to wash, and the flow-through was discarded. For a thorough removal of DNA, DNA digestion was carried out using the RNase-Free DNase Set (Qiagen). 10 μl of DNase 1 stock solution and 10 μl of Buffer RDD was added to each sample, directly onto the membrane, and incubated in the heating block for 15 min at 30 °C. 350 μl of Buffer RWT was added and centrifuged at 8000 × g for 15 s, where the runoff was discarded. This was repeated with 700 μl of Buffer RWT, followed by 500 μl of a milder RPE wash buffer. 500 μl of Buffer RPE was added again, and the spin columns were centrifuged for 2 min at 8000 × g to remove any remaining salts. The resultant runoff was discarded, the spin columns were placed in a new 2 ml collection tube and centrifuged at full speed for 1 min to further dry the membrane.

The spin columns were added to new 1.5 ml Eppendorf tubes following membrane drying to collect the resultant RNA. 40 μl of RNase free water was added to the columns to elute the RNA and centrifuged at 10,000 RPM for 1 min. This step was repeated by adding 20 μl of RNase free water to produce a higher concentration of RNA. The resulting RNA concentration (ng/ml) was measured using Nanodrop 1000 for cDNA reverse transcription. The purity of RNA was determined by the 260/280 absorbance ratio, which should be around 2.0 – 2.2. If the ratio was below this, the sample should be discarded due to contamination.

2.5.2 cDNA Synthesis

RNA lysate was used as a template for reverse transcription to cDNA using a commercially available miScript® II RT kit (Qiagen). Template RNA, 10x Nucleics Mix and 5x miScript HiFlex Buffer were thawed on ice and centrifuged briefly. The miScript Reverse Transcriptase Mix was removed from -20 °C freezer just before use and returned immediately after preparing the master mix. The reverse transcription master mix was prepared according to Table 2 on ice. The calculated volumes of RNA and RNase-free water were added to each tube to make up a total volume of 20 μl for each sample. The resultant mixture was mixed by centrifugation and placed on ice for 5 min for primers to anneal to the RNA templates. The microtubes were placed in the thermal cycler, incubated for 60 min at 37 °C and then 5 min at 95°C for the inactivation of miScript Reverse Transcriptase Mix. Another 30 μl of RNase-free water was added to the final cDNA and either used directly for real-time PCR (qPCR) or stored at -80 °C for future use.

2.5.3 DNA Isolation and Purification

DNA extraction and purification were carried out to analyse mouse mtDNA copy number. The QIAamp® DNA Mini Kit was used according to the manufacturer's instructions (Qiagen, Hilden, Germany). Frozen cardiac tissues (≤ 25 mg) were placed in a microcentrifuge tube with silica beads and homogenised in 180 μl of ATL lysis buffer using VelociRuptor V2 Microtube Homogeniser (10s, speed 7, 2 cycles). 20 μl of Proteinase K, which aids protein digestion and remove contaminations, was added to the homogenate. This was mixed by vortexing and incubated at 56 °C overnight until tissues were completely lysed (mixture turns clear). The clear medium is transferred into a new tube and centrifuged before adding 200 μL of AL lysis buffer, which is vortexed for 15 s for thorough mixing. The medium is subsequently incubated at 70 °C for 10 min, briefly centrifuged to ensure all droplets are removed from the lid. 200 μl of 100% (v/v) ethanol was added, mixed by

vortexing for another 15 s and briefly centrifuged again to remove droplets. This mixture was added to the spin columns (in a 2 ml collection tube) carefully and centrifuged at 6000 × g for 1 min. Resultant flow-through was discarded and the spin columns were placed in new collection tubes. 500 μl of wash buffer AW1 was added to the spin column and centrifuged at the same settings. The spin columns were placed in clean collection tubes and the runoff was discarded. 500 μl of wash buffer AW2 was added in the spin columns, centrifuged at 20000 × g for 3 min and transferred to new collection tubes. This was centrifuged at full speed for 1 min. Spin columns were put in new 1.5 ml microcentrifuge tubes. 100 μl of Elution buffer AE, which acts as a binding agent, was added. The columns were incubated at room temperature for 1 min and then centrifuged at 6000 × g for 1 min. This step was repeated with 80μl of buffer AE and incubated for 5 min to increase DNA yield. The resulting DNA concentration (ng/ml) was measured with Nanodrop 1000. An ideal A260/280 purity ratio of 1.7 – 1.9 was typical for DNA.

2.5.4 Quantitative Polymerase Chain Reaction (qPCR)

Lyophilised forward and reverse primers were reconstituted to 100 μM as primer stock and a working stock was made with 1:1 forward and reverse primers. For each gene of interest, the master mixes include 5 μL LightCycler® SYBR Green I Master (Roche), 0.2 μL primer working stock and 3.8 μL RNase free water. 9 μL of master mix and 1 μL of sample DNA were added to each well of the 386 well plate. Each sample was loaded in duplicate. The plate was sealed and centrifuged at 2400 rpm at 4 °C for 1 min. Roche LightCycler® 480 platform was used with the following qPCR conditions: preamplification at 95 °C for one cycle, amplification at 95 °C for 45 cycles.

Table 2.1 qPCR Primers for mRNA expression analysis.

Primer	Sequence
Mouse *ND1* Forward	5'- CTA GCA GAA ACA AAC CGG GC -3'
Mouse *ND1* Reverse	5'- CCG GCT GCG TAT TCT ACG TT -3'
Mouse *HK2* Forward	5'- GCC AGC CTC TCC TGA TTT TAG TGT -3'
Mouse *HK2* Reverse	5'- GGG AAC ACA AAA GAC CTC TTC TGG -3'
Mouse *Serca2A* Forward	5'- CTC CAT CTG CTT GTC CAT -3'
Mouse *Serca2A* Reverse	5'- GCG GTT ACT CCA GTA TTG -3'
Mouse *Serca3A* Forward	5'- GGG GTG GTG CTT CAG ATG TCT CTG C -3'
Mouse *Serca3A* Reverse	5'- CCT TTT TTT CAT CCA TGT GAT TCC -3'
Mouse *AT1* Forward	5'- TGT TCC TGC TGC TCA CGT GTC TC -3'
Mouse *AT1* Reverse	5'- CAT CAG CCA GAT GAT GAT GC -3'
Mouse *Mfn1* Forward	5'- GCA GAC AGC ACA TGG AGA GA -3'
Mouse *Mfn1* Reverse	5'- GAT CCG ATT CCG AGC TTC CG -3'
Mouse *Mfn2* Forward	5'- GGA GAC CAA C AA GGA CTG GA -3'
Mouse *Mfn2* Reverse	5'- TGC ACA GTG ACT TTC AAC CG -3'
Mouse *PINK1* Forward	5'- CAC ACT GTT CCT CGT TAT GAA GA-3'
Mouse *PINK1* Reverse	5'- CTT GAG ATC CCG ATG GGC AAT-3'
Mouse *Park2* Forward	5'- TCT TCC AGT GTA ACC ACC GTC -3'
Mouse *Park2* Reverse	5'- GGC AGG GAG TAG CCA AGT T -3'

2.5.5 Relative Expression Analysis

The cycle number (Ct) taken to generate the fluorescence signal above background by the LightCycler® 480 II Software was calculated and averaged for the duplicates of each sample. Relative expression of the gene of interest was calculated using the ΔΔCt method, relative to the housekeeping gene, and was expressed as fold change $2^{-\Delta\Delta Ct}$, shown in the equation below.

i. $\Delta Ct = Ct\ (\text{gene of interest}) - Ct\ (\text{housekeeping gene})$

ii. $\Delta\Delta Ct = \Delta Ct\ (\text{experimental sample}) - \Delta Ct\ (\text{control sample})$

iii. $\text{Relative expression} = 2^{-\Delta\Delta Ct}$

Equation 2.2 qPCR analysis to calculate relative expression of gene of interest.
(i) ΔCt is calculated to determine the difference between the target gene and reference gene within each sample. (ii) ΔΔCt is calculated to determine the change between experimental

and average of the control samples. (iii) Relative expression calculation between experimental and control samples.

2.6 Immunohistochemistry

Cardiac tissues were snap frozen in OCT compound in dry ice before being stored in -80 °C. Transverse cross-sections of the heart were cut using a Leica cryostat at a thickness of 12 μm and mounted on positively charged) SuperFrost® Plus slides (Fisher Scientific, Loughborough, U.K.). The slides were left to dry for an hour at room temperature before being wrapped in aluminium foil and stored at -80 °C for future use.

2.6.1 Immunofluorescence Staining of Frozen Sections

The slides were dried at room temperature and placed in -20 °C ice cold acetone for 10 min to fix the tissues. They were then washed in PBS (1X) for 5 min at room temperature to remove the OCT. The cut sections were circled with a wax pen to reduce the staining area. Slides were placed in a humidity chamber and washed again in PBS for 5 min, before blocking in 10% (v/v) Normal Goat Serum (in PBS) for 1 h at room temperature. To analyse the capillary density, Isolectin GS-B4, Biotin-XX conjugate, diluted 1:300 (in PBS) was used as the primary antibody and incubated overnight at 4 °C. The slides were washed in PBS for 5 min, three times. Secondary antibodies, Streptavidin Alexa Fluor 488 (Life Technologies S32354) (1:200 in PBS) and Rhodamine labelled Wheat Germ Agglutinin (WGA-Rho; Vector Labs RI-1022) (1:200 in PBS), were added and incubated at room temperature for 2 h in the dark. Slides were washed thrice again in PBS before being mounted using Vectashield with Dapi (Vector Lab H-1500). Coverslip was applied carefully to ensure that there were no air bubbles, sealed with clear nail varnish and allowed to dry at room temperature for 2 h.

2.6.2 Analysis of Capillary Density and Cardiomyocytes

Short axis views of the stained cardiac tissues were imaged using Nikon inverted microscope with a 40x objective lens. The images captured were with DAPI (nucleus), mCherry (cardiomyocyte boundaries) and GFPHQ (capillaries). The capillary density and number of cardiomyocytes per field of view were quantified and analysed with ImageJ.

2.7 RNA Sequencing

Tissue from apex of the heart was rapidly dissected, snapped frozen in dry ice and stored in -80 °C until further processing. Total RNA from apical cardiac tissues were extracted and sequenced by Novogene Co. (Cambridge, UK) as a commercial service project. The detailed protocol was previously described by Gao *et al.* (2021). The specifications for mRNA sequencing include total RNA ≥ 200 ng, purity of A260/280 between 1.8 – 2.0 and A260/230 ≥ 1.8. RNA quality determined by the RNA integrity number of ≥ 4.0 with a smooth base line was measured using Agilent 2100 Bioanalyser system. RNA library preparation was constructed by mRNA enrichment with poly (A) capture and cDNA reverse transcription. Following a library quality check, high throughput sequencing was performed on NovaSeq 6000 Illumina PE150 to generate 150 base-pair paired-end reads. As the raw sequenced reads of fastq format could be of low quality, or contained reads with adapters or ploy-N, they were first processed through in-house perl scripts to remove contamination. All downstream analyses were based on clean, high-quality data.

Reference genome and gene model annotation files were downloaded directly from the genome website for reads mapping. The reference genome was indexed using Hisat2 v2.0.5 and paired-end clean reads were matched to the reference genome using Hisat2 v2.0.5. FeatureCounts v1.5.0-p3 was used to quantify the reads associated with each gene. Gene expression levels were estimated using the expected number of Fragments per Kilobase of transcript sequence of per Millions base pairs sequences (FKPM), which was

derived from the reads count and gene length. Differential expression gene (DEG) analysis was performed with the DESeq2 R package (1.20.0); p-values were adjusted using the Benjamini & Hochberg false discovery rate method. Genes with adjusted p-value <0.05 and log2(foldchange) ≥ -0.6 and ≤ 0.6 were considered differentially expressed. Gene Ontology (GO) analysis of DEG was conducted by clusterProfiler R package and GO terms with adjusted p-value <0.05 were considered significantly enriched DEG. Pathway analysis was performed based on the Kyoto Encyclopaedia of Genes and Genomes (KEGG) database, where pathways with adjusted p-value <0.05 and 3 or more DEGs were considered significantly different. Relevant DEGs were selected for validation using qPCR.

Table 2.2 Primer sequences for qPCR validation of RNA seq data.

Primer	Sequence
Mouse *Gm5900* Forward	5'- CAA CAG ACC AAG GCA GCA AAC
Mouse *Gm5900* Reverse	5'- CAC CAG AGG CAA ACG ATT GA -3'
Mouse *Gbp2b* Forward	5'- ACC TGG AGA CTT CAC TGG CT -3'
Mouse *Gbp2b* Reverse	5'- TTT ATT CAG CTG GTC CTC CTG TAT CC -3'
Mouse *mtND3* Forward	5'- TAG TTG CAT TCT GAC TCC CCC A -3'
Mouse *mtND3* Reverse	5'- GAG AAT GGT AGA CGT GCA GAG C -3'
Mouse *Nppa* Forward	5'- TCC CTC GTC TTG GCC TTT TG -3'
Mouse *Nppa* Reverse	5'- CCT CAT CTT CTA CCG GCA TC -3'
Mouse *Rpl29* Forward	5'- CAA GTC CAA GAA CCA CAC CAC -3'
Mouse *Rpl29* Reverse	5'- GCA AAG CGC ATG TTC CTC AG -3'
Mouse *Osbpl3* Forward	5'- TCT GCG TCC TGC AGA AGT CC -3'
Mouse *Osbpl3* Reverse	5'- GGT GGA GCT GAG AGT ATG AAG TCC -3'
Mouse *IL-6* Forward	5'- TGA ACA ACG ATG ATG CAC TTG -3'
Mouse *IL-6* Reverse	5'- CTG AAG GAC TCT GGC TTT GTC -3'
Mouse *Itgb3* Forward	5'- GCT CAT TGG CCT TGC TAC TC -3'
Mouse *Itgb3* Reverse	5'- CCC GGT AGG TGA TAT TGG TG -3'
Mouse *Myh6* Forward	5'- CAA TGC AGA GTC GGT GAA GG -3'
Mouse *Myh6* Reverse	5'- CCT CTG TCT GGT AGG TGA GC -3'
Mouse *Myh7* Forward	5'- CTC AAG CTG CTC AGC AAT CTA TTT -3'
Mouse *Myh7* Reverse	5'- GGA GCG CAA GTT TGT CAT AAG T -3'

2.8 Statistical Analysis

All data presented as mean ± S.E.M. Statistical significance difference ($P<0.05$) was calculated using double factor variance analysis (two-way ANOVA), followed by *post-hoc* Sidak method to compare the differences in genetic background and age using GraphPad Prism 10 software. One comparison between two groups was performed with Mann-Whitney U-test nonparametric data. For the RNA sequencing, genes were considered significantly up- or downregulated when adjusted p-value <0.05 and $|\log_2 \text{fold change}| > 1$. All results were statistically significant at p-values of $^*p<0.05$, $^{**}p<0.01$, $^{***}p<0.001$ and $^{****}p<0.0001$.

3 Loss of CSE Affects Cardiac Functions in an Age-dependent Manner

3.1 Introduction

Cardiomyopathies (CMs) encompass a heterogenous group of myocardial diseases that affects the structure and function of the heart, with heart failure (HF) and cardiomegaly being their most prominent features (Ciarambino *et al.*, 2021). They can arise in the absence of a secondary condition like hypertension or coronary heart disease (Maron *et al.*, 2006). According to the Heart Disease and Stroke Statistics (2022), there is a considerable number of CM diagnoses both in- and outpatient populations, with 18000 cases as the principal diagnosis and 1101000 cases among all diagnoses for inpatient hospitalisations. The Global Burden of Disease estimated that in 2020, around 371000 deaths were attributed to CM, with age-dependent increase in prevalence and mortality rates and affecting men more than women (Roth *et al.*, 2020). Among the younger population, sudden cardiac deaths (SCDs) and HF caused by CM were commonly observed (Bagnall *et al.*, 2016). However, the precise underlying mechanisms that contribute to cardiac maladaptation in CM remain unclear. CMs are classified into four subtypes: dilated cardiomyopathy (DCM), hypertrophic cardiomyopathy (HCM), restrictive cardiomyopathy (RCM) and arrhythmogenic cardiomyopathy (ARVC). They are significant contributors to HF due to higher intracardiac pressures and reduced cardiac output (CO) (Ponikowski *et al.*, 2016). In addition, CMs are often under-recognised as they are typically asymptomatic. Therefore, it is crucial to identify changes in cardiac structures and LV functions in the early stages to prevent subsequent complications and administer appropriate treatments.

Previous research has demonstrated that CSE, responsible for H_2S production in the heart, exerts cardioprotective effects and plays a vital role in maintaining cardiovascular homeostasis. Loss of CSE causes marked reductions in H_2S production, which can exacerbate the symptoms of various CVDs such as atherosclerosis, myocardial infarction and hypertension (Yang *et al.*, 2008; Wang *et al.*, 2009; Elrod *et al.*, 2007). Wang *et al.* (2009) first showed the protective effects of the CSE/H_2S pathway in an apolipoprotein-E

knockout (apoE$^{-/-}$) mouse model, where administration of NaHS as a H_2S donor significantly reduced the size of atherosclerotic plaque and intracellular adhesion molecule-1 (ICAM-1). In a later study using the same mouse model, H_2S was found to inhibit the expressions of chemokines and chemokine receptors on stimulated macrophages, hence preventing the progression of atherosclerosis by mediating the inflammatory response and reducing macrophages accumulation in lesion sites of blood vessels (Zhang *et al.*, 2012a). In a rat model of doxorubicin-induced DCM, H_2S improved LV function and structure, inhibited cardiomyocyte apoptosis, and decreased oxidative stress (Yu *et al.*, 2017). H_2S has also been shown to attenuate cardiac fibrosis in diabetic CM by regulating redox homeostasis and inhibiting cardiac fibroblasts activation (Zheng *et al.*, 2015). Recently, Gong *et al.* (2022a) demonstrated that CSE deficiency exacerbated diabetic CM through increased oxidative stress, mitochondrial damage, and necroptosis, but these effects were mitigated by the administration of exogenous H_2S.

The onset of hypertension was observed at 8 weeks in mice with CSE deletion, as most of the endogenous H_2S produced in the cardiovascular system was eliminated. Consequently, CSE knockout (CSE$^{-/-}$) mice have been considered a valuable rodent model for studying H_2S in the heart (Yang *et al.*, 2008). Our lab has previously reported the importance CSE, as its deletion led to compromised vascular functions and complications in the maternal circulation during pregnancy (unpublished). Moreover, CSE mRNA expression and H_2S levels have been shown to decrease with age (Mys *et al.*, 2022). However, the long-term effects of CSE absence and how it affects general cardiac functions later in life in the absence of external stressors (i.e., pregnancy) have not been elucidated. Therefore, this study aims to investigate the changes in cardiac functions under physiological conditions without the presence of CSE enzyme.

We hypothesise that the CSE/H_2S pathway is essential in maintaining cardiovascular homeostasis, and CSE deletion could induce progressive cardiac dysfunction, leading to CM

and HF overtime, in addition to the effects of age-associated cardiovascular changes. To determine the role of CSE in general cardiovascular adaptations overtime, male C57BL/6Jx129SvEv $CSE^{+/+}$ and $CSE^{-/-}$ mice were utilised, and a time-course echocardiography study was conducted over 14 months at various time-points (2-, 6-, 9-, 12-, 14-months). These specific timepoints were selected based on the relationship between mice developmental stages and human age. Mice at 2 and 6 months old mice were in the onset of adulthood, while those at 9, 12 and 14 months old mice were considered matured with reproductive senescence, and 16 to 18 months old were considered old (Dutta and Sengupta, 2016). Due to time constraint, ultrasound images of the heart were only taken up until 14 months. By serially assessing LV functions in the $CSE^{+/+}$ and $CSE^{-/-}$ mice, we aim to determine the onset of cardiac dysfunctions in mature $CSE^{-/-}$ mice and the type of CM that could arise without this enzyme.

3.2 Results

3.2.1 Loss of CSE causes systolic dysfunction in older $CSE^{-/-}$ mice

CSE is primarily responsible for the generation of H_2S in the cardiovascular system (Yang *et al.*, 2008). To investigate the impact of loss of the CSE on cardiac functions under physiological conditions, male $CSE^{+/+}$ and $CSE^{-/-}$ mice were subjected to serial echocardiograms at 2-, 6-, 9-, 12- and 14-months of age. Various parameters reflecting the systolic function of the LV was analysed using Fujifilm's Vevo Lab 5.5.0 program. End diastolic volume (EDV), the volume of blood in the LV at the end of diastolic filling; end systolic volume (ESV), the residual volume at the end of contraction; CO and LV ejection fraction (EF), CO and echocardiographic volumes, including and, were analysed using the bi-plane Simpson's method, by tracing the LV in systole and diastole.

As shown in Figure 3.1A, all the parameters (CO, EF, ESV and EDV) measured showed no significant differences between $CSE^{+/+}$ and $CSE^{-/-}$ mice at 2-month baseline, and

up to 12-month. However, significant differences between the two groups were observed at 14-month. Specifically, CO and EF were significantly decreased, and the EDV and ESV were significantly increased in $CSE^{-/-}$ mice as compared to $CSE^{+/+}$ mice, suggesting that loss of CSE induced age-dependent LV dysfunction. Furthermore, we found that EDV and ESV progressively increased in $CSE^{-/-}$ mice after 6 months as compared to baseline (Figure 3.1C, D). Interestingly, EF was significantly reduced in older $CSE^{-/-}$ mice at 12- and 14 months as compared to their baseline measurements (Figure 3.1B). In contrast, no significant differences in these parameters at different time points were observed in $CSE^{+/+}$ mice. EF indicates the percentage of blood ejected during systole relative to EDV and it is considered the most important measure when looking at systolic functions and a predictor of HF in clinical settings (Kosaraju *et al.*, 2017). There was also an age-dependent increase in the CO of older $CSE^{+/+}$ mice, as seen in 9 and 14 months as compared to baseline (Figure 3.1A). However, 14-month-old $CSE^{-/-}$ mice exhibited significantly lower CO compared to the controls, indicating inefficient pumping and deficiency in mechanisms of the heart. Our results indicated that loss of CSE led to progressive deterioration of the LV systolic functions.

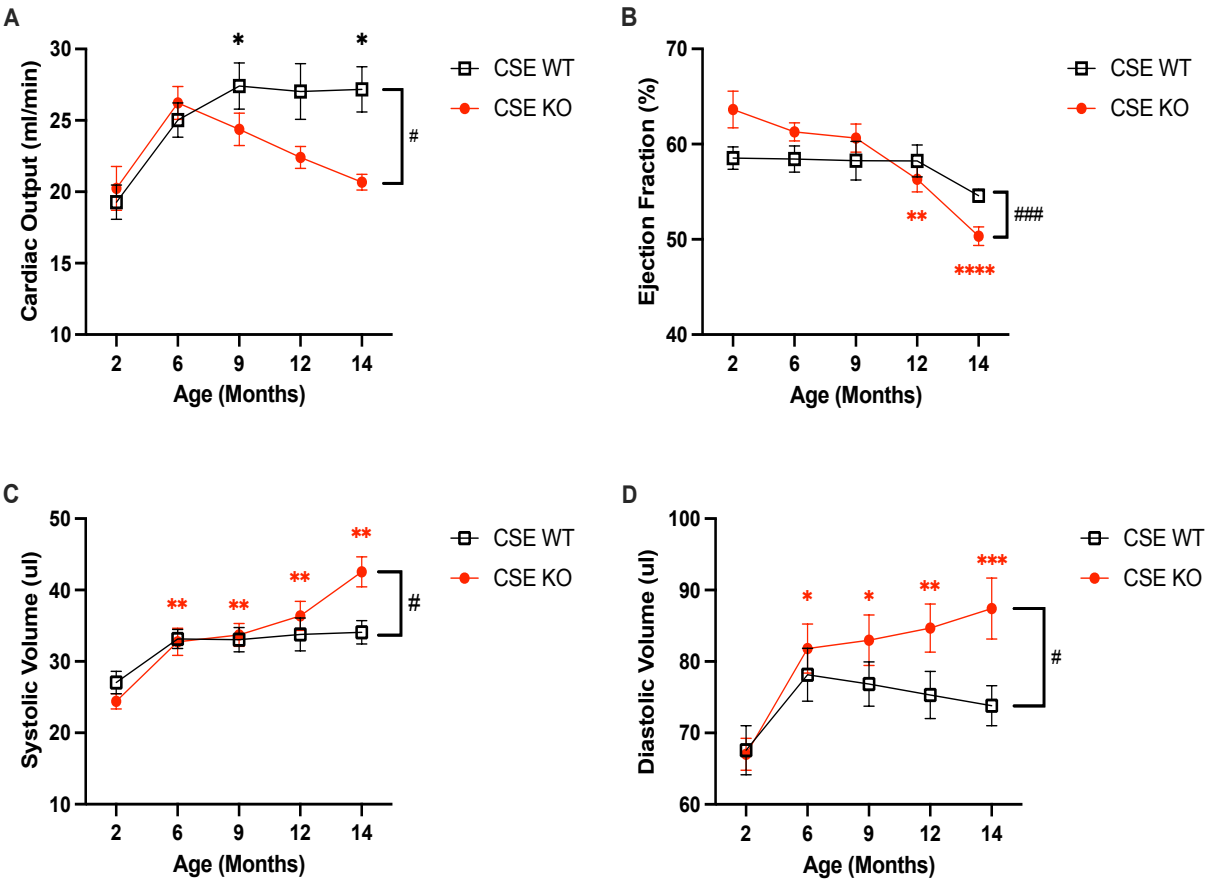

Figure 3.1 Heart functions were significantly affected in older mice lacking CSE enzyme. Echocardiography was used to determine the heart functions of $CSE^{+/+}$ and $CSE^{-/-}$ mice over 14 months. **(A)** Cardiac output (CO) and **(B)** ejection fraction (LVEF) was similar at 2 months baseline but was significantly reduced in $CSE^{-/-}$ mice at 14 months when compared to $CSE^{+/+}$. The **(C)** end systolic volume (ESV) and **(D)** end diastolic volume (EDV) of $CSE^{-/-}$ mice were both significantly increased overtime and when being compared to $CSE^{+/+}$ (n=12-15). Data are expressed as mean ± SEM. Statistical analysis was performed using two-way ANOVA analysis and post-hoc Sidak's test. # represents the significant differences between the two genotypes ($CSE^{+/+}$ and $CSE^{-/-}$ groups) at the same time point. # $p<0.05$ and ### $p< 0.001$ vs age matched $CSE^{+/+}$ mice. * represents the significant differences across different time points (relative to 2-month baseline), corresponding to the colour of the specific group (i.e. red= $CSE^{-/-}$ mice, black= $CSE^{+/+}$ mice). * $p<0.05$, ** $p <0.01$, *** $p<0.001$, **** $p<0.0001$ vs baseline.

3.2.2 Loss of CSE causes diastolic dysfunction in older $CSE^{-/-}$ mice

Systolic and diastolic dysfunction often coexist in HF. Diastolic dysfunction refers to abnormal mechanical properties of the heart, such as impaired LV diastolic distensibility, filling and relaxation, regardless of normal or depressed LVEF in symptomatic or asymptomatic patients (Jovin *et al.*, 2013). To determine whether the LV diastolic dysfunction was affected in the absence of CSE, colour Doppler echocardiography of the mitral valve inflow was employed and analysed. The isovolumetric relaxation time (IVRT), isovolumetric contraction time (IVCT), E/A ratio and deceleration time (DT) were the main parameters calculated. The myocardial performance index (MPI), also known as the Tei index, is a function of the sum of IVRT and IVCT, divided by the aortic ejection time (AET) (Table 1).

The MPI, which indicates the overall LV function, was significantly increased in the 14-month-old $CSE^{-/-}$ mice as compared to at 2-month baseline. Their MPI were also significantly higher than the $CSE^{+/+}$ mice at 6 months (Figure 3.2A). This indicated the onset of diastolic dysfunction and reduced myocardial performance from middle-age. Moreover, a significant decrease in the E/A ratio was detected at 12 and 14 months with the loss of CSE compared to age-matched wild-type mice (Figure 3.2B). The IVRT was significantly prolonged in the $CSE^{-/-}$ mice at 2, 6 and 12 months as compared to $CSE^{+/+}$ mice, indicating stiffening of the LV chamber and relaxation issues (Figure 3.2C). In contrast, the IVCT of $CSE^{-/-}$ mice was significantly shorter at baseline, when then gradually increases and becomes significantly longer at 14 months as compared to 2 months (Figure 3.2D). Both IVRT and IVCT remained similar in the $CSE^{+/+}$ mice overtime. DT, representing the rate of decline of flow velocity in early diastole, showed an age-dependent increase from 9 to 12 months in $CSE^{+/+}$ mice and 12 to 14 months in $CSE^{-/-}$ mice, although not significantly different between the two groups (Figure 3.2E).

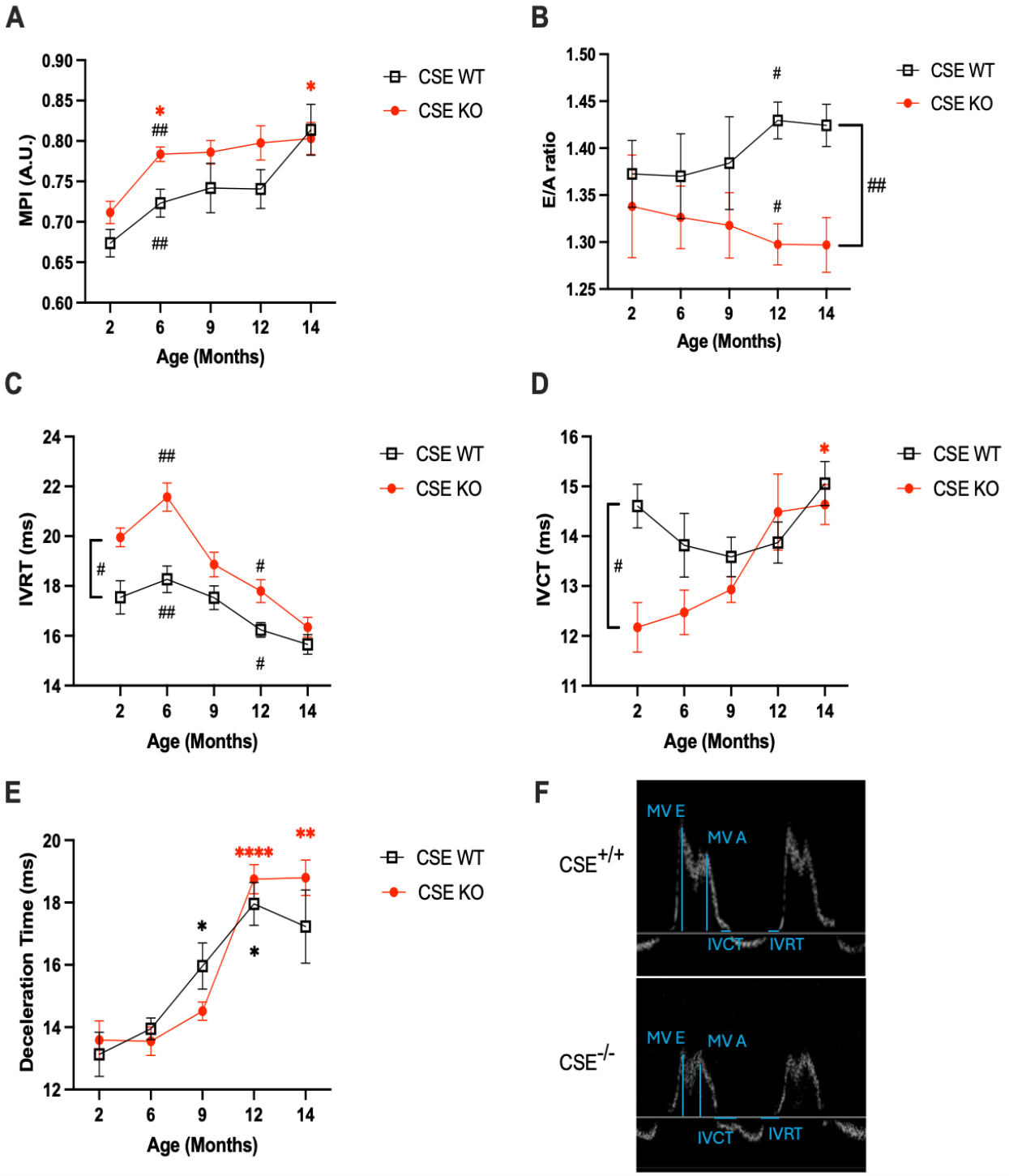

Figure 3.2 Altered cardiac time intervals measured using mitral flow indicated diastolic dysfunction in older mice without CSE.
Echocardiography was used to measure blood flow across the mitral valve of $CSE^{+/+}$ and $CSE^{-/-}$ mice overtime. **(A)** Myocardial performance index (MPI) was significantly increased in $CSE^{-/-}$ mice at 14 months and was higher than $CSE^{+/+}$ mice at 6 months. **(B)** E/A ratio was significantly lowered in 12 and 14 months $CSE^{-/-}$ mice. **(C)** Isovolumetric relaxation time (IVRT) and **(D)** isovolumetric contraction time (IVCT) was significantly higher and lower respectively in 2-month $CSE^{-/-}$ mice. However, the IVCT increased significantly at 14 months when lack of CSE. **(E)** Deceleration time (DT) significantly increased overtime in both older $CSE^{+/+}$ and $CSE^{-/-}$ mice. **(F)** Representative images of mitral inflow imaged using colour doppler waveform, highlighting lower E and A peaks, and prolonged IVCT and IVRT in $CSE^{-/-}$ mice. Data are expressed as mean ± SEM. p-value determined using two-way ANOVA

analysis. # represents the significant differences between $CSE^{+/+}$ and $CSE^{-/-}$ groups. # p<0.05 and ## p< 0.01 vs age-matched $CSE^{+/+}$ mice. * represents the significant differences across different timepoints (relative to 2 months). * p<0.05, ** p <0.01 and **** p<0.0001 vs baseline.

3.2.3 Progressive increase in left ventricular mass index in $CSE^{-/-}$ mice

To investigate whether loss of CSE plays a role in ventricular remodelling, the cardiac structural changes were determined. Specifically, the left ventricular mass index (LVMI), representing the myocardium mass to body weight ratio, was calculated using M-mode images of the PSLAX. As shown in Figure 3.3, the LVMI remained consistent at different timepoints in the $CSE^{+/+}$ mice. LVMI was also similar in both groups at 2 months. However, this was significantly elevated in older $CSE^{-/-}$ mice at 14 months, suggesting the presence of a larger heart and hypertrophy.

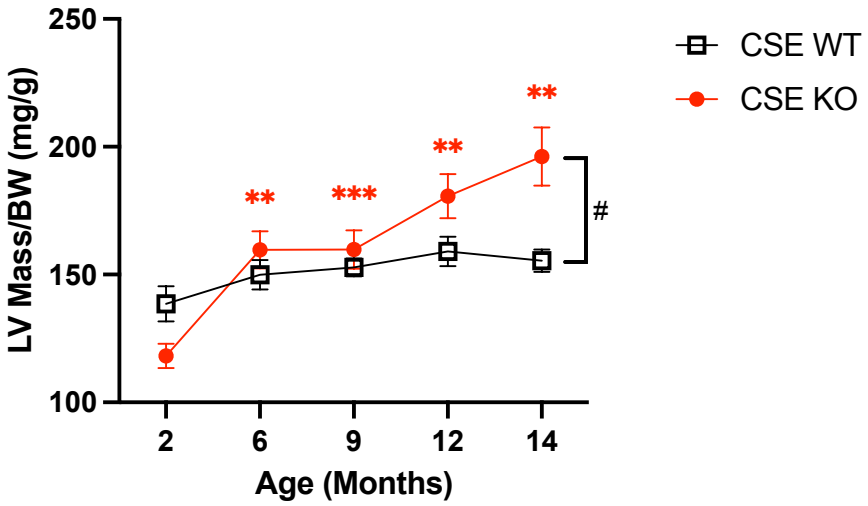

Figure 3.3 Left ventricular mass index (LVMI) is significantly increased in $CSE^{-/-}$ mice overtime compared to $CSE^{+/+}$ mice.
Echocardiography was used to measure the corrected LV mass, which takes the body weight into consideration. ** p<0.01 and *** p<0.001 were the significant difference relative to 2 months mice and # p<0.05 represents the significant difference between the 14-month $CSE^{+/+}$ and $CSE^{-/-}$ mice. Data expressed as mean ± SEM. Analysed by two-way ANOVA.

3.2.4 Age-dependent alterations in cardiac geometry in $CSE^{-/-}$ mice

CSE deficiency in a HF mouse model was found to substantially increase LV internal diameter (LVID) and exacerbate LVH (Wu *et al.*, 2022). Similar to LVMI, M-mode images

showing consecutive cardiac cycles were taken to observe changes in wall motions and thickness during systole and diastole. Figure 4.4 illustrates representative M-mode images of the PSLAX view of the heart in $CSE^{+/+}$ and $CSE^{-/-}$ mice at 2, 9 and 14 months. Parameters of heart dimensions, such as the thickness of the left ventricle posterior wall (LVPW), interventricular septum (IVS) and LVID were measured using these M-mode images during systole and diastole.

As shown in Figure 3.5A and B, LVID measured in both systole and diastole were similar in $CSE^{+/+}$ and $CSE^{-/-}$ mice at baseline and the other time points. From 6 months onwards, LVID was significantly increased in $CSE^{-/-}$ mice when compared to baseline, indicating that loss of CSE led to a progressive dilated LV phenotype, corresponding to the increasing EDV and ESV as described previously in this study. Interestingly, these changes were also observed in $CSE^{+/+}$ mice, but at later timepoints. We found that in the absence of CSE, there was a trend towards earlier and more pronounced LV remodelling compared to age matched $CSE^{+/+}$ mice. This difference was particularly evident in the 14-month $CSE^{-/-}$ mice, as evident from the M-mode images in Figure 3.4. In terms of wall thickness, LVPW remained consistent across all groups except for the LVPW measured at 14 months in $CSE^{-/-}$ mice, where a significant increase in the thickness was observed as compared to the baseline (Figure 3.5E). In contrast, while the IVS thickness remained consistent at different timepoints in $CSE^{+/+}$ mice, it was significantly increased in $CSE^{-/-}$ mice from 6 months onwards when compared to baseline. Interestingly, we found that the septal wall was significantly thinner in $CSE^{-/-}$ mice compared to the $CSE^{+/+}$ mice at baseline (Figure 3.5C, D). The thickness subsequently recovered in the $CSE^{-/-}$ mice, showing no significant difference when compared to the wild-type controls. These changes indicated that lack of CSE led to significant age-related structural remodelling, rather than differences between the two phenotypes.

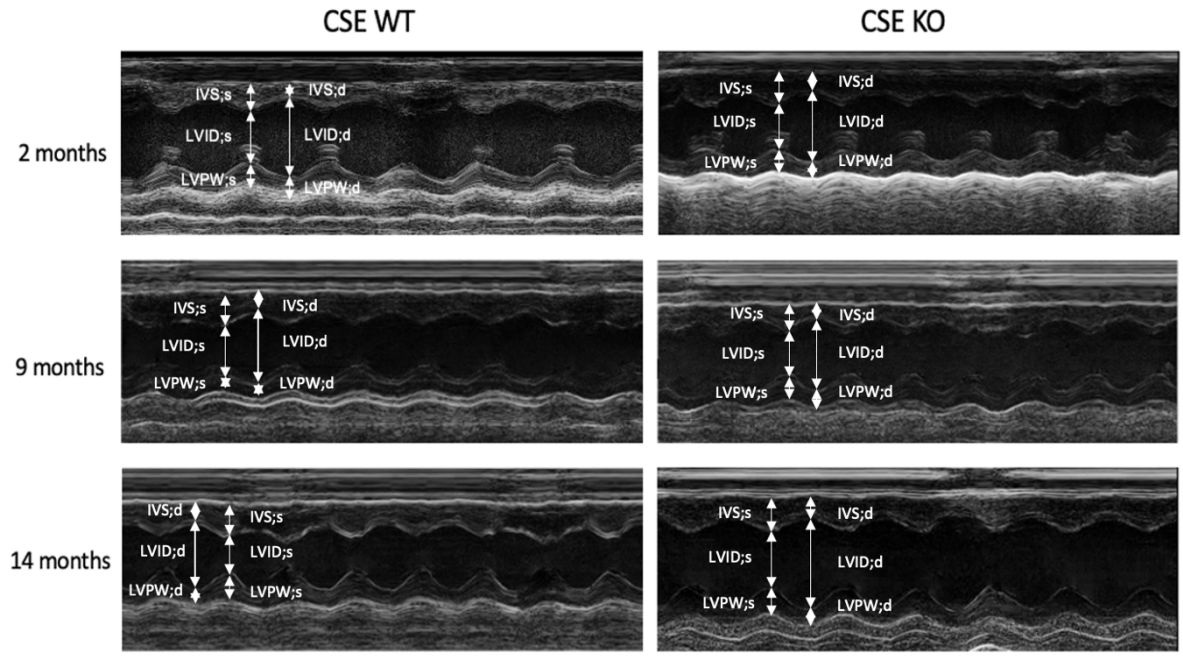

Figure 3.4 Representative M-mode images of the heart in parasternal long axis view showing the changes in wall motions and thickness during cardiac cycles.
Significant dilation and increase in thickness of IVS can be observed in the older $CSE^{-/-}$ mice as compared to younger counterparts and controls. IVS: interventricular septum; LVID: left ventricular diameter; LVPW: left ventricular posterior free wall; d: diastole; s: systole.

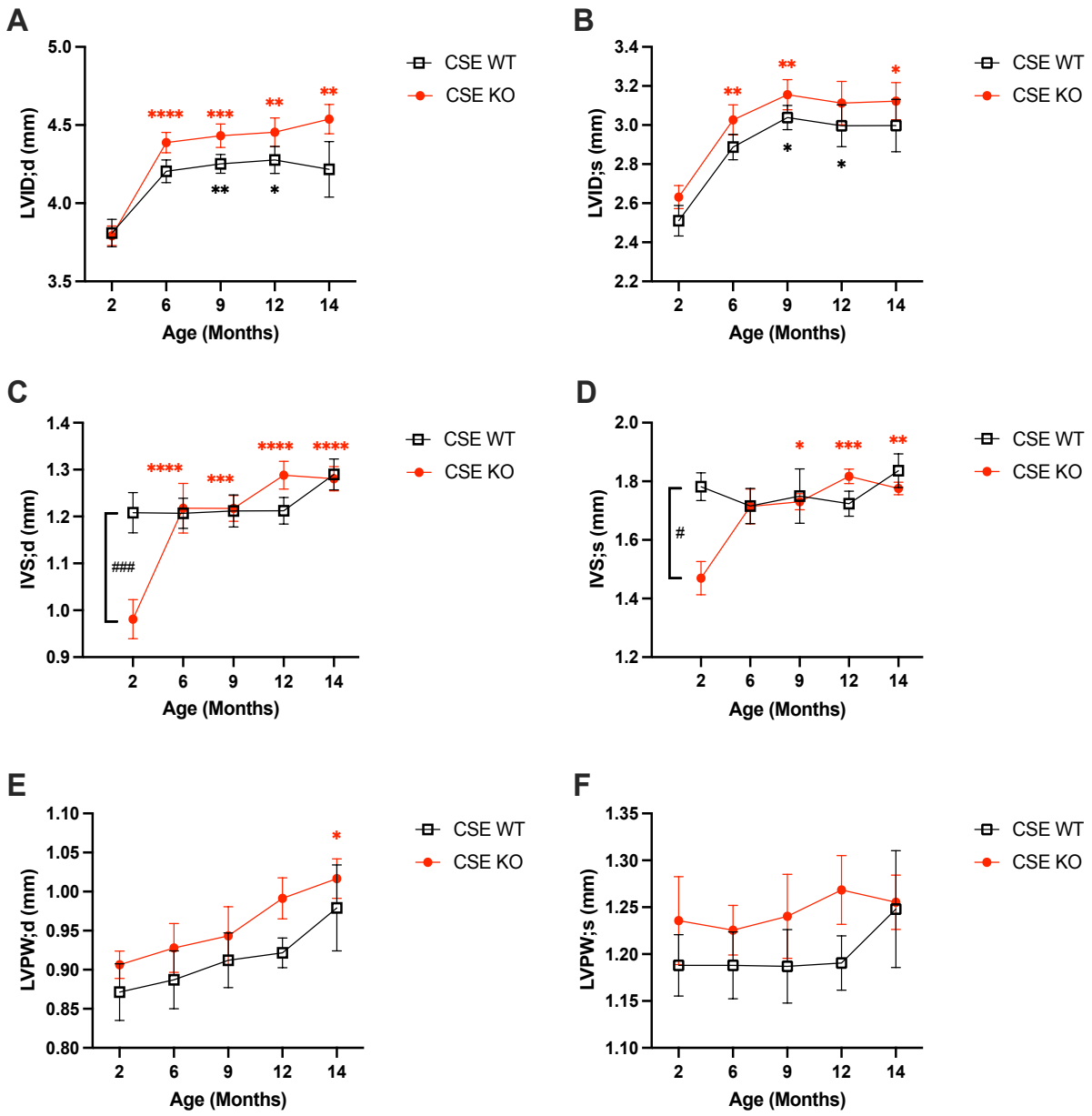

Figure 3.5 Left ventricular cavities were enlarged in both CSE$^{+/+}$ and CSE$^{-/-}$ mice and the interventricular septum (IVS) was thickened in CSE$^{-/-}$ mice as the mice become older.
Cavity size measured using left ventricular internal diameter (LVID) from the M-mode images during both **(A)** diastole and **(B)** systole showed chamber dilation overtime. Wall thickness of IVS in both **(C)** diastole and **(D)** systole was significantly lower in CSE$^{-/-}$ mice (at 2 months but has significantly increased when at 6 and 9 months respectively. The LVPW thickness during both **(E)** diastole and **(F)** systole remains relatively unchanged except for 14-month CSE$^{-/-}$ mice during diastole. Data was analysed with two-way ANOVA and expressed as mean ± SEM. # represents the significant differences between CSE WT and KO groups. # p<0.05 and ### p< 0.001 vs age-matched CSE$^{+/+}$ mice. * represents the significant differences across different timepoints (relative to 2 months). * p<0.05, ** p <0.01, ***p<0.001 and **** p<0.0001 vs baseline.

3.3 Discussion

H_2S has long been recognised to be important in maintaining healthy cardiac functions (Kolluru *et al.*, 2023). While many studies have shown its cardioprotective effects through anti-inflammation, vasodilation, anti-oxidation, and anti-apoptosis of the heart, the relationship between CSE/H_2S pathway and HF is not yet fully understood (Yang *et al.*, 2008; Su *et al.*, 2009; Sivarajah *et al.*, 2009). The aim of this longitudinal study was to investigate the role of CSE/H_2S pathway in murine hearts and how its dysregulation could impair cardiac functions and lead to the development of CM overtime. We found that CSE-deficient mice progressively developed systolic and diastolic dysfunction. A trend towards LV remodelling was also observed as the mice grew older, compared to age-matched wild-type controls. Cardiac functions were significantly compromised in $CSE^{-/-}$ mice, as reflected by the significantly lower CO, EF and E/A ratios, along with increased cardiac volumes and MPI. Structural changes, including a remarkable increase in LVMI and LVID after the 2-month baseline, indicated the potential presence of LV hypertrophy and dilation in $CSE^{-/-}$ mice as they age. Age-related LV remodelling was as prominent in the controls, and their LVMI remained relatively consistent overtime. Therefore, this study demonstrated that CSE plays a critical role in preserving cardiovascular adaptations in the mice, particularly in later stages of life.

3.3.1 Dysregulation of CSE/H_2S leads to age-dependent systolic and diastolic dysfunction

It has been previously proven that levels of H_2S are reduced in CSE-deficient mice (Mani *et al.*, 2013). Yang *et al.* (2008) reported an 80% reduction in endogenous H_2S production in the hearts and aortas of homozygous $CSE^{-/-}$ and 50% decrease in heterozygous mutant mice. H_2S bioavailability has been used as an indicative biomarker for CVDs, as patients with coronary or peripheral artery disease had significantly reduced plasma sulfide metabolite levels (Rajpal *et al.*, 2018). A clinical study also showed that the

total plasma sulfide in patients negatively correlates to the severity of chronic congestive HF, with low sulfide levels predicting higher mortality rates (Kovačić *et al.*, 2012). Additionally, plasma H_2S levels decline in human subjects aged 50 to 80 (Chen *et al.*, 2005). Therefore, it is likely that the reduction in H_2S levels, exacerbated by ageing, may render the heart more susceptible to damage, contributing to systolic and diastolic dysfunction and eventually leading to HF.

During HF, the metabolic demand of the heart is not met. Usually, HFrEF patients exhibit both systolic and diastolic dysfunction, although diastolic dysfunction can occur without systolic impairment in certain cases. In the present study, systolic deterioration was evidenced by both the reduced CO and EF, as well as increased cardiac volumes in the older $CSE^{-/-}$ mice. However, these clinical manifestations were absent in $CSE^{+/+}$ mice, which coincides with findings in healthy adults where overall systolic function should remain stable when resting during ageing (Akasheva *et al.*, 2015). There is usually inverse correlation of LV volumes with age, where both EDV and ESV were found to reduce in healthy ageing (Agrawal and Nagueh, 2022). However, in CSE-deficient mice, EDV and ESV was progressively increased, leading to a larger blood volume in the LV after each contraction. Depending on the cardiac phase (systolic or diastolic) and the degree of enlargement, cardiac function and overload could be affected differently (Yoshida *et al.*, 2017). According to the Frank-Starling law of the heart, greater EDV leads to more LV contractions due to increased passive stretching of myofibrils. The increase in EDV compensates for chamber dilation to preserve CO. Conversely, an increase of ESV might suggest supressed cardiac function and enhanced cardiac overload, which is detrimental to the heart (Yoshida *et al.*, 2017). In this study, the elevated EDV and ESV were associated with age-dependent reduced CO and EF in $CSE^{-/-}$ mice, suggesting that CSE plays an important role in maintaining cardiac homeostasis under normal condition.

Cardiac time intervals, particularly IVCT, are critical predictors of cardiac function and HF in the general population (Alhakak *et al.*, 2020). Prolonged IVCT has been associated with CVDs, ageing, lower LVEF, higher LVMI, systolic and diastolic blood pressure (Alhakak *et al.*, 2020). Increased IVRT, indicating diastolic dysfunction, is associated with higher blood pressure, advancing age, male sex and an elevated risk of subsequent HF (Alhakak *et al.*, 2023). MPI has been widely used as a reliable method for assessing global LV function in various heart diseases, as it accounts for both systolic and diastolic performance (Bruch *et al.*, 2000; Poulsen *et al.*, 2000). It has also been shown to be an important indicator for cardiac dysfunctions as it could provide early prognosis and correlates strongly with the severity of HF (Dujardin *et al.*, 1998). Recently, the Copenhagen City Heart Study (CCHS) (2023) investigated longitudinal changes of cardiac time intervals in 1064 individuals without CVDs based on echocardiographic examinations performed 10.5 years apart. The study found that IVCT, IVRT and MPI increased significantly with age, providing insights into future HF risks. Interestingly, in our study, IVCT, IVRT and MPI remained consistent in the wild-type controls. Changes in cardiac time intervals in the absence of CSE are indicators of impaired filling and diastolic dysfunction, which are usually associated with HFpEF. The prolonged IVCT observed in $CSE^{-/-}$ mice over time may result from deterioration of myocardial contractility, leading to a slower rise in pressure. It is likely that as LV systolic function progressively worsens, the time taken for LV pressure to reach the same level as the aorta increases, resulting in longer IVCT (Biering-Sørensen *et al.*, 2016). The significantly prolonged IVRT in $CSE^{-/-}$ mice over the time course of the longitudinal study suggested impaired relaxation and LV stiffening, indicating the presence of progressive diastolic dysfunction due to slower early diastolic relaxation. Consequently, this leads to increased MPI, calculated as (IVCT+IVRT)/AET (Su *et al.*, 2007).The progressive rise in MPI reflects the presence of both systolic and diastolic dysfunction in $CSE^{-/-}$ mice, with a trend of prolonged IVCT and significantly longer IVRT respectively, and overall deteriorated global LV performance further confirmed the importance of CSE in maintaining the LV function.

In addition, our results showed that many changes in the cardiac parameters occurred from 6 months onwards, suggesting a gradual decline in LV function starting from an early age in $CSE^{-/-}$ mice. it has been demonstrated that an increased prevalence of diastolic dysfunctions was associated with the development of HF, even in healthy participants with advancing age (Kane *et al.*, 2011). Impaired ventricular relaxation, considered as grade 1 diastolic dysfunction, has been recorded in humans around 50 years old (Pyszko *et al.*, 2018). This would correspond to about 15 months mice age (Flurkey *et al.*, 2007). Decline in E/A ratio, an indicator of diastolic dysfunction, is associated with declines with ageing (Lakatta and Levy, 2003). In this study, we found that $CSE^{-/-}$ mice displayed impaired ventricular relaxation patterns, such as increased IVRT and decreased E/A ratio. Some of these patterns were observed as early as 2-month-old. It has been reported that the levels of total plasma sulfide are decreased as diastolic functions deteriorates from normal (Grade 0) to moderate (Grade 2) diastolic dysfunction in patients (Glavnik Poznic *et al.*, 2018). Taken together, our findings suggest that CSE plays an important role in regulating cardiac diastolic function, and that loss of CSE could potentially lead to the development of diastolic dysfunction early in adulthood.

3.3.2 CSE deletion influenced cardiac functions more than its structure

DCM and HCM are some common clinical conditions that cause LV remodelling, which leads to LV dilation and LVH respectively. During remodelling, the heart changes shape to maximise pumping efficiency as a compensatory mechanism in response to wall pressure and diastolic overload (Bornstein, Rao and Marwaha, 2021). $CSE^{-/-}$ mice exhibited age-dependent increase in LV mass, as indicated by the significantly higher LVMI compared to their age-matched $CSE^{+/+}$ counterparts, whose LVMI remained unchanged over time. This was in consistent with the findings from healthy individuals. Hees *et al.* (2002) found that the cardiac mass either remained the same or even decreased with age in healthy male

participants. This was primarily due to the shortening of LV length along its long axis with no changes in myocardial wall thickness, resulting in a transition of a hemiellipsoid to hemispherical shape with age. Other studies showed that progressive thickening of LVPW was observed in wild-type mice from a young (4 months) to an older age (12 months), while their chamber size remained unchanged (Wu *et al.*, 2021).

Interestingly, although no significant differences in the LV wall thickness was observed between $CSE^{+/+}$ and $CSE^{-/-}$ mice phenotypes at later timepoints, the LVMI in $CSE^{-/-}$ mice was significantly increased compared to the wild-type controls at 14 months. It is likely that the progressive increase in LVMI in the $CSE^{-/-}$ mice arose from cumulative myocardium hypertrophy, specifically in the IVS as compared to the 2-month baseline. This hypertrophy further led to ventricular dilation and decreased EF overtime, ultimately causing HF. Cardiac hypertrophy, reflected by significant increase in IVS was only observed in spontaneously ageing C57Bl/6 mice at 24 months (De Moudt *et al.*, 2022). No significant changes were seen in middle-aged mice (around 9 to 12 months), which was the oldest age group that was used in this study. Although there were no significant differences between the two genotypes, it could be predicted that there will be progressive thickening of IVS, leading to LV remodelling at later stages without CSE. Therefore, LV remodelling could arise before 24 months and hypertrophic phenotype could be present when there is a dysregulation in CSE/H_2S pathway in the heart. Although most patients with HCM have smaller LV cavities, its dilation could mark end-stage of the disease caused by systolic dysfunction and continuous myocardial fibrosis (Rawlins, Bhan and Sharma, 2009). A study by Ahmad and colleagues (2016) showed a threefold reduction in CSE mRNA expression and H_2S concentration, accompanied by significant elevation in oxidative stress and collagen deposition in an isoproterenol-caffeine induced LVH rat model. While they observed a similar increase in LV indices and thickness during hypertrophy, they reported a reduction in LVID, which contradicted our findings. The exogenous administration of H_2S reversed the effects

on LV remodelling, suppressing LVH progression and attenuating endothelial dysfunction (Ahmad *et al.*, 2016).

Our study revealed a remarkably thin IVS in $CSE^{-/-}$ mice, indicating segmental abnormalities of the LV even at young age before hypertrophy was present. The asymmetrical increase of IVS with age may be attributed to replacement fibrosis, cardiomyocyte hypertrophy, or a combination of both, as observed in 60 – 70% of HCM cases. Other studies have also shown that it is more common to observe asymmetrical wall thickening, particularly in the septal than the posterior free wall (Méndez *et al.*, 2018). Another important contributing factor affecting LVH in ageing is changes in blood pressure (Aronow, 2017). All the clinical manifestations observed from this study demonstrated the classical signs of a hypertensive heart disease transitioning into dilated cardiac failure with reduced EF. It was shown that $CSE^{-/-}$ mice was associated with age-dependent hypertension, starting at 7 weeks of age regardless of gender (Yang *et al.*, 2008). Similar to the deletion of CSE, Peleli *et al.* (2020) found that 18-month-old aged $3\text{-}MST^{-/-}$ mice exhibited cardiac hypertrophy and reduced nitric oxide (NO) levels in heart, which could be the result of age-related hypertension. Our group has also previously demonstrated hypertension, abnormalities in angiogenesis and vascular dysfunctions with pregnancy in mice lacking CSE. In conclusion, the CSE/H_2S pathway is essential in maintaining normal cardiovascular functions as its dysregulation could result in systolic and diastolic dysfunction, and alterations in the heart geometry overtime with a hypertrophic phenotype.

3.3.3 Limitations

One major challenge of this study was the variations observed when assessing cardiac function, particularly in aged $CSE^{-/-}$ mice. This variability could potentially be attributed to batch-to-batch variations in the animals. In the present study, we investigated the LV volumes, CO, EF, cardiac time intervals and LV geometry using the bi-plane modified

Simpson method, which is considered more reliable and accurate compared to PSLAX B-mode view LV trace as it incorporates multiple short-axis (apical, midventricular and basal) views (Heinen *et al.*, 2018). However, using 2D images to calculate 3D volumes still has its limitations and cardiac parameters could be affected by anaesthesia as well. Furthermore, as echocardiography is operator dependent, it would also have been useful to assess intra- and interobserver variability to evaluate the repeatability of the data obtained. A better alternative, which is the gold standard, would be using cardiac MRI. Another limitation was the calculation of LVMI. It would have been useful to record the body weight of mice before each ultrasound scan to better consider the changes in body weight ratio. This could have been improved by measuring heart weight-to-tibia length ratio, which is a more stable unaffected by diet and lifestyle compared to body weight, although the latter was kept consistent throughout the experiment. Due to time constraint, we only managed to conduct ultrasound scans on mice up to 14 months. Examining older mice beyond 14 months would have provided insights, as LV contractile dysfunction became even more apparent at 18 months of age in C57BL/6J mice with serial echocardiography (Boyle *et al.*, 2011).

4 Underlying Mechanisms of Loss of CSE-induced Cardiac Dysfunction

4.1 Introduction

Structural abnormalities, impaired contractility, compromised cardiac output and abnormal energy metabolism are commonly observed collectively in failing hearts. Pathophysiological cellular mechanisms involved in cardiac dysfunction could contribute to myocardial remodelling, eventually leading to heart failure (HF). These signalling pathways in cardiac remodelling include impaired energy metabolism, mitochondrial dysfunction, hypertrophy, fibrosis and cardiomyocyte apoptosis (Schirone *et al.*, 2017). Cardiomyocytes undergo different compensatory hypertrophy as an adaptive response to different forms of stress. For instance, eccentric hypertrophy occurs with increased hemodynamic load, while concentric hypertrophy occurs in pressure overload, all aiming to maintain contractile function (You *et al.*, 2018). This initial hypertrophy proves to be a beneficial adaptation to meet the increased demand of the heart. However, if the stressors persist and become chronic, this leads to pathological hypertrophy that is associated with cardiac dysfunction and cardiomyopathy (CM).

Furthermore, cardiac remodelling affects calcium signalling, with dysregulation in intracellular calcium (Ca^{2+}) homeostasis due to defective function of the sarcoplasmic reticulum (SR) being the main cause of arrythmias and contractile dysfunction in HF (Luo and Anderson, 2013). Reductions in key Ca^{2+} handling gene expression and protein levels, such as sarco/endoplasmic reticulum Ca^{2+} ATPase 2 (SERCA2), have been not only associated with left ventricular hypertrophy (LVH) but also with severe diastolic dysfunction and failure in LV relaxation (Andersson *et al.*, 2009; Huang *et al.*, 2014). H_2S has been found to be a tight regulator of Ca^{2+} homeostasis (Yong *et al.*, 2010). In fact, Peng *et al.* (2022) recently reported that H_2S increases cardiac contractility by modulating the ubiquitination of SERCA2a and reducing cytosolic Ca^{2+} concentrations in a diabetic CM mouse model. Additionally, Ca^{2+} homeostasis is also essential for maintaining proper mitochondrial functions ATP production (Lai and Qiu, 2020). SERCA overexpression has been shown to

promote overall mitochondrial quality control in cardiac ischemia-reperfusion (I/R) injury by improving biogenesis, bioenergetics, fusion and mitophagy (Tan *et al.*, 2020). Given that healthy mitochondria serve as the powerhouse of cells, they are critically important for the energy-demanding heart to sustain rhythmic contractions and maintain cardiac output. Mitochondria quality, shape, size and number are tightly controlled by mitochondria dynamics, influencing overall cellular homeostasis and function (Cao and Zheng, 2019). Dysfunction or damage to the mitochondria can lead to energy deficits, impaired contractility and an increased risk of CVDs or HF (Pennanen *et al.*, 2014; Marín-García and Akhmedov, 2016). Furthermore, oxidative damage and depletion in mitochondrial DNA (mtDNA) leading to deranged mitochondria biogenesis contributes to pathological cardiac remodelling in end-stage ischemic HF (Pisano *et al.*, 2016). H_2S donors has been demonstrated to exert cardioprotective effects by decreasing cellular stress and preserving cardiac mitochondrial functions in various CVDs (Wüst *et al.*, 2016; Shimizu *et al.*, 2018).

Previously, our lab reported downregulation in SERCA2a and peroxisome proliferator-activated receptor gamma coactivator 1-alpha (PGC1α) mRNA in cardiac tissue from pregnant $CSE^{-/-}$ mice, alongside pathological signs of CM. PGC1α plays a crucial role in regulating mitochondria antioxidants, metabolism, and biogenesis (Lu *et al.*, 2010). Furthermore, increased oxidative stress has been observed in the $CSE^{-/-}$ hearts, suggesting that global deletion of CSE gene leads to mitochondrial dysfunction, possibly due to reduced transcription of PGC1α. However, the efficiency of the electron transport chain (McFarland *et al.*) and their ability to oxidise substrates have not been elucidated. The hypothesis of this chapter is that deletion of the CSE gene could cause myocyte hypertrophy and is linked to perturbations in cardiac bioenergetics, leading to impaired calcium signalling and mitochondria dysfunction. The aim of this study was to investigate the importance of the CSE gene in maintaining a healthy cardiomyocyte population and cardiac calcium homeostasis. Furthermore, we evaluated the role of endogenously produced H_2S on

mitochondrial function in isolated murine cardiac mitochondria, thereby demonstrating how CSE deletion affects cardiac mitochondrial oxidative phosphorylation (OXPHOS), biogenesis and dynamics.

4.2 Results

4.2.1 Structural Changes of LV at Cellular Level

In cardiac hypertrophy, a condition characterised by the thickening of LV wall, several structural changes occur at the cellular level, including cardiomyocytes, the individual muscle cells that make up the myocardium. To examine these cellular changes, the number of cardiomyocytes, total capillaries density, capillary-to-cardiomyocyte ratio and cardiomyocyte size were calculated using immunofluorescence staining of frozen isolated LV sections from 2, 9 and 16 months $CSE^{+/+}$ and $CSE^{-/-}$ mice.

As shown in Figure 4.1 and 4.2A, the size of cardiomyocyte was significantly larger in the 9- and 16-month timepoints. In addition, the size of cardiomyocyte in $CSE^{-/-}$ mice was increased in an age-dependent manner, suggesting that CSE deficiency induced hypertrophy was present at the cellular level. These changes coincided with a reduction in the number of cardiomyocytes per area in the $CSE^{-/-}$ mice (Figure 4.2B). Interestingly, while age-dependent reduction in the total capillary density per mm^2 was observed in both $CSE^{+/+}$ and $CSE^{-/-}$ mice, the capillary density was significantly increased in $CSE^{-/-}$ mice compared to the wild-type controls at different timepoints. Furthermore, the number of capillaries per cardiomyocyte was significantly increased in $CSE^{-/-}$ mice (Figure 4.2C, D).

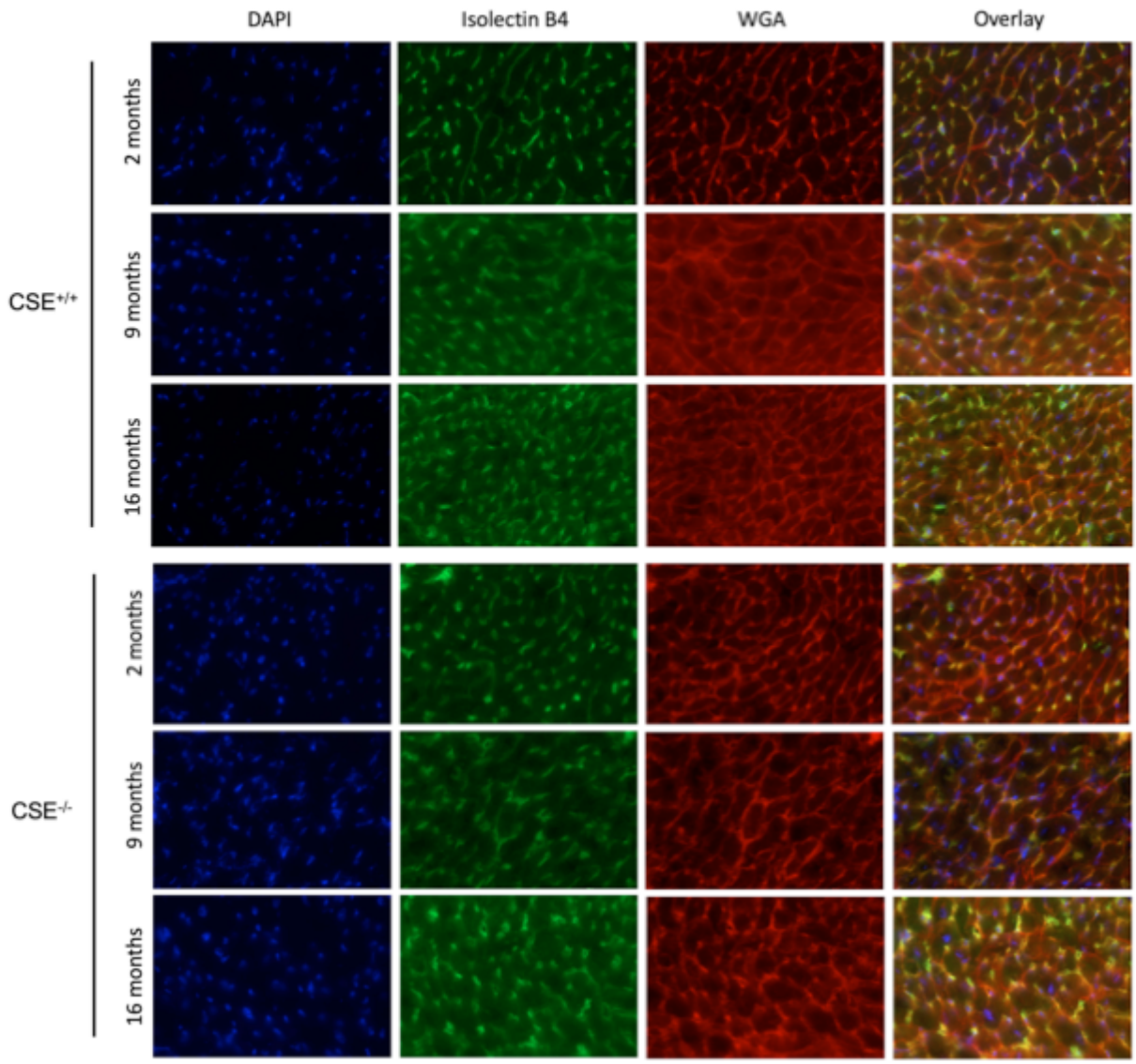

Figure 4.1 CSE deletion increased capillary/cardiomyocyte ratio in older mice.
Representative micrographs of the LV tissue in $CSE^{+/+}$ and $CSE^{-/-}$ mice at 2, 9 and 16 months. Cardiac tissues were incubated with DAPI (blue), isolectin B4 (green) and WGA (red) to identify the nucleus, capillary density and cardiomyocyte borders respectively. Taken at 40x magnification, scale bar 10μm. Analysis conducted by ImageJ software, capillaries and cardiomyocytes were manually counted in at least 4 micrograph images of endocardium per mouse. (n=6)

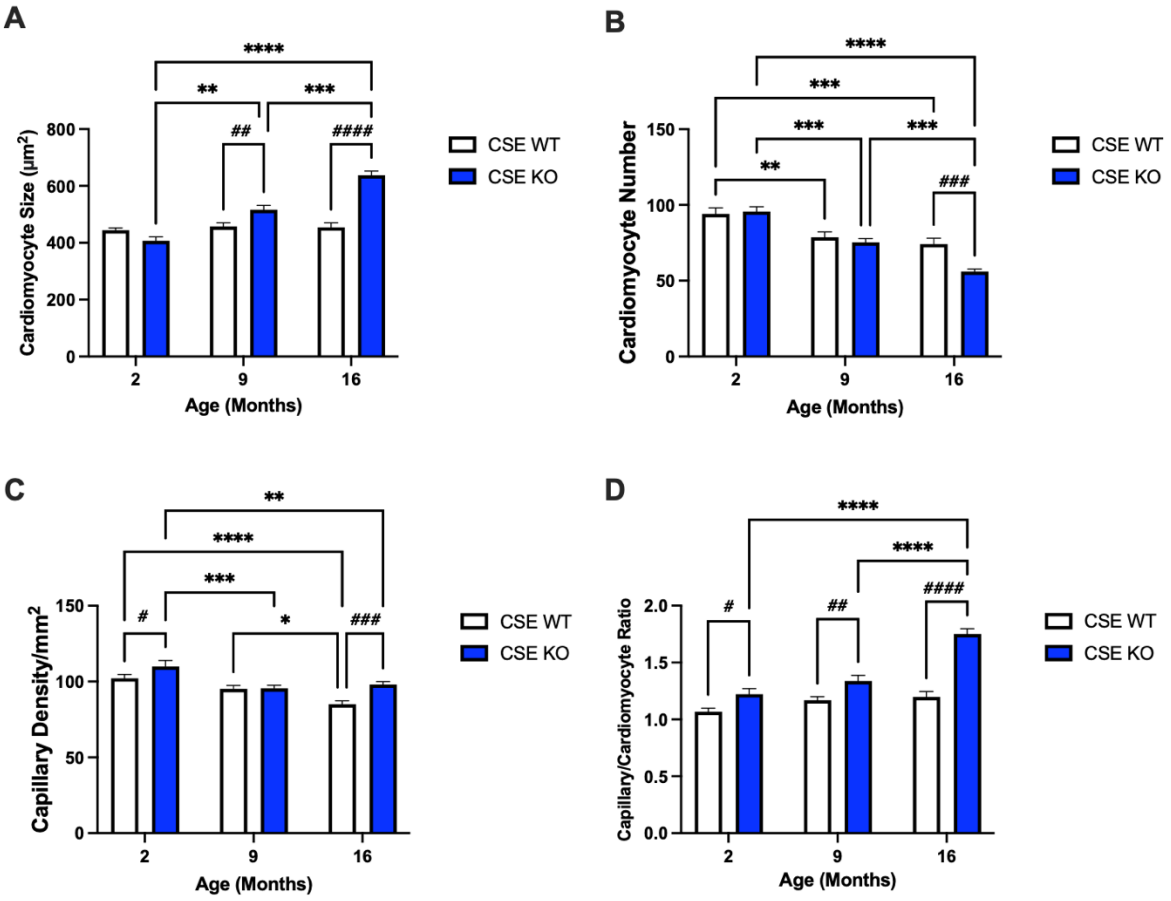

Figure 4.2 Loss of CSE results in hypertrophy at the cellular level.
(A) Cardiomyocyte size and **(B)** total numbers present in the micrograph of LV taken at 40× magnification. Significant increase in **(C)** capillary density may be due to compensatory remodelling and **(D)** cardiomyocyte/capillary ratio indicate the presence of cardiomyocyte hypertrophy. Data are displayed as mean ± SEM, n=6 mice per group, with at least 6 images per mouse. Two-way ANOVA and Sidak post-hoc test used for statistics. # $p<0.05$, ## $p<0.01$, ### $p<0.001$ and #### $p< 0.0001$ vs age-matched $CSE^{+/+}$ mice. * represents the significant differences across different timepoints (relative to 2 months). * $p<0.05$, ** $p <0.01$, ***$p<0.001$ and **** $p<0.0001$ vs baseline.

4.2.2 Molecular changes in the hearts of $CSE^{-/-}$ mice

To investigate the underlying mechanisms of CSE deficiency-induced cardiomyocyte hypertrophy, cardiac gene expression of angiotensin II Type I receptor (AT1) was measured in the $CSE^{-/-}$ mice. Activation of AT1 has been shown to stimulate signalling pathways associated with LV hypertrophy (Hunyady and Turu, 2004). We found that AT1 expression in the heart was significantly upregulated in $CSE^{-/-}$ mice compared to the wild-type controls at 16 months (Figure 4.3A).

In addition, Ca^{2+} homeostasis is essential for the heart and its contractility for efficient excitation-contraction (EC) coupling of the cardiomyocytes. Impaired Ca^{2+} signalling by defective SERCA in SR was found to cause irregular contraction, cardiac dysfunction and accelerated HF (Park and Oh, 2013). To explore the role of CSE in cellular Ca^{2+} homeostasis, the gene expression of cardiac was measured in the LV tissues of younger 2 months and older 16 months $CSE^{+/+}$ and $CSE^{-/-}$ mice using qPCR. As hypothesised, the loss of CSE affected SERCA2a as it was downregulated by approximately 30% at 2 months, indicating impaired Ca^{2+} signalling in SR of cardiomyocytes and may lead to relaxation issues of the heart due to calcium overload. This reduction was sustained at 16 months, suggesting the decrease in SERCA2a in young mice at 2 months persisted throughout the lifespan (Figure 4.3B). However, this significant decrease was not seen in Serca3a mRNA expression, indicating that CSE deletion predominantly affects the 2a isoform (Figure 4.3C).

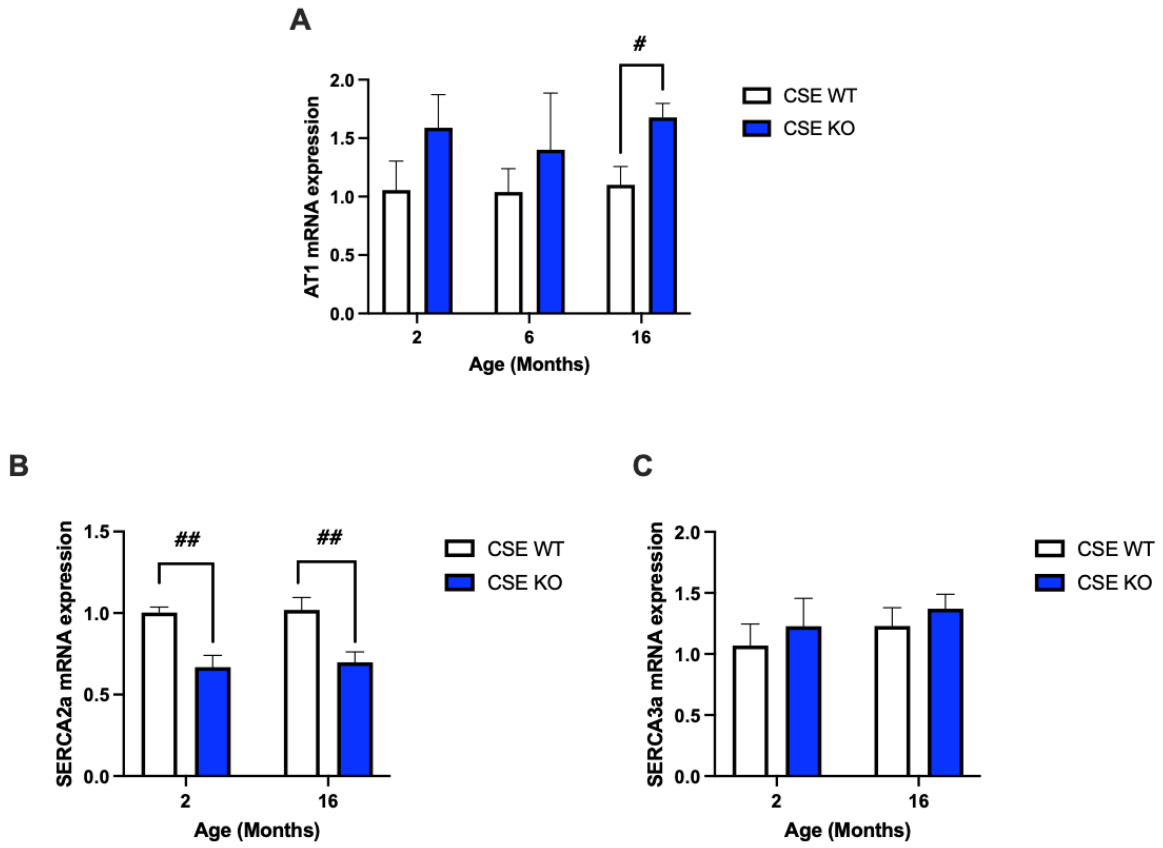

Figure 4.3 Altered mRNA expressions of Ca^{2+} signalling with CSE deletion.
(A) AT1 expression (relative to β-actin) was significantly increased in 16-month $CSE^{-/-}$ mice. Gene expression of **(B)** SERCA2a was decreased in both 2 and 16 months $CSE^{-/-}$ mice whereas expression levels of **(C)** SERCA3a showed no significant changes. Data are expressed as mean ± SEM (n= 5). Two-way ANOVA was used to test statistical significant difference: # $p<0.05$ and ## $p<0.01$.

4.2.3 CSE deletion reduced cardiac mitochondria biogenesis

Mitochondria biogenesis plays an important role in cardiac contractility by controlling the content of mitochondria and hence, oxidative metabolism for energy production in the heart (Rimbaud, Garnier and Ventura-Clapier, 2009). Alterations in the function of mitochondria was found to be linked to mitochondria content, as disruption in mtDNA expression can lead to OXPHOS deficiency and mitochondria dysfunction (Kühl *et al.*, 2017). Decline in respiratory chain function has been implicated with reduced mtDNA and cardiac dysfunction (Hansson *et al.*, 2004). To evaluate the effects of loss of CSE on mitochondria biogenesis, the mitochondrial DNA content, represented as the ratio of mitochondrial DNA (ND1) copy number to nuclear DNA (HK2) copy number (mtDNA/nDNA), was determined. As shown in Figure 4.4, the mtDNA content was significantly reduced in $CSE^{-/-}$ mice at 16

months when compared to age-matched wild-type controls. Furthermore, this reduction was age-dependent, suggesting that the deletion of CSE has an impact on mitochondria biogenesis, which may then affect mitochondrial function.

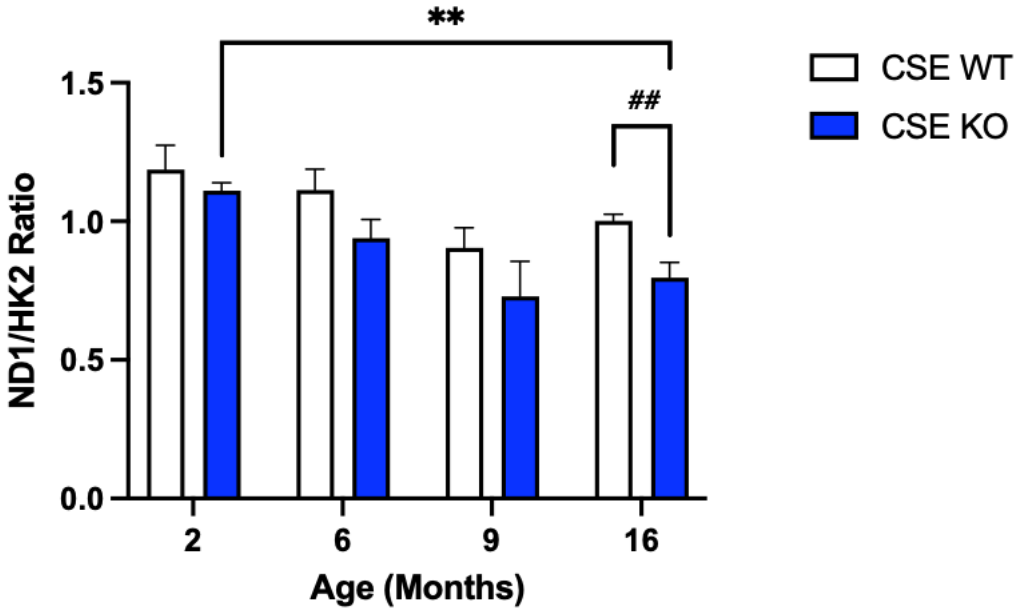

Figure 4.4 Decreased mitochondria content in older CSE$^{-/-}$ mice.
The mtDNA content, indicative of mitochondrial biogenesis, was reduced at 16 months as compared to the controls and 2 months CSE$^{-/-}$ mice. Data mean ± SEM. n= 6. Two-way ANOVA ** p<0.01 vs 2 months CSE$^{-/-}$ mice, ## p<0.01 vs age-matched controls.

4.2.4 Cardiac mitochondrial respiration and OXPHOS are affected in CSE$^{-/-}$ mice

Being the most metabolically demanding organ in the body, the heart relies on the ATP produced by OXPHOS for its optimal function (Rosca and Hoppel, 2010). Healthy mitochondria bioenergetics is essential for maintaining metabolic and cardiovascular functions, especially in age-related diseases (Dai, Rabinovitch and Ungvari, 2012). Moreover, the CSE/H_2S pathway has been shown to regulate mitochondria functions by stimulating ATP generation and enzymatic activity of the ETC (Módis *et al.*, 2016). To investigate the role of CSE in regulating cardiac mitochondrial activity, the bioenergetics

functions of isolated cardiac mitochondria were determined at different timepoints, at 2, 9 and 16 months, using the Seahorse-Agilent technology.

The ability of cardiac mitochondria to oxidise substrates, specifically pyruvate, at complex I was determined by calculating mitochondrial respiratory control ratio (RCR), based on the oxygen consumption rates representative of state 3 and state 4_o. State 3 and state 4_o respiration represents ADP and non-ADP dependent respiration respectively (Brand and Nicholls, 2011). As shown in Figure 4.5A, the mitochondrial RCR in response to pyruvate was significantly reduced in $CSE^{-/-}$ mice at baseline compared to $CSE^{+/+}$ mice. In addition, we found that there was an age-dependent reduction in the mitochondrial ability to oxidise pyruvate with CSE deletion. These results indicated that without CSE, the mitochondria were less able to respire and sustain ATP-dependent energetic demands. Next, the ability of cardiac mitochondria for succinate oxidation at complex II was determined in the presence of rotenone, a complex I inhibitor (Figure 4.5B) (Boutagy *et al.*, 2015). The mitochondrial RCR in response succinate in $CSE^{+/+}$ and $CSE^{-/-}$ mice showed no significant differences. However, we observed age-related changes in the mitochondrial RCR at complex II. As shown in Figure 4.5B, the RCR reduced by approximately 20% at 16 months as compared to 2 months in the wild-type controls. Interestingly, in the $CSE^{-/-}$ mice, the RCR increased approximately 30% at 9 months compared to baseline, but subsequently reduced to similar levels to the 2-month baseline at 16 months. The overall RCR of complex I is much higher than that of complex II, suggesting that the cardiac mitochondria have a higher capacity for pyruvate substrate oxidation than using succinate as sole substrate. Taken together, these results suggest that CSE plays a key role in regulating mitochondrial respiration at complex I but not at complex II. Next, we investigated the protein levels total OXPHOS enzymes of the isolated cardiac tissue using western blot analysis. We found that the expression of OXPHOS was significantly decreased in the heart tissue of $CSE^{-/-}$ mice at different timepoints compared to the wild-type controls (Figure 4.5C, D).

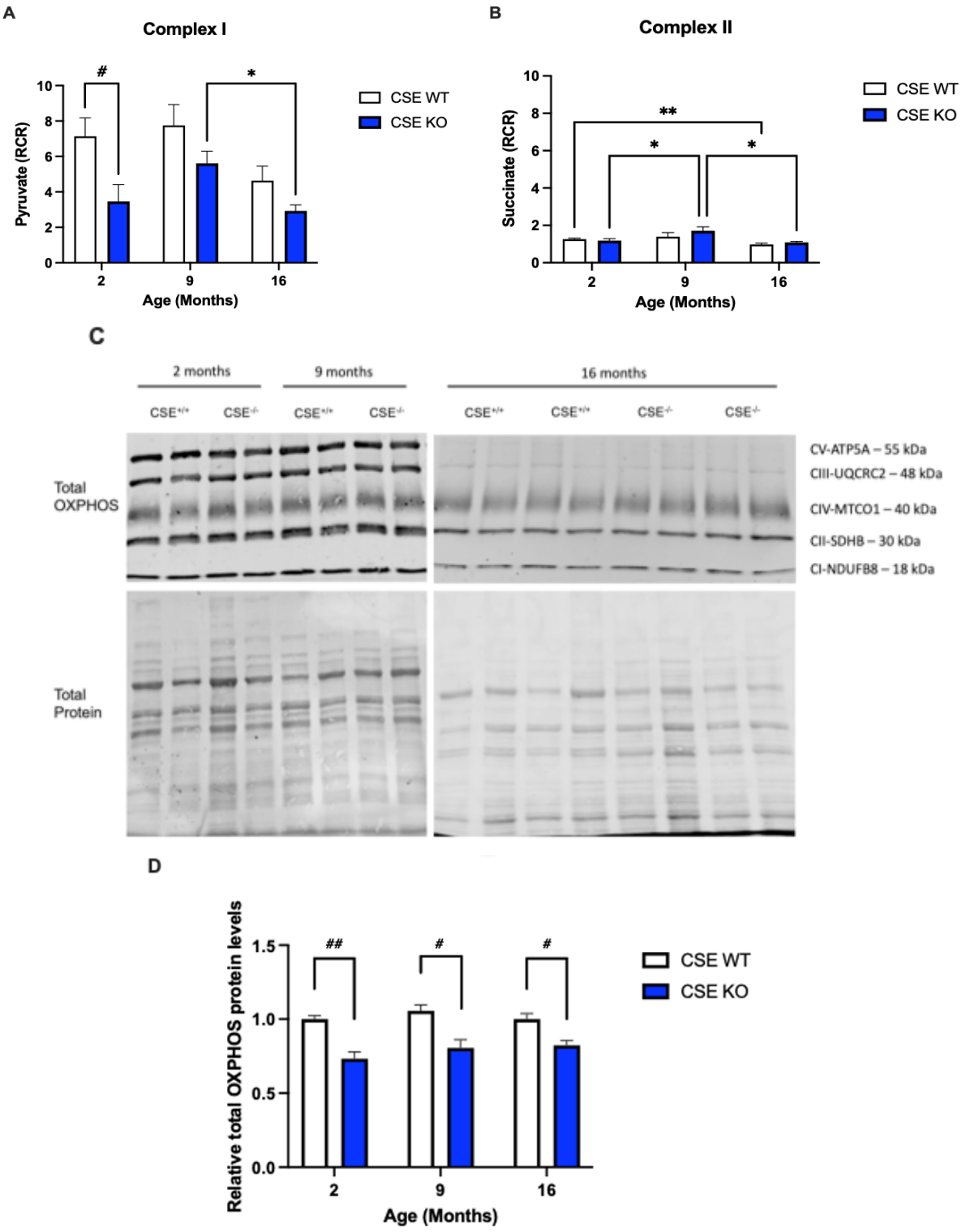

Figure 4.5 Loss of CSE affects cardiac mitochondria respiration in Complex I. Mitochondria oxygen consumption was calculated using respiratory control ratio (RCR) of **(A)** pyruvate and **(B)** succinate as substrates in complex I and II respectively. **(C)** Western blot densitometric analysis of total OXPHOS protein band (Complex I – V) normalised to intensity of total protein staining. **(D)** Total OXPHOS proteins was significantly reduced in $CSE^{-/-}$ mice. Data mean ± SEM. n= 5-8. Two-way ANOVA * $p<0.05$, ** $p<0.01$ between different time points and # $p<0.05$, ## $p<0.01$ vs $CSE^{+/+}$ mice.

4.2.5 Dysregulation of cardiac mitochondrial dynamics in $CSE^{-/-}$ mice

Mitochondria dynamics, which refers to the process of biogenesis, fission, fusion and mitophagy, is particularly important for cardiomyocytes. Impairments in mitochondrial dynamics is implicated in structural heart diseases including CM (Morciano *et al.*, 2023). Fission and fusion of mitochondria was evaluated by studying the expressions of proteins involved in these processes, including mitofusins (Mfn1 and Mfn2) in the outer mitochondrial membrane (OMM) and cytosolic GTPase dynamin-related protein 1 (Drp1) that is recruited to the OMM to regulate fission, in the cardiac tissues of younger (2 months) and older (16 months) $CSE^{+/+}$ and $CSE^{-/-}$ mice. Furthermore, PINK1 and Parkin mitophagy pathway, which is involved in the process of selective removal of damaged or dysfunctional mitochondria to preserve cellular function and integrity, was also investigated.

Gene expression of fusion protein Mfn1 was not only significantly reduced in the $CSE^{-/-}$ mice at 16 months when compared to the baseline but was also significantly lesser than $CSE^{+/+}$ mice (Figure 4.6A). Furthermore, the protein levels significantly depleted by approximately 75% in both age groups with the loss of CSE (Figure 4.6A and D). Similarly, the mRNA levels of Mfn2 in $CSE^{-/-}$ mice were almost halved at both ages and protein levels showed a marked reduction at 2 months (Figure 4.6B and E). This suggests that mitochondrial fusion was significantly reduced with CSE deletion, affecting both Mfn1 and Mfn2. There was also significant decrease in Drp1 protein levels at 2 months and 16 months when CSE is not present, indicative of reduced fission in the cardiac mitochondria at basal conditions (Figure 4.7). It could be mean that the $CSE^{-/-}$ hearts would not be able to cope when under circumstances where there are extreme energy demands, for instance during pregnancy or diabetes, as the cardiac mitochondria could not undergo fission and fusion as required and thus, resulting in cardiac failure.

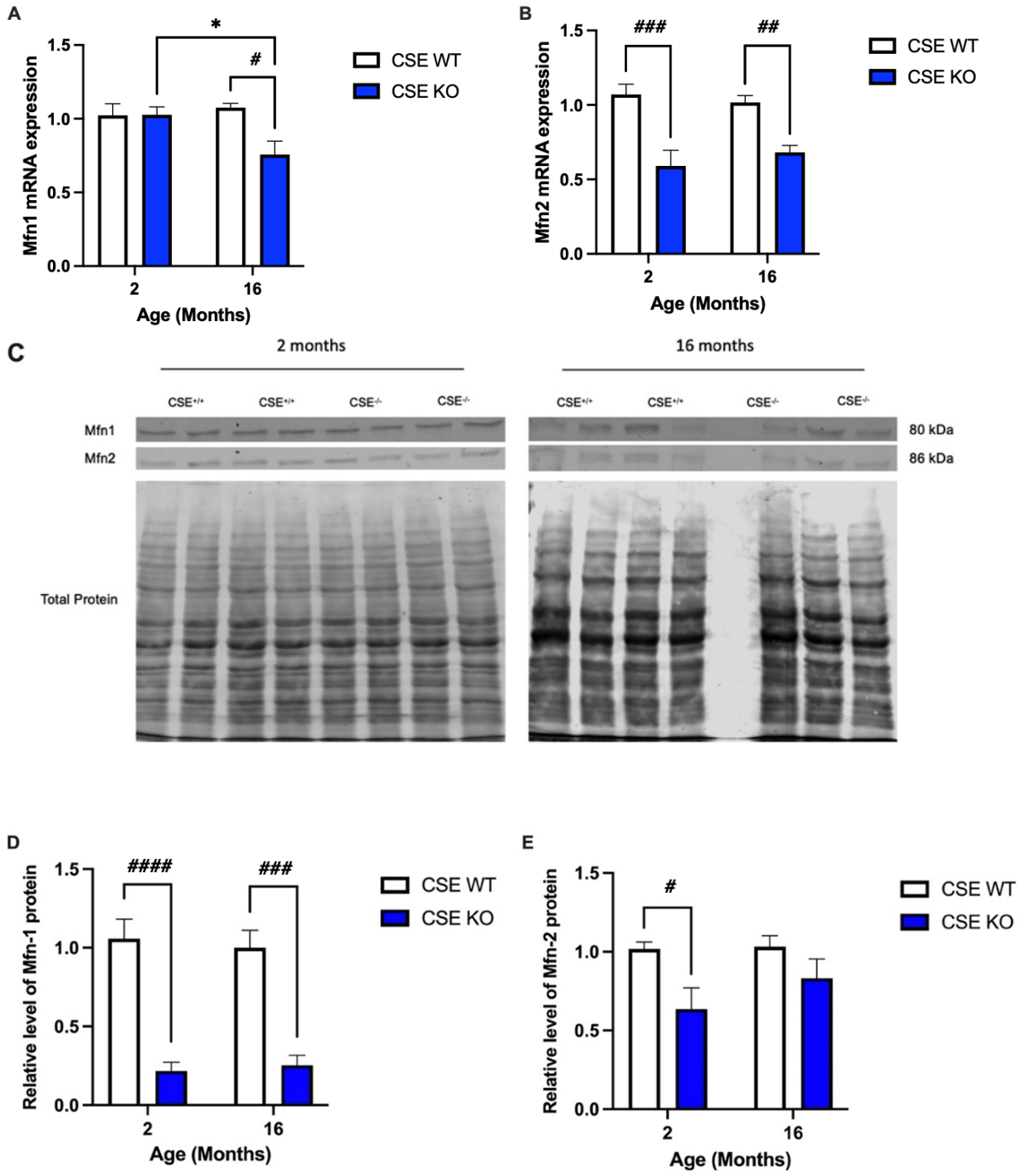

Figure 4.6 Decreased fusion in cardiac mitochondria when CSE is not present.
mRNA expression of (A) Mfn1 was significantly decreased in older CSE$^{-/-}$ mice whereas (B) Mfn2 gene expression remains unchanged in both ages. (C) Densitometry analysis on blots showing reductions in protein levels of (D) Mfn1, but not (E) Mfn2, relative to the total protein loaded. Results are mean ± SEM (n=4). Significance determined by two-way ANOVA whereby * $p<0.05$ between time points and # $p<0.05$, ## $p<0.01$, ### $p<0.001$ and #### $p<0.0001$ vs controls.

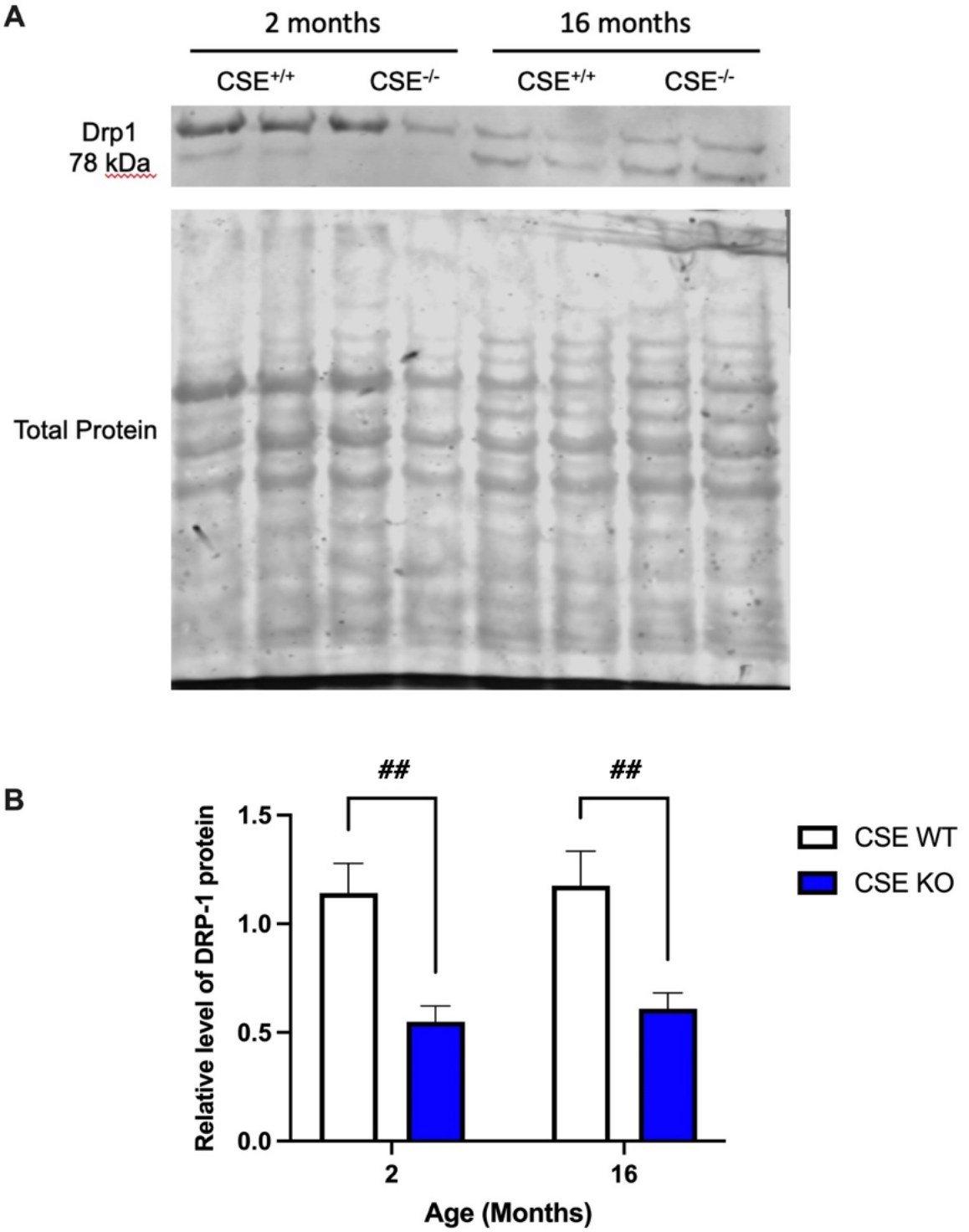

Figure 4.7 Reduced mitochondrial fission in cardiac tissue with the loss of CSE.
Protein levels of Drp1 in isolated heart tissue in 2 and 16 months was measured using densitometry analysis, normalised to total proteins loaded, on western blots n=4-6. Data mean ± SEM, statistical analysis using two-way ANOVA ## $p<0.01$.

Mitophagy is the process of clearance of damaged mitochondria through autophagy, mediated by PINK1/Parkin signalling pathway. After mitochondrial fission occurs to segregate the damaged mitochondria, PINK1 accumulates on the depolarised surface, phosphorylate Ser65 to trigger Parkin translocation and activation to induce mitophagy (Youle and Narendra, 2011). Dysregulation in this pathway could cause mitochondrial and cardiac dysfunction due to accumulation of defective mitochondria, leading to HF (Morales *et al.*, 2020). As shown in Figure 4.8, PINK1 mRNA expression markedly increased by an estimate of 40%, in the absence of CSE at 16 months. However, CSE deletion did not change the PINK1 protein levels, suggesting that post-translational modification could be affected. Preliminary data in Figure 4.9 shows the reduction in Ser65 proteins in 2 months $CSE^{-/-}$ mice by immunofluorescence staining, which indicated a marked decrease in Parkin ser65 phosphorylation upon PINK1 activation when CSE is not present. However, although the mRNA levels of Parkin showed an increasing trend in $CSE^{-/-}$ mice, it did not show significant difference (Figure 4.10A). Preliminary immunofluorescence staining of the Parkin proteins in 2 months heart remained unchanged as well.

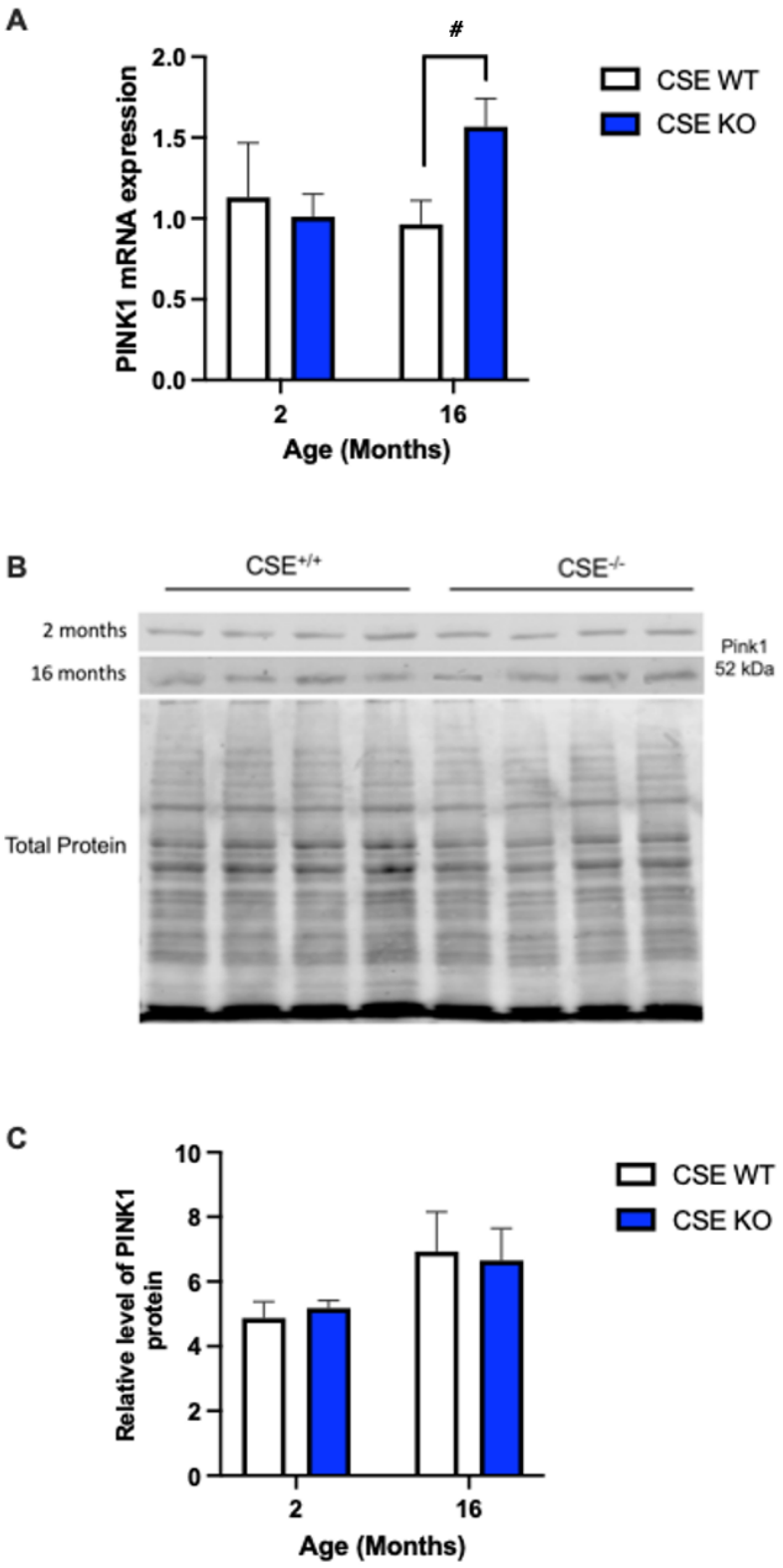

Figure 4.8 Increased PINK1 mRNA expression, but not protein levels, in 16 months CSE$^{-/-}$ mice. PINK1 **(A)** gene expression significantly upregulated in 16 months CSE$^{-/-}$ mice whereas their **(B-C)** protein levels showed no changes. Data mean ± SEM, statistical analysis using two-way ANOVA # $p<0.05$.

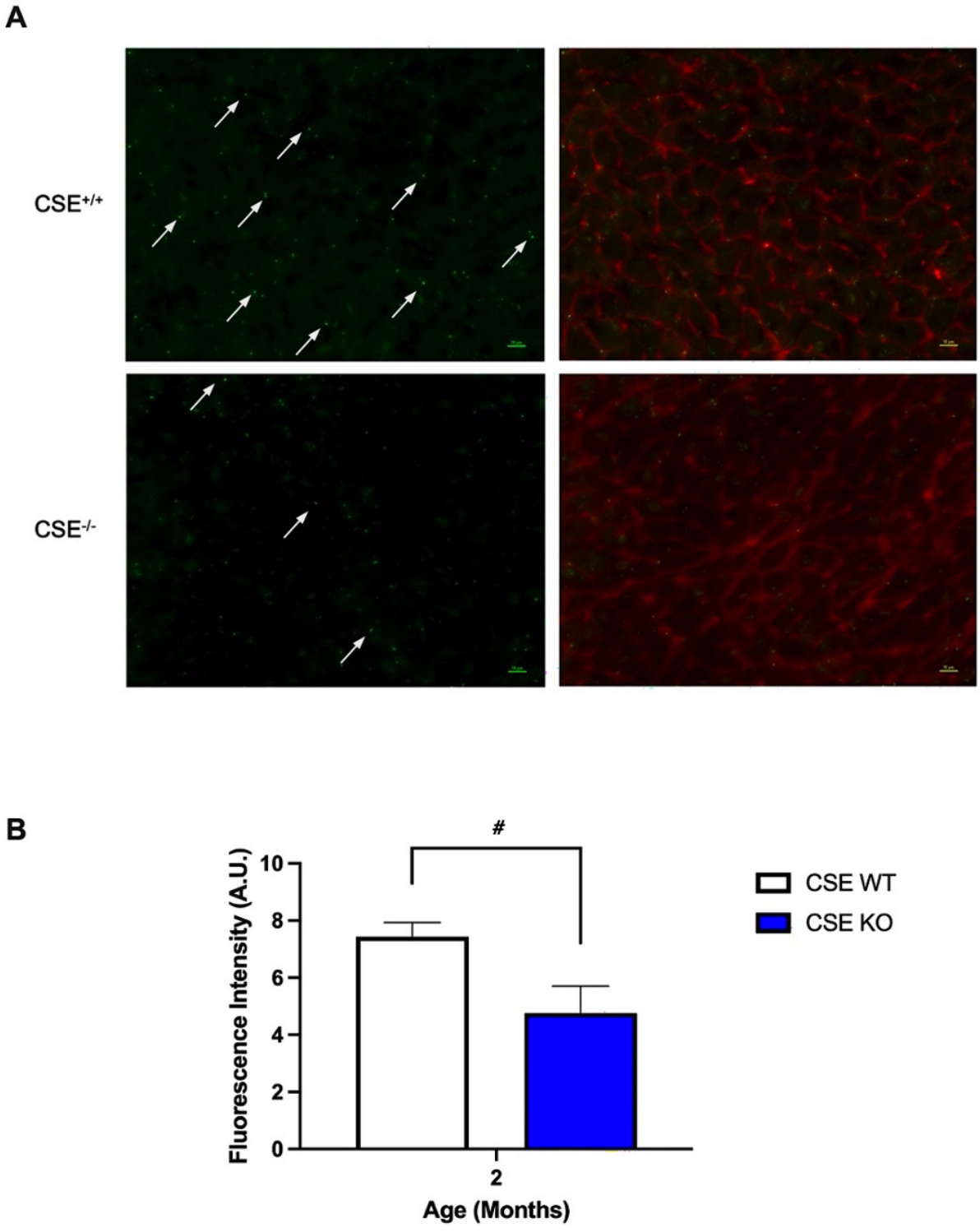

Figure 4.9 PINK1 phosphorylation of Parkin Ser65 was reduced in CSE$^{-/-}$ mice.
Preliminary data (n=2) showing the protein expression of Ser65, as reflected by fluorescence intensity. WGA (red) to identify cardiomyocyte borders and phospho-Parkin (Ser65) antibody (green) to identify Ser65 localisation (as shown by the arrows). Data expressed as mean ± SEM, Mann-Whitney test # $p<0.05$.

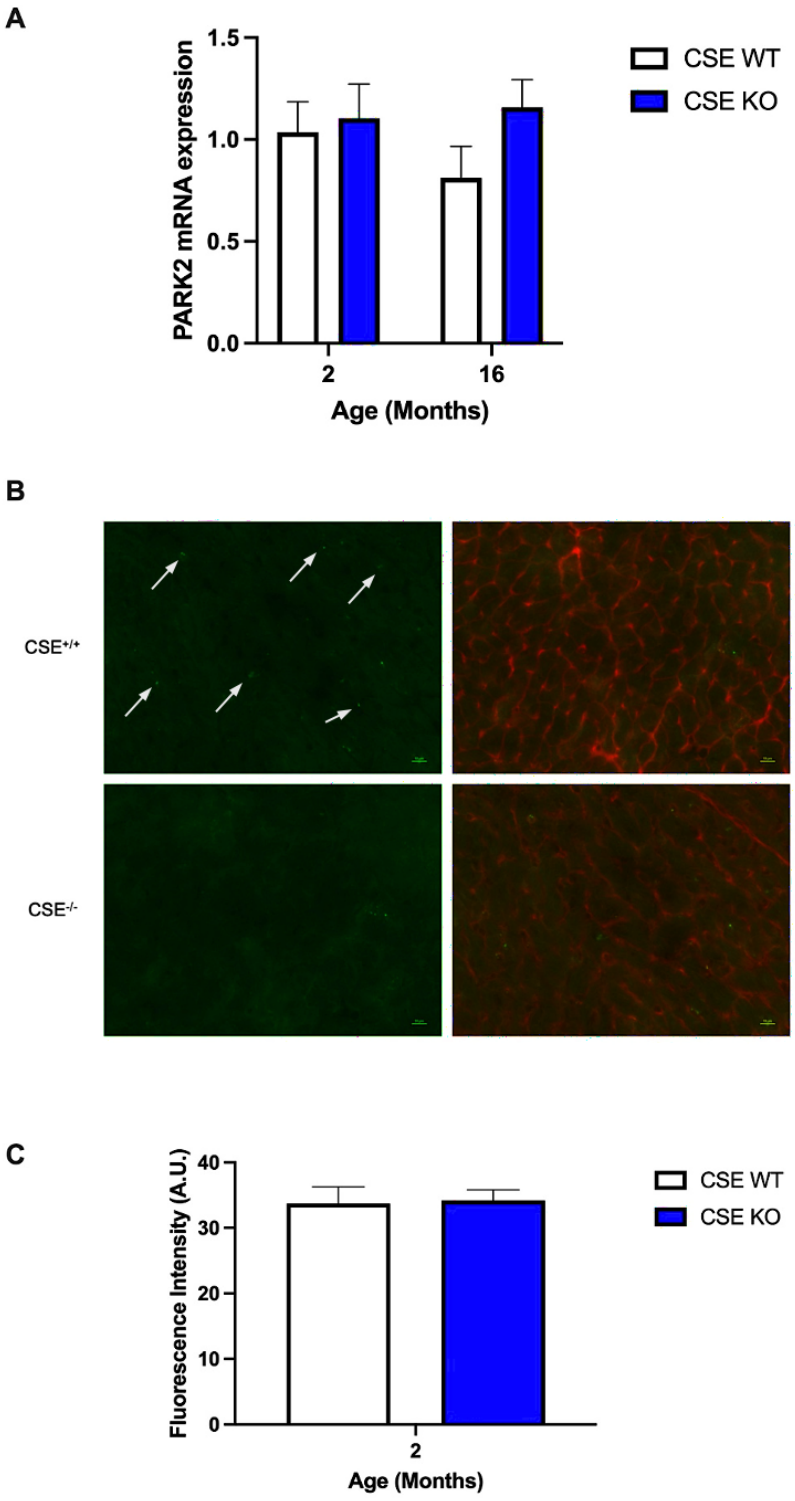

Figure 4.10 mRNA and protein levels of Parkin showed no difference between the two genotypes.
(A) Park2 mRNA expression (n=6) and **(B-C)** immunofluorescence staining of Parkin proteins (n=3) measured by the fluorescence intensity did not change with the loss of CSE. WGA (red) to identify cardiomyocyte borders and anti-Parkin antibody (green) to identify Parkin localisation (as shown by the arrows). Data expressed as mean ± SEM and two-way ANOVA or Mann-Whitney test was used for statistics for mRNA expression and fluorescence intensity respectively.

4.3 Discussion

HF manifests as a final stage of many CVDs, including CMs. Cardiac performance relies on proper regulation of cellular mechanisms and pathways in the cardiomyocytes, as they are the main regulators of myocardial contraction. Cellular phenotypic transformation in cardiomyocytes, endothelial cells and fibroblasts is induced during the progression of HF, leading to reduced contractility and myocardial fibrosis caused by abnormal ECM remodelling (Zhu *et al.*, 2022). Furthermore, altered Ca^{2+} handling and mitochondria dysfunctions were also associated with HF (Gorski, Ceholski and Hajjar, 2015). These mechanisms are chemically linked as EC coupling is one of the most energy consuming processes in the heart, and mitochondria is the main supplier of ATP to maintain this myocardial energetics (Pinz *et al.*, 2011). Profound cardiovascular functional and structural changes were seen in the previous study (Chapter 3), reflecting the importance of CSE/H_2S pathway in maintaining normal myocardial functions. In this study, we explored the effects of CSE at the cellular level, and how its deletion would impact cardiomyocytes, calcium signalling and the cardiac mitochondria at younger 2 months and older 16 months age. It is evident that the cardiac dysfunction could be due to cardiomyocyte hypertrophy, reduced SERCA2a and altered mitochondria functions and dynamics with the global deletion of CSE in the heart.

4.3.1 CSE deletion results in cardiomyocyte hypertrophy

Cardiac hypertrophy often precedes HF as a response to the increased workload and is characterised by LV wall thickening and cardiomyocyte hypertrophy. Indeed, structural changes in the cardiomyocytes from $CSE^{-/-}$ mice showed significant hypertrophy as reflected by the increased size and reduced number in the present study. Previously, Gong *et al.* (2022a) also found similar enlargement of cardiomyocytes in CSE KO diabetic mice, along with exacerbated CM and severe fibrosis from the increased deposition of interstitial and perivascular collagen. In a heart regeneration model using neonatal mouse, CSE inhibition

resulted in reduced proliferation of cardiomyocytes due to ROS-induced cellular damage and fibrosis (Pei *et al.*, 2020). Moreover, the upregulation in AT1 gene expression at 16 months further supported the hypertrophic phenotype of $CSE^{-/-}$ hearts. Zou *et al.* (2004) demonstrated that AT1 receptor can be activated to induce cardiomyocyte hypertrophy *in vivo* and *in vitro* by converting mechanical stress from pressure overload into biochemical signals. This was shown to be orchestrated by the increased angiotensin II (Ang-II), a vasoconstrictor, in both pressure and volume overload mouse models (You *et al.*, 2018). Likewise, cardiac hypertrophy models showed upregulated Ang-II content, accompanied by marked reductions in CSE expression and endogenous H_2S levels (Hu *et al.*, 2021). H_2S administration was found to reduce the binding affinity of AT1 and Ang-II to inhibit downstream signalling by Ang-II, hence alleviating hypertension and reducing oxidative stress (Zhao *et al.*, 2008; Al-Magableh, Kemp-Harper and Hart, 2015). Taken together, this finding suggests that loss of CSE-induced hypertrophy could be associated with AT1 and the renin-angiotensin system.

Interestingly, there was an increase in both the capillary density and capillary/cardiomyocyte ratio with the loss of CSE. The results in this study were contradictory to what was usually observed in HF, where there would be reduced capillary density and angiogenesis due to low levels of circulating H_2S and downregulation in VEGF (Cai *et al.*, 2007; Mohammed *et al.*, 2015). One possible explanation for the increased capillary density is that the heart could be in the compensatory hypertrophy phase. It was shown that angiogenesis plays a crucial role in the development of cardiac hypertrophy in a TAC mouse model as the increased number of micro vessels per cardiomyocyte preserved cardiac functions (Sano *et al.*, 2007). However, our results may also indicate the presence of pathogenic capillary growth in $CSE^{-/-}$ hearts, as previously shown in a coronary ischemic congestive HF rat model (Chen *et al.*, 2015). Unlike normal angiogenesis, this increased capillary density was caused by ischemia-reperfusion induced inflammation and pressure overload, with changes in morphology such as narrower lumen, irregular arrangement,

increased bifurcations with significantly shortened capillary segments (Chen *et al.*, 2015). Previous studies by our lab in pregnancy also showed similar increasing trend in capillary density, coupled with hypertension and systolic dysfunction, in the $CSE^{-/-}$ mice. In our study, the increased capillary density could be due to loss of CSE-induced inflammation (Chapter 5). Therefore, although there was increased capillary-to-cardiomyocyte ratio, which may arise from the presence of compensatory hypertrophy in mature hearts, the capillaries could be functionally defective. This finding suggests that capillary density does not necessarily correlate to improved myocardial functions, as there could be impaired perfusion and lack of tissue oxygenation. Further research using electron microscopy would be needed to study the changes in capillary microarchitecture to further support the cardiac dysfunction.

4.3.2 Loss of CSE disturb cardiac mitochondria respiration and mitochondrial dynamics

Mitochondria play a crucial role in providing energy for cellular functions, especially in the cardiovascular system. Defective mitochondria are commonly associated with myocardial dysfunction and have been implicated in various CVDs, leading to energy deficits, impaired contractility and myocyte death (Morciano *et al.*, 2023). Cardiac metabolism depends on the bioavailability of substrates in its environment, such as fatty acids, glucose, lactate, amino acids or ketones (Stanley, Recchia and Lopaschuk, 2005). OXPHOS is responsible for over 95% of the ATP production in the heart. Under physiological conditions, fatty acid oxidation contributes to 60–90% of the energy, while pyruvate oxidation accounts for the remaining 10–40% (Tham *et al.*, 2015). However, substrate switch occurs during LVH and HF, where substrate metabolism shifts away from fatty acid oxidation to glucose oxidation for more efficient ATP production (Taegtmeyer, 2002). This metabolic alteration affects mitochondria function, reduces overall ATP generation, and increases ROS production.

The results here showed that CSE deficiency induced mitochondrial dysfunction in the heart, characterised by reduced biogenesis, bioenergetics, and dynamics. Reduced mitochondria ETC efficiency, as reflected by lower RCR in isolated mitochondria, was observed in the $CSE^{-/-}$ hearts at 2 months in response to pyruvate, a complex I substrate. This indicated that $CSE^{-/-}$ mitochondria were less able to respire and sustain ATP-dependant energetic demands, potentially driven by the reduced total OXPHOS protein levels and mitochondrial content in the $CSE^{-/-}$ hearts. The decrease in mitochondrial proteins expression suggests the reduced activity of complexes, and therefore leading to lesser OXPHOS and energy production capacity to meet cardiac energy demand, causing HF. Interestingly, the RCR in response to succinate, which reflects complex II respiration, was not significantly different between the $CSE^{+/+}$ and $CSE^{-/-}$ mice, suggesting that complex II function may be preserved in CSE-deficient hearts. Previous findings from our lab also observed that RCR of $CSE^{-/-}$ pregnant mice, but not the controls, was significantly decreased due to the marked reductions in active state 3 respiration. This may suggest that the CSE-mediated reductions could be stress-related, as pregnancy is an energy-demanding condition. Using a cardiac ageing rat model, Tatarkova *et al.* (2011) found that the activities of complexes only significantly decreased in 26 months old senescent mice, with complex IV being most affected and followed by complex I. They saw no differences in 6 months adult mice and 15 months old-age mice, which supported our results above. Interestingly, Brandt *et al.* (2017) also found no age-related changes in respiratory rates and ATP production between young (approx. 5 months) and old (approx. 18 months) isolated mouse cardiac mitochondria. This was accompanied by little or no changes in mitochondria morphology levels of antioxidants and production of hydrogen peroxide.

Complex I, also known as proton-pumping NADH-ubiquinone oxidoreductase, serves as the entry-point of the mitochondria transport chain for NADH (Wirth *et al.*, 2016). On the other hand, Complex II, an enzyme known as succinate dehydrogenase, acts as the connection between the ETC and tricarboxylic acid (TCA) cycle, facilitating electron transfer

of flavin adenine dinucleotide ($FADH_2$) (Stepanova *et al.*, 2016). In line with previous findings, Wüst *et al.* (2016) reported a substantial reduction in the OXPHOS capacity of the mediated by complex I and complex II in cardiac hypertrophy and HF. Notably, they also showed that the complex I protein content was significantly diminished, while complex II less affected, supporting our results. However, other studies on chronic HF have stated that the poor quality of complex I, rather than its density, may be the reason for the disease progression (Scheubel *et al.*, 2002; Wüst *et al.*, 2016). Our lab has previously observed disturbances in mitochondrial bioenergetics in CSE-silenced HUVEC cells, leading to enhanced glycolysis and ROS generation. This indicates that H_2S modulates endothelial functions through metabolic signalling (Sanchez-Aranguren *et al.*, 2020a). The dysregulation of the CSE/H_2S pathway may contribute to increased ROS levels, which could potentially lead to the mitochondria dysfunction in cardiomyocyte observed in this study.

In addition, Ca^{2+} signalling is reduced in the cardiomyocytes of $CSE^{-/-}$ mice. Ca^{2+} homeostasis, controlled by EC coupling in ventricular myocytes, is crucial in vascular smooth muscle tone and cardiac systolic-diastolic function as it affects both myocardial contraction and electrical activity of the heart (Huang *et al.*, 2018). Defective Ca^{2+} signalling was shown to be a hallmark of cardiac hypertrophy and cardiac dysfunction (Roderick *et al.*, 2007). SERCA is one of the main Ca^{2+} handling proteins located in the SR that is responsible for the removal of Ca^{2+} during relaxation and its deficiency is associated with HF (Lyon *et al.*, 2011). Reduction in SERCA2a activity could lead to impaired relaxation and Ca^{2+} overload in the cytosol as the intracellular Ca^{2+} was not removed efficiently into the SR (Zhang *et al.*, 2018; Røe *et al.*, 2019). Our current results demonstrated that SERCA2a, the main isoform that is found in the heart, was significantly downregulated with the loss of CSE in both ages. This explained the systolic and diastolic dysfunction seen in the previous chapter in $CSE^{-/-}$ mice. Hence, when Ca^{2+} signalling in the heart is hampered by dysregulation of the CSE/H_2S pathway, cardiac function and contractility are compromised.

Furthermore, cardiac Ca^{2+} dynamics is intricately linked with mitochondria and its ATP production (Williams, Boyman and Lederer, 2015). The coordination between mitochondria and Ca^{2+} signalling in the SR is crucial in maintaining cellular energy balance, modulating contractility, and regulating cell survival. Their interdependent relationship is dependent on SR Ca^{2+} stimulating ATP synthesis in the mitochondria during EC-coupling by enhancing the activity of key enzymes involved in the ETC. Accordingly, 30 to 40% of the ATP produced is used to drive Ca^{2+} cycling whereas the remaining is used to fuel cardiac contraction (Stanley, Recchia and Lopaschuk, 2005; Dorn II and Maack, 2013). Intracellular Ca^{2+} was found to be responsible for inducing CSE translocation into the mitochondria to increase both H_2S and ATP production in the mitochondria under stress conditions via Tom20 (Fu *et al.*, 2012). Therefore, in this case, mitochondrial ATP production was affected with the loss of CSE due to changes in Ca^{2+} signalling.

Recently, it was also found that the overexpression of SERCA enhanced mitochondrial quality control and protected microcirculation against I/R damage (Tan *et al.*, 2020). Conversely, regulation of mitochondria dynamics is equally pivotal in maintaining Ca^{2+} homeostasis as well. Chen *et al.* (2012) reported the importance of fusion protein, Mfn2, as a physical contact in SR-mitochondria Ca^{2+} interaction in mouse cardiomyocytes. Mfn2 KO hearts displayed changes in mitochondria morphology, impaired SR-mitochondria tethering, reduced mitochondria bioenergetics and increased ROS production. In our study, the reduced Mfn2 expression with CSE deletion could also in turn affect Ca^{2+} regulation. We speculated that impaired mitochondria dynamics may precede defective Ca^{2+} regulation by SERCA2a. Therefore, alterations in SR-mitochondria Ca^{2+} modulation will result in dysregulation in energy supply and demand in the heart, exacerbating myocardial oxidative stress in failing hearts.

Indeed, mitochondria biogenesis, dynamics, including fission, fusion and mitophagy were dysregulated in the heart of $CSE^{-/-}$ mice. The decrease in mitochondria content could

either result from reduced biogenesis or dynamics (Ishihara *et al.*, 2015). Reduced mtDNA replication and subsequent loss of mtDNA encoded proteins, resulted from oxidative stress-induced DNA damage are associated with CM and HF in human (Karamanlidis *et al.*, 2010). Impaired mitochondrial biogenesis is also a constant feature of cardiac remodelling and HF, regardless of the underlying aetiology and disease progression stages (Pisano *et al.*, 2016). During the pathogenesis of HF, expression levels of PGC1α, the master regulator of mitochondria biogenesis, is commonly reported to be downregulated, which contributes to mitochondrial dysfunction in rodent models (Arany *et al.*, 2006). A previous study by Shimizu *et al.* (2018) using the same $CSE^{-/-}$ mouse model revealed significant depletion in mitochondria content due to markedly reduced PGC1α in the nucleus at 8 weeks, which was not observed in our present study. H_2S was found to induce biogenesis via AMPK activation, leading to deacetylation and phosphorylation of PGC1α in cardiomyocytes (Shimizu *et al.*, 2018).

Mitochondria dynamics, including fission, fusion and mitophagy, are highly interconnected to mitochondrial biogenesis (Morciano *et al.*, 2023). The delicate balance of these processes act as a quality control mechanism to maintain cellular homeostasis. Both reduced fusion and fission was observed in the $CSE^{-/-}$ mice, as reflected by decreased levels of OMM fusion protein Mfn1 and fission protein Drp1. CSE deficiency could cause disruptions in the mitochondria network and an accumulation of damaged mitochondria. Mfn1 and Mfn2 have been shown to play important roles in modulating cardiac mitochondrial respiration and morphology, and combined ablation of Mfn1 and Mfn2 resulted in small, round mitochondria with disorganised cristae and reduced oxygen consumption, leading to a sudden onset of progressive lethal DCM (Chen, Liu and Dorn, 2011). Moreover, it has been demonstrated that depletion in Mfn1 levels alone led to the development of smaller mitochondria, and a fragmented and disorganised mitochondrial network, which subsequently impaired the network excitability and electrical instability of cardiomyocytes in

HF animal models (Goh *et al.*, 2016; Wüst *et al.*, 2016). Notably, Mfn1, but not Mfn2, was found significantly reduced in failing hearts of non-responding patients with idiopathic CM (Hsiao *et al.*, 2021). Furthermore, this suppression led to metabolic dysfunction in cardiomyocytes, reduced cardiac functions and enhanced replacement fibrosis *in vivo* (Hsiao *et al.*, 2021). Interestingly, we showed that Mfn1 was more affected by CSE deletion compared to Mfn2, suggesting a regulatory role of CSE on Mfn1 and mitochondrial integrity in the heart.

In theory, mitochondrial fusion and fission has opposing effects as reduced fusion is typically accompanied by increased fission in disease states (Chen and Knowlton, 2011). Enhanced Drp1 activation or single mutation in Drp1, a GTPase crucial for mitochondrial fission, is associated with cardiac hypertrophy and chronic HF. Inhibition of Drp1 with mitochondrial division inhibitor-1 (midiv-1) reversed these response (Ashrafian *et al.*, 2010; Chang *et al.*, 2013). The loss of CSE decreased Drp1 gene expression levels in 16-month-old mice, indicating that the decrease in mitochondrial fusion was accompanied by reduced mitochondrial fission with CSE deletion. Reduced levels of Drp1 could indicate increased accumulation of defective mitochondria due to insufficient fission. Mitochondrial fission is linked to induction of mitophagy as dysfunctional mitochondria are segregated for degradation. These processes are essential in mitochondrial quality control (Twig *et al.*, 2008). Inhibition of fission has been shown to increase cellular apoptosis and hinder mitophagy in cardiomyocytes (Lee *et al.*, 2011b). Therefore, downregulation of Drp1 expression is likely to have a big impact on mitophagy in $CSE^{-/-}$ hearts, which will lead to the accumulation of larger, defective mitochondria in the cardiomyocytes.

Furthermore, another important mitophagy pathway, PINK1/Parkin signalling pathway, is affected by loss of CSE in the heart. Although there were no differences in the protein expressions of PINK1 and Parkin in the wild-type or $CSE^{-/-}$ mice, phosphorylation of Parkin at Ser65 residue was reduced in the heart tissue lack of CSE at 16 months. It has

been demonstrated that the phosphorylation at Ser65 by PINK1 plays a key role in the translocation of Parkin to the damaged mitochondria, and subsequently facilitates the mitophagy process (McWilliams *et al.*, 2018). Upregulation of SIRT1/PINK1/Parkin pathway by exogenous H_2S administration protects cardiomyocytes against cellular senescence in oxidative stress induced ageing (Hao *et al.*, 2022). Taken together, our data suggest that CSE/ H_2S pathway plays a crucial role in the mitochondrial quality control mechanisms. Dysregulation of this pathway may contribute to cellular stress in the heart and pathogenesis of CM.

4.3.3 Limitations

There were some limitations of using isolated mitochondria from tissues to quantify mitochondria dysfunction. Firstly, the *in vitro* properties of the isolated mitochondria might differ from their *in vivo* state. The isolation process itself could have disrupted the mitochondria network. Despite using optimal centrifugation speeds to preserve the mitochondrial membranes, there might have been potential changes in the membrane integrity with the loss of CSE. This could have influenced mitochondria sensitivity to centrifugation and thus impacted the integrity of the isolated mitochondria (Horan, Pichaud and Ballard, 2012). To address this, future studies could measure the RCR of mitochondria in cultured, permeabilised cardiomyocytes where mitochondria functions and structural interactions are preserved (Picard *et al.*, 2012). Furthermore, in the mitochondria dynamics section, 9-month mice were not assessed due their unavailability. Investigating changes at this time point is crucial as it signifies the onset of cardiac dysfunction in $CSE^{-/-}$ mice. The end number of animals should be increased for immunofluorescence staining of the respective proteins, extending the analysis to include 9- and 16- months mice as well.

5 Consequences of CSE deficiency on the cardiac gene expression

5.1 Introduction

CVDs are often caused by a combined influence of environmental and genetic factors, leading to disruptions in expressions of gene transcripts, proteins, molecular networks and the transcriptome itself (Kathiresan and Srivastava, 2012). These alterations subsequently affect cellular and physiological pathways, resulting in LV remodelling and dysfunction in the heart. Therefore, it is crucial to enhance our understanding of gene functions regulation in cardiac physiology and diseases. The underlying molecular events occurring in the heart when the CSE enzyme is not present is not fully understood. RNA sequencing (RNA-seq) has emerged as a valuable tool for investigating the underlying molecular mechanisms involved in the development and progression of CVDs. By utilising next-generation sequencing, RNA-seq allows the study of gene expression and identification of changes in the cellular transcriptome (Kukurba and Montgomery, 2015). The transcriptome refers to the complete set of RNA molecules present in a cell or tissue, which includes messenger-RNA (mRNA), non-coding RNA and small RNA molecules (Wang, Gerstein and Snyder, 2009). By analysing the transcriptome using RNA-seq, researchers can gain insights into the gene expression and its activity, identifying differentially expressed genes (DEGs) associated with the development of diseases at different stages (Adams, 2008). RNA-seq has been used for genetic testing in various diseases, including inherited CVDs like HCM, to establish correct prevalence of undiagnosed cases (Hata *et al.*, 2019). Liu *et al.* (2015) demonstrated the feasibility of using RNA-seq to classify disease status with an extremely small dataset. They sequenced LV tissues from six individuals (three controls, one with ischemic heart disease and two with DCM), identifying genes associated with HF, which were further validated in a larger cohort of 313 individuals with failing or non-failing hearts (Liu *et al.*, 2015). In addition, RNA-seq has proven effective in gene profiling in mouse hearts, enabling the detection of early changes in cardiac hypertrophy or HF (Matkovich *et al.*, 2010; Lee *et al.*, 2011a).

In the echocardiography study (Chapter 3), we observed pathological cardiac remodelling and functional alterations in global CSE deficiency with reduced H_2S biosynthesis, highlighting the significance of H_2S in the pathophysiology of CM. The CSE knockout-induced changes were primarily examined from 9 months onwards. Hence, it is important to improve the understanding of molecular mechanisms that contribute to CSE/H_2S pathway in heart, as this knowledge could pave the way for potential cardioprotective H_2S therapy. However, there are limited studies investigating transcriptome alterations related to the role of endogenous CSE in the heart. Recently, Huang *et al.* (2023) performed RNA-seq in isolated cardiomyocytes from CSE KO mice with HFpEF and reported significantly alterations in mitochondria function and metabolism pathways. Ellmers *et al.* (2020) compared gene networks in a myocardial infarction model between CSE wild-type and $CSE^{-/-}$ mice and found that expression levels of most genes were lower in $CSE^{-/-}$ mice compared to wild-type, suggesting the depletion of gene expression across the same gene network. However, there was no studies that directly compare the transcriptomic differences when there is loss of CSE in heart tissues. By leveraging the power of RNA-seq, we can gain deeper insights into cardiac transcriptomic alterations caused by the loss of endogenous CSE, potentially identify therapeutic target and biomarkers for diagnosis, prognosis and personalised treatment approaches involving H_2S.

We hypothesised that there is differential gene expression between $CSE^{+/+}$ and $CSE^{-/-}$ mice at baseline (2 months) and when $CSE^{-/-}$ mice start to exhibit cardiac dysfunction at 9 months. We expect that genes related to cardiac remodelling and dysfunction will undergo significant alterations, leading to cardiomyocyte hypertrophy and mitochondrial dysfunction as demonstrated in the previous chapter. The aim of this chapter is to identify molecular mechanism underlying the cardiac dysfunction in CSE deletion using RNA-seq. The significant pathways and genes involved were characterised, comparing changes in mRNA between younger (2 months old) and adult (9 months old) mice using transcriptome profiling of cardiac tissue from $CSE^{+/+}$ and $CSE^{-/-}$ mice. Gene set enrichment analysis (GSEA)

including gene ontology (GO) and Kyoto Encyclopaedia of Genes and Genomes (KEGG) pathways were used to examine the upregulated and downregulated DEGs. Moreover, important mRNA targets were validated by qPCR. To the best of our knowledge, this study represents the first RNA sequencing analysis of a CSE model in heart to compare young and adult mice.

5.2 Results

5.2.1 Gene expression in the hearts of $CSE^{+/+}$ and $CSE^{-/-}$ mice

DEG is essential for understanding the molecular basis of a disease. To determine the effect of CSE in the regulation of gene expression in hearts, DEG analysis was performed at 2 months (baseline) and 9 months (onset of cardiac dysfunction) in $CSE^{+/+}$ and $CSE^{-/-}$ mice. Table 5.1 and 5.2 showed all the significant DEGs that were affected by the loss of CSE. Interestingly, Gbp2b and Gm5900 genes were upregulated in 2 and 9 months $CSE^{-/-}$ mice, suggesting that the deletion of CSE enzyme directly affects these two genes. The complete DEG list is available in the supplementary materials. Volcano plots and clustering heatmaps were used to visualise the DEGs, using an adjusted p-value <0.05 and $\log_2$fold change >1 or < -1 (2-fold greater or lesser change in expression). A total of 26533 genes were identified from the heart samples in 2 months $CSE^{+/+}$ and $CSE^{-/-}$ mice and 24489 genes in the 9 months mice. In the 2-month group, only 7 genes (6 upregulated and 1 downregulated) showed significant expression changes in $CSE^{-/-}$ mice compared to controls (Figure 5.1). Similarly, at 9 months, 38 (12 upregulated and 26 downregulated) were significantly differentially expressed (Figure 5.3). The results indicate that loss of CSE leads to an increasing number of genes being dysregulated over time, and it is associated with the onset of cardiac dysfunction.

Clustering heatmaps provided a comprehensive overview of gene expression patterns and identified functionally related gene clusters. These genes were arranged in

rows and with the genotypes represented in the columns. Each cell in the heatmap corresponds to the expression level of a specific gene in a sample, colour-coded from red (highest expression) to blue (lowest expression). Heatmaps in figure 5.2 and 5.4 displayed dysregulated genes in $CSE^{-/-}$ mice compared to $CSE^{+/+}$ mice, with 7 DEGs at 2 months and 38 DEGs at 9 months.

Table 5.1 DEGs in 2 months cardiac heart tissue with global CSE deletion

Upregulated DEGs			
Gene	**log_2foldchange**	**padj**	**Gene description**
Gbp2b	8.55	7.89E-07	guanylate binding protein 2b
Nxpe4	5.12	3.18E-24	neurexophilin and PC-esterase domain family, member 4
Gm5900	3.74	0.015	predicted pseudogene 5900
Pdzd3	3.69	9.07E-07	PDZ domain containing 3
Cd59a	2.16	2.00E-21	CD59a antigen
Klra9	1.81	0.038	killer cell lectin-like receptor subfamily A, member 9
Downregulated DEGs			
Gene	**log_2foldchange**	**padj**	**Gene description**
Car3	-3.88	0.0014	carbonic anhydrase 3

Table 5.2 DEGs in 9 months cardiac heart tissue with global CSE deletion

Upregulated DEGs

Gene	log_2foldchange	padj	Gene description
Gbp2b	9.73	8.66E-12	guanylate binding protein 2b
Gm18190	5.99	0.048	predicted gene, 18190
Gm5900	4.74	6.70E-07	predicted pseudogene 5900
AC151284.2	3.19	0.050	microtubule-associated protein 7 (Map7) pseudogene
Ddc	3.16	0.021	dopa decarboxylase
Rpl34-ps1	2.98	8.07E-07	ribosomal protein L34, pseudogene 1
2610507I01Rik	2.92	0.002	RIKEN cDNA 2610507I01 gene
Nppa	2.21	0.0006	natriuretic peptide type A
Gramd1b	1.73	8.53E-06	GRAM domain containing 1B
Mfap1b	1.46	0.039	microfibrillar-associated protein 1B
Osbpl3	1.30	0.005	oxysterol binding protein-like 3
Eif3j1	1.25	0.039	eukaryotic translation initiation factor 3, subunit J1

Downregulated DEGs

Gene	log_2foldchange	padj	Gene description
Gm32171	-9.00	5.17E-09	predicted gene, 32171
Rpl29	-8.07	4.51E-63	ribosomal protein L29
Gm3650	-7.11	7.52E-11	predicted gene 3650
Rpl34	-7.03	5.70E-58	ribosomal protein L34
BC002163	-6.89	2.63E-38	cDNA sequence BC002163
Gm14085	-6.50	1.18E-22	predicted gene 14085
Gm44608	-6.12	0.002	predicted gene 44608
Pcna-ps2	-5.25	1.48E-15	proliferating cell nuclear antigen pseudogene 2
Gm6166	-4.63	6.93E-09	predicted gene 6166
Gm10709	-4.45	0.0009	predicted gene 10709
Gm7993	-4.41	5.88E-06	predicted gene 7993
Eif3j2	-3.87	1.27E-32	eukaryotic translation initiation factor 3, subunit J2
Slc15a2	-3.49	1.60E-09	solute carrier family 15 (H+/peptide transporter), member 2
Gm1821	-2.96	2.49E-07	predicted gene 1821
Gm10154	-2.78	1.75E-06	predicted gene 10154
Klra9	-2.40	0.032	killer cell lectin-like receptor subfamily A, member 9
Duoxa1	-2.35	0.039	dual oxidase maturation factor 1
Negr1	-2.21	0.033	neuronal growth regulator 1
Hba-a2	-1.89	0.0002	hemoglobin alpha, adult chain 2
Gchfr	-1.89	0.0003	GTP cyclohydrolase I feedback regulator
Hbb-bs	-1.87	0.002	hemoglobin, beta adult s chain
Hbb-bt	-1.82	0.0009	hemoglobin, beta adult t chain
Tent5c	-1.68	0.012	terminal nucleotidyltransferase 5C
Alas2	-1.47	0.005	aminolevulinic acid synthase 2, erythroid
mt-Nd3	-1.32	0.011	mitochondrially encoded NADH dehydrogenase 3
Gm5617	-1.26	0.043	predicted gene 5617

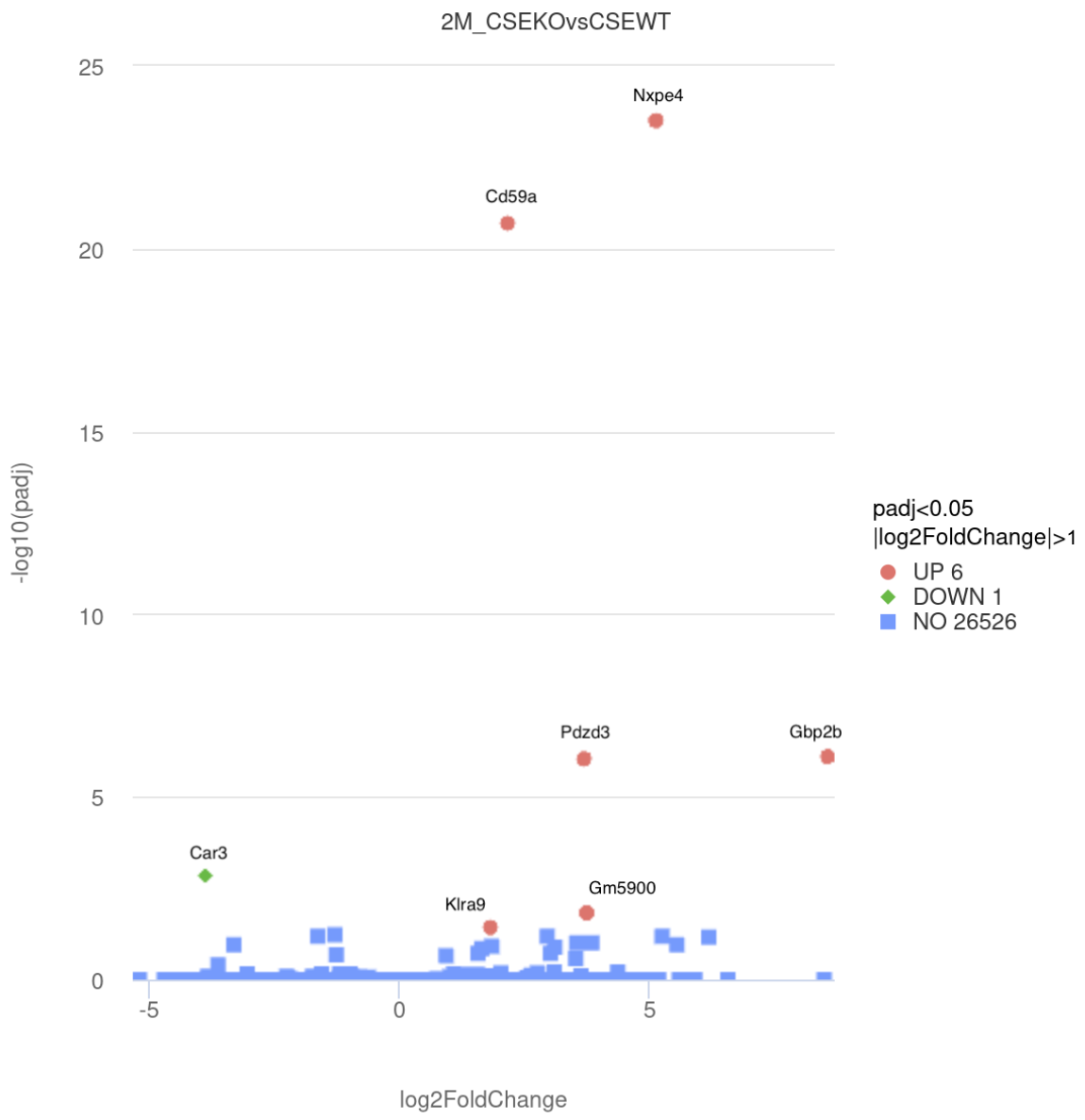

Figure 5.1 Volcano plot of DEGs between 2-month CSE$^{+/+}$ and CSE$^{-/-}$ mice hearts.
All detected transcripts in 2 months mouse hearts with $\log_2$(fold change) against -$\log_{10}$(p-adjusted) value. Each dot represents a DEG. Upregulated and downregulated DEGs with adjusted p-value < 0.05 and $|\log_2(\text{fold change})|$ >1 were indicated in red and green respectively.

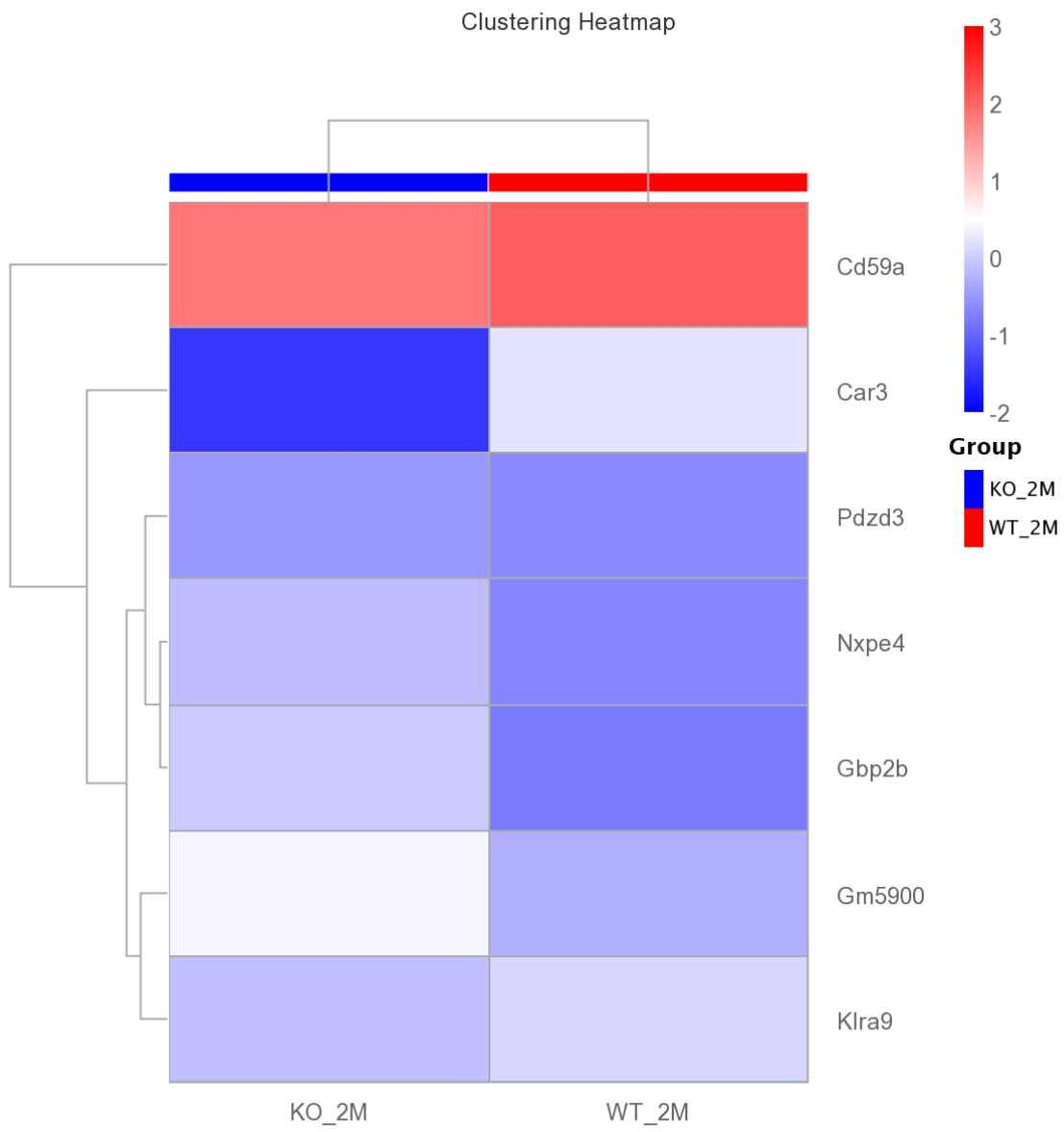

Figure 5.2 Clustering heatmap for 2 months mice showing up- and downregulated genes. Hierarchical clustering heatmap showing the expression patterns of DEGs in $CSE^{+/+}$ and $CSE^{-/-}$ mice, with the different genes on the y-axis and experimental conditions on the x-axis. The colour key represents the z-score which shows the degree of change, with the highest expression values (red) as upregulated and the lowest (blue) being those that were downregulated.

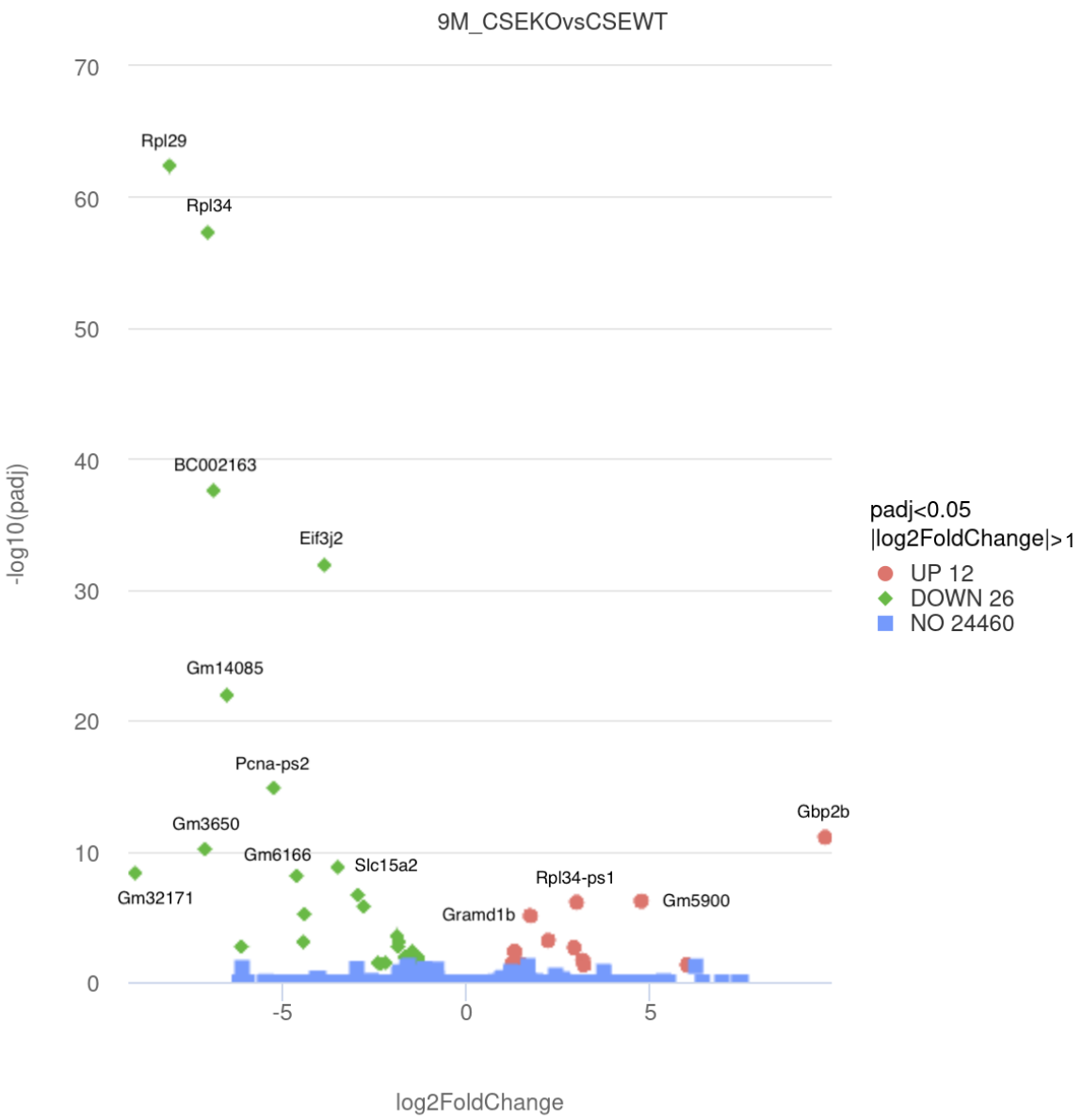

Figure 5.3 Volcano plot of DEGs between 9-month CSE$^{+/+}$ and CSE$^{-/-}$ mice hearts.
All detected transcripts in 9 months mouse hearts with $\log_2$(fold change) against -$\log_{10}$(p-adjusted) value. Each dot represents a DEG. Upregulated and downregulated DEGs with adjusted p-value< 0.05 and $|\log_2(\text{fold change})|$ >1 were indicated in red and green respectively.

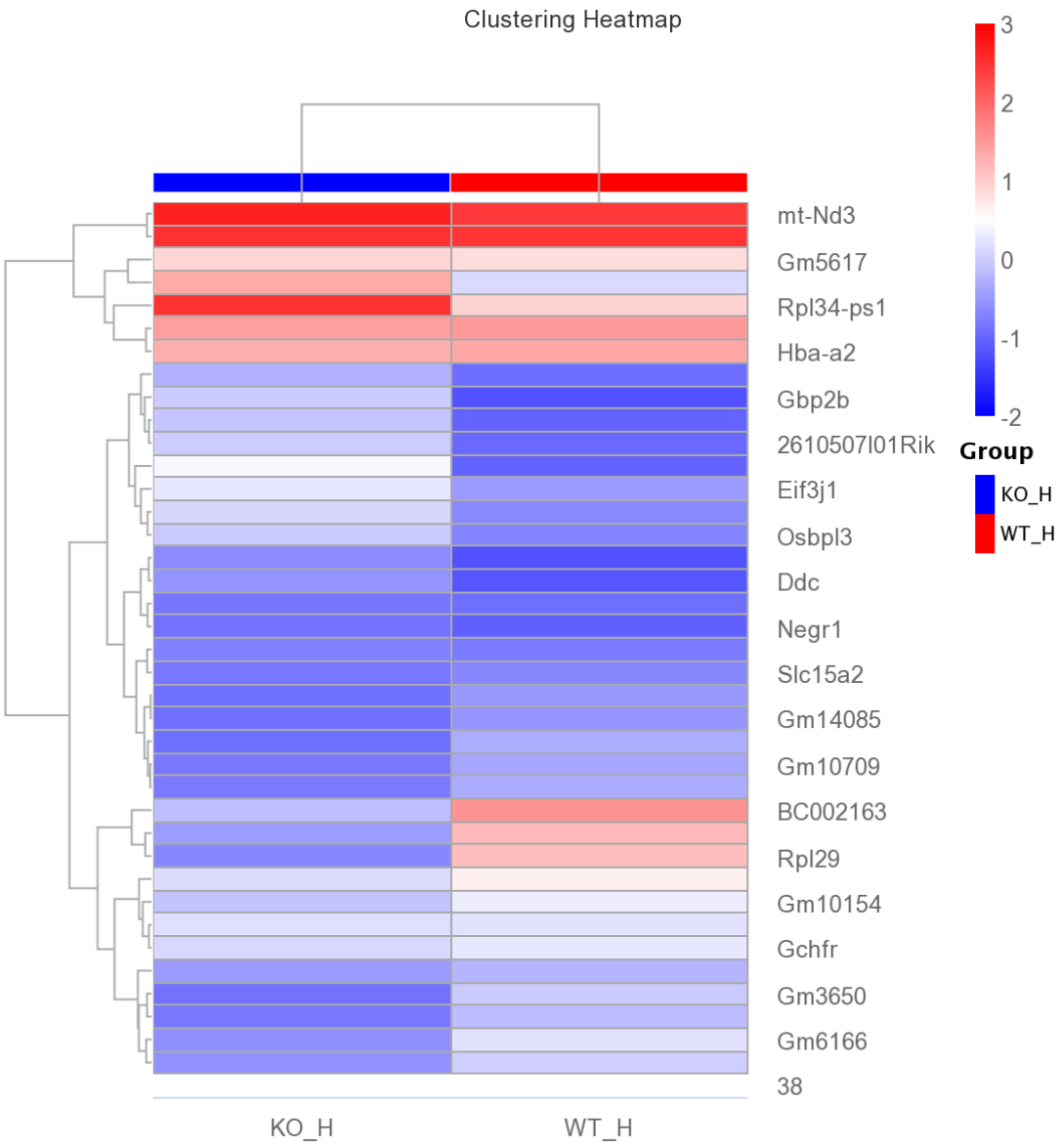

Figure 5.4 Clustering heatmap for 9 months mice showing up- and downregulated genes. Hierarchical clustering heatmap showing the expression patterns of DEGs in older $CSE^{+/+}$ and $CSE^{-/-}$ mice, with the different genes on the y-axis and experimental conditions on the x-axis. The colour key represents the z-score which shows the degree of change, with the highest expression values (red) as upregulated and the lowest (blue) being those that were downregulated.

5.2.2 Enriched GO analysis of DEGs in 2- and 9-months mice

To gain a better understanding of the biological response caused by the loss of CSE, GO analysis was performed (Young *et al.*, 2010). Depending on their functional roles, GO enrichment analysis of significantly enriched DEGs between $CSE^{+/+}$ and $CSE^{-/-}$ mice was categorised into biological processes (BP), cellular components (CC) and molecular functions (MF). The bar graphs depict all enriched GO terms in the different categories (Figure 5.5, 5.7, 5.9 and 5.11). Significantly enriched GO terms were determined based on an adjusted p-value <0.05, represented by red dots in the dot plots below. The x-axis displays the gene ratio, which is the ratio of the number of DEGs in the pathway to the total number of genes annotated in that pathway. A higher gene ratio indicates a greater degree of enrichment. The p value reflects the confidence level, with lower values indicating stronger results, and the size of the dots corresponds to the number of genes.

At 2 months, the GO analysis revealed that upregulated DEGs were implicated in 6 BP and 1 CC, while the downregulated DEG was associated with 71 BP. Among the upregulated BP, those related to cardiovascular inflammation stood out, including “response to type 1 interferon”, “pyroptosis” and “cellular response to interferon-alpha”. The only upregulated CC was “inflammasome complex”. The top 5 enriched GO terms for downregulated DEGs included “response to purine-containing compound”, “response to lipopolysaccharide”, “ageing”, “positive regulation of kidney development” and “ERK1 and ERK2 cascade”.

In comparison to the 2 months mice, the 9-month mice exhibited a larger number of enriched GO terms (padj< 0.05) due to a greater presence of DEGs. A total of 176 GO terms were significantly enriched, which includes 123 BP, 24 CC and 14 MF for the upregulated DEGs. As for the downregulated DEGs, 10 CC and 5 MF were affected. Among the upregulated DEGs, the most enriched GO terms in BP related in heart functions included

“cardiac muscle fibre development”, “muscle contraction”, “cardiac muscle tissue development”, “regulation of blood vessel size”, “cardiac muscle hypertrophy in response to stress”, “cardiac muscle adaptation” and “actin filament-based movement". The affected CC suggested that alterations in actin-myosin filament and ECM interactions, as the top 5 GO terms included “myosin filament”, “myosin complex”, “myosin II complex”, “integrin complex” and “protein complex involved in cell adhesion”. Similarly in MF, the most enriched GO included “actin filament binding”, “actin binding”, “actin-dependent ATPase activity”, “microfilament motor activity” and “extracellular matrix binding”. Regarding the downregulated DEGs, the top 5 enriched GO terms were related to structural constituents of the ribosomes and its functions. The CC terms included “cytosolic ribosome”, “cytosolic part”, “ribosomal subunit”, “cytosolic large ribosomal subunit” and “ribosome”. Mitochondrial structure and potentially functions were also affected, with CC terms associated with “inner mitochondrial membrane protein complex” and “mitochondrial membrane part”. The MF for the downregulated DEGs included “structural constituent of ribosome”, “oxygen binding”, “peroxidase activity”, “structural molecule activity” and “oxidoreductase activity, acting on peroxide as acceptor”.

Together, these data suggest that DEGs between $CSE^{-/-}$ mice and the controls are enriched for inflammation, intracellular metabolism and processes, heart contraction and ribosome related genes.

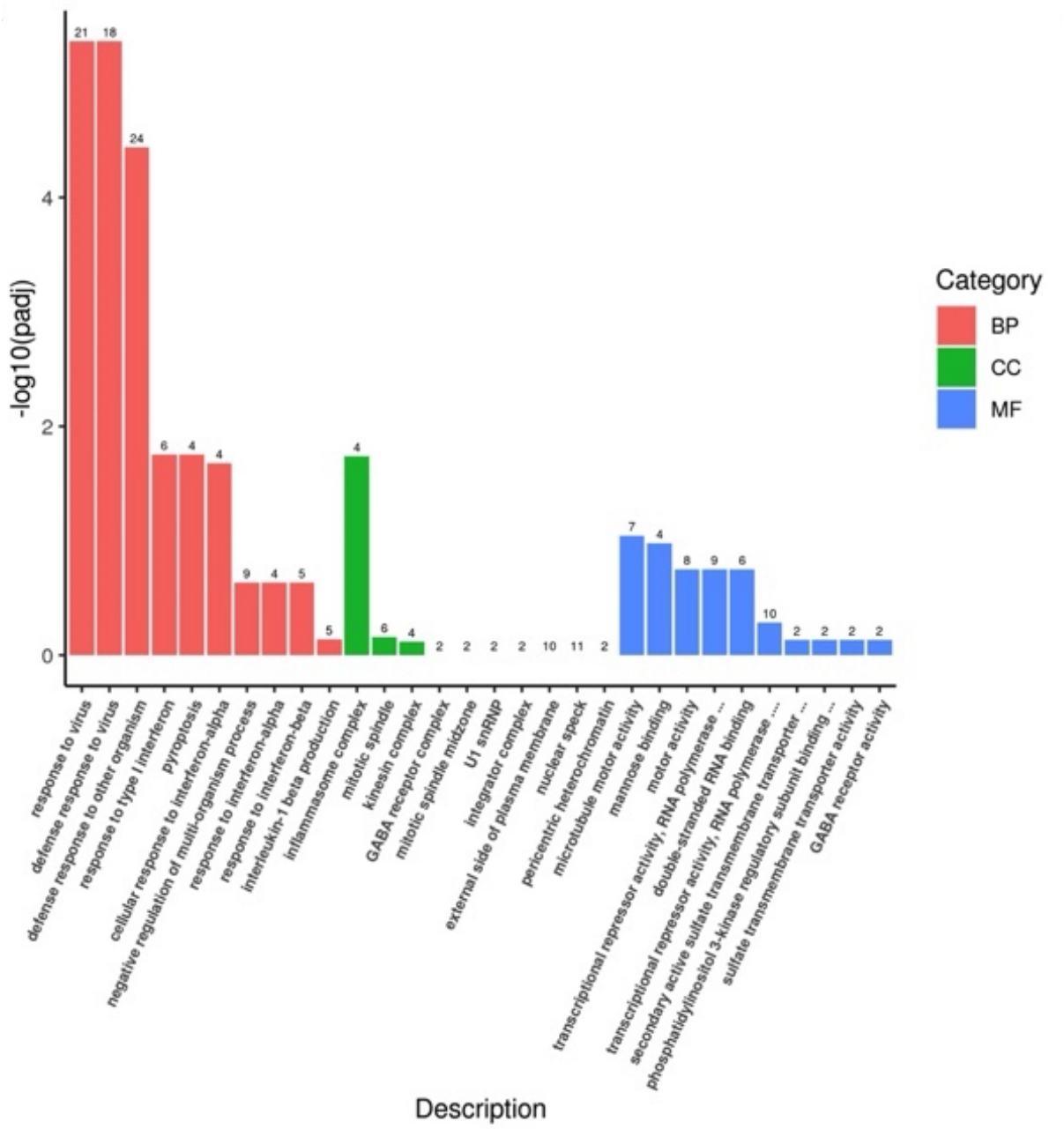

Figure 5.5 Functional analyses of upregulated DEGs at 2 months with loss of CSE.
Bar graph showing the GO enrichment of upregulated genes in $CSE^{-/-}$ mice at baseline, where terms associated with inflammation and viral response stood out. The pink columns represent overall changes in biological processes (BP) GO terms, green columns represent the cellular components (CC) GO terms and blue columns represent molecular functions (MF) GO terms. The number of genes significantly upregulated ($p<0.05$) is stated on top on each column.

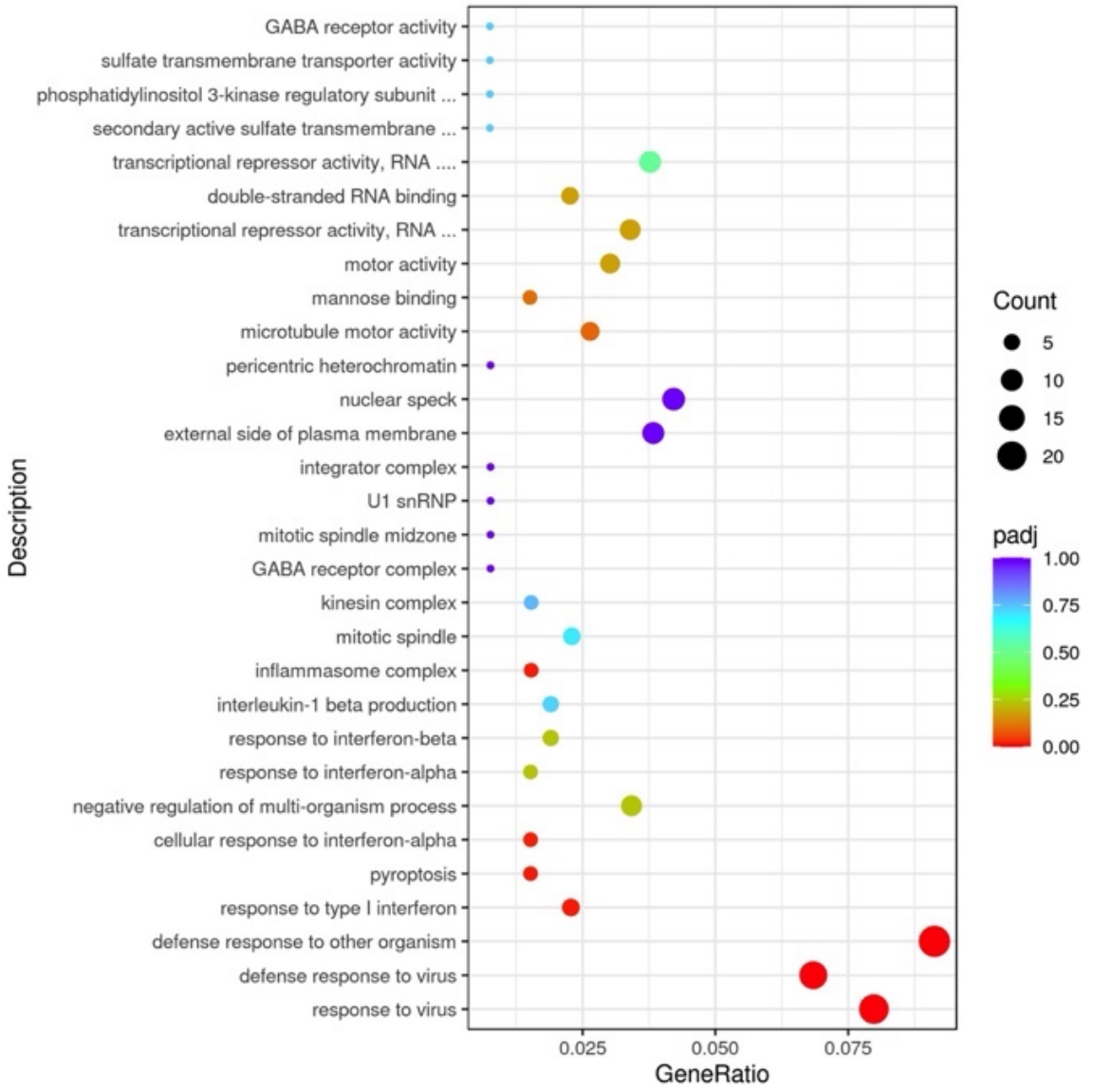

Figure 5.6 Enriched GO terms of upregulated DEGs in 2 months CSE$^{-/-}$ mice.
Upregulated terms in scatterplot to see significant changes in MF, CC and BP. GO terms (padj <0.05) are represented by the red dots on the scatterplot and the size of the dot reflects the number of genes affected.

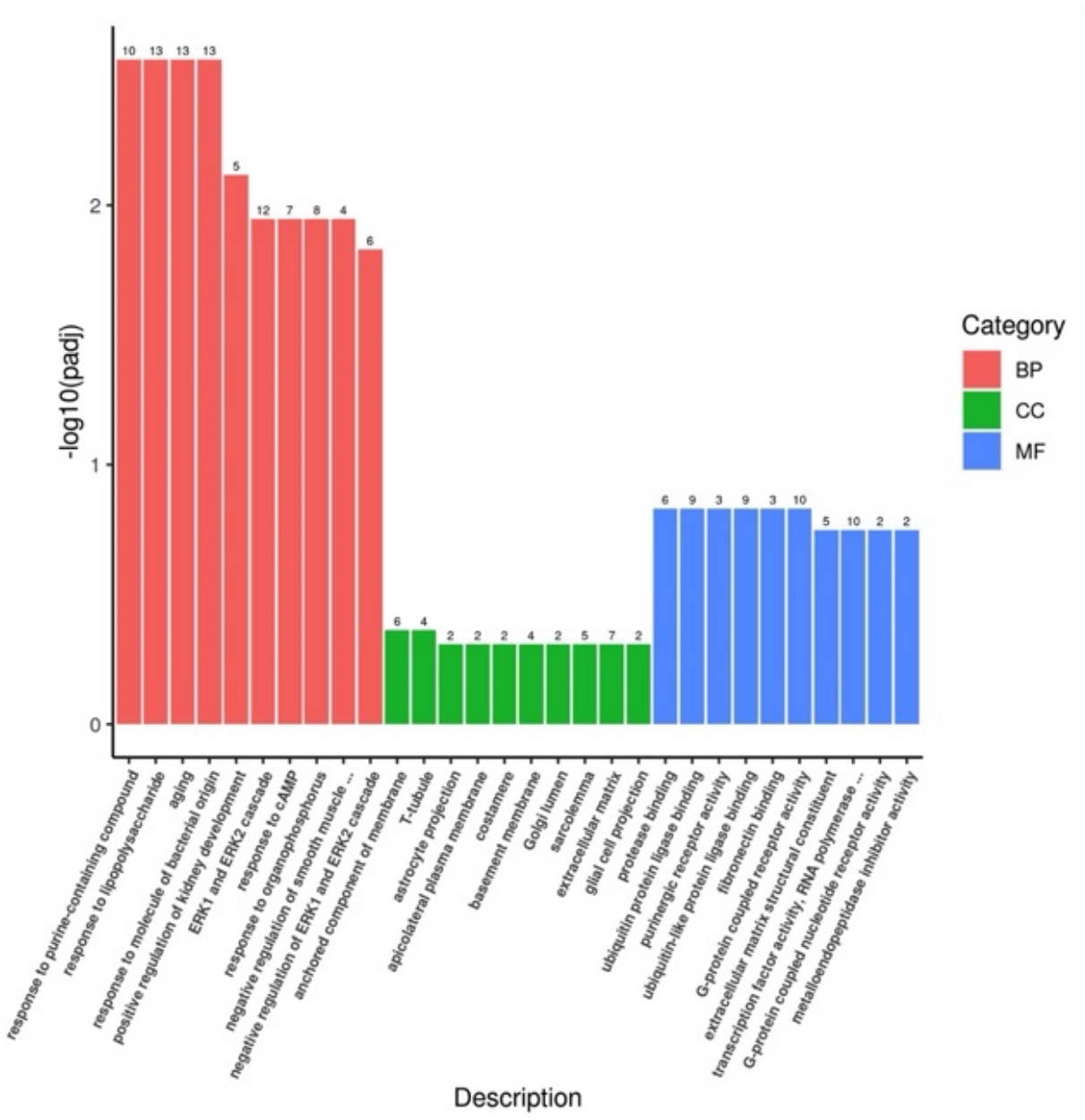

Figure 5.7 Functional analyses of downregulated DEGs at 2 months with loss of CSE.
Bar graph showing the GO enrichment of downregulated genes associated in $CSE^{-/-}$ mice at baseline. The pink columns represent overall changes in biological processes (BP) GO terms, green columns represent the cellular components (CC) and blue columns represent molecular functions (MF) GO terms. The number of genes significantly upregulated ($p<0.05$) is stated on top on each column.

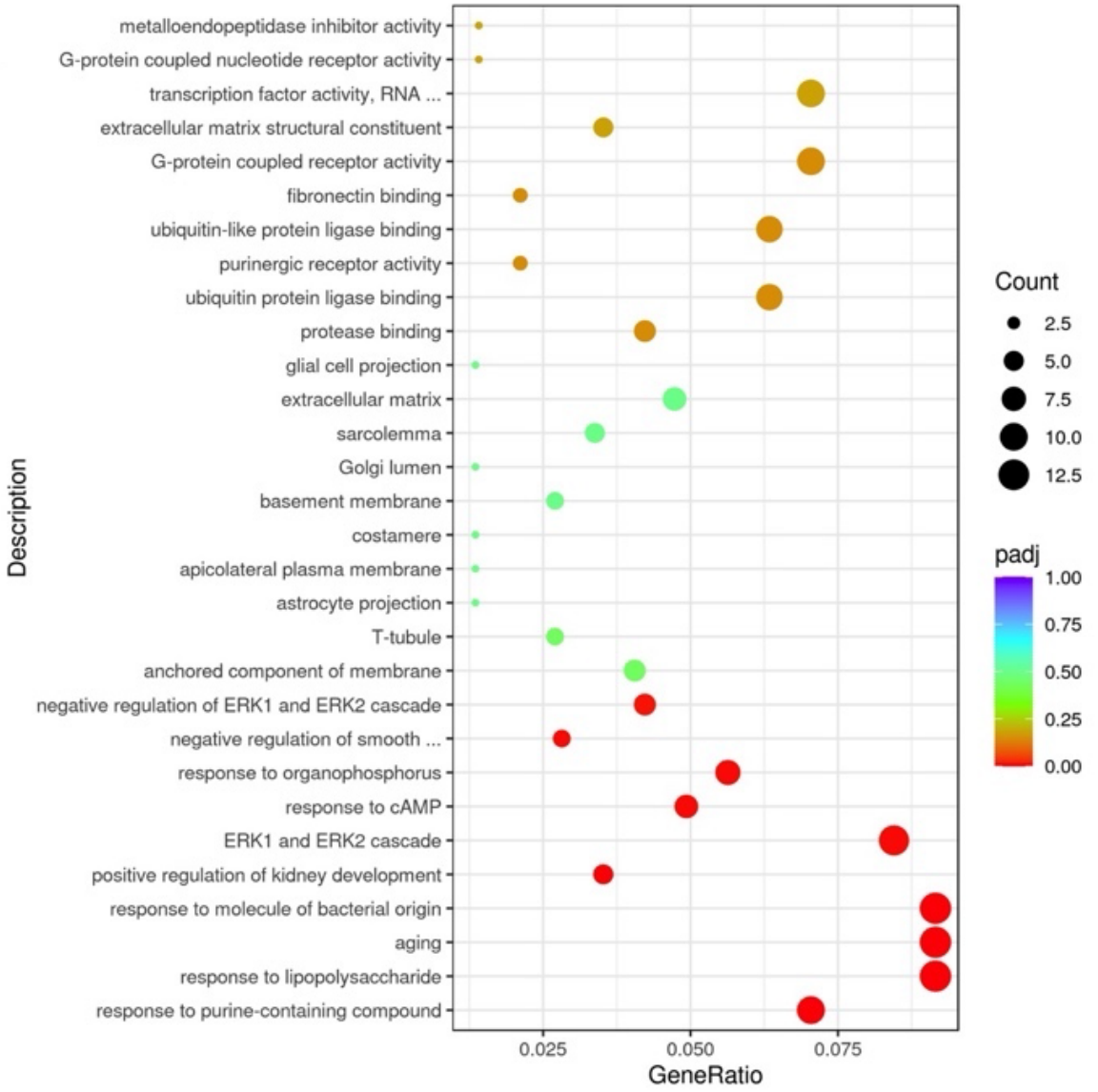

Figure 5.8 Enriched GO terms of downregulated DEGs in 2 months CSE$^{-/-}$ mice.
Downregulated terms in scatterplot to see significant changes in MF, CC and BP. GO terms (padj <0.05) are represented by the red dots on the scatterplot and the size of the dot reflects the number of genes affected.

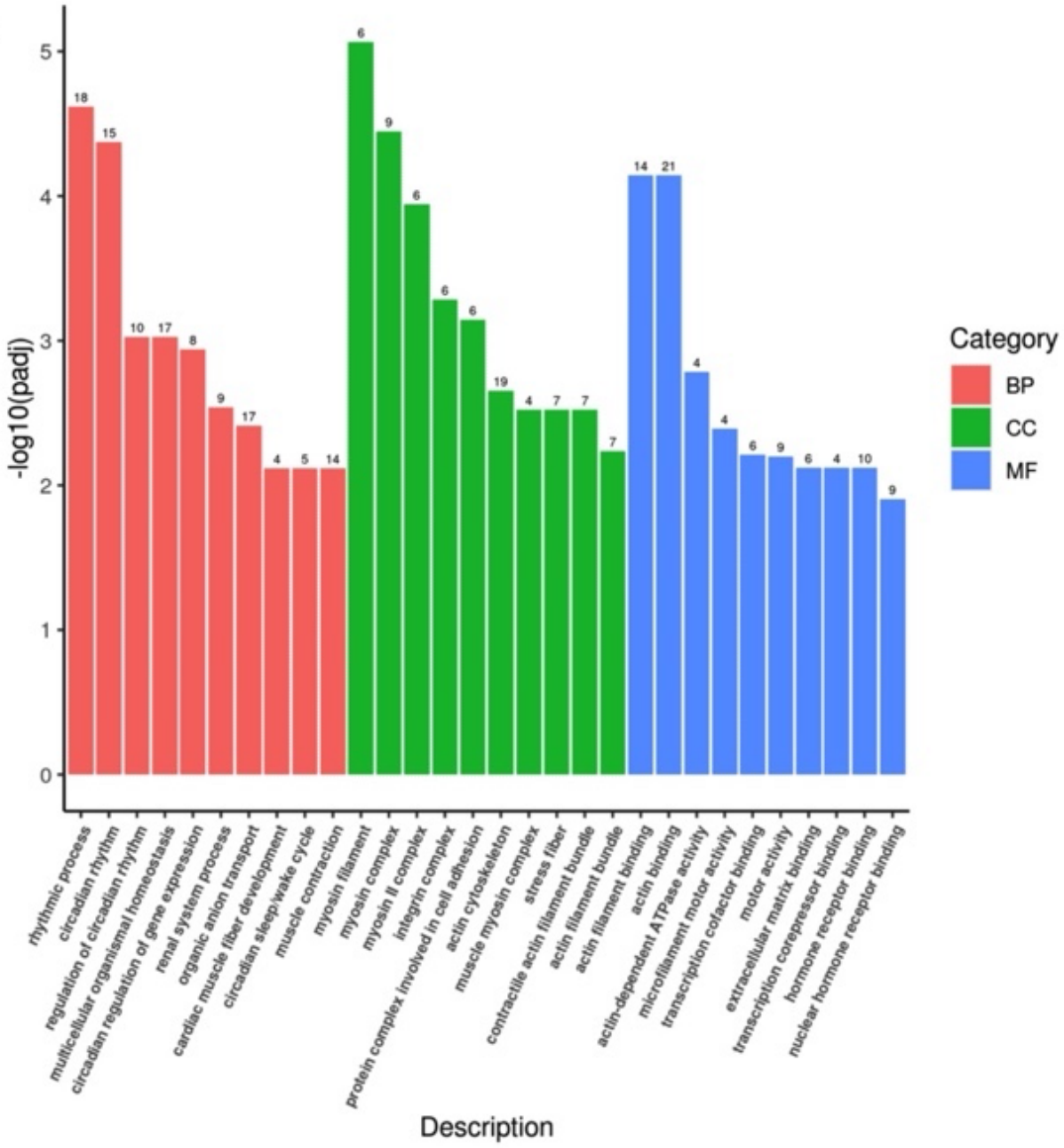

Figure 5.9 Functional analyses of upregulated DEGs at 9 months in CSE$^{-/-}$ mice.
Bar graph showing the GO enrichment of upregulated genes in older CSE$^{-/-}$ mice. The pink columns represent overall changes in biological processes (BP) GO terms, green columns represent the cellular components (CC) GO terms and blue columns represent molecular functions (MF) GO terms. The number of genes significantly upregulated ($p<0.05$) is stated on top on each column.

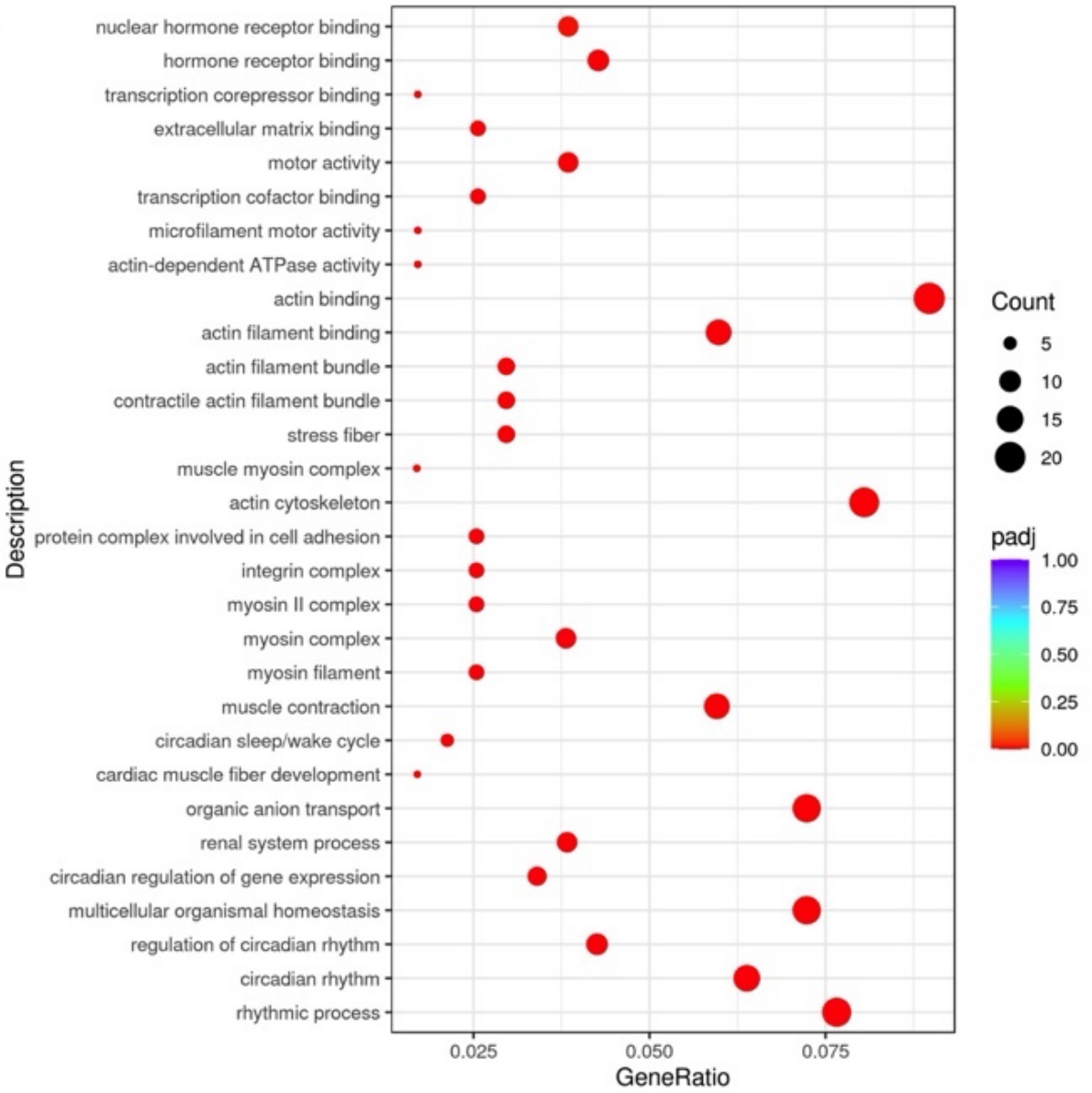

Figure 5.10 Enriched GO terms of upregulated DEGs in 9 months CSE$^{-/-}$ mice.
Upregulated terms in scatterplot to see significant changes in MF, CC and BP, including changes in actin-myosin activities and ECM interactions. GO terms (padj <0.05) are represented by the red dots on the scatterplot and the size of the dot reflects the number of genes affected.

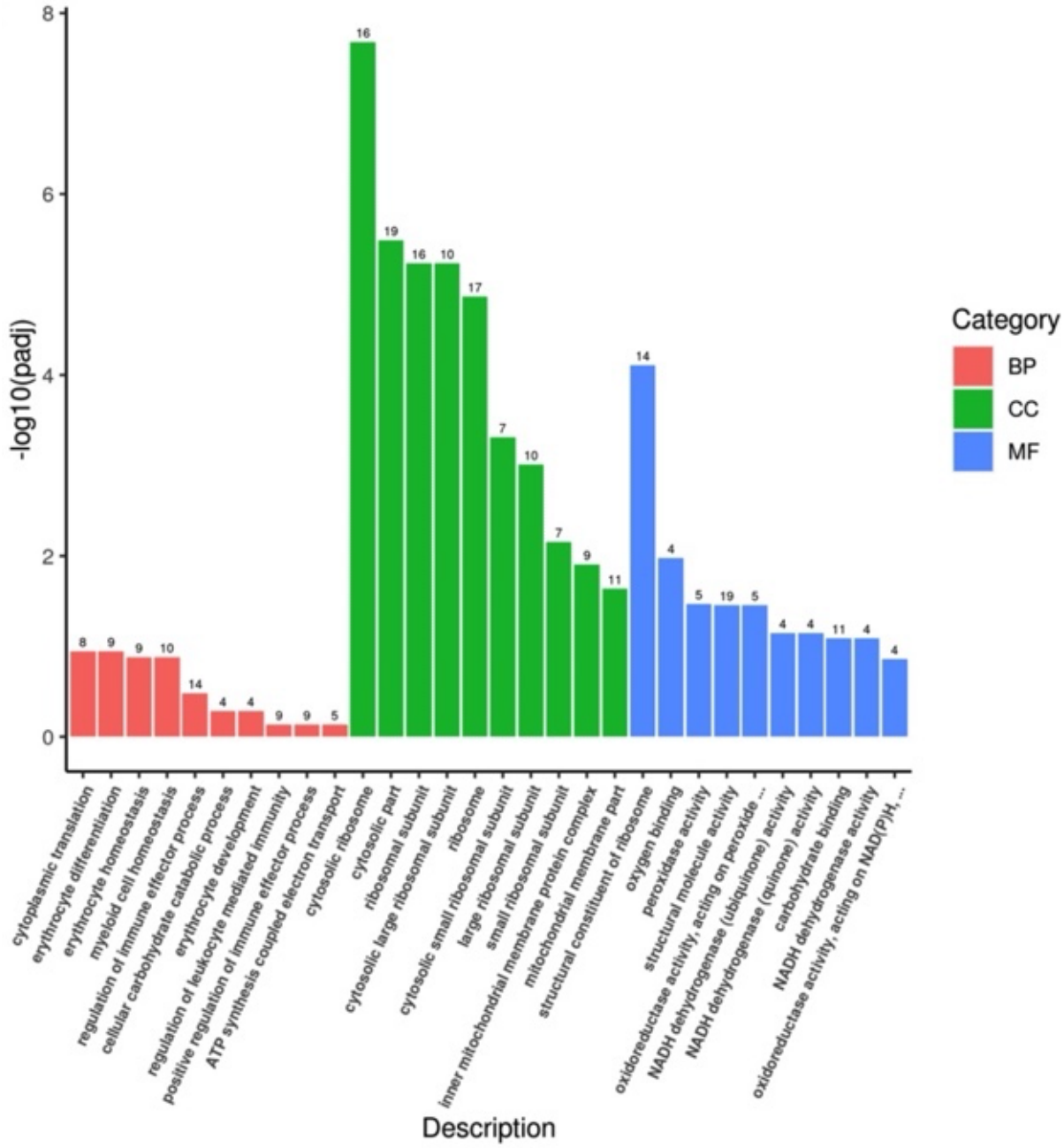

Figure 5.11 Functional analyses of downregulated DEGs at 9 months in CSE$^{-/-}$ mice.
Bar graph showing the GO enrichment of downregulated genes in older CSE$^{-/-}$ mice. The pink columns represent overall changes in biological processes (BP) GO terms, green columns represent the cellular components (CC) GO terms and blue columns represent molecular functions (MF) GO terms. The number of genes significantly upregulated ($p<0.05$) is stated on top on each column.

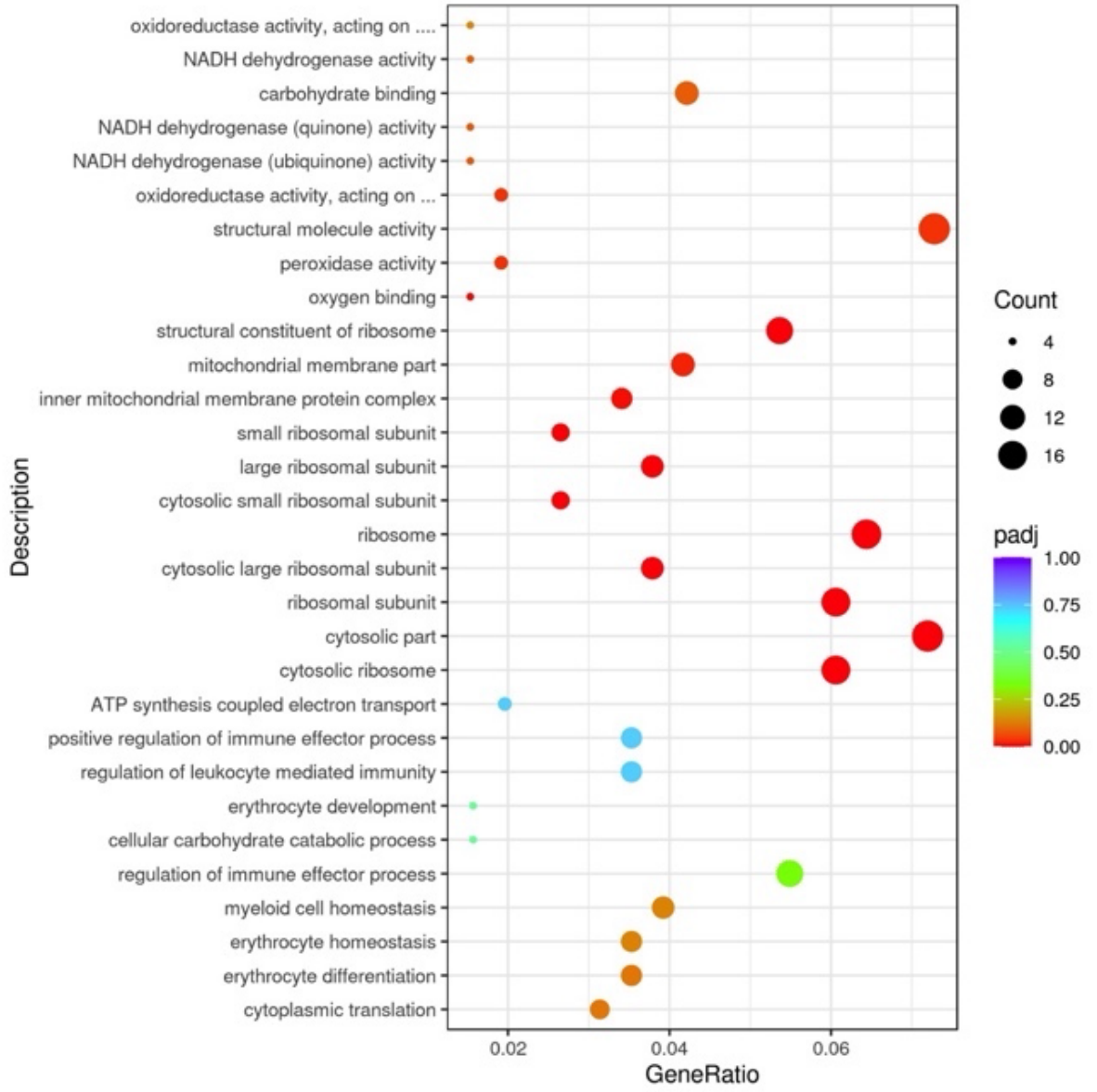

Figure 5.12 Enriched GO terms of downregulated DEGs in 9 months CSE$^{-/-}$ mice.
Downregulated terms in scatterplot to see significant changes in MF, CC and BP, including reduced ribosomal and mitochondrial functions. GO terms (padj <0.05) are represented by the red dots on the scatterplot and the size of the dot reflects the number of genes affected.

5.2.3 KEGG pathway enrichment analysis

To further explore the relationship between enriched GO terms and to visualise the changes in molecular signalling pathways that were differentially regulated with CSE deletion related to cardiac dysfunction, the DEGs were subjected to KEGG pathway analysis to determine which significant pathways were enriched for these genes. KEGG is a comprehensive biological database that integrates information on genes and proteins to depict cellular pathways and their interactions (Kanehisa and Goto, 2000). Among the DEGs, there were two upregulated pathways ("Hepatitis C" and "Measles") and no downregulated pathways in the 2-month-old mice, suggesting that CSE was involved in inflammation and viral infection. This will warrant further investigation but will not be covered in this study. In contrast, the 9-month-old mice showed enrichment of DEGs in 6 KEGG pathways. Two pathways, "circadian rhythm" and "hypertrophic cardiomyopathy (HCM)", were upregulated (Figure 5.13), while four pathways including "ribosome", "malaria", "African trypanosomiasis" and "Parkinson disease", were downregulated (Figure 5.14). In this study, we mainly focused on investigating two of the most enriched pathways, the HCM and ribosomal pathways (Figure 5.15). Details of the identified genes in the significantly enriched pathways are provided in Table 5.2. These data suggest that CSE plays a key role in regulating the genes involved in HCM and ribosome pathway, and loss of CSE leads to dysregulation of these genes, subsequently the development of CM.

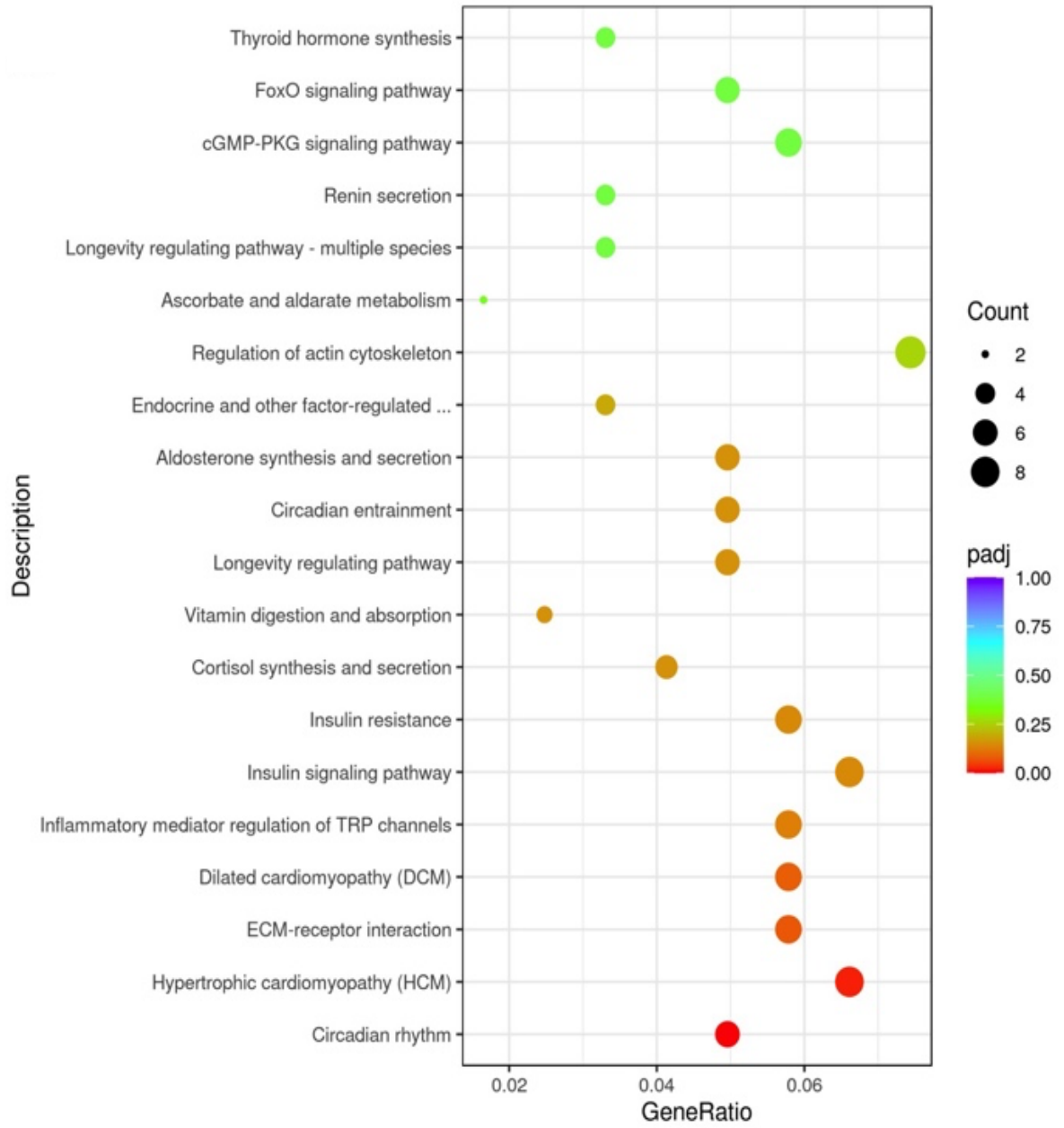

Figure 5.13 KEGG pathways upregulated in 9 months CSE$^{-/-}$ mice.
Significantly enriched pathways affected with upregulated DEGs, including HCM and circadian rhythm. Significantly affected KEGG pathways (padj <0.05) were represented by red dots on the scatterplot; size of the dot reflects the number of genes affected.

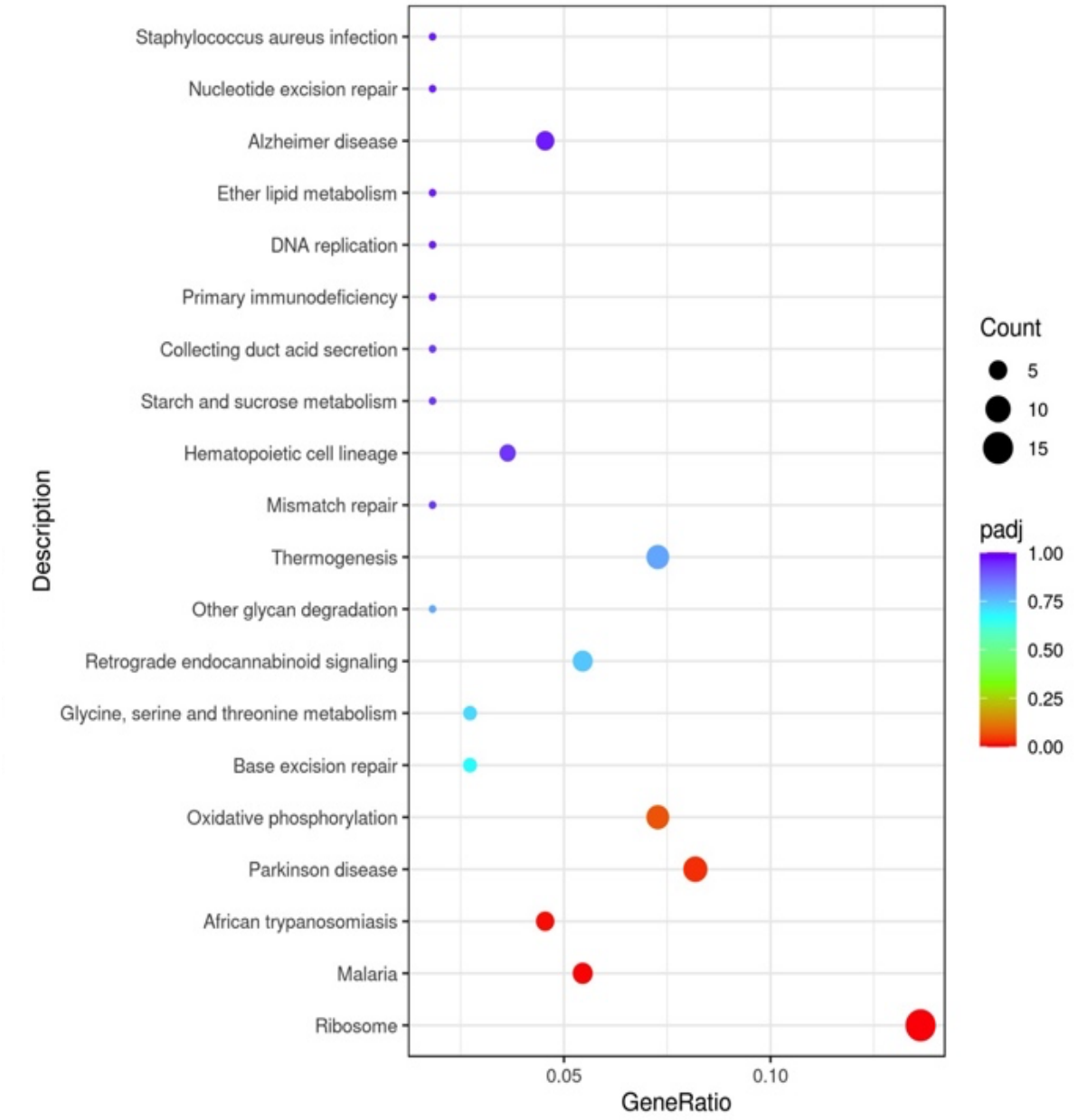

Figure 5.14 KEGG pathways downregulated in 9 months CSE$^{-/-}$ mice.
Significantly enriched pathways affected with downregulated DEGs, which include ribosome, malaria, African trypanosomiasis and Parkinson disease. Significantly affected KEGG pathways (padj <0.05) were represented by red dots on the scatterplot; size of the dot reflects the number of genes affected.

Table 5.3 Genes that were significantly changed in the 9 months CSE$^{-/-}$ mice hearts that were enriched in the KEGG upregulated HCM and downregulated ribosome pathways.

Most enriched pathways	Description	q-value	Gene name
Upregulated	HCM KEGGID: mmu05410	0.00489	Itga11/Myh6/Itga3/Itgb3/Prkab1/Il6/ Myh7/Itga9
Downregulated	Ribosome KEGGID: mmu03010	1.94E-0.6	Rpl29/Rpl34/Rplp1/Mrpl1/Rps15a/ Rps14/Rps21/Rpl36al/Rpl35a/Rpl1 7/Rpl3/Rps19/Rps12/Rpl26/Rpl39

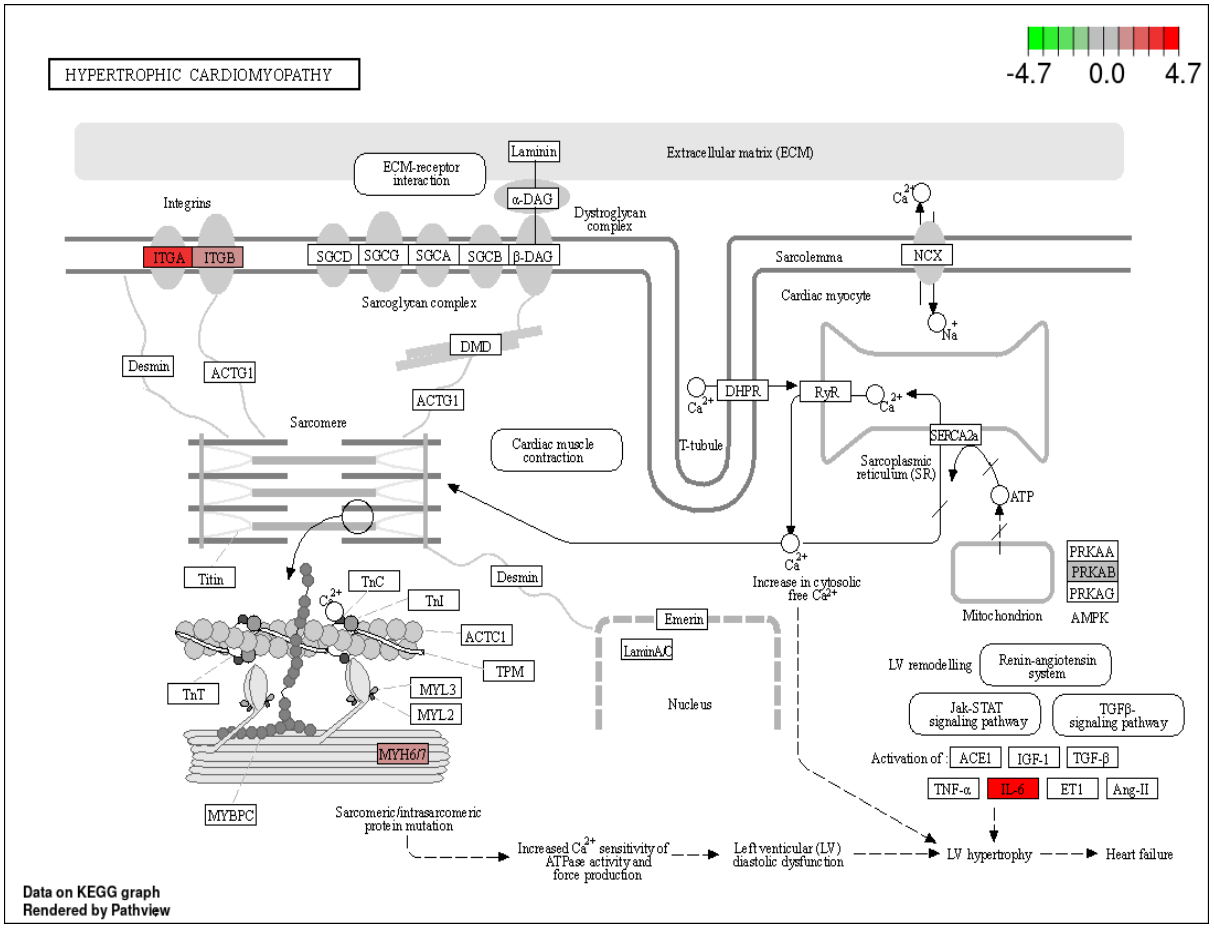
HYPERTROPHIC CARDIOMYOPATHY
-4.7
0.0
4.7
Extracellular matrix (ECM)
Laminin
ECM-receptor interaction
Integrins
α-DAG
Dystroglycan complex
ITGA
ITGB
SGCD
SGCG
SGCA
SGCB
β-DAG
Sarcoglycan complex
Sarcolemma
NCX
Cardiac myocyte
DMD
Desmin
ACTG1
Sarcomere
DHPR
RyR
T-tubule
Cardiac muscle contraction
SERCA2a
Sarcoplasmic reticulum (SR)
ATP
Titin
TnC
TnI
TnT
TPM
ACTC1
MYL3
MYL2
MYH6/7
MYBPC
Emerin
LaminA/C
Nucleus
Increase in cytosolic free Ca2+
Mitochondrion
PRKAA
PRKAB
PRKAG
AMPK
LV remodelling
Renin-angiotensin system
Jak-STAT signaling pathway
TGFβ-signaling pathway
Activation of :
ACE1
IGF-1
TGF-β
TNF-α
IL-6
ET1
Ang-II
Sarcomeric/intrasarcomeric protein mutation
Increased Ca2+ sensitivity of ATPase activity and force production
Left venticular (LV) diastolic dysfunction
LV hypertrophy
Heart failure
Data on KEGG graph
Rendered by Pathview

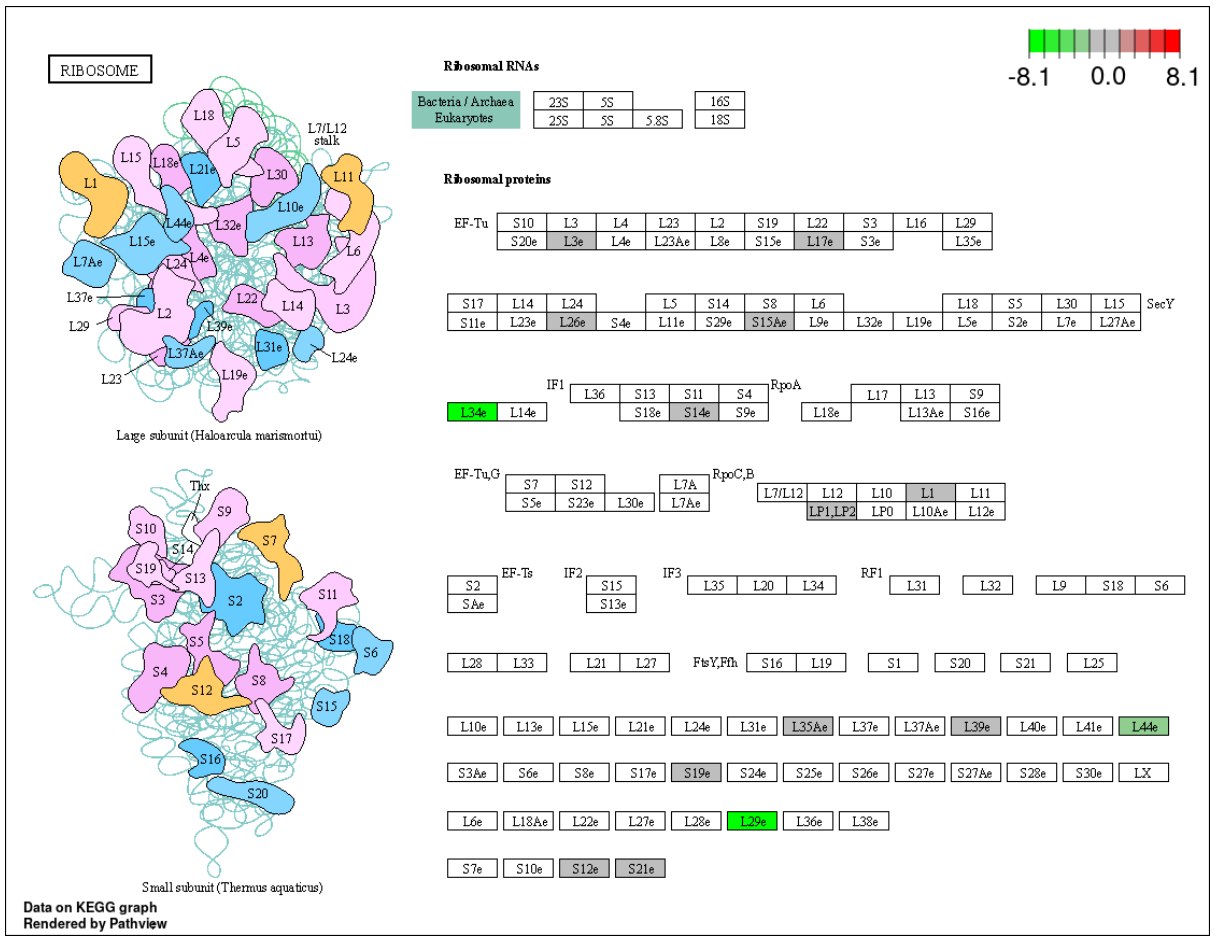
RIBOSOME
-8.1
0.0
8.1
Ribosomal RNAs
Bacteria / Archaea
Eukaryotes
23S
5S
16S
25S
5S
5.8S
18S
Ribosomal proteins
Large subunit (Haloarcula marismortui)
Small subunit (Thermus aquaticus)
Data on KEGG graph
Rendered by Pathview

Figure 5.15 Differential regulation KEGG pathways showing HCM (top) and ribosome (bottom) at 9 months.
Red represents upregulated genes and green represents downregulated genes in the hearts of $CSE^{-/-}$ mice compared to $CSE^{+/+}$ mice. Figure generated from KEGG pathway enrichment analysis and KEGG module enrichment analysis.

5.2.4 qPCR validation of relevant DEGs in 2- and 9-month-old $CSE^{+/+}$ and $CSE^{-/-}$ mice

RNA-seq data were validated using qPCR. RNA was isolated from the hearts obtained from 2- and 9-month-old $CSE^{+/+}$ and $CSE^{-/-}$ mice (n=8 per group). As shown in Figure 5.7, the mRNA expression of Gm5900 and Gbp2b were significantly increased in both 2- and 9-month-old $CSE^{-/-}$ mice compared to the wild-type controls. Similarly, the mRNA expression of hypertrophy marker, Nppa, was significantly upregulated in the 9-month $CSE^{-/-}$ group. Furthermore, the expression of ribosomal protein, Rpl29, was significantly downregulated in $CSE^{-/-}$ mice in both age groups. These qPCR data were consistent with the RNA-seq results. However, the mRNA expression of the two most affected genes, mtND3 and Osbpl3, as shown in the RNA-seq results, were not significantly affected by the loss of CSE (Figure 5.7C, F).

Next, we examined the mRNA expressions of some of the important genes identified in the KEGG pathways. Although the relative expressions of myosin heavy chains in cardiac muscle filaments Myh6 and Myh7 remained unchanged, the levels of pro-inflammatory cytokines Il-6 and integrin Itgb3 were both significantly increased at 9 months.

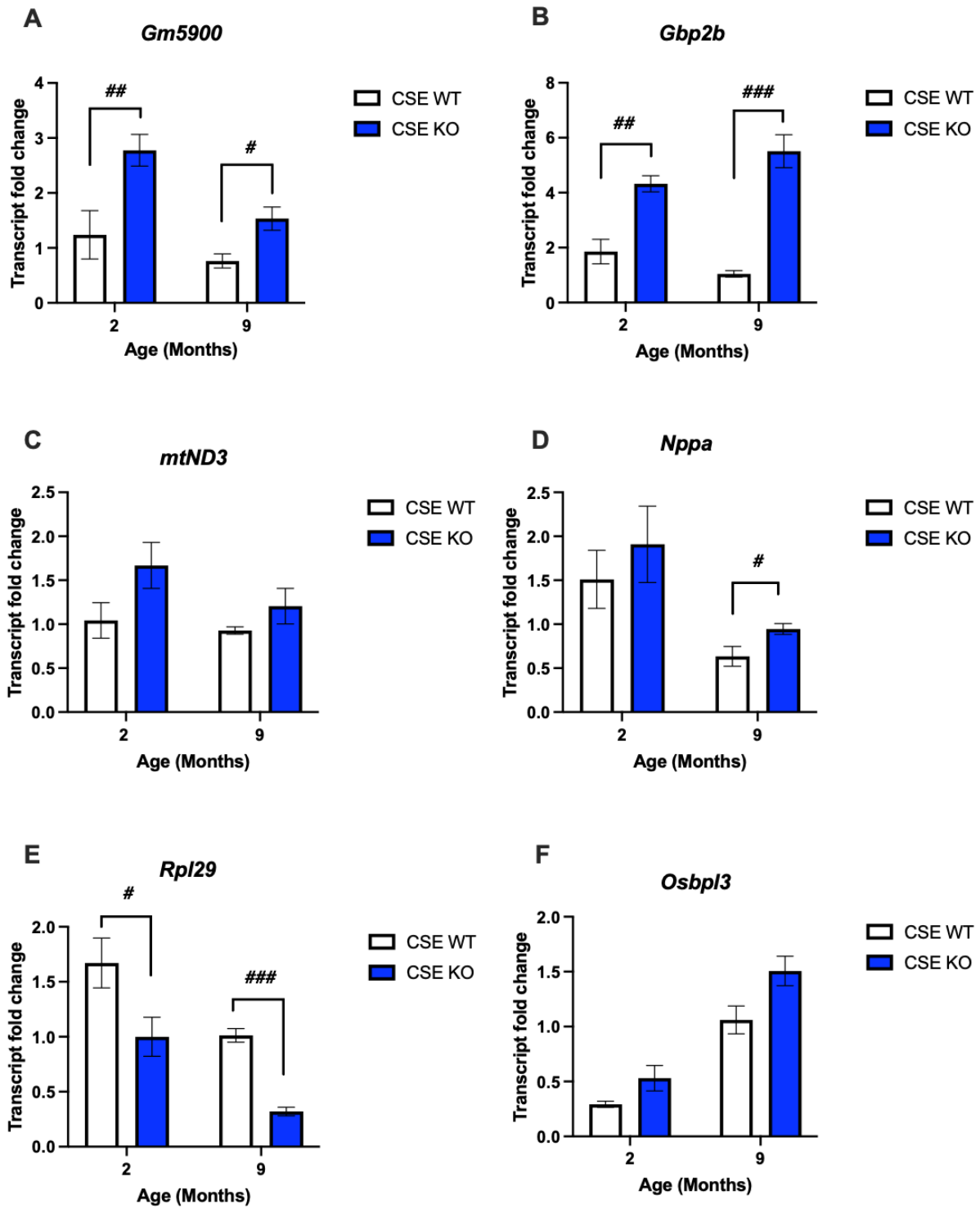

Figure 5.16 Transcript levels of DEGs related to cardiac dysfunction in hearts of 9 months CSE$^{-/-}$ mice.
qPCR analysis of **(A)** Gm5900, **(B)** Gbp2b, **(C)** mtND3, **(D)** Nppa, **(E)** Rpl29, **(F)** Osbpl3 transcript levels, normalised to actin and expressed as fold change relative to average of controls. n= 8. Data expressed as mean ± SEM. Mann-Whitney test # p<0.05, ## p<0.01 and ### p<0.001.

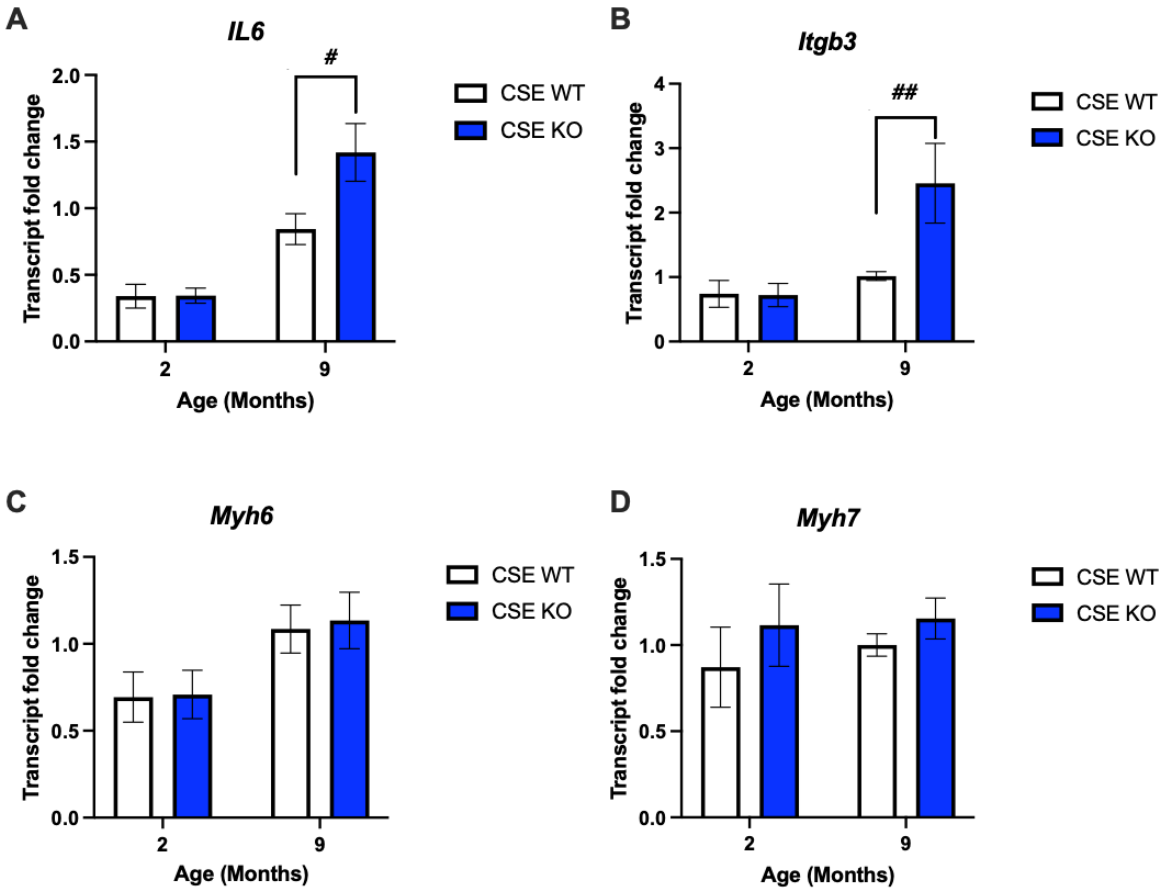

Figure 5.17 qPCR validation of DEGs related to HCM pathway in 9 months CSE$^{-/-}$ hearts. Transcript levels of **(A)** Il6 and **(B)** Itgb3 were significantly increased, whereas **(C)** Myh6 and **(D)** Myh7 transcript levels showed no significant difference, normalised to actin and expressed as fold change relative to average of controls. n= 8. Data expressed as mean ± SEM. Mann-Whitney test # $p<0.05$ and ## $p<0.01$.

5.3 Discussion

The RNA-seq data presented in this chapter provided the first insight into the age-dependent changes in cardiac gene expression in CSE$^{-/-}$ mice. We found that these changes, including DEGs, GO and KEGG pathways, were associated with the onset of the major cardiac dysfunction. These findings revealed some of the potential or biomarkers for non-end stage CM patients.

5.3.1 Loss of CSE results in cardiac inflammation

Cardiac inflammation is a key process in the development of CVDs (Deten *et al.*, 2002). Increased levels of pro-inflammatory cytokines released by myocardium, such as IL-6

and TNF-α, have been linked with HF (Fiordelisi *et al.*, 2019). Notably, an elevated level of IL-6 is a risk factor of CVD and is associated with depressed contractile function and hypertrophy in the heart (Fontes, Rose and Čiháková, 2015). H_2S deficiency due to CSE KO were previously shown to have a pro-inflammatory phenotype in animal and cellular models of atherosclerosis and diabetic CM (Bourque *et al.*, 2018; Gong *et al.*, 2022a). In this study, our data aligns with these findings, as we found an age-dependent upregulation of IL-6 in the hearts of $CSE^{-/-}$ mice, potentially contributing to cardiac dysfunction.

Furthermore, we observed an upregulation of Gbp2b, an intracellular host defence guanylate-binding protein (Gbps), in $CSE^{-/-}$ mice. Gbp2b expression is increased by interferon gamma (IFN-γ) stimulation in macrophages, vascular epithelial cells and endothelial cells, to protect these cells against intracellular infections (Sohrabi *et al.*, 2018). This gene has been found to be expressed in the proinflammatory neutrophil cluster 1 at the early stage of experimental autoimmune myocarditis. It has been proposed that the upregulation of Gbp2b contributes to the inflammatory process during the transition of myocarditis to CM and HF (Hua *et al.*, 2020). In addition, the GO terms in $CSE^{-/-}$ mice were significantly enriched for inflammation. Pyroptosis, a pro-inflammatory mode of programmed cell death, was one of the BP affected. Previously, reduced H_2S levels in high-fat diet mice was found to increase cardiac pyroptosis, contributing to adverse cardiac remodelling and dysfunction, ultimately leading to diabetic CM (Kar *et al.*, 2019). Recently, H_2S was demonstrated to alleviate pyroptosis by inhibiting the NLRP3 inflammasome and upregulating the PI3K/AKT/mTOR signalling in kidney injury (Ni *et al.*, 2021; Hu *et al.*, 2023). In summary, it is likely that cardiac inflammation is present in the heart lacking CSE, leading to cardiac dysfunction.

5.3.2 CSE deletion contributes to the hypertrophic phenotype in adult mice

Cardiac remodelling, often characterised by cardiomyocyte hypertrophy, is a common observation in HF as a response to increased workload. Initially, hypertrophy develops as a compensatory mechanism to maintain cardiac output and reduce wall stress. However, this adaptive response can become pathological and unsustainable, eventually leading to LV functional decline and HF (Kehat and Molkentin, 2010). In this study, we found that the $CSE^{-/-}$ mice exhibited an age-dependent hypertrophic phenotype, which was accompanied by increased cardiac Nppa expression, a known marker of hypertrophy (Kresin *et al.*, 2019). Upregulated Nppa gene expression has been associated with increased myocardial stress and the reactivation of 'fetal gene program', and was found to be significantly increased in cardiomyocytes of patients with HCM or CHF (Sergeeva *et al.*, 2014; Man, Barnett and Christoffels, 2018; Wehrens *et al.*, 2022).

HCM is the most common inherited cardiac disorder with an autosomal dominant pattern. It affects approximately 1 in 500 in young adults and is a leading cause of SCDs in this population (Maron, Maron and Semsarian, 2012). Our KEGG pathway analysis revealed that HCM pathway was significantly upregulated and enriched in the 9 months old $CSE^{-/-}$ mice, with increased expressions of IL-6, integrins (Itga and Itgb) and myosin heavy chain (Myh6 and Myh7). These genes are related to pro-inflammatory response, signalling molecules and indicators of HCM, contraction defects respectively (Xue *et al.*, 2018). Recently, Ellmers *et al.* (2020) observed a similar increase in Nppa expression with CSE deletion and significant decrease in Nppa, Myh6 and Myh7 expression, accompanied by reduced hypertrophy and infarct size, increased LVEF and improved cardiac functions after GYY4137 administration.

Among the genes affected in KEGG analysis, mutations in the Myh7 and Mybp3 genes are implicated with familial HCM, accounting for half of the affected patients (Girolami

et al., 2010). An increase in Mhy7/Myh6 ratio, mainly driven by a reduction in Myh6 expression, is indicative of an HCM phenotype, suggesting functional impairments in cardiomyocytes and changes ECM dynamics and its interactions with receptors (Hsieh *et al.*, 2022). Interestingly, in our study, the gene expressions of Myh6 and Myh7 are not affected by the loss of CSE. On the other hand, Itgb3 was upregulated in 9 months $CSE^{-/-}$ mice. Itgb3 integrin plays a role in ECM accumulation and cardiac fibroblast proliferation. Maintaining a balanced expression of integrins is important for cardiomyocyte survival and the tissue maintenance of the heart as its dysregulation can contribute to cardiac fibrosis in a pressure-overload hypertrophied heart (Balasubramanian *et al.*, 2012). This upregulation could indicate the presence of potential fibrosis and stiffening in the $CSE^{-/-}$ hearts, which hallmark features of HCM. Therefore, our findings suggest that the loss of CSE may contribute to hypertrophic and fibrotic phenotypes as seen in HCM hearts, and its disease progression by affecting these critical genes.

5.3.3 CSE deletion leads to disturbed cardiac metabolism

Disturbed cardiac metabolism, coupled with inefficient sarcomere contraction is also associated with HCM (van der Velden *et al.*, 2018). Unlike other organs, where glucose was used as the primary energy substrate, the heart relies on fatty acid oxidation under normal circumstances (Stanley, Recchia and Lopaschuk, 2005). However, in a failing heart, reduced respiratory chain activity in the mitochondria leads to decreased ATP generation and a shift from fatty acid to carbohydrate metabolism for energy (Ritterhoff *et al.*, 2020).

In the DEG analysis, oxysterol-binding protein-like 3 (Osbpl3) and mitochondrially encoded NADH:ubiquinone oxidoreductase core subunit 3 (mt-ND3) were identified as upregulated and downregulated genes respectively in the 9 months $CSE^{-/-}$ mice, indicating that cardiac energetics may be affected. Osbpl3 belongs to the oxysterol-binding protein family, a group of intracellular lipid receptors that regulated lipid metabolism, synthesis and

transport (Olkkonen, 2015). Previously, Osbpl3 was found to be upregulated in patients with HFpEF (Andersson *et al.*, 2019). Increased expression of this gene can be associated with myocardial steatosis, a condition characterised by an accumulation of lipids in cardiomyocytes, leading to impaired cardiac metabolism and dysfunction (Wei *et al.*, 2016). In patients with coronary microvascular dysfunction and subclinical HFpEF, myocardial steatosis can contribute to HCM, leading to cardiac remodelling and diastolic dysfunction (Wei *et al.*, 2016).

Mt-ND3 is a subunit in NADH dehydrogenase (Complex I), which catalyses electron transfer from NADH to ubiquinone in the mitochondrial respiratory chain. Mutations in the ND3 gene can cause impairment in OXPHOS and decreased redox activities, often implicated in Complex I deficiency and Leigh syndrome (Miller *et al.*, 2014). Ahmed *et al.* (2017) reported that a defective mt-ND3 gene can cause perturbed redox activities, reduced complex I assembly and activity in patients with suspected Complex I deficiency. The reduction in the Complex I respiration in $CSE^{-/-}$ mice (Chapter 4) could be mediated by the downregulation of the ND3 gene as the election transfer process in the ETC is less efficient. It is likely that dysregulation of the CSE pathway in cardiomyocytes can cause impaired lipid metabolism and mitochondrial dysfunction, contributing to the contractile dysfunction. However, validation of the protein expression of these genes would be necessary.

5.3.4 Loss of CSE impairs protein translational machinery in the heart

The ribosome plays an important role in gene transcription and translation serv as a regulator of protein expression. Eukaryotic 80S ribosomes consist of a large 60S subunit and a small 40S subunit, composed of numerous ribosomal proteins (RPs) and ribosomal RNA (rRNA) (Goudarzi and Lindström, 2016). Mutations in ribosome subunits reduce ribosome function, leading to the dysregulation of downstream targets that are involved in cellular differentiation, growth, migration, proliferation and apoptosis (Wang *et al.*, 2015). We found

that the downregulated DEGs, for example Rpl29, were integral components of the cytosolic ribosomes. The KEGG analysis further revealed dysregulation in the ribosome pathway in the 9-month-old $CSE^{-/-}$ mice. Downregulation of Rpl29 expression may affect the protein translational process in the heart as it is sensitive to changes in cytosolic RPs. Haplo-insufficiency of cytoplasmic RP genes in the heart is known to lead to severe CM. (Casad *et al.*, 2011). Furthermore, as Rpl29 specifically controls the rate of protein translation, its downregulation could result in poor translation efficiency in ribosomes (Kirn-Safran *et al.*, 2007). In addition, endogenous Rpl29 has been demonstrated to play a role in angiogenesis through interaction with VEGF signalling pathway (Jones *et al.*, 2013) and regulates the expression of microRNA 22 (miR-22) in the brain and lungs (Ali *et al.*, 2020). Depletion of miR-22 in mice impairs cardiac development, and is associated with adverse cardiac remodelling (Huang *et al.*, 2013). Moreover, we speculate that the increased load and strain on the heart, attributed to increased cardiac volumes (Chapter 3), can result in dysregulation in protein translational mechanism with the loss of CSE and increasing age. Previous research found that impaired protein translation, caused by changes in biomechanical force signalling of the heart, is associated with the development of CM and HF (Simpson, Reader and Tzima, 2020). Dysfunctional protein translation machinery can lead to dysregulation in proteostasis and aggregation of misfolded proteins during HF progression (Gouveia *et al.*, 2023).

Specifically, during cardiac hypertrophy and remodelling, protein synthesis is enhanced due to increased numbers of ribosomes and translational signal in cardiomyocytes (Yan *et al.*, 2021). However, in our study, the cardiomyocyte hypertrophy was not attributed to increased protein synthesis as the “ribosomal pathway” was the first downregulated KEGG term. It is plausible that the loss of CSE results in reduced translation of contractile proteins, leading to decreased force production in the myofibrils (Vikhorev and Vikhoreva, 2018). Recently, Shiraishi *et al.* (2023) showed that depletion of RPL3L, a heart specific ribosome protein, resulted in reduced cardiac contractility and the development of DCM

through downregulation of proteins involved in cardiac muscle contraction. Interestingly, in a recent study by Zhou *et al.* (2020) both Rpl34 and Rpl29 were identified as downregulated DEGs in hypertensive hearts, contributing to the pathogenesis of DCM. These findings suggest that CSE might influence overallprotein synthesisribosomal protein expression.

In addition, the loss of CSE upregulated the expression of predicted pseudogene Gm5900. The function of this pseudogene is not fully understood. However, it has been demonstrated that Gm5900 is expressed in the hippocampus and upregulation of this gene is associated with cognitive impairment in a mouse model of Alzheimer's disease (Wang *et al.*, 2017). Gm5900 is functionally related to mammalian target of rapamycin (mTOR) activator 3 (LAMTOR3) that encodes mitogen-activated protein kinase scaffold protein 1 (MAPKSP1) (NCBI, 2023). Therefore, the loss of CSE may affect the MAPK or mTOR signalling pathway. The mTOR signalling pathway is a global translational regulator in cardiac tissues and its activation is crucial for the initiation of adaptive cardiac hypertrophy under stressed conditions (Sciarretta *et al.*, 2018). mTOR inhibition reduces the ability of the heart to adapt to increased loads as mTOR KO mice developed accelerated HF and fatal DCM without having compensatory hypertrophy (Zhang *et al.*, 2010). Furthermore, disruptions in mTOR signalling also affect cardiac metabolism and ATP generation, as it shifts from fatty acid to glucose oxidation before the onset of HF (Zhu *et al.*, 2013). As protein translation is a highly energy-dependent process, reduction in energy produced by mitochondria (Chapter 4) will decrease overall ribosomal functions to produce a functional protein.

It was only recently discovered that the dysregulation in pseudogenes was involved in the development and pathogenesis of CVDs (Qi *et al.*, 2021). Moreover, LAMTOR3 has been extensively studied in cancer and found in tumorigenesis and cancer progression (Deng *et al.*, 2019; Gong *et al.*, 2022b). Another cellular process that was regulated by LAMTOR3 is apoptosis, where it inhibited proliferation and increase the apoptosis of breast

cancer cells via the mTOR signalling pathway (Shi *et al.*, 2020). This suggests that the loss of CSE may potentially disrupt the same pathway in the heart, leading to increased myocyte apoptosis and contractile dysfunction. However, confirming the definitive function of a pseudogene can be challenging. They can play a functional role in regulating gene expression at transcriptional and post-transcriptional level, in particular for their parent gene (Hu, Yang and Mo, 2018). On the other hand, pseudogenes can also modulate and interfere with parent gene function by generating small interfering RNA (siRNA) causing gene silencing, or compete for stabilising RNA binding proteins (RBPs) to reduce parent gene expression (Guo *et al.*, 2014). Further experimental validation is necessary to determine whether a predicted pseudogene is indeed non-functional or if it may have regained functionality and can produce functional proteins in specific cases.

The findings from this RNA-seq study show that CSE deficiency might contribute to disturbed protein translation machinery, chronic inflammatory phenotype and the potential progression of HCM, even in young mice. With the advancements in bioinformatics and sequencing technology, many genes, including pseudogenes, are identifiable and discovered. These results from RNA-seq, together with our previous findings, revealed that CSE insufficiency contributes to the pathogenesis of CM and HF, suggesting the importance of the protective mechanism of CSE/H_2S pathway in the heart. These genes could be used as new biomarkers or therapeutic targets during the disease progression of CM and other CVDs.

5.3.5 Limitations

There were some limitations to this study. Firstly, the results collected were based on a small number of DEGs. Despite the q-values being statistically significant, the data might not be robust enough. Furthermore, this affects the reproducibility of the study as well. For this RNA-seq study, LV apex tissue was used for RNA extraction and analysis. Their

functional relevance at molecular or cellular relevance should be established in the future. The gene expression data could therefore be skewed by different cell types, such as endothelial cells and fibroblasts, present and does not represent the transcript changes in cardiomyocytes alone. This could be improved by performing RNA-seq in isolated cardiomyocytes from whole LV for the investigation of myocyte specific changes in gene expression. Furthermore, the results are based on bioinformatic information and does not reflect protein expression as it does not take post-transcriptional modifications into consideration. It would be essential to further validate the RNA-seq data using western blots to verify the protein expression in LV tissues. It would have been interesting to do RNA-seq in all the different timepoints as well, to observe the progressive mechanistic genetic changes during the progression of CM due to the loss of CSE.

6 General discussion and future work

6.1 General discussion and concluding remarks

The role of H_2S in cardioprotection is well-established (Shen *et al.*, 2015). Loss of CSE, the main H_2S-producing enzyme in the cardiovascular system, has been shown to cause various cardiovascular abnormalities, including endothelial dysfunction, ischemia-reperfusion injury, hypertension and HF (Yang *et al.*, 2008; Kondo *et al.*, 2013; Ellmers *et al.*, 2020). Previous studies from our lab highlighted the importance of CSE in cardiovascular adaptations during pregnancy, where $CSE^{-/-}$ mice struggled to meet increased metabolic demands. This was accompanied by disruptions in mitochondrial biogenesis and respiration in cardiac tissues. Despite the demonstrated functional activity of CSE in cardiac stress models such as pregnancy or TAC (Kondo *et al.*, 2013), its biological effects on age-related changes remained unexplored. This study represents the first longitudinal investigation into the progressive impact of CSE deletion on the heart without external stressors. It provides a comprehensive examination of cardiac functional, structural, and molecular changes in the $CSE^{+/+}$ and $CSE^{-/-}$ mice across different age. Moreover, only male mice were used in the experiments, owing to the established understanding that females, especially those in pre-menopause, possess enhanced cardioprotective mechanisms attributed to the antioxidative effects of oestrogen (Xiang *et al*., 2021). By mitigating the gender-related variability, this approach facilitates a more focus observation of age-related physiological cardiac changes.

Our results suggest a long-term decrease of CSE/H_2S pathway activity on both systolic and diastolic functions under basal conditions, with cardiac dysfunction preceding structural abnormalities. Furthermore, cellular and molecular analyses revealed mitochondrial dysfunction, alongside an inflammatory and hypertrophic phenotype in older CSE-deficient mice. According to the Frank-Starling mechanism, increased EDV (preload) or ESV (afterload) causes increased contractile force, resulting in higher SV and CO to sustain EF. However, in this study, older $CSE^{-/-}$ mice exhibited reduced EF and CO, suggesting structural remodelling with an enlarged chamber akin to DCM (Konstam and Abboud, 2017).

We also showed that CSE deletion induced cardiac dysfunction at 9 months in mice, equivalent to approximately 35 years in human (Wang *et al.*, 2020). Consistent with literature, CM typically affects individuals aged 20 to 60 (Hazebroek, Dennert and Heymans, 2012). Significant functional differences were observed at 14 months, which was about 51 years in human patients. However, changes in cellular mechanisms, including mitochondria function, were detectable as early as the 2-month baseline, equivalent to 15 human years, suggesting that CSE deletion accelerated dysregulation in underlying pathways, albeit without evident cardiac dysfunction at this stage. It can be speculated that systolic and diastolic dysfunction of the heart will further deteriorate in the $CSE^{-/-}$ mice beyond 14 months. Nonetheless, additional stressors, for instance pressure or volume overload and pregnancy, would be needed to induce alterations in geometrical structure of the heart as no significant differences were observed between both genotypes, other than age-related changes.

Diastolic dysfunction, a pathophysiological sign of HCM (Haland and Edvardsen, 2019), was evident in older $CSE^{-/-}$ mice. The reduced E/a ratio and increased deceleration time suggested abnormal relaxation, which correlated to grade 1 diastolic dysfunction in elderly patients (Dugo *et al.*, 2016). Furthermore, the prolonged IVRT throughout the longitudinal time course of $CSE^{-/-}$ mice indicated LV stiffening and poor myocardial relaxation, consistent with impaired LV relaxation in patients and during ageing (Appleton, 2008). Given that IVRT is a high energy-dependent period of active relaxation, this prolongation might be linked to reduced ATP production and impaired calcium signalling. Notably, this study revealed significant mitochondria dysfunction in $CSE^{-/-}$ mice, even at 2 months, as indicated by the diminished mitochondrial content, impaired OXPHOS signalling and disrupted mitochondria dynamics. It has been prviously shown that reduced RCR in $CSE^{-/-}$ mice was driven by significant reduction in state 3 active respiration (King *et al.*, 2014). These mitochondrial defects are consistent with those observed in human failing hearts, suggesting their role in HF progression (Lemieux *et al.*, 2011). The significant increase in EDV, greater than that of ESV, also indicated the presence of diastolic

dysfunction preceding systolic dysfunction. Overtime, IVCT is also likely to continue increasing as systolic function progressively deteriorates after 14 months without CSE.

The interplay between the CSE/H_2S pathway, Ca^{2+} regulation and mitochondria dynamics was also explored. Loss of CSE resulted in a nearly 40% reduction in the gene expression of Ca^{2+} channel SERCA2a, the main isoform in cardiac tissue, indicating a shift in Ca^{2+} homeostasis. Dysregulated Ca^{2+} signalling could lead to intracellular Ca^{2+} accumulation, affecting both cardiac contractility and mitochondria function. This aligns with previous findings associating increased Ca^{2+} concentration with increased vascular stiffness (Abi-Samra and Gutterman, 2016), providing insights into the observed relaxation issues in $CSE^{-/-}$ mice. Moreover, cardiac mitochondria isolated from $CSE^{-/-}$ mice exhibited diminished mtDNA content, defective OXPHOS and disrupted mitochondria dynamics. The reduction in Mfn2, a molecular tether crucial for facilitating Ca^{2+} transfer between cardiomyocyte mitochondria and SR, may have further downregulated Ca^{2+} signalling, potentially creating a mismatch between energy supply and demand (Chen *et al.*, 2012). Imbalances between ATP and Ca^{2+} are known to contribute to abnormalities in energy production and utilisation during HF (Gorski, Ceholski and Hajjar, 2015). While some molecular parameters were altered in $CSE^{-/-}$ mice at 2 months, functional changes indicative of cardiac dysfunction only became apparent at 9 months. This delay suggests initial activation of compensatory mechanisms to preserve cardiac function and ATP production, which became unsustainable with age and eventually leading to HF. It conceivable that there might be increased activities of CBS or 3-MST in endogenous H_2S production, but further studies would be needed to validate this hypothesis. These findings collectively suggest a close connection between mitochondria dysfunction and impaired Ca^{2+} cycling, potentially acting as a feedforward mechanism exacerbating HF.

Inflammation and oxidative stress are major contributors to LV remodelling and cardiac hypertrophy. Elevated levels of pro-inflammatory cytokines have been directly

proportional to cardiac functional impairments and the progression of chronic HF (Gullestad *et al.*, 2012). Notably, the RNA-seq data in this study revealed DEGs associated with heightened inflammatory responses, indicating a potential pro-inflammatory phenotype in mouse hearts following CSE deletion, potentially due to heightened oxidative stress. Furthermore, the increased capillary density observed in $CSE^{-/-}$ mice may also indicate an inflammatory response. Supporting this, previous research in our lab found endothelial dysfunction and hypertension pre-pregnancy due to low-grade inflammation induced by high-fat diet in 2 months female mice. Chronic systemic inflammation within the myocardium is a common pathogenic factor in HCM, eventually leading to end-stage CM and HF (Lillo *et al.*, 2023). Besides systemic inflammation that causes cardiac fibrosis and LV stiffening, oxidative stress and cellular senescence also play an important role in the cardiac ageing transition process. Previous research by Yang *et al.* (2013) proved that CSE deficiency doubled ROS levels and reduced intracellular antioxidant GSH protein levels, inducing premature cellular ageing. Moreover, complex I impairment, a major source of ROS in cardiac mitochondria (Karamanlidis *et al.*, 2013), exacerbated oxidative stress resulting from CSE loss. This can also be supported by CSE deletion in a myocardial I/R mouse model, where depletion in H_2S increased ROS production via reducing bioavailability of NO (King *et al.*, 2014). This oxidative stress may also be further contributed by dysregulated mitochondrial quality control mechanisms in the absence of CSE, as inadequate mitophagy may lead to the accumulation of defective mitochondria, triggering cardiomyocyte apoptosis and activating inflammatory pathways (Ikeda *et al.*, 2015). Taken together, loss of CSE leads to inflammation, increased oxidative stress and mitochondria dysfunction at the molecular level, contributing to cardiac maladaptation.

In summary, our findings suggest that CSE plays an important role in regulating cardiovascular function under normal physiological conditions, and dysregulation in the CSE/H_2S pathway could lead to HCM and HF overtime. Our study has identified novel mechanisms involved, including regulation of mitochondria function, calcium homeostasis

and inflammatory responses. These novel insights may give rise new therapeutic potential for HF.

6.2 Future direction

Under physiological conditions, the absence of CSE in mice could predispose them to CM, arising from mitochondrial dysfunction and underlying changes in the molecular processes. Echocardiography using ultrasound imaging revealed substantial systolic and diastolic dysfunction with the loss of CSE. Although ultrasound analysis is quick, non-invasive and allows real-time imaging of the beating heart, it would be interesting to combine this with pressure-volume loop analysis. Performing pressure-volume loop analysis in LV longitudinally could track the underlying molecular mechanisms and disease progression of CM in $CSE^{-/-}$ mice as it provides a picture of load-independent hemodynamic changes (Townsend, 2016). Time and cost constraints hindered my ability to gain proficiency in this technique. In addition, detecting early cardiac dysfunction using speckle tracking-based echocardiography (STE) could also enhance these assessments. STE directly evaluates myocardial deformation, has higher sensitivity to subtle changes in wall motion and captures cardiac motion better than M-mode images. By measuring the longitudinal and circumferential strain of LV walls, STE can detect deterioration in cardiac muscles at earlier stages (De Lucia *et al.*, 2019). Using this, Wu *et al.* (2021) was able to identify cardiac muscle defects and contractile dysfunction preceding cardiac dysfunction in conventional ultrasound. Future studies can use early intervention with exogenous H_2S in $CSE^{-/-}$ mice to investigate its effects on prevent disease progression.

Mitochondria-targeted therapies may also be valuable as they were shown to cause cardiomyocyte dysfunction in this study. At a cellular level, it would be interesting to investigate the changes in mitochondrial morphology using transmission electron microscope and MitoTracker staining and elucidate the underpinning mechanism behind the

reduced mtDNA content. Mitochondria metabolism using fatty acid oxidation and glycolysis can also be measured to investigate the stage where this switch occurs during ageing transition and when CSE/H_2S pathway is dysregulated. Fatty acid oxidation can be measured by using palmitoyl-L-carnitine as a substrate and glycolytic stress assay to assess glucose metabolism in mitochondria (Tran and Wang, 2019; Sanchez-Aranguren *et al.*, 2020b). Furthermore, while bulk tissue RNA-seq can detect overall transcriptomic changes in the heart caused by CSE, it would have been better to use isolated cardiomyocytes as the heart is composed of various cell types including fibroblasts, endothelial cells and smooth muscle cells. Future studies using single-cell RNA sequencing (scRNA-seq) could investigate the molecular shifts in different cell types involved with the absence of CSE, providing broader and novel therapeutic targets using H_2S (Iqbal *et al.*, 2021). If possible, dysregulation of CSE and H_2S should be further studied in patients with different types of CM of different age groups, extending this research to clinical applications.

7 References

Abe, K. and Kimura, H. (1996) 'The possible role of hydrogen sulfide as an endogenous neuromodulator', *Journal of Neuroscience,* 16(3), pp. 1066-1071.

Abi-Samra, F. and Gutterman, D. (2016) 'Cardiac contractility modulation: a novel approach for the treatment of heart failure', *Heart failure reviews,* 21(6), pp. 645-660.

Adams, J. (2008) 'Transcriptome: connecting the genome to gene function', *Nat Educ,* 1(1), pp. 195.

Agrawal, T. and Nagueh, S. F. (2022) 'Changes in cardiac structure and function with aging', *The Journal of Cardiovascular Aging,* 2(1), pp. 13.

Ahmad, A., Sattar, M. A., Rathore, H. A., Abdulla, M. H., Khan, S. A., Azam, M., Abdullah, N. A. and Johns, E. J. (2016) 'Up Regulation of cystathione γ lyase and Hydrogen Sulphide in the Myocardium Inhibits the Progression of Isoproterenol–Caffeine Induced Left Ventricular Hypertrophy in Wistar Kyoto Rats', *PloS one,* 11(3), pp. e0150137.

Ahmad, M., Wolberg, A. and Kahwaji, C. I. (2018) 'Biochemistry, electron transport chain'.

Ahmed, S. T., Alston, C. L., Hopton, S., He, L., Hargreaves, I. P., Falkous, G., Oláhová, M., McFarland, R., Turnbull, D. M. and Rocha, M. C. (2017) 'Using a quantitative quadruple immunofluorescent assay to diagnose isolated mitochondrial Complex I deficiency', *Scientific reports,* 7(1), pp. 15676.

Ahuja, P., Wanagat, J., Wang, Z., Wang, Y., Liem, D. A., Ping, P., Antoshechkin, I. A., Margulies, K. B. and MacLellan, W. R. (2013) 'Divergent mitochondrial biogenesis responses in human cardiomyopathy', *Circulation,* 127(19), pp. 1957-1967.

Akasheva, D. U., Plokhova, E. V., Tkacheva, O. N., Strazhesko, I. D., Dudinskaya, E. N., Kruglikova, A. S., Pykhtina, V. S., Brailova, N. V., Pokshubina, I. A. and Sharashkina, N. V. (2015) 'Age-related left ventricular changes and their association with leukocyte telomere length in healthy people', *PloS one,* 10(8), pp. e0135883.

Al-Magableh, M. R., Kemp-Harper, B. K. and Hart, J. L. (2015) 'Hydrogen sulfide treatment reduces blood pressure and oxidative stress in angiotensin II-induced hypertensive mice', *Hypertension Research,* 38(1), pp. 13-20.

Alhakak, A. S., Møgelvang, R., Schnohr, P., Modin, D., Brainin, P., Gislason, G. and Biering-Sørensen, T. (2020) 'The cardiac isovolumetric contraction time is an independent predictor

of incident heart failure in the general population', *International Journal of Cardiology,* 312, pp. 81-86.

Alhakak, A. S., Olsen, F. J., Skaarup, K. G., Lassen, M. C. H., Johansen, N. D., Espersen, C., Abildgaard, U., Jensen, G. B., Schnohr, P. and Marott, J. L. (2023) 'Changes in cardiac time intervals over a decade and the risk of incident heart failure: The Copenhagen City heart study', *International Journal of Cardiology*.

Ali, M. I., Li, L., Li, L., Yao, L., Liu, J., Gu, W., Huang, S., Wang, B. and Liu, G. (2020) 'The tissue specific regulation of miR22 expression in the lung and brain by ribosomal protein L29', *Scientific Reports,* 10(1), pp. 16242.

Andersson, C., Lin, H., Liu, C., Levy, D., Mitchell, G. F., Larson, M. G. and Vasan, R. S. (2019) 'Integrated multiomics approach to identify genetic underpinnings of heart failure and its echocardiographic precursors: Framingham heart study', *Circulation: Genomic and Precision Medicine,* 12(12), pp. e002489.

Andersson, K. B., Birkeland, J. A. K., Finsen, A. V., Louch, W. E., Sjaastad, I., Wang, Y., Chen, J., Molkentin, J. D., Chien, K. R. and Sejersted, O. M. (2009) 'Moderate heart dysfunction in mice with inducible cardiomyocyte-specific excision of the Serca2 gene', *Journal of molecular and cellular cardiology,* 47(2), pp. 180-187.

Appleton, C. P. (2008) 'Evaluation of diastolic function by two-dimensional and Doppler assessment of left ventricular filling including pulmonary venous flow', *Diastology: Clinical Approach to Diastolic Heart Failure*: Elsevier Inc., pp. 115-143.

Arany, Z., Novikov, M., Chin, S., Ma, Y., Rosenzweig, A. and Spiegelman, B. M. (2006) 'Transverse aortic constriction leads to accelerated heart failure in mice lacking PPAR-γ coactivator 1α', *Proceedings of the National Academy of Sciences,* 103(26), pp. 10086-10091.

Ariga, R., Tunnicliffe, E. M., Manohar, S. G., Mahmod, M., Raman, B., Piechnik, S. K., Francis, J. M., Robson, M. D., Neubauer, S. and Watkins, H. (2019) 'Identification of myocardial disarray in patients with hypertrophic cardiomyopathy and ventricular arrhythmias', *Journal of the American College of Cardiology,* 73(20), pp. 2493-2502.

Aronow, W. S. (2017) 'Hypertension and left ventricular hypertrophy', *Annals of translational medicine,* 5(15).

Ashrafian, H., Docherty, L., Leo, V., Towlson, C., Neilan, M., Steeples, V., Lygate, C. A., Hough, T., Townsend, S. and Williams, D. (2010) 'A mutation in the mitochondrial fission gene Dnm1l leads to cardiomyopathy', *Plos genetics,* 6(6), pp. e1001000.

Awtry, E. H. and Philippides, G. J. (2010) 'Alcoholic and cocaine-associated cardiomyopathies', *Progress in cardiovascular diseases,* 52(4), pp. 289-299.

Bagnall, R. D., Weintraub, R. G., Ingles, J., Duflou, J., Yeates, L., Lam, L., Davis, A. M., Thompson, T., Connell, V. and Wallace, J. (2016) 'A prospective study of sudden cardiac death among children and young adults', *New England Journal of Medicine,* 374(25), pp. 2441-2452.

Balasubramanian, S., Quinones, L., Kasiganesan, H., Zhang, Y., Pleasant, D. L., Sundararaj, K. P., Zile, M. R., Bradshaw, A. D. and Kuppuswamy, D. (2012) 'β3 integrin in cardiac fibroblast is critical for extracellular matrix accumulation during pressure overload hypertrophy in mouse'.

Bergmann, O., Bhardwaj, R. D., Bernard, S., Zdunek, S., Barnabé-Heider, F., Walsh, S., Zupicich, J., Alkass, K., Buchholz, B. A. and Druid, H. (2009) 'Evidence for cardiomyocyte renewal in humans', *Science,* 324(5923), pp. 98-102.

Bezawork-Geleta, A., Rohlena, J., Dong, L., Pacak, K. and Neuzil, J. (2017) 'Mitochondrial complex II: at the crossroads', *Trends in biochemical sciences,* 42(4), pp. 312-325.

BHF (2020) *Death rates - Heart and circulatory disease in context*. bhf.org.uk: British Heart Foundation. Available at: www.bhf.org.uk/what-we-do/our-research/heart-and-circulatory-diseases-in-numbers/heart-and-circulatory-disease-in-context.

Bibli, S.-I., Hu, J., Sigala, F., Wittig, I., Heidler, J., Zukunft, S., Tsilimigras, D. I., Randriamboavonjy, V., Wittig, J. and Kojonazarov, B. (2019) 'Cystathionine γ lyase sulfhydrates the RNA binding protein human antigen R to preserve endothelial cell function and delay atherogenesis', *Circulation,* 139(1), pp. 101-114.

Biering-Sørensen, T., Mogelvang, R., Schnohr, P. and Jensen, J. S. (2016) 'Cardiac time intervals measured by tissue Doppler imaging M-mode: association with hypertension, left ventricular geometry, and future ischemic cardiovascular diseases', *Journal of the American Heart Association,* 5(1), pp. e002687.

Bironaite, D., Daunoravicius, D., Bogomolovas, J., Cibiras, S., Vitkus, D., Zurauskas, E., Zasytyte, I., Rucinskas, K., Labeit, S. and Venalis, A. (2015) 'Molecular mechanisms behind progressing chronic inflammatory dilated cardiomyopathy', *BMC cardiovascular disorders,* 15(1), pp. 1-14.

Bollen, I. A., Schuldt, M., Harakalova, M., Vink, A., Asselbergs, F. W., Pinto, J. R., Krüger, M., Kuster, D. W. and van der Velden, J. (2017) 'Genotype-specific pathogenic effects in human dilated cardiomyopathy', *The Journal of physiology,* 595(14), pp. 4677-4693.

Bornstein, A. B., Rao, S. S. and Marwaha, K. (2021) 'Left ventricular hypertrophy', *StatPearls [Internet]*: StatPearls Publishing.

Bourque, C., Zhang, Y., Fu, M., Racine, M., Greasley, A., Pei, Y., Wu, L., Wang, R. and Yang, G. (2018) 'H2S protects lipopolysaccharide-induced inflammation by blocking NFκB transactivation in endothelial cells', *Toxicology and applied pharmacology,* 338, pp. 20-29.

Boutagy, N. E., Rogers, G. W., Pyne, E. S., Ali, M. M., Hulver, M. W. and Frisard, M. I. (2015) 'Using isolated mitochondria from minimal quantities of mouse skeletal muscle for high throughput microplate respiratory measurements', *JoVE (Journal of Visualized Experiments),* (104), pp. e53216.

Boyle, A. J., Shih, H., Hwang, J., Ye, J., Lee, B., Zhang, Y., Kwon, D., Jun, K., Zheng, D. and Sievers, R. (2011) 'Cardiomyopathy of aging in the mammalian heart is characterized by myocardial hypertrophy, fibrosis and a predisposition towards cardiomyocyte apoptosis and autophagy', *Experimental gerontology,* 46(7), pp. 549-559.

Brand, M. D. and Nicholls, D. G. (2011) 'Assessing mitochondrial dysfunction in cells', *Biochemical Journal,* 435(2), pp. 297-312.

Brandt, T., Mourier, A., Tain, L. S., Partridge, L., Larsson, N.-G. and Kühlbrandt, W. (2017) 'Changes of mitochondrial ultrastructure and function during ageing in mice and Drosophila', *Elife,* 6, pp. e24662.

Bruch, C., Schmermund, A., Marin, D., Katz, M., Bartel, T., Schaar, J. and Erbel, R. (2000) 'Tei-index in patients with mild-to-moderate congestive heart failure', *European heart journal,* 21(22), pp. 1888-1895.

Burke, M. A., Cook, S. A., Seidman, J. G. and Seidman, C. E. (2016) 'Clinical and mechanistic insights into the genetics of cardiomyopathy', *Journal of the American College of Cardiology,* 68(25), pp. 2871-2886.

Caforio, A. L., Adler, Y., Agostini, C., Allanore, Y., Anastasakis, A., Arad, M., Boehm, M., Charron, P., Elliott, P. M. and Eriksson, U. (2017) 'Diagnosis and management of myocardial involvement in systemic immune-mediated diseases: a position statement of the European Society of Cardiology Working Group on Myocardial and Pericardial Disease', *European heart journal,* 38(35), pp. 2649-2662.

Cai, W.-J., Wang, M.-J., Moore, P. K., Jin, H.-M., Yao, T. and Zhu, Y.-C. (2007) 'The novel proangiogenic effect of hydrogen sulfide is dependent on Akt phosphorylation', *Cardiovascular research,* 76(1), pp. 29-40.

Calvert, J. W., Jha, S., Gundewar, S., Elrod, J. W., Ramachandran, A., Pattillo, C. B., Kevil, C. G. and Lefer, D. J. (2009) 'Hydrogen sulfide mediates cardioprotection through Nrf2 signaling', *Circulation research,* 105(4), pp. 365-374.

Cao, Y.-P. and Zheng, M. (2019) 'Mitochondrial dynamics and inter-mitochondrial communication in the heart', *Archives of biochemistry and biophysics,* 663, pp. 214-219.

Carmeliet, P. (2003) 'Angiogenesis in health and disease', *Nature medicine,* 9(6), pp. 653-660.

Casad, M. E., Abraham, D., Kim, I.-M., Frangakis, S., Dong, B., Lin, N., Wolf, M. J. and Rockman, H. A. (2011) 'Cardiomyopathy is associated with ribosomal protein gene haplo-insufficiency in Drosophila melanogaster', *Genetics,* 189(3), pp. 861-870.

Chaanine, A. H., Joyce, L. D., Stulak, J. M., Maltais, S., Joyce, D. L., Dearani, J. A., Klaus, K., Nair, K. S., Hajjar, R. J. and Redfield, M. M. (2019) 'Mitochondrial morphology, dynamics, and function in human pressure overload or ischemic heart disease with preserved or reduced ejection fraction', *Circulation: Heart Failure,* 12(2), pp. e005131.

Chadda, K. R., Ajijola, O. A., Vaseghi, M., Shivkumar, K., Huang, C. L.-H. and Jeevaratnam, K. (2018) 'Ageing, the autonomic nervous system and arrhythmia: from brain to heart', *Ageing research reviews,* 48, pp. 40-50.

Chang, Y.-W., Chang, Y.-T., Wang, Q., Lin, J. J.-C., Chen, Y.-J. and Chen, C.-C. (2013) 'Quantitative phosphoproteomic study of pressure-overloaded mouse heart reveals dynamin-related protein 1 as a modulator of cardiac hypertrophy', *Molecular & Cellular Proteomics,* 12(11), pp. 3094-3107.

Charron, P., Arad, M., Arbustini, E., Basso, C., Bilinska, Z., Elliott, P., Helio, T., Keren, A., McKenna, W. J. and Monserrat, L. (2010) 'Genetic counselling and testing in cardiomyopathies: a position statement of the European Society of Cardiology Working Group on Myocardial and Pericardial Diseases', *European heart journal,* 31(22), pp. 2715-2726.

Chaudhary, K. R., El-Sikhry, H. and Seubert, J. M. (2011) 'Mitochondria and the aging heart', *Journal of geriatric cardiology: JGC,* 8(3), pp. 159.

Chen, J., Yaniz-Galende, E., Kagan, H. J., Liang, L., Hekmaty, S., Giannarelli, C. and Hajjar, R. (2015) 'Abnormalities of capillary microarchitecture in a rat model of coronary ischemic congestive heart failure', *American Journal of Physiology-Heart and Circulatory Physiology,* 308(8), pp. H830-H840.

Chen, L. and Knowlton, A. (2011) 'Mitochondrial dynamics in heart failure', *Congestive heart failure,* 17(6), pp. 257-261.

Chen, Y., Csordás, G., Jowdy, C., Schneider, T. G., Csordás, N., Wang, W., Liu, Y., Kohlhaas, M., Meiser, M. and Bergem, S. (2012) 'Mitofusin 2-containing mitochondrial-reticular microdomains direct rapid cardiomyocyte bioenergetic responses via interorganelle Ca2+ crosstalk', *Circulation research,* 111(7), pp. 863-875.

Chen, Y. and Dorn, G. W. (2013) 'PINK1-phosphorylated mitofusin 2 is a Parkin receptor for culling damaged mitochondria', *Science,* 340(6131), pp. 471-475.

Chen, Y., Liu, Y. and Dorn, G. W. (2011) 'Mitochondrial fusion is essential for organelle function and cardiac homeostasis', *Circulation research,* 109(12), pp. 1327-1331.

Chen, Y., Zhang, F., Yin, J., Wu, S. and Zhou, X. (2020) 'Protective mechanisms of hydrogen sulfide in myocardial ischemia', *Journal of Cellular Physiology,* 235(12), pp. 9059-9070.

Chen, Y.-H., Yao, W.-Z., Geng, B., Ding, Y.-L., Lu, M., Zhao, M.-W. and Tang, C.-S. (2005) 'Endogenous hydrogen sulfide in patients with COPD', *Chest,* 128(5), pp. 3205-3211.

Cheng, S., Fernandes, V. R., Bluemke, D. A., McClelland, R. L., Kronmal, R. A. and Lima, J. A. (2009) 'Age-related left ventricular remodeling and associated risk for cardiovascular outcomes: the Multi-Ethnic Study of Atherosclerosis', *Circulation: Cardiovascular Imaging,* 2(3), pp. 191-198.

Chiao, Y. A. and Rabinovitch, P. S. (2015) 'The aging heart', *Cold Spring Harbor perspectives in medicine,* 5(9), pp. a025148.

Chiku, T., Padovani, D., Zhu, W., Singh, S., Vitvitsky, V. and Banerjee, R. (2009) 'H2S biogenesis by human cystathionine γ-lyase leads to the novel sulfur metabolites lanthionine and homolanthionine and is responsive to the grade of hyperhomocysteinemia', *Journal of Biological Chemistry,* 284(17), pp. 11601-11612.

Chute, M., Aujla, P., Jana, S. and Kassiri, Z. (2019) 'The non-fibrillar side of fibrosis: contribution of the basement membrane, proteoglycans, and glycoproteins to myocardial fibrosis', *Journal of cardiovascular development and disease,* 6(4), pp. 35.

Ciarambino, T., Menna, G., Sansone, G. and Giordano, M. (2021) 'Cardiomyopathies: an overview', *International journal of molecular sciences,* 22(14), pp. 7722.

Cipolat, S., de Brito, O. M., Dal Zilio, B. and Scorrano, L. (2004) 'OPA1 requires mitofusin 1 to promote mitochondrial fusion', *Proceedings of the National Academy of Sciences,* 101(45), pp. 15927-15932.

Coppini, R., Ho, C. Y., Ashley, E., Day, S., Ferrantini, C., Girolami, F., Tomberli, B., Bardi, S., Torricelli, F. and Cecchi, F. (2014) 'Clinical phenotype and outcome of hypertrophic cardiomyopathy associated with thin-filament gene mutations', *Journal of the American College of Cardiology,* 64(24), pp. 2589-2600.

Corona-Villalobos, C. P., Sorensen, L. L., Pozios, I., Chu, L., Eng, J., Abraham, M. R., Abraham, T. P., Kamel, I. R. and Zimmerman, S. L. (2016) 'Left ventricular wall thickness in patients with hypertrophic cardiomyopathy: a comparison between cardiac magnetic resonance imaging and echocardiography', *The international journal of cardiovascular imaging,* 32, pp. 945-954.

Corsello, T., Komaravelli, N. and Casola, A. (2018) 'Role of hydrogen sulfide in NRF2-and sirtuin-dependent maintenance of cellular redox balance', *Antioxidants,* 7(10), pp. 129.

Cubero, J. S., Rivera, L. A.-P., Moral, R. P. and Melchor, L. S. (2004) 'Heart failure: etiology and approach to diagnosis', *Revista Española de Cardiología (English Edition),* 57(3), pp. 250-259.

Cui, H., Schaff, H. V., Lentz Carvalho, J., Nishimura, R. A., Geske, J. B., Dearani, J. A., Lahr, B. D., Lee, A. T., Bos, J. M. and Ackerman, M. J. (2021) 'Myocardial histopathology in patients with obstructive hypertrophic cardiomyopathy', *Journal of the American College of Cardiology,* 77(17), pp. 2159-2170.

Dai, D.-F., Rabinovitch, P. S. and Ungvari, Z. (2012) 'Mitochondria and cardiovascular aging', *Circulation research,* 110(8), pp. 1109-1124.

Dai, D.-F., Santana, L. F., Vermulst, M., Tomazela, D. M., Emond, M. J., MacCoss, M. J., Gollahon, K., Martin, G. M., Loeb, L. A. and Ladiges, W. C. (2009) 'Overexpression of catalase targeted to mitochondria attenuates murine cardiac aging', *Circulation,* 119(21), pp. 2789-2797.

Davies, P. F., Civelek, M., Fang, Y. and Fleming, I. (2013) 'The atherosusceptible endothelium: endothelial phenotypes in complex haemodynamic shear stress regions in vivo', *Cardiovascular research,* 99(2), pp. 315-327.

De Lucia, C., Wallner, M., Eaton, D. M., Zhao, H., Houser, S. R. and Koch, W. J. (2019) 'Echocardiographic strain analysis for the early detection of left ventricular systolic/diastolic dysfunction and dyssynchrony in a mouse model of physiological aging', *The Journals of Gerontology: Series A,* 74(4), pp. 455-461.

De Moudt, S., Hendrickx, J. O., Neutel, C., De Munck, D., Leloup, A., De Meyer, G. R., Martinet, W. and Fransen, P. (2022) 'Progressive aortic stiffness in aging C57Bl/6 mice displays altered contractile behaviour and extracellular matrix changes', *Communications Biology,* 5(1), pp. 605.

Debessa, C. R. G., Maifrino, L. B. M. and de Souza, R. R. (2001) 'Age related changes of the collagen network of the human heart', *Mechanisms of ageing and development,* 122(10), pp. 1049-1058.

Deng, L. H., Xu, F. H., Zeng, T., Xu, X. and Chao, H. C. (2019) 'Expression and Clinical Significance of Late Endosomal/Lysosomal Adaptor, Mitogen-activated Protein Kinase and Mammalian Target of Rapamycin Activator 3 in Bladder Carcinoma', *Zhongguo yi xue ke xue Yuan xue bao. Acta Academiae Medicinae Sinicae,* 41(5), pp. 601-608.

Deten, A., Volz, H. C., Briest, W. and Zimmer, H.-G. (2002) 'Cardiac cytokine expression is upregulated in the acute phase after myocardial infarction. Experimental studies in rats', *Cardiovascular research,* 55(2), pp. 329-340.

Dhalla, N. S., Elmoselhi, A. B., Hata, T. and Makino, N. (2000) 'Status of myocardial antioxidants in ischemia–reperfusion injury', *Cardiovascular research,* 47(3), pp. 446-456.

Dolinsky, V. W., Cole, L. K., Sparagna, G. C. and Hatch, G. M. (2016) 'Cardiac mitochondrial energy metabolism in heart failure: Role of cardiolipin and sirtuins', *Biochimica et Biophysica Acta (BBA)-Molecular and Cell Biology of Lipids,* 1861(10), pp. 1544-1554.

Dorn, G. W. (2015) 'Mitochondrial dynamism and heart disease: changing shape and shaping change', *EMBO molecular medicine,* 7(7), pp. 865-877.

Dorn II, G. W. and Maack, C. (2013) 'SR and mitochondria: calcium cross-talk between kissing cousins', *Journal of molecular and cellular cardiology,* 55, pp. 42-49.

Dugo, C. *et al.* (2016) 'Assessment and impact of diastolic function by echocardiography in elderly patients', *Journal of Geriatric Cardiology*, 13(3), pp. 252–260.

Dujardin, K. S., Tei, C., Yeo, T. C., Hodge, D. O., Rossi, A. and Seward, J. B. (1998) 'Prognostic value of a Doppler index combining systolic and diastolic performance in idiopathic-dilated cardiomyopathy', *The American journal of cardiology,* 82(9), pp. 1071-1076.

Dutta, S. and Sengupta, P. (2016) 'Men and mice: relating their ages', *Life sciences,* 152, pp. 244-248.

Edelberg, J. M., Sehnert, A. J., Mealiffe, M. E., Del Rio, C. L. and McDowell, R. (2022) 'The impact of mavacamten on the pathophysiology of hypertrophic cardiomyopathy: a narrative review', *American Journal of Cardiovascular Drugs,* 22(5), pp. 497-510.

EHN (2018) *European Cardiovascular Disease Statistics 2017*. ehn.org: European Heart Network. Available at: https://ehnheart.org/cvd-statistics.html.

Eijgenraam, T. R., Silljé, H. H. and de Boer, R. A. (2020) 'Current understanding of fibrosis in genetic cardiomyopathies', *Trends in cardiovascular medicine,* 30(6), pp. 353-361.

Ellmers, L. J., Templeton, E. M., Pilbrow, A. P., Frampton, C., Ishii, I., Moore, P. K., Bhatia, M., Richards, A. M. and Cameron, V. A. (2020) 'Hydrogen sulfide treatment improves post-infarct remodeling and long-term cardiac function in CSE knockout and wild-type mice', *International Journal of Molecular Sciences,* 21(12), pp. 4284.

Elrod, J. W., Calvert, J. W., Morrison, J., Doeller, J. E., Kraus, D. W., Tao, L., Jiao, X., Scalia, R., Kiss, L. and Szabo, C. (2007) 'Hydrogen sulfide attenuates myocardial ischemia-reperfusion injury by preservation of mitochondrial function', *Proceedings of the National Academy of Sciences,* 104(39), pp. 15560-15565.

Fang, L., Ellims, A. H., Beale, A. L., Taylor, A. J., Murphy, A. and Dart, A. M. (2017) 'Systemic inflammation is associated with myocardial fibrosis, diastolic dysfunction, and cardiac

hypertrophy in patients with hypertrophic cardiomyopathy', *American Journal of Translational Research,* 9(11), pp. 5063.

Fassone, E. and Rahman, S. (2012) 'Complex I deficiency: clinical features, biochemistry and molecular genetics', *Journal of medical genetics,* 49(9), pp. 578-590.

Ferrara, N., Komici, K., Corbi, G., Pagano, G., Furgi, G., Rengo, C., Femminella, G. D., Leosco, D. and Bonaduce, D. (2014) 'β-adrenergic receptor responsiveness in aging heart and clinical implications', *Frontiers in physiology,* 4, pp. 396.

Finocchiaro, G., Merlo, M., Sheikh, N., De Angelis, G., Papadakis, M., Olivotto, I., Rapezzi, C., Carr-White, G., Sharma, S. and Mestroni, L. (2020) 'The electrocardiogram in the diagnosis and management of patients with dilated cardiomyopathy', *European journal of heart failure,* 22(7), pp. 1097-1107.

Fiordelisi, A., Iaccarino, G., Morisco, C., Coscioni, E. and Sorriento, D. (2019) 'NFkappaB is a key player in the crosstalk between inflammation and cardiovascular diseases', *International Journal of Molecular Sciences,* 20(7), pp. 1599.

Flurkey, K., Currer, J., Harrison, D. and Fox, J. G. (2007) 'The mouse in biomedical research', *American College of Laboratory Animal Medicine series. Elsevier, AP: Amsterdam*.

Fontana, G. A. and Gahlon, H. L. (2020) 'Mechanisms of replication and repair in mitochondrial DNA deletion formation', *Nucleic acids research,* 48(20), pp. 11244-11258.

Fontes, J. A., Rose, N. R. and Čihák ová, D. (2015) 'The varying faces of IL-6: From cardiac protection to cardiac failure', *Cytokine,* 74(1), pp. 62-68.

Fu, M., Zhang, W., Wu, L., Yang, G., Li, H. and Wang, R. (2012) 'Hydrogen sulfide (H2S) metabolism in mitochondria and its regulatory role in energy production', *Proceedings of the National Academy of Sciences,* 109(8), pp. 2943-2948.

Furne, J., Springfield, J., Koenig, T., DeMaster, E. and Levitt, M. D. (2001) 'Oxidation of hydrogen sulfide and methanethiol to thiosulfate by rat tissues: a specialized function of the colonic mucosa', *Biochemical pharmacology,* 62(2), pp. 255-259.

Galati, G., Leone, O., Pasquale, F., Olivotto, I., Biagini, E., Grigioni, F., Pilato, E., Lorenzini, M., Corti, B. and Foà, A. (2016) 'Histological and histometric characterization of myocardial fibrosis in end-stage hypertrophic cardiomyopathy: a clinical-pathological study of 30 explanted hearts', *Circulation: Heart Failure,* 9(9), pp. e003090.

Gao, Q., Zhang, W., Zhao, Y., Tian, Y., Wang, Y., Zhang, J., Geng, M., Xu, M., Yao, C. and Wang, H. (2021) 'High-throughput screening in postimplantation haploid epiblast stem cells

reveals Hs3st3b1 as a modulator for reprogramming', *Stem Cells Translational Medicine,* 10(5), pp. 743-755.

Garcia-Canadilla, P., Cook, A. C., Mohun, T. J., Oji, O., Schlossarek, S., Carrier, L., McKenna, W. J., Moon, J. C. and Captur, G. (2019) 'Myoarchitectural disarray of hypertrophic cardiomyopathy begins pre-birth', *Journal of Anatomy,* 235(5), pp. 962-976.

Garfinkel, A. C., Seidman, J. G. and Seidman, C. E. (2018) 'Genetic pathogenesis of hypertrophic and dilated cardiomyopathy', *Heart failure clinics,* 14(2), pp. 139-146.

Gegg, M. E., Cooper, J. M., Chau, K.-Y., Rojo, M., Schapira, A. H. and Taanman, J.-W. (2010) 'Mitofusin 1 and mitofusin 2 are ubiquitinated in a PINK1/parkin-dependent manner upon induction of mitophagy', *Human molecular genetics,* 19(24), pp. 4861-4870.

Geisler, S., Holmström, K. M., Skujat, D., Fiesel, F. C., Rothfuss, O. C., Kahle, P. J. and Springer, W. (2010) 'PINK1/Parkin-mediated mitophagy is dependent on VDAC1 and p62/SQSTM1', *Nature cell biology,* 12(2), pp. 119-131.

Gersh, B. J., Maron, B. J., Bonow, R. O., Dearani, J. A., Fifer, M. A., Link, M. S., Naidu, S. S., Nishimura, R. A., Ommen, S. R. and Rakowski, H. (2011) '2011 ACCF/AHA guideline for the diagnosis and treatment of hypertrophic cardiomyopathy: a report of the American College of Cardiology Foundation/American Heart Association Task Force on practice guidelines developed in collaboration with the American Association for Thoracic Surgery, American Society of echocardiography, American Society of nuclear Cardiology, Heart Failure Society of America, Heart Rhythm Society, Society for Cardiovascular Angiography and Interventions, and Society of Thoracic Surgeons', *Journal of the American College of Cardiology,* 58(25), pp. e212-e260.

Girolami, F., Ho, C. Y., Semsarian, C., Baldi, M., Will, M. L., Baldini, K., Torricelli, F., Yeates, L., Cecchi, F. and Ackerman, M. J. (2010) 'Clinical features and outcome of hypertrophic cardiomyopathy associated with triple sarcomere protein gene mutations', *Journal of the American College of Cardiology,* 55(14), pp. 1444-1453.

Glancy, B., Kim, Y., Katti, P. and Willingham, T. B. (2020) 'The functional impact of mitochondrial structure across subcellular scales', *Frontiers in physiology,* 11, pp. 541040.

Glavnik Poznic, N., KOVAČIĆ, D., GOSLAR, T., MARŠ, T. and Podbregar, M. (2018) 'Total plasma sulfde in mild to moderate diastolic heart dysfunction', *Signa vitae: journal for intesive care and emergency medicine,* 14(2), pp. 35-40.

Goh, K. Y., Qu, J., Hong, H., Liu, T., Dell'Italia, L. J., Wu, Y., O'rourke, B. and Zhou, L. (2016) 'Impaired mitochondrial network excitability in failing guinea-pig cardiomyocytes', *Cardiovascular research,* 109(1), pp. 79-89.

Gong, W., Zhang, S., Chen, Y., Shen, J., Zheng, Y., Liu, X., Zhu, M. and Meng, G. (2022a) 'Protective role of hydrogen sulfide against diabetic cardiomyopathy via alleviating necroptosis', *Free Radical Biology and Medicine,* 181, pp. 29-42.

Gong, Y., Lv, Y., Xu, F., Xiu, Y., Lu, Y., Liu, Z. and Deng, L. (2022b) 'LAMTOR3 is a prognostic biomarker in kidney renal clear cell carcinoma', *Journal of Clinical Laboratory Analysis,* 36(9), pp. e24648.

Gorini, F., Bustaffa, E., Chatzianagnostou, K., Bianchi, F. and Vassalle, C. (2020) 'Hydrogen sulfide and cardiovascular disease: Doubts, clues, and interpretation difficulties from studies in geothermal areas', *Science of The Total Environment,* 743, pp. 140818.

Gorski, P. A., Ceholski, D. K. and Hajjar, R. J. (2015) 'Altered myocardial calcium cycling and energetics in heart failure—a rational approach for disease treatment', *Cell metabolism,* 21(2), pp. 183-194.

Goto, D., Kinugawa, S., Hamaguchi, S., Sakakibara, M., Tsuchihashi-Makaya, M., Yokota, T., Yamada, S., Yokoshiki, H., Tsutsui, H. and Investigators, J.-C. (2013) 'Clinical characteristics and outcomes of dilated phase of hypertrophic cardiomyopathy: report from the registry data in Japan', *Journal of Cardiology,* 61(1), pp. 65-70.

Goubern, M., Andriamihaja, M., Nübel, T., Blachier, F. and Bouillaud, F. (2007) 'Sulfide, the first inorganic substrate for human cells', *The FASEB Journal,* 21(8), pp. 1699-1706.

Goudarzi, K. M. and Lindström, M. S. (2016) 'Role of ribosomal protein mutations in tumor development', *International journal of oncology,* 48(4), pp. 1313-1324.

Gouveia, M., Teixeira, M., Schmidt, C., Lopes, M., Trindade, D., Magalhães, S., Henriques, A. G., Nunes, A., Santos, M. and Vieira, S. (2023) 'Impaired Extracellular Proteostasis in Patients with Heart Failure', *Archives of Medical Research,* 54(3), pp. 211-222.

Grünig, E., Tasman, J. A., Kücherer, H., Franz, W., Kübler, W. and Katus, H. A. (1998) 'Frequency and phenotypes of familial dilated cardiomyopathy', *Journal of the American College of Cardiology,* 31(1), pp. 186-194.

Guan, Q., Wang, X., Gao, L., Chen, J., Liu, Y., Yu, C., Zhang, N., Zhang, X. and Zhao, J. (2013) 'Hydrogen sulfide suppresses high glucose–induced expression of intercellular adhesion molecule-1 in endothelial cells', *Journal of cardiovascular pharmacology,* 62(3), pp. 278-284.

Gulati, A., Assomull, R., Morarji, K., Brown, T., Liodakis, E., Dweck, M. R., Khalique, Z., Morarji, J., Alpendurada, F. and Prasad, S. K. (2012) 'Prognostic significance of midwall fibrosis in dilated cardiomyopathy', *Journal of Cardiovascular Magnetic Resonance,* 14(1), pp. 1-2.

Gullestad, L., Ueland, T., Vinge, L. E., Finsen, A., Yndestad, A. and Aukrust, P. (2012) 'Inflammatory cytokines in heart failure: mediators and markers', *Cardiology,* 122(1), pp. 23-35.

Gunja-Smith, Z., Morales, A. R., Romanelli, R. and Woessner Jr, J. F. (1996) 'Remodeling of human myocardial collagen in idiopathic dilated cardiomyopathy. Role of metalloproteinases and pyridinoline cross-links', *The American journal of pathology,* 148(5), pp. 1639.

Guo, X., Lin, M., Rockowitz, S., Lachman, H. M. and Zheng, D. (2014) 'Characterization of human pseudogene-derived non-coding RNAs for functional potential', *PloS one,* 9(4), pp. e93972.

Haas, J., Frese, K. S., Peil, B., Kloos, W., Keller, A., Nietsch, R., Feng, Z., Müller, S., Kayvanpour, E., Vogel, B., Sedaghat-Hamedani, F., Lim, W.-K., Zhao, X., Fradkin, D., Köhler, D., Fischer, S., Franke, J., Marquart, S., Barb, I., Li, D. T., Amr, A., Ehlermann, P., Mereles, D., Weis, T., Hassel, S., Kremer, A., King, V., Wirsz, E., Isnard, R., Komajda, M., Serio, A., Grasso, M., Syrris, P., Wicks, E., Plagnol, V., Lopes, L., Gadgaard, T., Eiskjær, H., Jørgensen, M., Garcia-Giustiniani, D., Ortiz-Genga, M., Crespo-Leiro, M. G., Deprez, R. H. L. D., Christiaans, I., Van Rijsingen, I. A., Wilde, A. A., Waldenstrom, A., Bolognesi, M., Bellazzi, R., Mörner, S., Bermejo, J. L., Monserrat, L., Villard, E., Mogensen, J., Pinto, Y. M., Charron, P., Elliott, P., Arbustini, E., Katus, H. A. and Meder, B. (2015) 'Atlas of the clinical genetics of human dilated cardiomyopathy', *European Heart Journal,* 36(18), pp. 1123-1135.

Haland, T.F. and Edvardsen, T. (2019) ‘The role of echocardiography in management of hypertrophic cardiomyopathy’, *Journal of Echocardiography*, 18(2), pp. 77–85.

Haland, T. F., Hasselberg, N. E., Almaas, V. M., Dejgaard, L. A., Saberniak, J., Leren, I. S., Berge, K. E., Haugaa, K. H. and Edvardsen, T. (2017) 'The systolic paradox in hypertrophic cardiomyopathy', *Open Heart,* 4(1), pp. e000571.

Hansson, A., Hance, N., Dufour, E., Rantanen, A., Hultenby, K., Clayton, D. A., Wibom, R. and Larsson, N.-G. (2004) 'A switch in metabolism precedes increased mitochondrial biogenesis in respiratory chain-deficient mouse hearts', *Proceedings of the National Academy of Sciences,* 101(9), pp. 3136-3141.

Hao, J., Xi, Y., Jiao, L., Wen, X., Wu, R., Chang, G., Sun, F., Wei, C. and Li, H. (2022) 'Exogenous hydrogen sulfide inhibits the senescence of cardiomyocytes through modulating mitophagy in rats', *Cellular Signalling,* 100, pp. 110465.

Harman, D. (1972) 'The biologic clock: the mitochondria?', *Journal of the American Geriatrics Society,* 20(4), pp. 145-147.

Harraan, D. (1955) 'Aging: a theory based on free radical and radiation chemistry'.

Hasselberg, N. E., Haland, T. F., Saberniak, J., Brekke, P. H., Berge, K. E., Leren, T. P., Edvardsen, T. and Haugaa, K. H. (2018) 'Lamin A/C cardiomyopathy: young onset, high penetrance, and frequent need for heart transplantation', *Eur Heart J,* 39(10), pp. 853-860.

Hata, Y., Ichimata, S., Yamaguchi, Y., Hirono, K., Oku, Y., Ichida, F. and Nishida, N. (2019) 'Clinicopathological and genetic profiles of cases with myocyte disarray—investigation for establishing the autopsy diagnostic criteria for hypertrophic cardiomyopathy', *Journal of Clinical Medicine,* 8(4), pp. 463.

Hazebroek, M., Dennert, R. and Heymans, S. (2012) 'Idiopathic dilated cardiomyopathy: possible triggers and treatment strategies', *Netherlands Heart Journal,* 20(7), pp. 332-335.

Hees, P. S., Fleg, J. L., Lakatta, E. G. and Shapiro, E. P. (2002) 'Left ventricular remodeling with age in normal men versus women: novel insights using three-dimensional magnetic resonance imaging', *The American journal of cardiology,* 90(11), pp. 1231-1236.

Heinen, A., Raupach, A., Behmenburg, F., Hölscher, N., Flögel, U., Kelm, M., Kaisers, W., Nederlof, R., Huhn, R. and Gödecke, A. (2018) 'Echocardiographic analysis of cardiac function after infarction in mice: validation of single-plane long-axis view measurements and the bi-plane simpson method', *Ultrasound in Medicine & Biology,* 44(7), pp. 1544-1555.

Helms, A. S., Tang, V. T., O'Leary, T. S., Friedline, S., Wauchope, M., Arora, A., Wasserman, A. H., Smith, E. D., Lee, L. M. and Wen, X. W. (2020) 'Effects of MYBPC3 loss-of-function mutations preceding hypertrophic cardiomyopathy', *JCI insight,* 5(2).

Henein, M. Y., Vancheri, S., Longo, G. and Vancheri, F. (2022) 'The Role of Inflammation in Cardiovascular Disease', *International Journal of Molecular Sciences,* 23(21), pp. 12906.

Herman, D. S., Lam, L., Taylor, M. R., Wang, L., Teekakirikul, P., Christodoulou, D., Conner, L., DePalma, S. R., McDonough, B. and Sparks, E. (2012) 'Truncations of titin causing dilated cardiomyopathy', *New England Journal of Medicine,* 366(7), pp. 619-628.

Hershberger, R. E., Hedges, D. J. and Morales, A. (2013) 'Dilated cardiomyopathy: the complexity of a diverse genetic architecture', *Nature Reviews Cardiology,* 10(9), pp. 531-547.

Hildebrandt, T. M. (2011) 'Modulation of sulfide oxidation and toxicity in rat mitochondria by dehydroascorbic acid', *Biochimica et Biophysica Acta (BBA)-Bioenergetics,* 1807(9), pp. 1206-1213.

Hildebrandt, T. M. and Grieshaber, M. K. (2008) 'Three enzymatic activities catalyze the oxidation of sulfide to thiosulfate in mammalian and invertebrate mitochondria', *The FEBS journal,* 275(13), pp. 3352-3361.

Hirota, Y., Shimizu, G., Kaku, K., Saito, T., Kino, M. and Kawamura, K. (1984) 'Mechanisms of compensation and decompensation in dilated cardiomyopathy', *The American journal of cardiology,* 54(8), pp. 1033-1038.

Hoorntje, E. T., Bollen, I. A., Barge-Schaapveld, D. Q., van Tienen, F. H., Te Meerman, G. J., Jansweijer, J. A., van Essen, A. J., Volders, P. G., Constantinescu, A. A. and Van Den Akker, P. C. (2017) 'Lamin A/C-related cardiac disease: late onset with a variable and mild phenotype in a large cohort of patients with the lamin A/C p.(Arg331Gln) founder mutation', *Circulation: Cardiovascular Genetics,* 10(4), pp. e001631.

Horan, M. P., Pichaud, N. and Ballard, J. W. O. (2012) 'Quantifying mitochondrial dysfunction in complex diseases of aging', *Journals of Gerontology Series A: Biomedical Sciences and Medical Sciences,* 67(10), pp. 1022-1035.

Hoshikawa, E., Matsumura, Y., Kubo, T., Okawa, M., Yamasaki, N., Kitaoka, H., Furuno, T., Takata, J. and Doi, Y. L. (2011) 'Effect of left ventricular reverse remodeling on long-term prognosis after therapy with angiotensin-converting enzyme inhibitors or angiotensin II receptor blockers and β blockers in patients with idiopathic dilated cardiomyopathy', *The American journal of cardiology,* 107(7), pp. 1065-1070.

Hsiao, Y. T., Shimizu, I., Wakasugi, T., Yoshida, Y., Ikegami, R., Hayashi, Y., Suda, M., Katsuumi, G., Nakao, M. and Ozawa, T. (2021) 'Cardiac mitofusin-1 is reduced in non-responding patients with idiopathic dilated cardiomyopathy', *Scientific reports,* 11(1), pp. 6722.

Hsieh, J., Becklin, K. L., Givens, S., Komosa, E. R., Lloréns, J. E. A., Moriarity, B. S., Webber, B. R., Singh, B. N. and Ogle, B. M. (2022) 'Myosin heavy chain converter domain mutations drive early-stage changes in extracellular matrix dynamics in hypertrophic cardiomyopathy', *Frontiers in Cell and Developmental Biology,* 10, pp. 894635.

Hu, H.-J., Wang, X.-H., Liu, Y., Zhang, T.-Q., Chen, Z.-R., Zhang, C., Tang, Z.-H., Qu, S.-L., Tang, H.-F. and Jiang, Z.-S. (2021) 'Hydrogen sulfide ameliorates angiotensin II-induced atrial fibrosis progression to atrial fibrillation through inhibition of the Warburg Effect and endoplasmic reticulum stress', *Frontiers in Pharmacology,* 12, pp. 690371.

Hu, Q., Zhang, R., Zheng, J., Song, M., Gu, C. and Li, W. (2023) 'Hydrogen sulfide attenuates uranium-induced kidney cells pyroptosis via upregulation of PI3K/AKT/mTOR signaling', *Journal of biochemical and molecular toxicology,* 37(1), pp. e23220.

Hu, X., Yang, L. and Mo, Y.-Y. (2018) 'Role of pseudogenes in tumorigenesis', *Cancers,* 10(8), pp. 256.

Hua, X., Hu, G., Hu, Q., Chang, Y., Hu, Y., Gao, L., Chen, X., Yang, P.-C., Zhang, Y. and Li, M. (2020) 'Single-cell RNA sequencing to dissect the immunological network of autoimmune myocarditis', *Circulation,* 142(4), pp. 384-400.

Huang, H., Joseph, L. C., Gurin, M. I., Thorp, E. B. and Morrow, J. P. (2014) 'Extracellular signal-regulated kinase activation during cardiac hypertrophy reduces sarcoplasmic/endoplasmic reticulum calcium ATPase 2 (SERCA2) transcription', *Journal of molecular and cellular cardiology,* 75, pp. 58-63.

Huang, H., Sun, Z., Hill, M. A. and Meininger, G. A. (2018) 'A calcium mediated mechanism coordinating vascular smooth muscle cell adhesion during KCl activation', *Frontiers in Physiology,* 9, pp. 1810.

Huang, S., Chen, X., Pan, J., Zhang, H., Ke, J., Gao, L., Chang, A. C. Y., Zhang, J. and Zhang, H. (2023) 'Hydrogen sulfide alleviates heart failure with preserved ejection fraction in mice by targeting mitochondrial abnormalities via PGC-1α', *Nitric Oxide*.

Huang, Z.-P., Chen, J., Seok, H. Y., Zhang, Z., Kataoka, M., Hu, X. and Wang, D.-Z. (2013) 'MicroRNA-22 regulates cardiac hypertrophy and remodeling in response to stress', *Circulation research,* 112(9), pp. 1234-1243.

Hughes, S. (2004) 'The pathology of hypertrophic cardiomyopathy', *Histopathology,* 44(5), pp. 412-427.

Hunyady, L. and Turu, G. (2004) 'The role of the AT1 angiotensin receptor in cardiac hypertrophy: angiotensin II receptor or stretch sensor?', *Trends in Endocrinology & Metabolism,* 15(9), pp. 405-408.

Iaizzo, P. A. (2015) 'General Features of the Cardiovascular System', in Iaizzo, P.A. (ed.) *Handbook of Cardiac Anatomy, Physiology, and Devices*. Cham: Springer International Publishing, pp. 3-12.

Ikeda, Y., Shirakabe, A., Maejima, Y., Zhai, P., Sciarretta, S., Toli, J., Nomura, M., Mihara, K., Egashira, K. and Ohishi, M. (2015) 'Endogenous Drp1 mediates mitochondrial autophagy and protects the heart against energy stress', *Circulation research,* 116(2), pp. 264-278.

Inamdar, A. A. and Inamdar, A. C. (2016) 'Heart failure: diagnosis, management and utilization', *Journal of clinical medicine,* 5(7), pp. 62.

Iqbal, F., Lupieri, A., Aikawa, M. and Aikawa, E. (2021) 'Harnessing single-cell RNA sequencing to better understand how diseased cells behave the way they do in cardiovascular disease', *Arteriosclerosis, thrombosis, and vascular biology,* 41(2), pp. 585-600.

Ishihara, T., Ban-Ishihara, R., Maeda, M., Matsunaga, Y., Ichimura, A., Kyogoku, S., Aoki, H., Katada, S., Nakada, K. and Nomura, M. (2015) 'Dynamics of mitochondrial DNA nucleoids regulated by mitochondrial fission is essential for maintenance of homogeneously active mitochondria during neonatal heart development', *Molecular and cellular biology,* 35(1), pp. 211-223.

Ito, Y., Yoshida, M., Masuda, H., Maeda, D., Kudo-Asabe, Y., Umakoshi, M., Nanjo, H. and Goto, A. (2021) 'Disorganization of intercalated discs in dilated cardiomyopathy', *Scientific Reports,* 11(1), pp. 1-13.

Izumiya, Y., Shiojima, I., Sato, K., Sawyer, D. B., Colucci, W. S. and Walsh, K. (2006) 'Vascular endothelial growth factor blockade promotes the transition from compensatory cardiac hypertrophy to failure in response to pressure overload', *Hypertension,* 47(5), pp. 887-893.

Janicki, J. S. and Brower, G. L. (2002) 'The role of myocardial fibrillar collagen in ventricular remodeling and function', *Journal of cardiac failure,* 8(6), pp. S319-S325.

Jiang, H., Wu, H., Li, Z., Geng, B. and Tang, C. (2005) 'Changes of the new gaseous transmitter H2S in patients with coronary heart disease', *Di 1 jun yi da xue xue bao= Academic journal of the first medical college of PLA,* 25(8), pp. 951-954.

Jin, J.-y., Wei, X.-x., Zhi, X.-l., Wang, X.-h. and Meng, D. (2021) 'Drp1-dependent mitochondrial fission in cardiovascular disease', *Acta Pharmacologica Sinica,* 42(5), pp. 655-664.

Johansen, D., Ytrehus, K. and Baxter, G. F. (2006) 'Exogenous hydrogen sulfide (H 2 S) protects against regional myocardial ischemia–reperfusion injury: Evidence for a role of K ATP channels', *Basic research in cardiology,* 101, pp. 53-60.

John, G. B., Shang, Y., Li, L., Renken, C., Mannella, C. A., Selker, J. M., Rangell, L., Bennett, M. J. and Zha, J. (2005) 'The mitochondrial inner membrane protein mitofilin controls cristae morphology', *Molecular biology of the cell,* 16(3), pp. 1543-1554.

Jones, D. T., Lechertier, T., Reynolds, L. E., Mitter, R., Robinson, S. D., Kirn-Safran, C. B. and Hodivala-Dilke, K. M. (2013) 'Endogenous ribosomal protein L29 (RPL29): a newly identified regulator of angiogenesis in mice', *Disease models & mechanisms,* 6(1), pp. 115-124.

Jovin, I. S., Ebisu, K., Liu, Y. H., Finta, L. A., Oprea, A. D., Brandt, C. A., Dziura, J. and Wackers, F. J. (2013) 'Left Ventricular Ejection Fraction and Left Ventricular End-Diastolic Volume in Patients With Diastolic Dysfunction', *Congestive Heart Failure,* 19(3), pp. 130-134.

Kageyama, Y., Zhang, Z., Roda, R., Fukaya, M., Wakabayashi, J., Wakabayashi, N., Kensler, T. W., Reddy, P. H., Iijima, M. and Sesaki, H. (2012) 'Mitochondrial division ensures the survival of postmitotic neurons by suppressing oxidative damage', *Journal of Cell Biology,* 197(4), pp. 535-551.

Kalkhoran, S. B., Munro, P., Qiao, F., Ong, S.-B., Hall, A. R., Cabrera-Fuentes, H., Chakraborty, B., Boisvert, W. A., Yellon, D. M. and Hausenloy, D. J. (2017) 'Unique morphological characteristics of mitochondrial subtypes in the heart: the effect of ischemia and ischemic preconditioning', *Discoveries (Craiova, Romania),* 5(1).

Kamoun, P. (2004) 'Endogenous production of hydrogen sulfide in mammals', *Amino acids,* 26(3), pp. 243-254.

Kane, G. C., Karon, B. L., Mahoney, D. W., Redfield, M. M., Roger, V. L., Burnett, J. C., Jacobsen, S. J. and Rodeheffer, R. J. (2011) 'Progression of left ventricular diastolic dysfunction and risk of heart failure', *Jama,* 306(8), pp. 856-863.

Kanehisa, M. and Goto, S. (2000) 'KEGG: kyoto encyclopedia of genes and genomes', *Nucleic acids research,* 28(1), pp. 27-30.

Kar, S., Shahshahan, H. R., Hackfort, B. T., Yadav, S. K., Yadav, R., Kambis, T. N., Lefer, D. J. and Mishra, P. K. (2019) 'Exercise training promotes cardiac hydrogen sulfide biosynthesis and mitigates pyroptosis to prevent high-fat diet-induced diabetic cardiomyopathy', *Antioxidants,* 8(12), pp. 638.

Karamanlidis, G., Lee, C. F., Garcia-Menendez, L., Kolwicz Jr, S. C., Suthammarak, W., Gong, G., Sedensky, M. M., Morgan, P. G., Wang, W. and Tian, R. (2013) 'Mitochondrial complex I deficiency increases protein acetylation and accelerates heart failure', *Cell metabolism,* 18(2), pp. 239-250.

Karamanlidis, G., Nascimben, L., Couper, G. S., Shekar, P. S., del Monte, F. and Tian, R. (2010) 'Defective DNA replication impairs mitochondrial biogenesis in human failing hearts', *Circulation research,* 106(9), pp. 1541-1548.

Karwi, Q. G., Uddin, G. M., Ho, K. L. and Lopaschuk, G. D. (2018) 'Loss of metabolic flexibility in the failing heart', *Frontiers in cardiovascular medicine,* 5, pp. 68.

Kathiresan, S. and Srivastava, D. (2012) 'Genetics of human cardiovascular disease', *Cell,* 148(6), pp. 1242-1257.

Keam, S. J. (2022) 'Mavacamten: First Approval', *Drugs,* 82(10), pp. 1127-1135.

Kehat, I. and Molkentin, J. D. (2010) 'Molecular pathways underlying cardiac remodeling during pathophysiological stimulation', *Circulation,* 122(25), pp. 2727-2735.

Kimura, H. (2014) 'Production and physiological effects of hydrogen sulfide', *Antioxidants & redox signaling,* 20(5), pp. 783-793.

King, A. L., Polhemus, D. J., Bhushan, S., Otsuka, H., Kondo, K., Nicholson, C. K., Bradley, J. M., Islam, K. N., Calvert, J. W. and Tao, Y.-X. (2014) 'Hydrogen sulfide cytoprotective signaling is endothelial nitric oxide synthase-nitric oxide dependent', *Proceedings of the National Academy of Sciences,* 111(8), pp. 3182-3187.

Kirn-Safran, C. B., Oristian, D. S., Focht, R. J., Parker, S. G., Vivian, J. L. and Carson, D. D. (2007) 'Global growth deficiencies in mice lacking the ribosomal protein HIP/RPL29', *Developmental dynamics: an official publication of the American Association of Anatomists,* 236(2), pp. 447-460.

Klabunde, R. (2011) *Cardiovascular physiology concepts.* Lippincott Williams & Wilkins.

Kohl, J. B., Mellis, A. T. and Schwarz, G. (2019) 'Homeostatic impact of sulfite and hydrogen sulfide on cysteine catabolism', *British Journal of Pharmacology,* 176(4), pp. 554-570.

Kolluru, G. K., Shackelford, R. E., Shen, X., Dominic, P. and Kevil, C. G. (2023) 'Sulfide regulation of cardiovascular function in health and disease', *Nature Reviews Cardiology,* 20(2), pp. 109-125.

Kolluru, G. K., Shen, X. and Kevil, C. G. (2013) 'A tale of two gases: NO and H2S, foes or friends for life?', *Redox biology,* 1(1), pp. 313-318.

Kondo, K., Bhushan, S., King, A. L., Prabhu, S. D., Hamid, T., Koenig, S., Murohara, T., Predmore, B. L., Gojon Sr, G. and Gojon Jr, G. (2013) 'H2S protects against pressure overload–induced heart failure via upregulation of endothelial nitric oxide synthase', *Circulation,* 127(10), pp. 1116-1127.

Konstam, M. A. and Abboud, F. M. (2017) 'Ejection fraction: misunderstood and overrated (changing the paradigm in categorizing heart failure)', *Circulation,* 135(8), pp. 717-719.

Kosaraju, A., Goyal, A., Grigorova, Y. and Makaryus, A. N. (2017) 'Left ventricular ejection fraction'.

Kovačić, D., Glavnik, N., Marinšek, M., Zagožen, P., Rovan, K., Goslar, T., Marš, T. and Podbregar, M. (2012) 'Total plasma sulfide in congestive heart failure', *Journal of cardiac failure,* 18(7), pp. 541-548.

Kresin, N., Stücker, S., Krämer, E., Flenner, F., Mearini, G., Münch, J., Patten, M., Redwood, C., Carrier, L. and Friedrich, F. W. (2019) 'Analysis of contractile function of permeabilized human hypertrophic cardiomyopathy multicellular heart tissue', *Frontiers in physiology,* 10, pp. 239.

Kubalova, Z., Terentyev, D., Viatchenko-Karpinski, S., Nishijima, Y., Györke, I., Terentyeva, R., Da Cuñha, D. N., Sridhar, A., Feldman, D. S. and Hamlin, R. L. (2005) 'Abnormal intrastore calcium signaling in chronic heart failure', *Proceedings of the National Academy of Sciences,* 102(39), pp. 14104-14109.

Kühl, I., Miranda, M., Atanassov, I., Kuznetsova, I., Hinze, Y., Mourier, A., Filipovska, A. and Larsson, N.-G. (2017) 'Transcriptomic and proteomic landscape of mitochondrial dysfunction reveals secondary coenzyme Q deficiency in mammals', *Elife,* 6, pp. e30952.

Kühlbrandt, W. (2015) 'Structure and function of mitochondrial membrane protein complexes', *BMC biology,* 13, pp. 1-11.

Kukat, C., Davies, K. M., Wurm, C. A., Spåhr, H., Bonekamp, N. A., Kühl, I., Joos, F., Polosa, P. L., Park, C. B. and Posse, V. (2015) 'Cross-strand binding of TFAM to a single mtDNA molecule forms the mitochondrial nucleoid', *Proceedings of the National Academy of Sciences,* 112(36), pp. 11288-11293.

Kukurba, K. R. and Montgomery, S. B. (2015) 'RNA sequencing and analysis', *Cold Spring Harbor Protocols,* 2015(11), pp. pdb. top084970.

Kuusisto, J., Kärjä, V., Sipola, P., Kholová, I., Peuhkurinen, K., Jääskeläinen, P., Naukkarinen, A., Ylä-Herttuala, S., Punnonen, K. and Laakso, M. (2012) 'Low-grade inflammation and the phenotypic expression of myocardial fibrosis in hypertrophic cardiomyopathy', *Heart,* 98(13), pp. 1007-1013.

Lai, L. and Qiu, H. (2020) 'The physiological and pathological roles of mitochondrial calcium uptake in heart', *International Journal of Molecular Sciences,* 21(20), pp. 7689.

Lakatta, E. G. and Levy, D. (2003) 'Arterial and cardiac aging: major shareholders in cardiovascular disease enterprises: Part II: the aging heart in health: links to heart disease', *Circulation,* 107(2), pp. 346-354.

Lee, D. S., Gona, P., Vasan, R. S., Larson, M. G., Benjamin, E. J., Wang, T. J., Tu, J. V. and Levy, D. (2009) 'Relation of disease pathogenesis and risk factors to heart failure with preserved or reduced ejection fraction: insights from the framingham heart study of the national heart, lung, and blood institute', *Circulation,* 119(24), pp. 3070-3077.

Lee, H., Smith, S. B. and Yoon, Y. (2017) 'The short variant of the mitochondrial dynamin OPA1 maintains mitochondrial energetics and cristae structure', *Journal of Biological Chemistry,* 292(17), pp. 7115-7130.

Lee, J.-H., Gao, C., Peng, G., Greer, C., Ren, S., Wang, Y. and Xiao, X. (2011a) 'Analysis of transcriptome complexity through RNA sequencing in normal and failing murine hearts', *Circulation research,* 109(12), pp. 1332-1341.

Lee, Y., Lee, H.-Y., Hanna, R. A. and Gustafsson, Å. B. (2011b) 'Mitochondrial autophagy by Bnip3 involves Drp1-mediated mitochondrial fission and recruitment of Parkin in cardiac myocytes', *American journal of physiology-heart and circulatory physiology,* 301(5), pp. H1924-H1931.

Lemieux, H., Semsroth, S., Antretter, H., Höfer, D. and Gnaiger, E. (2011) 'Mitochondrial respiratory control and early defects of oxidative phosphorylation in the failing human heart', *The international journal of biochemistry & cell biology,* 43(12), pp. 1729-1738.

Leyva, F., Taylor, R. J., Foley, P. W., Umar, F., Mulligan, L. J., Patel, K., Stegemann, B., Haddad, T., Smith, R. E. and Prasad, S. K. (2012) 'Left ventricular midwall fibrosis as a predictor of mortality and morbidity after cardiac resynchronization therapy in patients with nonischemic cardiomyopathy', *Journal of the American College of Cardiology,* 60(17), pp. 1659-1667.

Li, L., Bhatia, M., Zhu, Y. Z., Zhu, Y. C., Ramnath, R. D., Wang, Z. J., Anuar, F. B. M., Whiteman, M., Salto-Tellez, M. and Moore, P. K. (2005) 'Hydrogen sulfide is a novel mediator of lipopolysaccharide-induced inflammation in the mouse', *The FASEB Journal,* 19(9), pp. 1196-1198.

Li, L., Salto-Tellez, M., Tan, C.-H., Whiteman, M. and Moore, P. K. (2009) 'GYY4137, a novel hydrogen sulfide-releasing molecule, protects against endotoxic shock in the rat', *Free Radical Biology and Medicine,* 47(1), pp. 103-113.

Li, L., Whiteman, M., Guan, Y. Y., Neo, K. L., Cheng, Y., Lee, S. W., Zhao, Y., Baskar, R., Tan, C.-H. and Moore, P. K. (2008) 'Characterization of a novel, water-soluble hydrogen sulfide–releasing molecule (GYY4137) new insights into the biology of hydrogen sulfide', *Circulation,* 117(18), pp. 2351-2360.

Li, Z., Polhemus, D. J. and Lefer, D. J. (2018) 'Evolution of hydrogen sulfide therapeutics to treat cardiovascular disease', *Circulation Research,* 123(5), pp. 590-600.

Lillo, R., Graziani, F., Franceschi, F., Iannaccone, G., Massetti, M., Olivotto, I., Crea, F. and Liuzzo, G. (2023) 'Inflammation across the spectrum of hypertrophic cardiac phenotypes', *Heart Failure Reviews*, pp. 1-11.

Limongelli, G., Tome-Esteban, M., Dejthevaporn, C., Rahman, S., Hanna, M. G. and Elliott, P. M. (2010) 'Prevalence and natural history of heart disease in adults with primary mitochondrial respiratory chain disease', *European journal of heart failure,* 12(2), pp. 114-121.

Liu, M., Lv, J., Pan, Z., Wang, D., Zhao, L. and Guo, X. (2022) 'Mitochondrial dysfunction in heart failure and its therapeutic implications', *Frontiers in Cardiovascular Medicine,* 9, pp. 945142.

Liu, Y., Morley, M., Brandimarto, J., Hannenhalli, S., Hu, Y., Ashley, E. A., Tang, W. W., Moravec, C. S., Margulies, K. B. and Cappola, T. P. (2015) 'RNA-Seq identifies novel myocardial gene expression signatures of heart failure', *Genomics,* 105(2), pp. 83-89.

Lo Sasso, G., Schlage, W. K., Boué, S., Veljkovic, E., Peitsch, M. C. and Hoeng, J. (2016) 'The Apoe−/− mouse model: a suitable model to study cardiovascular and respiratory diseases in the context of cigarette smoke exposure and harm reduction', *Journal of translational medicine,* 14(1), pp. 146.

Lopaschuk, G. D., Ussher, J. R., Folmes, C. D., Jaswal, J. S. and Stanley, W. C. (2010) 'Myocardial fatty acid metabolism in health and disease', *Physiological reviews,* 90(1), pp. 207-258.

Lopes, L. R., Rahman, M. S. and Elliott, P. M. (2013) 'A systematic review and meta-analysis of genotype–phenotype associations in patients with hypertrophic cardiomyopathy caused by sarcomeric protein mutations', *Heart,* 99(24), pp. 1800-1811.

Lopes, L. R., Syrris, P., Guttmann, O. P., O'Mahony, C., Tang, H. C., Dalageorgou, C., Jenkins, S., Hubank, M., Monserrat, L. and McKenna, W. J. (2015) 'Novel genotype–phenotype associations demonstrated by high-throughput sequencing in patients with hypertrophic cardiomyopathy', *Heart,* 101(4), pp. 294-301.

López, B. a., González, A. and Díez, J. (2010) 'Circulating biomarkers of collagen metabolism in cardiac diseases', *Circulation,* 121(14), pp. 1645-1654.

Losón, O. C., Song, Z., Chen, H. and Chan, D. C. (2013) 'Fis1, Mff, MiD49, and MiD51 mediate Drp1 recruitment in mitochondrial fission', *Molecular biology of the cell,* 24(5), pp. 659-667.

Louzao-Martinez, L., Vink, A., Harakalova, M., Asselbergs, F. W., Verhaar, M. C. and Cheng, C. (2016) 'Characteristic adaptations of the extracellular matrix in dilated cardiomyopathy', *International Journal of Cardiology,* 220, pp. 634-646.

Lu, Z., Xu, X., Hu, X., Fassett, J., Zhu, G., Tao, Y., Li, J., Huang, Y., Zhang, P. and Zhao, B. (2010) 'PGC-1α regulates expression of myocardial mitochondrial antioxidants and myocardial oxidative stress after chronic systolic overload', *Antioxidants & redox signaling,* 13(7), pp. 1011-1022.

Luo, M. and Anderson, M. E. (2013) 'Mechanisms of altered Ca2+ handling in heart failure', *Circulation research,* 113(6), pp. 690-708.

Lyon, A. R., Bannister, M. L., Collins, T., Pearce, E., Sepehripour, A. H., Dubb, S. S., Garcia, E., O'Gara, P., Liang, L. and Kohlbrenner, E. (2011) 'SERCA2a gene transfer decreases sarcoplasmic reticulum calcium leak and reduces ventricular arrhythmias in a model of chronic heart failure', *Circulation: Arrhythmia and Electrophysiology,* 4(3), pp. 362-372.

Maack, C., Kartes, T., Kilter, H., Schäfers, H.-J., Nickenig, G., Böhm, M. and Laufs, U. (2003) 'Oxygen free radical release in human failing myocardium is associated with increased activity of rac1-GTPase and represents a target for statin treatment', *Circulation,* 108(13), pp. 1567-1574.

Mahadevan, V. (2018) 'Anatomy of the heart', *Surgery (Oxford),* 36(2), pp. 43-47.

Mahmaljy, H., Yelamanchili, V. S. and Singhal, M. (2022) 'Dilated Cardiomyopathy', *StatPearls*. Treasure Island (FL).

Mahon, N. G., Murphy, R. T., MacRae, C. A., Caforio, A. L., Elliott, P. M. and McKenna, W. J. (2005) 'Echocardiographic evaluation in asymptomatic relatives of patients with dilated cardiomyopathy reveals preclinical disease', *Annals of internal medicine,* 143(2), pp. 108-115.

Man, J., Barnett, P. and Christoffels, V. M. (2018) 'Structure and function of the Nppa–Nppb cluster locus during heart development and disease', *Cellular and Molecular Life Sciences,* 75, pp. 1435-1444.

Mani, S., Li, H., Untereiner, A., Wu, L., Yang, G., Austin, R. C., Dickhout, J. G., Lhoták, Š., Meng, Q. H. and Wang, R. (2013) 'Decreased endogenous production of hydrogen sulfide accelerates atherosclerosis', *Circulation,* 127(25), pp. 2523-2534.

Marín-García, J. and Akhmedov, A. T. (2016) 'Mitochondrial dynamics and cell death in heart failure', *Heart failure reviews,* 21, pp. 123-136.

Maron, B. J., Desai, M. Y., Nishimura, R. A., Spirito, P., Rakowski, H., Towbin, J. A., Rowin, E. J., Maron, M. S. and Sherrid, M. V. (2022) 'Diagnosis and Evaluation of Hypertrophic Cardiomyopathy', *Journal of the American College of Cardiology,* 79(4), pp. 372-389.

Maron, B. J., Maron, M. S. and Semsarian, C. (2012) 'Genetics of hypertrophic cardiomyopathy after 20 years: clinical perspectives', *Journal of the American College of Cardiology,* 60(8), pp. 705-715.

Maron, B. J., Towbin, J. A., Thiene, G., Antzelevitch, C., Corrado, D., Arnett, D., Moss, A. J., Seidman, C. E. and Young, J. B. (2006) 'Contemporary Definitions and Classification of the Cardiomyopathies', *Circulation,* 113(14), pp. 1807-1816.

Maron, M. S., Rowin, E. J. and Maron, B. J. (2017) 'How to image hypertrophic cardiomyopathy', *Circulation: Cardiovascular Imaging,* 10(7), pp. e005372.

Martínez, J., Marmisolle, I., Tarallo, D. and Quijano, C. (2020) 'Mitochondrial bioenergetics and dynamics in secretion processes', *Frontiers in Endocrinology,* 11, pp. 319.

Martínez-Reyes, I. and Chandel, N. S. (2020) 'Mitochondrial TCA cycle metabolites control physiology and disease', *Nature communications,* 11(1), pp. 102.

Massera, D., McClelland, R. L., Ambale-Venkatesh, B., Gomes, A. S., Hundley, W. G., Kawel-Boehm, N., Yoneyama, K., Owens, D. S., Garcia, M. J. and Sherrid, M. V. (2019) 'Prevalence of unexplained left ventricular hypertrophy by cardiac magnetic resonance imaging in MESA', *Journal of the American Heart Association,* 8(8), pp. e012250.

Mathai, J. C., Missner, A., Kügler, P., Saparov, S. M., Zeidel, M. L., Lee, J. K. and Pohl, P. (2009) 'No facilitator required for membrane transport of hydrogen sulfide', *Proceedings of the National Academy of Sciences,* 106(39), pp. 16633-16638.

Matkovich, S. J., Zhang, Y., Van Booven, D. J. and Dorn, G. W. (2010) 'Deep mRNA sequencing for in vivo functional analysis of cardiac transcriptional regulators: application to Gαq', *Circulation research,* 106(9), pp. 1459-1467.

McCrohon, J., Moon, J., Prasad, S., McKenna, W., Lorenz, C., Coats, A. and Pennell, D. (2003) 'Differentiation of heart failure related to dilated cardiomyopathy and coronary artery disease using gadolinium-enhanced cardiovascular magnetic resonance', *Circulation,* 108(1), pp. 54-59.

McDonagh, T. A., Metra, M., Adamo, M., Gardner, R. S., Baumbach, A., Böhm, M., Burri, H., Butler, J., Čelutkienė, J. and Chioncel, O. (2021) '2021 ESC Guidelines for the diagnosis and treatment of acute and chronic heart failure: Developed by the Task Force for the diagnosis and treatment of acute and chronic heart failure of the European Society of Cardiology (ESC) With the special contribution of the Heart Failure Association (HFA) of the ESC', *European heart journal,* 42(36), pp. 3599-3726.

McFarland, R., Kirby, D. M., Fowler, K. J., Ohtake, A., Ryan, M. T., Amor, D. J., Fletcher, J. M., Dixon, J. W., Collins, F. A. and Turnbull, D. M. (2004) 'De novo mutations in the mitochondrial ND3 gene as a cause of infantile mitochondrial encephalopathy and complex I deficiency', *Annals of Neurology: Official Journal of the American Neurological Association and the Child Neurology Society,* 55(1), pp. 58-64.

McKenna, W. J., Maron, B. J. and Thiene, G. (2017) 'Classification, epidemiology, and global burden of cardiomyopathies', *Circulation research,* 121(7), pp. 722-730.

McLelland, G.-L., Goiran, T., Yi, W., Dorval, G., Chen, C. X., Lauinger, N. D., Krahn, A. I., Valimehr, S., Rakovic, A. and Rouiller, I. (2018) 'Mfn2 ubiquitination by PINK1/parkin gates the p97-dependent release of ER from mitochondria to drive mitophagy', *Elife,* 7, pp. e32866.

McWilliams, T. G., Barini, E., Pohjolan-Pirhonen, R., Brooks, S. P., Singh, F., Burel, S., Balk, K., Kumar, A., Montava-Garriga, L. and Prescott, A. R. (2018) 'Phosphorylation of Parkin at serine 65 is essential for its activation in vivo', *Royal Society Open Biology,* 8(11), pp. 180108.

Mears, J. A., Lackner, L. L., Fang, S., Ingerman, E., Nunnari, J. and Hinshaw, J. E. (2011) 'Conformational changes in Dnm1 support a contractile mechanism for mitochondrial fission', *Nature structural & molecular biology,* 18(1), pp. 20-26.

members, A. T. F. and Elliott, P. M. and Anastasakis, A. and Borger, M. A. and Borggrefe, M. and Cecchi, F. and Charron, P. and Hagege, A. A. and Lafont, A. and Limongelli, G. and Mahrholdt, H. and McKenna, W. J. and Mogensen, J. and Nihoyannopoulos, P. and Nistri, S. and Pieper, P. G. and Pieske, B. and Rapezzi, C. and Rutten, F. H. and Tillmanns, C. and

Watkins, H. and Contributor, A. and O'Mahony, C. and Guidelines, E. C. f. P. and Zamorano, J. L. and Achenbach, S. and Baumgartner, H. and Bax, J. J. and Bueno, H. and Dean, V. and Deaton, C. and Erol, Ç. and Fagard, R. and Ferrari, R. and Hasdai, D. and Hoes, A. W. and Kirchhof, P. and Knuuti, J. and Kolh, P. and Lancellotti, P. and Linhart, A. and Nihoyannopoulos, P. and Piepoli, M. F. and Ponikowski, P. and Sirnes, P. A. and Tamargo, J. L. and Tendera, M. and Torbicki, A. and Wijns, W. and Windecker, S. and Reviewers, D. and Hasdai, D. and Ponikowski, P. and Achenbach, S. and Alfonso, F. and Basso, C. and Cardim, N. M. and Gimeno, J. R. and Heymans, S. and Holm, P. J. and Keren, A. and Kirchhof, P. and Kolh, P. and Lionis, C. and Muneretto, C. and Priori, S. and Salvador, M. J. and Wolpert, C. and Zamorano, J. L. and Frick, M. and Aliyev, F. and Komissarova, S. and Mairesse, G. and Smajić, E. and Velchev, V. and Antoniades, L. and Linhart, A. and Bundgaard, H. and Heliö, T. and Leenhardt, A. and Katus, H. A. and Efthymiadis, G. and Sepp, R. and Thor Gunnarsson, G. and Carasso, S. and Kerimkulova, A. and Kamzola, G. and Skouri, H. and Eldirsi, G. and Kavoliuniene, A. and Felice, T. and Michels, M. and Hermann Haugaa, K. and Lenarczyk, R. and Brito, D. and Apetrei, E. and Bokheria, L. and Lovic, D. and Hatala, R. and Garcia Pavía, P. and Eriksson, M. and Noble, S. and Srbinovska, E. and Özdemir, M. and Nesukay, E. and Sekhri, N. (2014) '2014 ESC Guidelines on diagnosis and management of hypertrophic cardiomyopathy: The Task Force for the Diagnosis and Management of Hypertrophic Cardiomyopathy of the European Society of Cardiology (ESC)', *European Heart Journal,* 35(39), pp. 2733-2779.

Méndez, C., Soler, R., Rodríguez, E., Barriales, R., Ochoa, J. P. and Monserrat, L. (2018) 'Differential diagnosis of thickened myocardium: an illustrative MRI review', *Insights into Imaging,* 9, pp. 695-707.

Mestroni, L., Brun, F., Spezzacatene, A., Sinagra, G. and Taylor, M. R. (2014) 'Genetic Causes of Dilated Cardiomyopathy', *Prog Pediatr Cardiol,* 37(1-2), pp. 13-18.

Michels, V. V., Moll, P. P., Miller, F. A., Tajik, A. J., Chu, J. S., Driscoll, D. J., Burnett, J. C., Rodeheffer, R. J., Chesebro, J. H. and Tazelaar, H. D. (1992) 'The frequency of familial dilated cardiomyopathy in a series of patients with idiopathic dilated cardiomyopathy', *New England Journal of Medicine,* 326(2), pp. 77-82.

Mikami, Y., Shibuya, N., Kimura, Y., Nagahara, N., Ogasawara, Y. and Kimura, H. (2011) 'Thioredoxin and dihydrolipoic acid are required for 3-mercaptopyruvate sulfurtransferase to produce hydrogen sulfide', *Biochemical Journal,* 439(3), pp. 479-485.

Miller, D. K., Menezes, M. J., Simons, C., Riley, L. G., Cooper, S. T., Grimmond, S. M., Thorburn, D. R., Christodoulou, J. and Taft, R. J. (2014) 'Rapid identification of a novel complex I MT-ND3 m. 10134C> A mutation in a Leigh syndrome patient', *Plos one,* 9(8), pp. e104879.

Mirut, R., Stephan, A. E. and Pirici, D. (2018) 'Histopathological aspects of the myocardium in dilated cardiomyopathy', *Current Health Sciences Journal,* 44(3), pp. 243.

Mitruț, R., Pirici, D., Stepan, A. E., Mărgăritescu, C., Simionescu, C. E., Kesse, A. and Militaru, C. (2019) 'Histopathological and Morphometric Study of Fibrosis and Nuclear

Pleomorphism in Dilated Cardiomyopathy', *Current Health Sciences Journal,* 45(1), pp. 73-78.

Módis, K., Coletta, C., Erdélyi, K., Papapetropoulos, A. and Szabo, C. (2013) 'Intramitochondrial hydrogen sulfide production by 3-mercaptopyruvate sulfurtransferase maintains mitochondrial electron flow and supports cellular bioenergetics', *The FASEB Journal,* 27(2), pp. 601-611.

Módis, K., Ju, Y., Ahmad, A., Untereiner, A. A., Altaany, Z., Wu, L., Szabo, C. and Wang, R. (2016) 'S-Sulfhydration of ATP synthase by hydrogen sulfide stimulates mitochondrial bioenergetics', *Pharmacological research,* 113, pp. 116-124.

Mohammed, S. F., Hussain, S., Mirzoyev, S. A., Edwards, W. D., Maleszewski, J. J. and Redfield, M. M. (2015) 'Coronary microvascular rarefaction and myocardial fibrosis in heart failure with preserved ejection fraction', *Circulation,* 131(6), pp. 550-559.

Monte-Nieto, G. d., Fischer, J. W., Gorski, D. J., Harvey, R. P. and Kovacic, J. C. (2020) 'Basic biology of extracellular matrix in the cardiovascular system, part 1/4: JACC Focus Seminar', *Journal of the American College of Cardiology,* 75(17), pp. 2169-2188.

Moraga, P. and Collaborators, G. C. o. D. (2017) 'Global, regional, and national age-sex specific mortality for 264 causes of death, 1980-2016: a systematic analysis for the Global Burden of Disease Study 2016', *The Lancet,* 390(10100), pp. 1151-1210.

Morales, P. E., Arias-Durán, C., Ávalos-Guajardo, Y., Aedo, G., Verdejo, H. E., Parra, V. and Lavandero, S. (2020) 'Emerging role of mitophagy in cardiovascular physiology and pathology', *Molecular aspects of medicine,* 71, pp. 100822.

Morciano, G., Boncompagni, C., Ramaccini, D., Pedriali, G., Bouhamida, E., Tremoli, E., Giorgi, C. and Pinton, P. (2023) 'Comprehensive Analysis of Mitochondrial Dynamics Alterations in Heart Diseases', *International Journal of Molecular Sciences,* 24(4), pp. 3414.

Movassagh, M. and Foo, R. S.-Y. (2008) 'Simplified apoptotic cascades', *Heart failure reviews,* 13, pp. 111-119.

Mustafa, A. K., Gadalla, M. M., Sen, N., Kim, S., Mu, W., Gazi, S. K., Barrow, R. K., Yang, G., Wang, R. and Snyder, S. H. (2009) 'H2S signals through protein S-sulfhydration', *Science signaling,* 2(96), pp. ra72-ra72.

Mustafa, A. K., Sikka, G., Gazi, S. K., Steppan, J., Jung, S. M., Bhunia, A. K., Barodka, V. M., Gazi, F. K., Barrow, R. K. and Wang, R. (2011) 'Hydrogen sulfide as endothelium-derived hyperpolarizing factor sulfhydrates potassium channels', *Circulation research,* 109(11), pp. 1259-1268.

Mys, L., Goshovska, Y., Strutynska, N., Fedichkina, R., Korkach, Y., Strutynskyi, R. and Sagach, V. (2022) 'Pyridoxal-5-phosphate induced cardioprotection in aging associated with up-expression of cystathionine-γ-lyase, 3-mercaptopyruvate sulfurtransferase, and ATP-sensitive potassium channels', *European Journal of Clinical Investigation,* 52(2), pp. e13683.

Narendra, D. P., Jin, S. M., Tanaka, A., Suen, D.-F., Gautier, C. A., Shen, J., Cookson, M. R. and Youle, R. J. (2010) 'PINK1 is selectively stabilized on impaired mitochondria to activate Parkin', *PLoS biology,* 8(1), pp. e1000298.

NCBI (2023) *Gm5900 predicted pseudogene 5900 [Mus musculus (house mouse)]*. NCBI: NIH. Available at: https://www.ncbi.nlm.nih.gov/gene/545987.

Neubauer, S. (2007) 'The failing heart—an engine out of fuel', *New England Journal of Medicine,* 356(11), pp. 1140-1151.

Ni, J., Jiang, L., Shen, G., Xia, Z., Zhang, L., Xu, J., Feng, Q., Qu, H., Xu, F. and Li, X. (2021) 'Hydrogen sulfide reduces pyroptosis and alleviates ischemia-reperfusion-induced acute kidney injury by inhibiting NLRP3 inflammasome', *Life Sciences,* 284, pp. 119466.

Nicholson, C. K., Lambert, J. P., Molkentin, J. D., Sadoshima, J. and Calvert, J. W. (2013) 'Thioredoxin 1 is essential for sodium sulfide–mediated cardioprotection in the setting of heart failure', *Arteriosclerosis, Thrombosis, and Vascular Biology,* 33(4), pp. 744-751.

Nollet, E. E., Duursma, I., Rozenbaum, A., Eggelbusch, M., Wüst, R. C., Schoonvelde, S. A., Michels, M., Jansen, M., van der Wel, N. N. and Bedi Jr, K. C. (2023) 'Mitochondrial dysfunction in human hypertrophic cardiomyopathy is linked to cardiomyocyte architecture disruption and corrected by improving NADH-driven mitochondrial respiration', *European heart journal,* 44(13), pp. 1170-1185.

Nourani, M., Mirzaie, M., Sadr-Ameli, M. A., Fazelifar, A. and Haghjoo, M. (2023) 'Role of Surface Electrocardiography in Differentiation between Obstructive and Non-obstructive Hypertrophic Cardiomyopathy', *The Journal of Tehran University Heart Center,* 18(1), pp. 46.

Olivetti, G., Melissari, M., Capasso, J. and Anversa, P. (1991) 'Cardiomyopathy of the aging human heart. Myocyte loss and reactive cellular hypertrophy', *Circulation research,* 68(6), pp. 1560-1568.

Olkkonen, V. M. (2015) 'OSBP-related protein family in lipid transport over membrane contact sites', *Lipid insights,* 8, pp. LPI. S31726.

Olson, K. R. and Straub, K. D. (2015) 'The role of hydrogen sulfide in evolution and the evolution of hydrogen sulfide in metabolism and signaling', *Physiology*.

Ommen, S. R., Mital, S., Burke, M. A., Day, S. M., Deswal, A., Elliott, P., Evanovich, L. L., Hung, J., Joglar, J. A. and Kantor, P. (2020) '2020 AHA/ACC guideline for the diagnosis and

treatment of patients with hypertrophic cardiomyopathy: a report of the American College of Cardiology/American Heart Association Joint Committee on Clinical Practice Guidelines', *Journal of the American College of Cardiology,* 76(25), pp. e159-e240.

Pan, L. L., Liu, X. H., Gong, Q. H., Yang, H. B. and Zhu, Y. Z. (2012) 'Role of cystathionine γ-lyase/hydrogen sulfide pathway in cardiovascular disease: a novel therapeutic strategy?', *Antioxidants & redox signaling,* 17(1), pp. 106-118.

Pankiv, S., Clausen, T. H., Lamark, T., Brech, A., Bruun, J.-A., Outzen, H., Øvervatn, A., Bjørkøy, G. and Johansen, T. (2007) 'p62/SQSTM1 binds directly to Atg8/LC3 to facilitate degradation of ubiquitinated protein aggregates by autophagy', *Journal of biological chemistry,* 282(33), pp. 24131-24145.

Papapetropoulos, A., Pyriochou, A., Altaany, Z., Yang, G., Marazioti, A., Zhou, Z., Jeschke, M. G., Branski, L. K., Herndon, D. N. and Wang, R. (2009) 'Hydrogen sulfide is an endogenous stimulator of angiogenesis', *Proceedings of the National Academy of Sciences,* 106(51), pp. 21972-21977.

Park, W. J. and Oh, J. G. (2013) 'SERCA2a: a prime target for modulation of cardiac contractility during heart failure', *BMB reports,* 46(5), pp. 237.

Parks, S. B., Kushner, J. D., Nauman, D., Burgess, D., Ludwigsen, S., Peterson, A., Li, D., Jakobs, P., Litt, M. and Porter, C. B. (2008) 'Lamin A/C mutation analysis in a cohort of 324 unrelated patients with idiopathic or familial dilated cardiomyopathy', *American heart journal,* 156(1), pp. 161-169.

Patten, I. S., Rana, S., Shahul, S., Rowe, G. C., Jang, C., Liu, L., Hacker, M. R., Rhee, J. S., Mitchell, J. and Mahmood, F. (2012) 'Cardiac angiogenic imbalance leads to peripartum cardiomyopathy', *Nature,* 485(7398), pp. 333-338.

Paulus, W. J. and Tschöpe, C. (2013) 'A novel paradigm for heart failure with preserved ejection fraction: comorbidities drive myocardial dysfunction and remodeling through coronary microvascular endothelial inflammation', *Journal of the American College of Cardiology,* 62(4), pp. 263-271.

Pei, J., Wang, F., Pei, S., Bai, R., Cong, X., Nie, Y. and Chen, X. (2020) 'Hydrogen sulfide promotes cardiomyocyte proliferation and heart regeneration via ROS scavenging', *Oxidative medicine and cellular longevity,* 2020.

Peleli, M., Bibli, S.-I., Li, Z., Chatzianastasiou, A., Varela, A., Katsouda, A., Zukunft, S., Bucci, M., Vellecco, V. and Davos, C. H. (2020) 'Cardiovascular phenotype of mice lacking 3-mercaptopyruvate sulfurtransferase', *Biochemical pharmacology,* 176, pp. 113833.

Pelliccia, F., Limongelli, G., Rosano, G. M., Vitale, C., Bossone, E., Calabrò, P. and Gaudio, C. (2022) 'Nuclear factor-kappa B predicts long-term clinical outcome in patients with

hypertrophic cardiomyopathy: 10-year follow-up study', *European Journal of Preventive Cardiology,* 29(3), pp. e108-e111.

Peng, S., Zhao, D., Li, Q., Wang, M., Zhang, S., Pang, K., Huang, J., Lu, F., Chen, H. and Zhang, W. (2022) 'Hydrogen Sulfide Regulates SERCA2a Ubiquitylation via Muscle RING Finger-1 S-Sulfhydration to Affect Cardiac Contractility in db/db Mice', *Cells,* 11(21), pp. 3465.

Pennanen, C., Parra, V., Lopez-Crisosto, C., Morales, P. E., Del Campo, A., Gutierrez, T., Rivera-Mejías, P., Kuzmicic, J., Chiong, M. and Zorzano, A. (2014) 'Mitochondrial fission is required for cardiomyocyte hypertrophy mediated by a Ca2+-calcineurin signaling pathway', *Journal of cell science,* 127(12), pp. 2659-2671.

Pérez-Serra, A., Toro, R., Sarquella-Brugada, G., de Gonzalo-Calvo, D., Cesar, S., Carro, E., Llorente-Cortes, V., Iglesias, A., Brugada, J. and Brugada, R. (2016) 'Genetic basis of dilated cardiomyopathy', *International Journal of Cardiology,* 224, pp. 461-472.

Perry, T. L., Hansen, S. and MacDougall, L. (1966) 'Homolanthionine excretion in homocystinuria', *Science,* 152(3730), pp. 1750-1752.

Phillips, D., Covian, R., Aponte, A. M., Glancy, B., Taylor, J. F., Chess, D. and Balaban, R. S. (2012) 'Regulation of oxidative phosphorylation complex activity: effects of tissue-specific metabolic stress within an allometric series and acute changes in workload', *American Journal of Physiology-Regulatory, Integrative and Comparative Physiology,* 302(9), pp. R1034-R1048.

Picard, F., Brehm, M., Fassbach, M., Pelzer, B., Scheuring, S., Küry, P., Strauer, B. E. and Schwartzkopff, B. (2006) 'Increased cardiac mRNA expression of matrix metalloproteinase-1 (MMP–1) and its inhibitor (TIMP–1) in DCM patients', *Clinical research in cardiology,* 95(5), pp. 261-269.

Picard, M., Wright, K. J., Ritchie, D., Thomas, M. M. and Hepple, R. T. (2012) 'Mitochondrial function in permeabilized cardiomyocytes is largely preserved in the senescent rat myocardium'.

Pinto, Y. M., Elliott, P. M., Arbustini, E., Adler, Y., Anastasakis, A., Böhm, M., Duboc, D., Gimeno, J., De Groote, P. and Imazio, M. (2016) 'Proposal for a revised definition of dilated cardiomyopathy, hypokinetic non-dilated cardiomyopathy, and its implications for clinical practice: a position statement of the ESC working group on myocardial and pericardial diseases', *European heart journal,* 37(23), pp. 1850-1858.

Pinz, I., Tian, R., Belke, D., Swanson, E., Dillmann, W. and Ingwall, J. S. (2011) 'Compromised myocardial energetics in hypertrophied mouse hearts diminish the beneficial effect of overexpressing SERCA2a', *Journal of Biological Chemistry,* 286(12), pp. 10163-10168.

Pisano, A., Cerbelli, B., Perli, E., Pelullo, M., Bargelli, V., Preziuso, C., Mancini, M., He, L., Bates, M. G. and Lucena, J. R. (2016) 'Impaired mitochondrial biogenesis is a common feature to myocardial hypertrophy and end-stage ischemic heart failure', *Cardiovascular Pathology,* 25(2), pp. 103-112.

Polhemus, D. J., Calvert, J. W., Butler, J. and Lefer, D. J. (2014) 'The cardioprotective actions of hydrogen sulfide in acute myocardial infarction and heart failure', *Scientifica,* 2014.

Polhemus, D. J., Kondo, K., Bhushan, S., Bir, S. C., Kevil, C. G., Murohara, T., Lefer, D. J. and Calvert, J. W. (2013) 'Hydrogen sulfide attenuates cardiac dysfunction after heart failure via induction of angiogenesis', *Circulation: Heart Failure,* 6(5), pp. 1077-1086.

Polhemus, D. J., Li, Z., Pattillo, C. B., Gojon Sr, G., Gojon Jr, G., Giordano, T. and Krum, H. (2015) 'A novel hydrogen sulfide prodrug, SG 1002, promotes hydrogen sulfide and nitric oxide bioavailability in heart failure patients', *Cardiovascular therapeutics,* 33(4), pp. 216-226.

Ponikowski, P., Voors, A. A., Anker, S. D., Bueno, H., Cleland, J. G., Coats, A. J., Falk, V., González-Juanatey, J. R., Harjola, V.-P. and Jankowska, E. A. (2016) '2016 ESC Guidelines for the diagnosis and treatment of acute and chronic heart failure', *Kardiologia Polska (Polish Heart Journal),* 74(10), pp. 1037-1147.

Poulsen, S. H., Jensen, S. E., Nielsen, J. C., Møller, J. E. and Egstrup, K. (2000) 'Serial changes and prognostic implications of a Doppler-derived index of combined left ventricular systolic and diastolic myocardial performance in acute myocardial infarction', *The American journal of cardiology,* 85(1), pp. 19-25.

Pyszko, J., Václavík, J., Václavík, T., Kociánová, E., Kamasová, M., Lazárová, M. and Táborský, M. (2018) 'Effects of age on left ventricular diastolic function', *Cor et Vasa*.

Qi, Y., Wang, X., Li, W., Chen, D., Meng, H. and An, S. (2021) 'Pseudogenes in cardiovascular disease', *Frontiers in Molecular Biosciences,* 7, pp. 622540.

Qipshidze, N., Metreveli, N., Mishra, P. K., Lominadze, D. and Tyagi, S. C. (2012) 'Hydrogen sulfide mitigates cardiac remodeling during myocardial infarction via improvement of angiogenesis', *International journal of biological sciences,* 8(4), pp. 430.

Rajpal, S., Katikaneni, P., Deshotels, M., Pardue, S., Glawe, J., Shen, X., Akkus, N., Modi, K., Bhandari, R. and Dominic, P. (2018) 'Total sulfane sulfur bioavailability reflects ethnic and gender disparities in cardiovascular disease', *Redox Biology,* 15, pp. 480-489.

Rapezzi, C., Arbustini, E., Caforio, A. L., Charron, P., Gimeno-Blanes, J., Heliö, T., Linhart, A., Mogensen, J., Pinto, Y. and Ristic, A. (2013) 'Diagnostic work-up in cardiomyopathies: bridging the gap between clinical phenotypes and final diagnosis. A position statement from the ESC Working Group on Myocardial and Pericardial Diseases', *European heart journal,* 34(19), pp. 1448-1458.

Rawlins, J., Bhan, A. and Sharma, S. (2009) 'Left ventricular hypertrophy in athletes', *European Journal of Echocardiography,* 10(3), pp. 350-356.

Revsbech, I. G., Shen, X., Chakravarti, R., Jensen, F. B., Thiel, B., Evans, A. L., Kindberg, J., Fröbert, O., Stuehr, D. J. and Kevil, C. G. (2014) 'Hydrogen sulfide and nitric oxide metabolites in the blood of free-ranging brown bears and their potential roles in hibernation', *Free Radical Biology and Medicine,* 73, pp. 349-357.

Riahi, S. and Rowley, C. N. (2014) 'Why can hydrogen sulfide permeate cell membranes?', *Journal of the American Chemical Society,* 136(43), pp. 15111-15113.

Ribatti, D. (2009) 'William Harvey and the discovery of the circulation of the blood', *Journal of Angiogenesis Research,* 1(1), pp. 3.

Rimbaud, S., Garnier, A. and Ventura-Clapier, R. (2009) 'Mitochondrial biogenesis in cardiac pathophysiology', *Pharmacological reports,* 61(1), pp. 131-138.

Ritterhoff, J., Young, S., Villet, O., Shao, D., Neto, F. C., Bettcher, L. F., Hsu, Y.-W. A., Kolwicz Jr, S. C., Raftery, D. and Tian, R. (2020) 'Metabolic remodeling promotes cardiac hypertrophy by directing glucose to aspartate biosynthesis', *Circulation research,* 126(2), pp. 182-196.

Rizvi, F., Preston, C. C., Emelyanova, L., Yousufuddin, M., Viqar, M., Dakwar, O., Ross, G. R., Faustino, R. S., Holmuhamedov, E. L. and Jahangir, A. (2021) 'Effects of aging on cardiac oxidative stress and transcriptional changes in pathways of reactive oxygen species generation and clearance', *Journal of the American Heart Association,* 10(16), pp. e019948.

Roberts, W. C., Siegel, R. J. and McManus, B. M. (1987) 'Idiopathic dilated cardiomyopathy: analysis of 152 necropsy patients', *The American journal of cardiology,* 60(16), pp. 1340-1355.

Roderick, H. L., Higazi, D., Smyrnias, I., Fearnley, C., Harzheim, D. and Bootman, M. (2007) 'Calcium in the heart: when it's good, it's very very good, but when it's bad, it's horrid', *Biochemical Society transactions,* 35(5), pp. 957-961.

Rodrigues, P., Santos-Ribeiro, S., Teodoro, T., Gomes, F. V., Leal, I., Reis, J. P., Goff, D. C., Gonçalves, A. and Lima, J. A. (2018) 'Association between alcohol intake and cardiac remodeling', *Journal of the American College of Cardiology,* 72(13), pp. 1452-1462.

Røe, Å. T., Ruud, M., Espe, E. K., Manfra, O., Longobardi, S., Aronsen, J. M., Norden, E. S., Husebye, T., Kolstad, T. R. and Cataliotti, A. (2019) 'Regional diastolic dysfunction in post-infarction heart failure: role of local mechanical load and SERCA expression', *Cardiovascular research,* 115(4), pp. 752-764.

Rohde, J. A., Roopnarine, O., Thomas, D. D. and Muretta, J. M. (2018) 'Mavacamten stabilizes an autoinhibited state of two-headed cardiac myosin', *Proceedings of the National Academy of Sciences,* 115(32), pp. E7486-E7494.

Rosca, M. G. and Hoppel, C. L. (2010) 'Mitochondria in heart failure', *Cardiovascular research,* 88(1), pp. 40-50.

Roth, G. A., Mensah, G. A., Johnson, C. O., Addolorato, G., Ammirati, E., Baddour, L. M., Barengo, N. C., Beaton, A. Z., Benjamin, E. J. and Benziger, C. P. (2020) 'Global burden of cardiovascular diseases and risk factors, 1990–2019: update from the GBD 2019 study', *Journal of the American College of Cardiology,* 76(25), pp. 2982-3021.

Rubinshtein, R., Glockner, J. F., Ommen, S. R., Araoz, P. A., Ackerman, M. J., Sorajja, P., Bos, J. M., Tajik, A. J., Valeti, U. S. and Nishimura, R. A. (2010) 'Characteristics and clinical significance of late gadolinium enhancement by contrast-enhanced magnetic resonance imaging in patients with hypertrophic cardiomyopathy', *Circulation: Heart Failure,* 3(1), pp. 51-58.

Rubiś, P., Wiśniowska-Śmialek, S., Wypasek, E., Biernacka-Fijalkowska, B., Rudnicka-Sosin, L., Dziewiecka, E., Faltyn, P., Khachatryan, L., Karabinowska, A. and Kozanecki, A. (2016) 'Fibrosis of extracellular matrix is related to the duration of the disease but is unrelated to the dynamics of collagen metabolism in dilated cardiomyopathy', *Inflammation Research,* 65(12), pp. 941-949.

Sabbah, H. N. (2020) 'Targeting the mitochondria in heart failure: a translational perspective', *JACC: Basic to Translational Science,* 5(1), pp. 88-106.

Sabbah, H. N., Gupta, R. C., Singh-Gupta, V., Zhang, K. and Lanfear, D. E. (2018) 'Abnormalities of mitochondrial dynamics in the failing heart: normalization following long-term therapy with elamipretide', *Cardiovascular drugs and therapy,* 32, pp. 319-328.

Sahebekhtiari, N., Nielsen, C. B., Johannsen, M. and Palmfeldt, J. (2016) 'Untargeted metabolomics analysis reveals a link between ETHE1-mediated disruptive redox state and altered metabolic regulation', *Journal of Proteome Research,* 15(5), pp. 1630-1638.

Sanchez-Aranguren, L. C., Ahmad, S., Dias, I. H., Alzahrani, F. A., Rezai, H., Wang, K. and Ahmed, A. (2020a) 'Bioenergetic effects of hydrogen sulfide suppress soluble Flt-1 and soluble endoglin in cystathionine gamma-lyase compromised endothelial cells', *Scientific reports,* 10(1), pp. 15810.

Sanchez-Aranguren, L. C., Rezai, H., Ahmad, S., Alzahrani, F. A., Sparatore, A., Wang, K. and Ahmed, A. (2020b) 'MZe786 rescues cardiac mitochondrial activity in high sFlt-1 and low HO-1 environment', *Antioxidants,* 9(7), pp. 598.

Sanchez-Contreras, M., Sweetwyne, M. T., Tsantilas, K. A., Whitson, J. A., Campbell, M. D., Kohrn, B. F., Kim, H. J., Hipp, M. J., Fredrickson, J. and Nguyen, M. M. (2023) 'The multi-

tissue landscape of somatic mtdna mutations indicates tissue specific accumulation and removal in aging', *Elife,* 12, pp. e83395.

Sangaralingham, S. J., Huntley, B. K., Martin, F. L., McKie, P. M., Bellavia, D., Ichiki, T., Harders, G. E., Chen, H. H. and Burnett Jr, J. C. (2011) 'The aging heart, myocardial fibrosis, and its relationship to circulating C-type natriuretic peptide', *Hypertension,* 57(2), pp. 201-207.

Sano, M., Minamino, T., Toko, H., Miyauchi, H., Orimo, M., Qin, Y., Akazawa, H., Tateno, K., Kayama, Y. and Harada, M. (2007) 'p53-induced inhibition of Hif-1 causes cardiac dysfunction during pressure overload', *Nature,* 446(7134), pp. 444-448.

Savarese, G. and Lund, L. H. (2017) 'Global public health burden of heart failure', *Cardiac failure review,* 3(1), pp. 7.

Sbodio, J. I., Snyder, S. H. and Paul, B. D. (2019) 'Regulators of the transsulfuration pathway', *British journal of pharmacology,* 176(4), pp. 583-593.

Scheubel, R. J., Tostlebe, M., Simm, A., Rohrbach, S., Prondzinsky, R., Gellerich, F. N., Silber, R.-E. and Holtz, J. (2002) 'Dysfunction of mitochondrial respiratory chain complex I in human failing myocardium is not due to disturbed mitochondrial gene expression', *Journal of the American College of Cardiology,* 40(12), pp. 2174-2181.

Schirone, L., Forte, M., Palmerio, S., Yee, D., Nocella, C., Angelini, F., Pagano, F., Schiavon, S., Bordin, A. and Carrizzo, A. (2017) 'A review of the molecular mechanisms underlying the development and progression of cardiac remodeling', *Oxidative medicine and cellular longevity,* 2017.

Schultheiss, H.-P., Fairweather, D., Caforio, A. L., Escher, F., Hershberger, R. E., Lipshultz, S. E., Liu, P. P., Matsumori, A., Mazzanti, A. and McMurray, J. (2019) 'Dilated cardiomyopathy', *Nature reviews Disease primers,* 5(1), pp. 1-19.

Schwartz, B. G., Rezkalla, S. and Kloner, R. A. (2010) 'Cardiovascular effects of cocaine', *Circulation,* 122(24), pp. 2558-2569.

Sciarretta, S., Forte, M., Frati, G. and Sadoshima, J. (2018) 'New insights into the role of mTOR signaling in the cardiovascular system', *Circulation research,* 122(3), pp. 489-505.

Searcy, D. G. and Lee, S. H. (1998) 'Sulfur reduction by human erythrocytes', *Journal of Experimental Zoology,* 282(3), pp. 310-322.

Sedaghat-Hamedani, F., Kayvanpour, E., Tugrul, O. F., Lai, A., Amr, A., Haas, J., Proctor, T., Ehlermann, P., Jensen, K. and Katus, H. A. (2018) 'Clinical outcomes associated with sarcomere mutations in hypertrophic cardiomyopathy: a meta-analysis on 7675 individuals', *Clinical Research in Cardiology,* 107, pp. 30-41.

Sergeeva, I. A., Hooijkaas, I. B., Van Der Made, I., Jong, W. M., Creemers, E. E. and Christoffels, V. M. (2014) 'A transgenic mouse model for the simultaneous monitoring of ANF and BNP gene activity during heart development and disease', *Cardiovascular research,* 101(1), pp. 78-86.

Shen, Y., Shen, Z., Luo, S., Guo, W. and Zhu, Y. Z. (2015) 'The cardioprotective effects of hydrogen sulfide in heart diseases: from molecular mechanisms to therapeutic potential', *Oxidative Medicine and Cellular Longevity,* 2015.

Sheng, S.-y., Li, J.-m., Hu, X.-y. and Wang, Y. (2023) 'Regulated cell death pathways in cardiomyopathy', *Acta Pharmacologica Sinica*, pp. 1-15.

Shi, K.-Y., Fan, L.-Y., Xu, D., Ren, L.-P., Wang, L.-P., Chen, L.-Y. and Wang, L.-J. (2020) 'MiR-20a suppresses proliferation and facilitates apoptosis of breast cancer cells via the MTOR signaling pathway', *European Review for Medical & Pharmacological Sciences,* 24(22).

Shibuya, N., Koike, S., Tanaka, M., Ishigami-Yuasa, M., Kimura, Y., Ogasawara, Y., Fukui, K., Nagahara, N. and Kimura, H. (2013) 'A novel pathway for the production of hydrogen sulfide from D-cysteine in mammalian cells', *Nature communications,* 4(1), pp. 1-7.

Shimada, Y. J., Raita, Y., Liang, L. W., Maurer, M. S., Hasegawa, K., Fifer, M. A. and Reilly, M. P. (2021) 'Comprehensive proteomics profiling reveals circulating biomarkers of hypertrophic cardiomyopathy', *Circulation: Heart Failure,* 14(7), pp. e007849.

Shimizu, Y., Polavarapu, R., Eskla, K.-L., Nicholson, C. K., Koczor, C. A., Wang, R., Lewis, W., Shiva, S., Lefer, D. J. and Calvert, J. W. (2018) 'Hydrogen sulfide regulates cardiac mitochondrial biogenesis via the activation of AMPK', *Journal of molecular and cellular cardiology,* 116, pp. 29-40.

Shiraishi, C., Matsumoto, A., Ichihara, K., Yamamoto, T., Yokoyama, T., Mizoo, T., Hatano, A., Matsumoto, M., Tanaka, Y. and Matsuura-Suzuki, E. (2023) 'RPL3L-containing ribosomes determine translation elongation dynamics required for cardiac function', *Nature communications,* 14(1), pp. 2131.

Silva, A. C., Pereira, C., Fonseca, A. C. R., Pinto-do-Ó, P. and Nascimento, D. S. (2021) 'Bearing my heart: the role of extracellular matrix on cardiac development, homeostasis, and injury response', *Frontiers in Cell and Developmental Biology,* 8, pp. 1705.

Simmonds, S. J., Cuijpers, I., Heymans, S. and Jones, E. A. (2020) 'Cellular and molecular differences between HFpEF and HFrEF: a step ahead in an improved pathological understanding', *Cells,* 9(1), pp. 242.

Simpson, L. J., Reader, J. S. and Tzima, E. (2020) 'Mechanical regulation of protein translation in the cardiovascular system', *Frontiers in Cell and Developmental Biology,* 8, pp. 34.

Sisakian, H. (2014) 'Cardiomyopathies: Evolution of pathogenesis concepts and potential for new therapies', *World journal of cardiology,* 6(6), pp. 478.

Sivarajah, A., Collino, M., Yasin, M., Benetti, E., Gallicchio, M., Mazzon, E., Cuzzocrea, S., Fantozzi, R. and Thiemermann, C. (2009) 'Anti-apoptotic and anti-inflammatory effects of hydrogen sulfide in a rat model of regional myocardial I/R', *Shock,* 31(3), pp. 267-274.

Sliwa, K., Hilfiker-Kleiner, D., Petrie, M., Mebazaa, A., Pieske, B., Buchmann, E., Regitz-Zagrosek, V., Schaufelberger, M., Tavazzi, L. and Van Veldhuisen, D. (2010) 'Heart Failure Association of the European Society of Cardiology Working Group on Peripartum Cardiomyopathy. Current state of knowledge on aetiology, diagnosis, management, and therapy of peripartum cardiomyopathy: a position statement from the Heart Failure Association of the European Society of Cardiology Working Group on peripartum cardiomyopathy', *Eur J Heart Fail,* 12(8), pp. 767-778.

Smirnova, E., Griparic, L., Shurland, D.-L. and Van Der Bliek, A. M. (2001) 'Dynamin-related protein Drp1 is required for mitochondrial division in mammalian cells', *Molecular biology of the cell,* 12(8), pp. 2245-2256.

Sohrabi, Y., Volkova, V., Kobets, T., Havelková, H., Krayem, I., Slapničková, M., Demant, P. and Lipoldová, M. (2018) 'Genetic regulation of guanylate-binding proteins 2b and 5 during leishmaniasis in mice', *Frontiers in immunology,* 9, pp. 130.

Song, M., Franco, A., Fleischer, J. A., Zhang, L. and Dorn, G. W. (2017) 'Abrogating mitochondrial dynamics in mouse hearts accelerates mitochondrial senescence', *Cell metabolism,* 26(6), pp. 872-883. e5.

Song, M., Gong, G., Burelle, Y., Gustafsson, Å. B., Kitsis, R. N., Matkovich, S. J. and Dorn, G. W. (2015a) 'Interdependence of Parkin-mediated mitophagy and mitochondrial fission in adult mouse hearts', *Circulation research,* 117(4), pp. 346-351.

Song, M., Mihara, K., Chen, Y., Scorrano, L. and Dorn, G. W. (2015b) 'Mitochondrial fission and fusion factors reciprocally orchestrate mitophagic culling in mouse hearts and cultured fibroblasts', *Cell metabolism,* 21(2), pp. 273-286.

Sonobe, T. and Haouzi, P. (2016) 'H2S concentrations in the heart after acute H2S administration: methodological and physiological considerations', *American Journal of Physiology-Heart and Circulatory Physiology,* 311(6), pp. H1445-H1458.

Soufen, H., Salemi, V., Aneas, I., Ramires, F., Benício, A., Benvenuti, L., Krieger, J. and Mady, C. (2008) 'Collagen content, but not the ratios of collagen type III/I mRNAs, differs among hypertensive, alcoholic, and idiopathic dilated cardiomyopathy', *Brazilian Journal of Medical and Biological Research,* 41, pp. 1098-1104.

Stanley, W. C., Recchia, F. A. and Lopaschuk, G. D. (2005) 'Myocardial substrate metabolism in the normal and failing heart', *Physiological reviews,* 85(3), pp. 1093-1129.

Steenman, M. and Lande, G. (2017) 'Cardiac aging and heart disease in humans', *Biophysical reviews,* 9(2), pp. 131-137.

Stepanova, A., Shurubor, Y., Valsecchi, F., Manfredi, G. and Galkin, A. (2016) 'Differential susceptibility of mitochondrial complex II to inhibition by oxaloacetate in brain and heart', *Biochimica et Biophysica Acta (BBA)-Bioenergetics,* 1857(9), pp. 1561-1568.

Su, H. M., Lin, T. H., Voon, W. C., Lee, K. T., Chu, C. S., Yen, H. W., Lai, W. T. and Sheu, S. H. (2007) 'Correlation of Tei index obtained from tissue Doppler echocardiography with invasive measurements of left ventricular performance', *Echocardiography,* 24(3), pp. 252-257.

Su, Y.-W., Liang, C., Jin, H.-F., Tang, X.-Y., Han, W., Chai, L.-J., Zhang, C.-Y., Geng, B., Tang, C.-S. and Du, J.-B. (2009) 'Hydrogen sulfide regulates cardiac function and structure in adriamycin-induced cardiomyopathy', *Circulation Journal,* 73(4), pp. 741-749.

Subramaniam, S. R. and Chesselet, M.-F. (2013) 'Mitochondrial dysfunction and oxidative stress in Parkinson's disease', *Progress in neurobiology,* 106, pp. 17-32.

Sun, Y.-G., Cao, Y.-X., Wang, W.-W., Ma, S.-F., Yao, T. and Zhu, Y.-C. (2008) 'Hydrogen sulphide is an inhibitor of L-type calcium channels and mechanical contraction in rat cardiomyocytes', *Cardiovascular research,* 79(4), pp. 632-641.

Szabó, C. (2007) 'Hydrogen sulphide and its therapeutic potential', *Nature reviews Drug discovery,* 6(11), pp. 917-935.

Szabo, C. and Papapetropoulos, A. (2017) 'International union of basic and clinical pharmacology. CII: pharmacological modulation of H2S levels: H2S donors and H2S biosynthesis inhibitors', *Pharmacological reviews,* 69(4), pp. 497-564.

Szabo, C., Ransy, C., Módis, K., Andriamihaja, M., Murghes, B., Coletta, C., Olah, G., Yanagi, K. and Bouillaud, F. (2014) 'Regulation of mitochondrial bioenergetic function by hydrogen sulfide. Part I. Biochemical and physiological mechanisms', *British journal of pharmacology,* 171(8), pp. 2099-2122.

Szczesny, B., Módis, K., Yanagi, K., Coletta, C., Le Trionnaire, S., Perry, A., Wood, M. E., Whiteman, M. and Szabo, C. (2014) 'AP39, a novel mitochondria-targeted hydrogen sulfide donor, stimulates cellular bioenergetics, exerts cytoprotective effects and protects against the loss of mitochondrial DNA integrity in oxidatively stressed endothelial cells in vitro', *Nitric oxide,* 41, pp. 120-130.

Taegtmeyer, H. 2002. Switching metabolic genes to build a better heart. Am Heart Assoc.

Tan, Y., Mui, D., Toan, S., Zhu, P., Li, R. and Zhou, H. (2020) 'SERCA overexpression improves mitochondrial quality control and attenuates cardiac microvascular ischemia-reperfusion injury', *Molecular Therapy-Nucleic Acids,* 22, pp. 696-707.

Tatarkova, Z., Kuka, S., Racay, P., Lehotský, J., Dobrota, D., Mistuna, D. and Kaplán, P. (2011) 'Effects of aging on activities of mitochondrial electron transport chain complexes and oxidative damage in rat heart', *Physiological research,* 60(2), pp. 281.

Tayal, U., Gregson, J., Buchan, R., Whiffin, N., Halliday, B. P., Lota, A., Roberts, A. M., Baksi, A. J., Voges, I. and Jarman, J. W. (2022) 'Moderate excess alcohol consumption and adverse cardiac remodelling in dilated cardiomyopathy', *Heart,* 108(8), pp. 619-625.

Taylor, R. J., Umar, F., Lin, E. L., Ahmed, A., Moody, W. E., Mazur, W., Stegemann, B., Townend, J. N., Steeds, R. P. and Leyva, F. (2015) 'Mechanical effects of left ventricular midwall fibrosis in non-ischemic cardiomyopathy', *Journal of Cardiovascular Magnetic Resonance,* 18(1), pp. 1-8.

Tejado, B. S. M. and Jou, C. (2018) 'Histopathology in HCM', *Global cardiology science & practice,* 2018(3).

Tham, Y. K., Bernardo, B. C., Ooi, J. Y., Weeks, K. L. and McMullen, J. R. (2015) 'Pathophysiology of cardiac hypertrophy and heart failure: signaling pathways and novel therapeutic targets', *Archives of toxicology,* 89, pp. 1401-1438.

Thygesen, K., Alpert, J. S., White, H. D., TASK FORCE MEMBERS: Chairpersons: Kristian Thygesen , J. S. A., Harvey D. White *, Biomarker Group: Allan S. Jaffe, C., Fred S. Apple , Marcello Galvani , Hugo A. Katus , L. Kristin Newby , Jan Ravkilde, ECG Group: Bernard Chaitman, C.-o., Peter M. Clemmensen , Mikael Dellborg , Hanoch Hod , Pekka Porela, Imaging Group: Richard Underwood, C., Jeroen J. Bax , George A. Beller , Robert Bonow , Ernst E. Van Der Wall, Intervention Group: Jean-Pierre Bassand, C.-o., William Wijns, Coordinator , T. Bruce Ferguson , Philippe G. Steg , Barry F. Uretsky , David O. Williams, Clinical Investigation Group: Paul W. Armstrong, C., Elliott M. Antman , Keith A. Fox , Christian W. Hamm , E. Magnus Ohman , Maarten L. Simoons and Global Perspective Group: Philip A. Poole-Wilson, C., Enrique P. Gurfinkel , José-Luis Lopez-Sendon , Prem Pais , Shanti Mendis , Jun-Ren Zhu (2007) 'Universal definition of myocardial infarction', *circulation,* 116(22), pp. 2634-2653.

Toldo, S., Das, A., Mezzaroma, E., Chau, V. Q., Marchetti, C., Durrant, D., Samidurai, A., Van Tassell, B. W., Yin, C. and Ockaili, R. A. (2014) 'Induction of microRNA-21 with exogenous hydrogen sulfide attenuates myocardial ischemic and inflammatory injury in mice', *Circulation: Cardiovascular Genetics,* 7(3), pp. 311-320.

Towbin, J. and Bowles, N. (2002) 'The failing heart', *Nature,* 415(6868), pp. 227-233.

Townsend, D. (2016) 'Measuring pressure volume loops in the mouse', *JoVE (Journal of Visualized Experiments),* (111), pp. e53810.

Tran, D. H. and Wang, Z. V. (2019) 'Glucose metabolism in cardiac hypertrophy and heart failure', *Journal of the American Heart Association,* 8(12), pp. e012673.

Trifunovic, A., Wredenberg, A., Falkenberg, M., Spelbrink, J. N., Rovio, A. T., Bruder, C. E., Bohlooly-Y, M., Gidlöf, S., Oldfors, A. and Wibom, R. (2004) 'Premature ageing in mice expressing defective mitochondrial DNA polymerase', *Nature,* 429(6990), pp. 417-423.

Tromp, J., Lim, S. L., Tay, W. T., Teng, T.-H. K., Chandramouli, C., Ouwerkerk, W., Wander, G. S., Sawhney, J. P., Yap, J. and MacDonald, M. R. (2019) 'Microvascular disease in patients with diabetes with heart failure and reduced ejection versus preserved ejection fraction', *Diabetes Care,* 42(9), pp. 1792-1799.

Tromp, J., Paniagua, S. M., Lau, E. S., Allen, N. B., Blaha, M. J., Gansevoort, R. T., Hillege, H. L., Lee, D. E., Levy, D. and Vasan, R. S. (2021) 'Age dependent associations of risk factors with heart failure: pooled population based cohort study', *Bmj,* 372.

Tsao, C., Aday, A., Almarzooq, Z., Alonso, A., Beaton, A., Bittencourt, M., Boehme, A., Buxton, A., Carson, A. and Commodore-Mensah, Y. (2022) 'American heart association council on epidemiology and prevention statistics committee and stroke statistics subcommittee', *Heart disease and stroke statistics-2022 update: A report from the American Heart Association. Circulation,* 145(8), pp. e153-e639.

Tschöpe, C., Ammirati, E., Bozkurt, B., Caforio, A. L. P., Cooper, L. T., Felix, S. B., Hare, J. M., Heidecker, B., Heymans, S., Hübner, N., Kelle, S., Klingel, K., Maatz, H., Parwani, A. S., Spillmann, F., Starling, R. C., Tsutsui, H., Seferovic, P. and Van Linthout, S. (2021) 'Myocarditis and inflammatory cardiomyopathy: current evidence and future directions', *Nature Reviews Cardiology,* 18(3), pp. 169-193.

Tsipis, A. (2018) *Current Perspectives on Cardiomyopathies.* BoD–Books on Demand.

Twig, G., Elorza, A., Molina, A. J., Mohamed, H., Wikstrom, J. D., Walzer, G., Stiles, L., Haigh, S. E., Katz, S. and Las, G. (2008) 'Fission and selective fusion govern mitochondrial segregation and elimination by autophagy', *The EMBO journal,* 27(2), pp. 433-446.

Tzoulaki, I., Murray, G. D., Lee, A. J., Rumley, A., Lowe, G. D. and Fowkes, F. G. R. (2005) 'C-reactive protein, interleukin-6, and soluble adhesion molecules as predictors of progressive peripheral atherosclerosis in the general population: Edinburgh Artery Study', *Circulation,* 112(7), pp. 976-983.

van der Velden, J., Tocchetti, C. G., Varricchi, G., Bianco, A., Sequeira, V., Hilfiker-Kleiner, D., Hamdani, N., Leite-Moreira, A. F., Mayr, M. and Falcao-Pires, I. (2018) 'Metabolic changes in hypertrophic cardiomyopathies: scientific update from the Working Group of Myocardial Function of the European Society of Cardiology', *Cardiovascular research,* 114(10), pp. 1273-1280.

Varnava, A. M., Elliott, P. M., Baboonian, C., Davison, F., Davies, M. J. and McKenna, W. J. (2001) 'Hypertrophic cardiomyopathy: histopathological features of sudden death in cardiac troponin T disease', *Circulation,* 104(12), pp. 1380-1384.

Velicki, L., Jakovljevic, D. G., Preveden, A., Golubovic, M., Bjelobrk, M., Ilic, A., Stojsic, S., Barlocco, F., Tafelmeier, M. and Okwose, N. (2020) 'Genetic determinants of clinical phenotype in hypertrophic cardiomyopathy', *BMC cardiovascular disorders,* 20(1), pp. 1-10.

Vikhorev, P. G. and Vikhoreva, N. N. (2018) 'Cardiomyopathies and related changes in contractility of human heart muscle', *International journal of molecular sciences,* 19(8), pp. 2234.

Villard, E., Duboscq-Bidot, L., Charron, P., Benaiche, A., Conraads, V., Sylvius, N. and Komajda, M. (2005) 'Mutation screening in dilated cardiomyopathy: prominent role of the beta myosin heavy chain gene', *European heart journal,* 26(8), pp. 794-803.

Viswanathan, S. K., Sanders, H. K., McNamara, J. W., Jagadeesan, A., Jahangir, A., Tajik, A. J. and Sadayappan, S. (2017) 'Hypertrophic cardiomyopathy clinical phenotype is independent of gene mutation and mutation dosage', *PloS one,* 12(11), pp. e0187948.

Vitvitsky, V., Yadav, P. K., Kurthen, A. and Banerjee, R. (2015) 'Sulfide oxidation by a noncanonical pathway in red blood cells generates thiosulfate and polysulfides', *Journal of Biological Chemistry,* 290(13), pp. 8310-8320.

Vogiatzi, G., Lazaros, G., Oikonomou, E., Lazarou, E., Vavuranakis, E. and Tousoulis, D. (2022) 'Role of genetic testing in cardiomyopathies: A primer for cardiologists', *World Journal of Cardiology,* 14(1), pp. 29.

Volkova, M. and Russell, R. (2011) 'Anthracycline cardiotoxicity: prevalence, pathogenesis and treatment', *Current cardiology reviews,* 7(4), pp. 214-220.

Wahls, S. A. (2012) 'Causes and evaluation of chronic dyspnea', *American family physician,* 86(2), pp. 173-182.

Walsh, R., Rutland, C., Thomas, R. and Loughna, S. (2009) 'Cardiomyopathy: a systematic review of disease-causing mutations in myosin heavy chain 7 and their phenotypic manifestations', *Cardiology,* 115(1), pp. 49-60.

Wang, H., Song, P., Du, L., Tian, W., Yue, W., Liu, M., Li, D., Wang, B., Zhu, Y. and Cao, C. (2011) 'Parkin ubiquitinates Drp1 for proteasome-dependent degradation: implication of dysregulated mitochondrial dynamics in Parkinson disease', *Journal of Biological Chemistry,* 286(13), pp. 11649-11658.

Wang, J., Liu, Y., Cheng, X., Zhang, X., Liu, F., Liu, G., Qiao, S., Ni, M., Zhou, W. and Zhang, Y. (2017) 'The effects of LW-AFC on the hippocampal transcriptome in senescence-

accelerated mouse prone 8 strain, a mouse model of Alzheimer's disease', *Journal of Alzheimer's Disease,* 57(1), pp. 227-240.

Wang, R. (2002) 'Two's company, three's a crowd: can H2S be the third endogenous gaseous transmitter?', *FASEB J,* 16(13), pp. 1792-8.

Wang, S. *et al.* (2020) 'Correlation between mouse age and human age in anti-tumor research: Significance and Method Establishment', *Life Sciences*, 242, pp. 117242.

Wang, W., Nag, S., Zhang, X., Wang, M. H., Wang, H., Zhou, J. and Zhang, R. (2015) 'Ribosomal proteins and human diseases: pathogenesis, molecular mechanisms, and therapeutic implications', *Medicinal research reviews,* 35(2), pp. 225-285.

Wang, Y., Zhao, X., Jin, H., Wei, H., Li, W., Bu, D., Tang, X., Ren, Y., Tang, C. and Du, J. (2009) 'Role of hydrogen sulfide in the development of atherosclerotic lesions in apolipoprotein E knockout mice', *Arteriosclerosis, thrombosis, and vascular biology,* 29(2), pp. 173-179.

Wang, Z., Gerstein, M. and Snyder, M. (2009) 'RNA-Seq: a revolutionary tool for transcriptomics', *Nature reviews genetics,* 10(1), pp. 57-63.

Weber, K. T. (1989) 'Cardiac interstitium in health and disease: the fibrillar collagen network', *Journal of the American College of Cardiology,* 13(7), pp. 1637-1652.

Wehrens, M., de Leeuw, A. E., Wright-Clark, M., Eding, J. E., Boogerd, C. J., Molenaar, B., van der Kraak, P. H., Kuster, D. W., van der Velden, J. and Michels, M. (2022) 'Single-cell transcriptomics provides insights into hypertrophic cardiomyopathy', *Cell Reports,* 39(6).

Wei, J., Nelson, M. D., Szczepaniak, E. W., Smith, L., Mehta, P. K., Thomson, L. E., Berman, D. S., Li, D., Bairey Merz, C. N. and Szczepaniak, L. S. (2016) 'Myocardial steatosis as a possible mechanistic link between diastolic dysfunction and coronary microvascular dysfunction in women', *American Journal of Physiology-Heart and Circulatory Physiology,* 310(1), pp. H14-H19.

Weissler-Snir, A., Hindieh, W., Gruner, C., Fourey, D., Appelbaum, E., Rowin, E., Care, M., Lesser, J. R., Haas, T. S. and Udelson, J. E. (2017) 'Lack of phenotypic differences by cardiovascular magnetic resonance imaging in MYH7 (β-myosin heavy chain)-versus MYBPC3 (myosin-binding protein C)-related hypertrophic cardiomyopathy', *Circulation: Cardiovascular Imaging,* 10(2), pp. e005311.

Westermann, B. (2010) 'Mitochondrial fusion and fission in cell life and death', *Nature reviews Molecular cell biology,* 11(12), pp. 872-884.

Wexler, R., Elton, T., Pleister, A. and Feldman, D. (2009) 'Cardiomyopathy: an overview', *American family physician,* 79(9), pp. 778.

Whiteman, M., Li, L., Rose, P., Tan, C.-H., Parkinson, D. B. and Moore, P. K. (2010) 'The effect of hydrogen sulfide donors on lipopolysaccharide-induced formation of inflammatory mediators in macrophages', *Antioxidants & redox signaling,* 12(10), pp. 1147-1154.

WHO (2021) *Cardiovascular diseases (CVDs)*. who.int: WHO. Available at: https://www.who.int/news-room/fact-sheets/detail/cardiovascular-diseases-(cvds).

Wilkins, E., Wilson, L., Wickramasinghe, K., Bhatnagar, P., Leal, J., Luengo-Fernandez, R., Burns, R., Rayner, M. and Townsend, N. (2017) 'European cardiovascular disease statistics 2017'.

Williams, G. S., Boyman, L. and Lederer, W. J. (2015) 'Mitochondrial calcium and the regulation of metabolism in the heart', *Journal of molecular and cellular cardiology,* 78, pp. 35-45.

Wintner, E. A., Deckwerth, T. L., Langston, W., Bengtsson, A., Leviten, D., Hill, P., Insko, M. A., Dumpit, R., VandenEkart, E. and Toombs, C. F. (2010) 'A monobromobimane-based assay to measure the pharmacokinetic profile of reactive sulphide species in blood', *British journal of pharmacology,* 160(4), pp. 941-957.

Wirth, C., Brandt, U., Hunte, C. and Zickermann, V. (2016) 'Structure and function of mitochondrial complex I', *Biochimica et Biophysica Acta (BBA)-Bioenergetics,* 1857(7), pp. 902-914.

Wu, D., Hu, Q., Liu, X., Pan, L., Xiong, Q. and Zhu, Y. Z. (2015) 'Hydrogen sulfide protects against apoptosis under oxidative stress through SIRT1 pathway in H9c2 cardiomyocytes', *Nitric Oxide,* 46, pp. 204-212.

Wu, D., Tan, B., Sun, Y. and Hu, Q. (2022) 'Cystathionine γ lyase S-sulfhydrates Drp1 to ameliorate heart dysfunction', *Redox Biology,* 58, pp. 102519.

Wu, W., Sun, X., Shi, X., Lai, L., Wang, C., Xie, M., Qin, G. and Qiu, H. (2021) 'Hsp22 deficiency induces age-dependent cardiac dilation and dysfunction by impairing autophagy, metabolism, and oxidative response', *Antioxidants,* 10(10), pp. 1550.

Wüst, R. C., de Vries, H. J., Wintjes, L. T., Rodenburg, R. J., Niessen, H. W. and Stienen, G. J. (2016) 'Mitochondrial complex I dysfunction and altered NAD (P) H kinetics in rat myocardium in cardiac right ventricular hypertrophy and failure', *Cardiovascular Research,* 111(4), pp. 362-372.

Xiang, D. *et al.* (2021) 'Protective effects of estrogen on cardiovascular disease mediated by oxidative stress', *Oxidative Medicine and Cellular Longevity*, pp. 1–15.

Xue, J., Zhou, D., Poulsen, O., Hartley, I., Imamura, T., Xie, E. X. and Haddad, G. G. (2018) 'Exploring miRNA-mRNA regulatory network in cardiac pathology in Na+/H+ exchanger isoform 1 transgenic mice', *Physiological Genomics,* 50(10), pp. 846-861.

Yan, Y., Tang, R., Li, B., Cheng, L., Ye, S., Yang, T., Han, Y.-C., Liu, C., Dong, Y. and Qu, L.-H. (2021) 'The cardiac translational landscape reveals that micropeptides are new players involved in cardiomyocyte hypertrophy', *Molecular Therapy,* 29(7), pp. 2253-2267.

Yang, G., Wu, L., Jiang, B., Yang, W., Qi, J., Cao, K., Meng, Q., Mustafa, A. K., Mu, W. and Zhang, S. (2008) 'H2S as a physiologic vasorelaxant: hypertension in mice with deletion of cystathionine γ-lyase', *Science,* 322(5901), pp. 587-590.

Yang, G., Zhao, K., Ju, Y., Mani, S., Cao, Q., Puukila, S., Khaper, N., Wu, L. and Wang, R. (2013) 'Hydrogen sulfide protects against cellular senescence via S-sulfhydration of Keap1 and activation of Nrf2', *Antioxidants & redox signaling,* 18(15), pp. 1906-1919.

Yang, J., Minkler, P., Grove, D., Wang, R., Willard, B., Dweik, R. and Hine, C. (2019) 'Non-enzymatic hydrogen sulfide production from cysteine in blood is catalyzed by iron and vitamin B6', *Communications biology,* 2(1), pp. 194.

Yin, P., Zhao, C., Li, Z., Mei, C., Yao, W., Liu, Y., Li, N., Qi, J., Wang, L. and Shi, Y. (2012) 'Sp1 is involved in regulation of cystathionine γ-lyase gene expression and biological function by PI3K/Akt pathway in human hepatocellular carcinoma cell lines', *Cellular signalling,* 24(6), pp. 1229-1240.

Yong, Q. C., Choo, C. H., Tan, B. H., Low, C.-M. and Bian, J.-S. (2010) 'Effect of hydrogen sulfide on intracellular calcium homeostasis in neuronal cells', *Neurochemistry international,* 56(3), pp. 508-515.

Yoshida, J., Kawai, M., Minai, K., Ogawa, K., Ogawa, T. and Yoshimura, M. (2017) 'Associations between left ventricular cavity size and cardiac function and overload determined by natriuretic peptide levels and a covariance structure analysis', *Scientific Reports,* 7(1), pp. 2037.

You, J., Wu, J., Zhang, Q., Ye, Y., Wang, S., Huang, J., Liu, H., Wang, X., Zhang, W. and Bu, L. (2018) 'Differential cardiac hypertrophy and signaling pathways in pressure versus volume overload', *American Journal of Physiology-Heart and Circulatory Physiology,* 314(3), pp. H552-H562.

Youle, R. J. and Narendra, D. P. (2011) 'Mechanisms of mitophagy', *Nature reviews Molecular cell biology,* 12(1), pp. 9-14.

Young, M. D., Wakefield, M. J., Smyth, G. K. and Oshlack, A. (2010) 'Gene ontology analysis for RNA-seq: accounting for selection bias', *Genome biology,* 11(2), pp. 1-12.

Yu, Z., Zhang, W., Zhang, M., Jin, M., Xu, W. and Zhou, X. (2017) 'Gas signaling molecule hydrogen sulfide attenuates doxorubicin-induced dilated cardiomyopathy', *Oncotarget,* 8(56), pp. 95425.

Zaiser, E., Sehnert, A. J., Duenas, A., Saberi, S., Brookes, E. and Reaney, M. (2020) 'Patient experiences with hypertrophic cardiomyopathy: a conceptual model of symptoms and impacts on quality of life', *Journal of Patient-Reported Outcomes,* 4(1), pp. 1-11.

Zanardo, R. C., Brancaleone, V., Distrutti, E., Fiorucci, S., Cirino, G., Wallace, J. L., Zanardo, R. C., Brancaleone, V., Distrutti, E. and Fiorucci, S. (2006) 'Hydrogen sulfide is an endogenous modulator of leukocyte-mediated inflammation', *The FASEB journal,* 20(12), pp. 2118-2120.

Zhang, C. Y., Li, X. H., Zhang, T., Fu, J. and Cui, X. D. (2013) 'Hydrogen sulfide upregulates heme oxygenase-1 expression in rats with volume overload-induced heart failure', *Biomedical Reports,* 1(3), pp. 454-458.

Zhang, D., Contu, R., Latronico, M. V., Zhang, J., Rizzi, R., Catalucci, D., Miyamoto, S., Huang, K., Ceci, M. and Gu, Y. (2010) 'MTORC1 regulates cardiac function and myocyte survival through 4E-BP1 inhibition in mice', *The Journal of clinical investigation,* 120(8), pp. 2805-2816.

Zhang, H., Guo, C., Wu, D., Zhang, A., Gu, T., Wang, L. and Wang, C. (2012a) 'Hydrogen sulfide inhibits the development of atherosclerosis with suppressing CX3CR1 and CX3CL1 expression', *PloS one,* 7(7), pp. e41147.

Zhang, R., Sun, Y., Tsai, H., Tang, C., Jin, H. and Du, J. (2012b) 'Hydrogen sulfide inhibits L-type calcium currents depending upon the protein sulfhydryl state in rat cardiomyocytes', *PloS one,* 7(5), pp. e37073.

Zhang, S., Liu, X., Bawa-Khalfe, T., Lu, L.-S., Lyu, Y. L., Liu, L. F. and Yeh, E. T. (2012c) 'Identification of the molecular basis of doxorubicin-induced cardiotoxicity', *Nature medicine,* 18(11), pp. 1639-1642.

Zhang, Y., Ikeno, Y., Qi, W., Chaudhuri, A., Li, Y., Bokov, A., Thorpe, S. R., Baynes, J. W., Epstein, C. and Richardson, A. (2009) 'Mice deficient in both Mn superoxide dismutase and glutathione peroxidase-1 have increased oxidative damage and a greater incidence of pathology but no reduction in longevity', *Journals of Gerontology Series A: Biomedical Sciences and Medical Sciences,* 64(12), pp. 1212-1220.

Zhang, Y., Jiao, L., Sun, L., Li, Y., Gao, Y., Xu, C., Shao, Y., Li, M., Li, C. and Lu, Y. (2018) 'LncRNA ZFAS1 as a SERCA2a inhibitor to cause intracellular Ca2+ overload and contractile dysfunction in a mouse model of myocardial infarction', *Circulation research,* 122(10), pp. 1354-1368.

Zhao, L., Liu, X., Zhang, J., Dong, G., Xiao, W. and Xu, X. (2020) 'Hydrogen sulfide alleviates skeletal muscle fibrosis via attenuating inflammation and oxidative stress', *Frontiers in Physiology,* 11, pp. 533690.

Zhao, W., Zhang, J., Lu, Y. and Wang, R. (2001) 'The vasorelaxant effect of H2S as a novel endogenous gaseous KATP channel opener', *The EMBO journal,* 20(21), pp. 6008-6016.

Zhao, X., Zhang, L.-K., Zhang, C.-Y., Zeng, X.-J., Yan, H., Jin, H.-F., Tang, C.-S. and Du, J.-B. (2008) 'Regulatory effect of hydrogen sulfide on vascular collagen content in spontaneously hypertensive rats', *Hypertension Research,* 31(8), pp. 1619-1630.

Zheng, D., Dong, S., Li, T., Yang, F., Yu, X., Wu, J., Zhong, X., Zhao, Y., Wang, L. and Xu, C. (2015) 'Exogenous hydrogen sulfide attenuates cardiac fibrosis through reactive oxygen species signal pathways in experimental diabetes mellitus models', *Cellular physiology and biochemistry,* 36(3), pp. 917-929.

Zhou, N., Chen, X., Xi, J., Ma, B., Leimena, C., Stoll, S., Qin, G., Wang, C. and Qiu, H. (2020) 'Genomic characterization reveals novel mechanisms underlying the valosin-containing protein-mediated cardiac protection against heart failure', *Redox Biology,* 36, pp. 101662.

Zhu, C., Su, Y., Juriasingani, S., Zheng, H., Veramkovich, V., Jiang, J., Sener, A., Whiteman, M., Lacefield, J. and Nagpal, D. (2019) 'Supplementing preservation solution with mitochondria-targeted H2S donor AP39 protects cardiac grafts from prolonged cold ischemia–reperfusion injury in heart transplantation', *American Journal of Transplantation,* 19(11), pp. 3139-3148.

Zhu, L., Wang, W., Ren, C., Wang, Y., Zhang, G., Liu, J. and Wang, W. (2022) 'Cellular phenotypic transformation in heart failure caused by coronary heart disease and dilated cardiomyopathy: delineating at single-cell level', *Biomedicines,* 10(2), pp. 402.

Zhu, Y., Soto, J., Anderson, B., Riehle, C., Zhang, Y. C., Wende, A. R., Jones, D., McClain, D. A. and Abel, E. D. (2013) 'Regulation of fatty acid metabolism by mTOR in adult murine hearts occurs independently of changes in PGC-1α', *American Journal of Physiology-Heart and Circulatory Physiology,* 305(1), pp. H41-H51.

Zhu, Y. Z., Wang, Z. J., Ho, P., Loke, Y. Y., Zhu, Y. C., Huang, S. H., Tan, C. S., Whiteman, M., Lu, J. and Moore, P. K. (2007) 'Hydrogen sulfide and its possible roles in myocardial ischemia in experimental rats', *Journal of Applied Physiology,* 102(1), pp. 261-268.

Zile, M. R., Baicu, C. F., S. Ikonomidis, J., Stroud, R. E., Nietert, P. J., Bradshaw, A. D., Slater, R., Palmer, B. M., Van Buren, P. and Meyer, M. (2015) 'Myocardial stiffness in patients with heart failure and a preserved ejection fraction: contributions of collagen and titin', *Circulation,* 131(14), pp. 1247-1259.

Zorov, D. B., Juhaszova, M. and Sollott, S. J. (2014) 'Mitochondrial reactive oxygen species (ROS) and ROS-induced ROS release', *Physiological reviews,* 94(3), pp. 909-950.

Zou, Y., Akazawa, H., Qin, Y., Sano, M., Takano, H., Minamino, T., Makita, N., Iwanaga, K., Zhu, W. and Kudoh, S. (2004) 'Mechanical stress activates angiotensin II type 1 receptor without the involvement of angiotensin II', *Nature cell biology,* 6(6), pp. 499-506.

Appendix A – Consumables

2-beta Mercaptoethanol	Sigma-Aldrich, Dorset, UK
30% Protogel casting kit	Gene Flow, Lichfield, UK
4x Laemmli sample buffer	Bio-rad, Watford, UK
Acetone	University stores
Alexa Fluor 488	Life Technologies, UK
Bradford protein assay Reagent A	Bio-rad, Watford, UK
Bradford protein assay Reagent B	Bio-rad, Watford, UK
Bradford protein assay Reagent S	Bio-rad, Watford, UK
BSA	Sigma-Aldrich, Dorset, UK
Calcium chloride	Sigma-Aldrich, Dorset, UK
EDTA	Sigma-Aldrich, Dorset, UK
EGTA	Sigma-Aldrich, Dorset, UK
Ethanol	University stores
Evoscript	Roche, Basel, Switzerland
Eye cream	Provided by vet
Fluormount	Sigma-Aldrich, Dorset, UK
Goat serum	Vector Labs, California, USA
Isoflurane	Provided by vet
Isolectin B4	Vector Labs, California, USA
Licor blocking buffer	Licor, Nebraska, USA
Licor REVERT total protein stain kit	Licor, Nebraska, USA
Licor secondary antibodies	Licor, Nebraska, USA
Mannitol	Sigma-Aldrich, Dorset, UK
Methanol	University stores
Milk-dried skimmed powder	Marvel, UK
miRNeasy kit	Qiagen, Hilden, Germany
OCT compound	Scientific Laboatory Supplies
Phosphate buffer saline (PBS)	Lonza, Basel, Switzerland
Precision plus protein dual colour standards	Bio-rad, Watford, UK
Primers	ID Technologies
Protease inhibitor	Sigma-Aldrich, Dorset, UK
QIAamp DNA mini kit	Qiagen, Hilden, Germany
Qishredder	Qiagen, Hilden, Germany
Qizol reagent	Qiagen, Hilden, Germany

Reagent diluent	R and D systems, Minnsota, USA
RIPA buffer	Milipore, UK
RNase free water	Qiagen, Hilden, Germany
Running buffer	Gene Flow, Lichfield, UK
Seahorse medium XF Base	Agilent Technologies, UK
Seahorse XF Calibrant solution	Agilent Technologies, UK
Streptavidin, Alexa Fluor 488 conjugate	Vector Labs, California, USA
Sucrose	Sigma-Aldrich, Dorset, UK
SYBR green	Roche, Basel, Switzerland
TBS	Santa Cruz
Transfer buffer	Gene Flow, Lichfield, UK
Transfer buffer	Gene Flow, Lichfield, UK
Triton	Sigma-Aldrich, Dorset, UK
Trypan blue	Sigma-Aldrich, Dorset, UK
Tween-20	Sigma-Aldrich, Dorset, UK
Ultrasound gel	Scientific Laboratory Supplies
WGA	Vector Labs, California, USA